THE REACTIONS OF GROUP IVB HYDRIDES WITH CARBONYL COMPLEXES OF COBALT AND MANGANESE.

A Thesis Submitted

to the

University of Waikato

In **Fulfilment**

Of the Requirements

For the Degree of

Doctor of Philosophy

by

Stephen Paul Foster MSc (Hons)

University of Waikato November 1982.

TO

My Parents

and

Margaret.

CONTENTS

LIST OF TABLES AND FIGURES

ABSTRACT

The use of the hydrides as reagents for building group IVB - transition metal complexes has been investigated.

The reactions of the simple hydrides; Me_3GeH, Me_2GeH_2, $MeGeH_3$, GeH_4, Me_2SiH_2, Me_2SnH_2, $MeSnH_3$, and SnH_4, with $Co_2(CO)_8$ have been examined, and the effect determined of, reactant ratios and amount of CO present, on the products obtained. Limited evidence was obtained for the synthesis of the new compounds; $MeGe[Co(CO)_4]_3$, $HGe[Co(CO)_4]_3$, $Me_2SiHCo(CO)_4$ and $(OC)_4CoMe_2SiOCCo_3(CO)_9$. Me_2GeH_2 replaces a bridging CO group:

$$Me_2GeH_2 + Co_2(CO)_8 \rightarrow Me_2GeCo_2(CO)_7 + H_2 + CO$$

$$Me_2GeH_2 + Me_2GeCo_2(CO)_7 \rightarrow (Me_2Ge)_2Co_2(CO)_6 + H_2 + CO$$

In the reactions of the polygermanes; Me_3GeGeH_3, Me_3SiGeH_3, Ge_2H_6, Ge_3H_8 and $(GeH_3)_2SiMe_2$ with $Co_2(CO)_8$, the M'-Ge (M' = Si or Ge) bonds were quantitatively cleaved, and the new compound $Ge_2Co_6(CO)_{20}$, was isolated. This compound is assigned the structure:

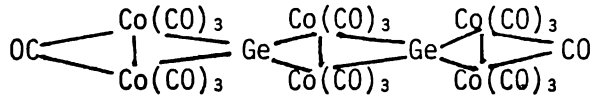

on spectroscopic evidence.

Me_2GeH_2 also replaces a bridging CO group in the germanium - cobalt carbonyl species, to produce the new compounds; $Me_2Ge_2Co_4(CO)_{13}$ and $(Me_2Ge)_2Ge_2Co_6(CO)_{18}$. An X-ray crystallographic study on $Me_2Ge_2Co_4(CO)_{13}$ although showing the:

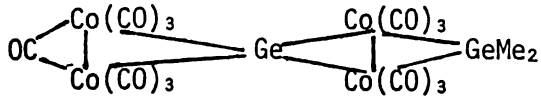

skeleton, failed to refine properly. The reactions of Me_2SiH_2 and Me_2SnH_2 with germanium - cobalt carbonyl species failed to give a similar result.

$MeGeH_3$ and $GeCo_4(CO)_{14}$ produced initially the analogous $Me(H)Ge_2Co_4(CO)_{13}$. However when left for 6 months, an unexpected

rearrangement yielded $(MeGe)_2Co_4(CO)_{11}$. X-ray crystallography showed an irregular square bipyramidal stucture, containing 5-coordinated square pyramidal germanium. This is the first example of such a group IVB - transition metal cluster.

The decarbonylation of $Ge_2Co_6(CO)_{20}$ yielded the new compound $[(OC)_4CoGe]_2Co_4(CO)_{11}$:

$$Ge_2Co_6(CO)_{20} \xrightarrow[\text{hexane}]{60\,^0C} [(OC)_4CoGe]_2Co_4(CO)_{11} + CO$$

which was found by X-ray crystallography to have a similar square bipyramidal stucture.

The new tin hydrides; $MeSnH_2Mn(CO)_5$ and $Me_2SnHMn(CO)_5$, have been prepared by the established route :

$$Me_{(3-x)}SnH_xCl + NaMn(CO)_5 \longrightarrow Me_{(3-x)}SnH_xMn(CO)_5 + NaCl$$
$$(x = 1,2)$$

and characterised spectroscopically.

ACKNOWLEDGEMENTS

I should sincerely like to thank my supervisors, Professor K.M. Mackay and Dr. B.K. Nicholson, for their stimulating discussion, guidance and constant encouragement throughout this work.

I gratefully acknowledge the helpful assistance of the following people :

(i) The technical staff of the University, particuarly Mr G. Purdy the University Glassblower, Mr F. Bailey the University Draughtsman, and Mr A. Brennan, for the running of mass spectra.

(ii) Messrs R. Thomson and P. Watkinson, for the running of Fourier Transform N.M.R. spectra.

(iii) The Universities of Adelaide's and Auckland's Crystallographic Departments, for the collection of intensity data. Special thanks are due to , Professor N. Waters, Associate Professor J. Waters, and Dr. A. Jones, of the University of Auckland, for their patience and assistance.

(iv) Mr R. Croft of the University's Computing Centre and Dr A.L. Wilkins for help with the crystallographic programs.

(v) Dr A.M. Cartner, for helpful discussion.

(vi) Mr C.C Scott, for the drawing of the diagrams.

(vii) The Chemistry Secretaries. Throughout this work the Chemistry Dept. has been fortunate to have had such bright, helpful and efficient secretaries as Mrs S. Buick, Mrs J.O. Smith, Mrs B. Hughes and Miss F.M. Annan.

(viii) Mrs H. Bloxam for her patient, efficient, and when necessary, speedy preparation of the typescript.

(ix) The University for a Study Award.

(x) My contemporaries and good friends, Mr D.V Dass, Dr J. Dunbar and Mr H.J. van Enckevort,who have during this work, helped, amused and distracted me, mostly simultaneously.

Finally, I am especially grateful to my wife Margaret, whose encouragement and support was always given and appreciated.

ABBREVIATIONS

The following abbreviations have been used in this work.

Bu_2O	di-n-butyl ether
Et_2O	diethyl ether
THF	tetrahydrofuran
R	alkyl or aryl group
Me	methyl
Et	ethyl
Tol	toluene
Bu	butyl
Ph	phenyl
nmr	nuclear magnetic resonance
IR	infrared
ν	stretch
δ	deformation
ρ	rock
vs	very strong
s	strong
m	medium
w	weak
vw	very weak
sh	shoulder
br	broad
M'	group IVB element
E	main group atom
M	transition metal
X	halogen

CHAPTER 1. INTRODUCTION.

1.1. GENERAL.

Recently, a considerable volume of work in modern Inorganic Chemistry has been concerned with metal carbonyl chemistry. These compounds, in addition to their unusual bonding properties and wide and varied structural chemistry (1) show the ability to catalyse the rates of certain reaction systems. (2,3,4)

In addition to the binary metal carbonyls there is an extensive group of compounds in which a main group hetero-atom is bonded to one or more transition metal atoms. Although most of the main group atoms on the right-hand side of the periodic table form these type of compounds, one of the more interesting groups involves the group IVB metallic elements (Si,Ge,Sn and Pb) whose members show a readiness to form catenated compounds amongst themselves. (5)

A large proportion of the work on these compounds has been carried out on the first row transition metals, in particular manganese, iron and cobalt. Of the second and third row elements, the most studied are platinum, ruthenium, osmium and rhodium. (6)

There are several excellent reviews (6, 7, 8, 9, 60) which comprehensively cover the chemistry of these compounds and so in this chapter only parts of direct interest to the work in this thesis will be covered.

1.2 GROUP IVB - COBALT CARBONYLS.

1.2.1. GENERAL.

Carbonyls containing cobalt bonded to a heavier Group IVB element (Si, Ge, Sn and Pb) have so far been found in three different structural classes:

(i) those in which M^1 is bonded to a terminal $-Co(CO)_4$ group (Fig.1(a))

(ii) those in which M^1 bridges a cobalt-cobalt bond (Fig.1(b))

(iii) those in which M^1 triply bridges a triangle of cobalt atoms. (Fig.1(c))

1.2.2. COMPOUNDS CONTAINING TERMINAL COBALT TETRACARBONYL GROUPS.

The known compounds of the types $R_{4-n}M^1\{Co(CO)_4\}_n$ are listed in Table 1.1. The general type is found for M^1 = Si to Pb and n = 1 to 4.

For the monocobalt species, a wide range of substituents on M^1 are known, including alkyl, aryl, halide and other transition metals. Also known are the polygermanyl compounds, $GeH_3GeH_2Co(CO)_4$ and $\{GeH_2Co(CO)_4\}_2$ (28) containing Ge-Ge metal bonds in addition to the Ge-Co bond.

Infrared spectroscopy is a powerful tool for the analysis of these compounds. For compounds of type $R_3M^1Co(CO)_4$ with C_{3v} symmetry, $2a_1+e$ carbonyl stretching modes are predicted and generally observed. Replacing M^1 by a heavier group IVB atom generally shifts bands by 1-2 cm^{-1} to lower frequency (27). The replacement of substituents by less electronegative groups also leads

FIGURE 1.1 STRUCTURAL TYPES OF GROUP IVB - COBALT CARBONYLS

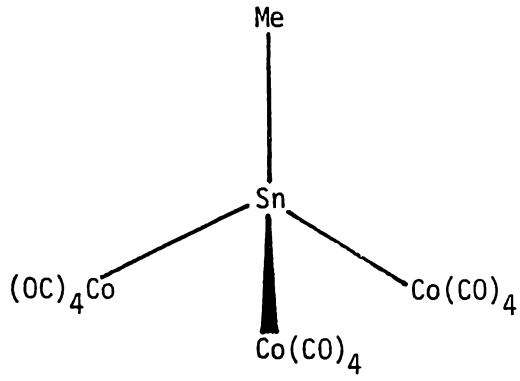

(A) $MeSn[Co(CO)_4]_3$ Ref. 31

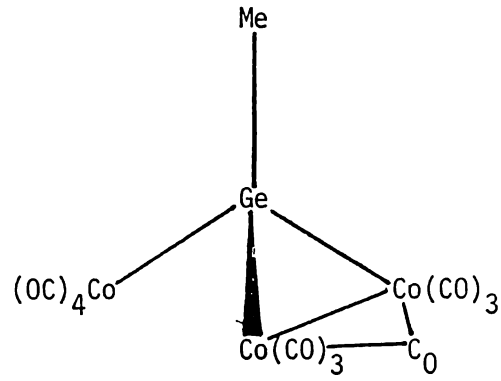

(B) $MeGe[Co(CO)_4][Co_2(CO)_7]$ Ref. 52

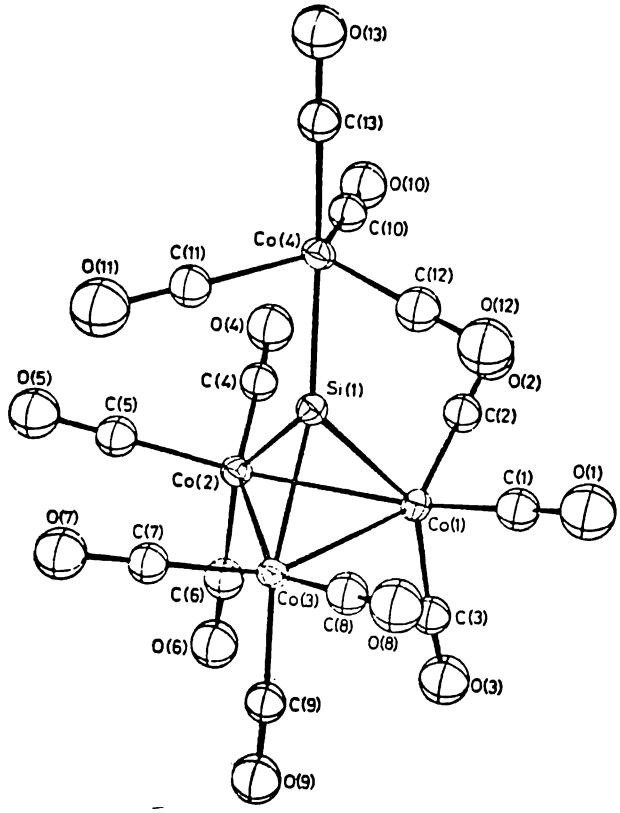

(C) $SiCo_4(CO)_{13}$ Ref. 62

TABLE 1.1. Terminal -$Co(CO)_4$ Derivatives of Si, Ge, Sn and Pb

One -$Co(CO)_4$ Group per Atom

Compound	References
$R_3M^1Co(CO)_4$	
M^1=Si, R_3=H_3	10
Me_3	11
Et_3	11
Ph_3	12
$(OMe)_3$	13
$(OEt)_3$	13
F_3	11
Cl_3	12
$(C_6H_5)_3$	14
Me and H_2	15
Me and F_2	16
Me and Ph and α-Np	17
Me and Ph and neo -C_5H_{11}	17
$Ph_2$and H	13
Ph and Cl_2	13
Special case.	
Me_2HSi-$SiMe_2Co(CO)_4$	18
M^1=Ge, R_3=H_3	19
Me_3	20
Et_3	20
Ph_3	21
Cl_3	22, 23
Br_3	22, 23
I_3	22, 23

TABLE 1.1. (Continued)

Compound	References
Me and H_2	24
Me and I_2	22
Me_2 and H	25
Me_2 and Cl	22
Ph and Cl_2	22
Ph and I_2	22
Ph_2 and Cl	22
Ph_2 and I	22
Ph_2 and $Mn(CO)_5$	26
Me and Cl_2	27
Me and Br_2	27
Special Cases	
$GeH_3GeH_2Co(CO)_4$	28
$(CO)_4CoGeH_2GeH_2Co(CO)_4$	28
M^1=Sn, R_3=Me_3	20
Et_3	29
Bu_3	30
Ph_3	21
Cl_3	23
Br_3	23
I_3	23
Me and Cl_2	31, 32
Me and Br_2	31, 32
Me and I_2	31, 32
Me_2 and Cl	23, 32
Me_2 and Br	23, 32

TABLE 1.1. (Continued)

Compound		References
	Me_2 and I	23, 32
	Ph and Cl_2	23
	Ph and Br_2	23
	Ph and I_2	23
	$Ph_2Mn(CO)_5$ and Cl	33
	Ph_2 and Cl	22
	Ph_2 and Br	23
	Ph_2 and I	23
	Ph_2 and $Mn(CO)_5$	34
	$(acac)_2$ and Cl	35
M^1=Pb, R_3=Me_3		22
	Et_3	22
	Ph_3	22
	$(C_6H_{11})_3$	30
Two $-Co(CO)_4$ Groups per Atom		
$R_2M^1\{Co(CO)_4\}_2$		
M^1=Si, R_2=H_2		36
M^1=Ge, R_2=Cl_2		22
	I_2	37
	Me_2	22, 38
	Ph_2	39
	I and Me	22
	Br_2	27
	Me and Cl	27
	Me and Br	27

TABLE 1.1. (Continued)

Compound	References
M^1=Sn, R_2=Cl_2	37, 40
Br_2	37, 40
I_2	37, 40
Me_2	21, 22, 41, 42
Ph_2	22, 40
Me and Cl	22, 31
Ph and Cl	22
$(n\text{-}Pr)_2$	31
(n-Pr) and Cl	31
$(n\text{-}Bu)_2$	21, 31
(n-Bu) and Cl	22, 31
$(CH_2{=}CH)_2$	41
$(CH_2{=}CH)$ and Cl	22, 43
$(CH_3COO)_2$	23
$(acac)_2$	35
M^1=Pb, R_2=Ph_2	30
Three $-Co(CO)_4$ Groups per Atom	
R $M^1\{Co(CO)_4\}_3$	
M^1=Ge, R =Ph	44
Cl, Br	27
M^1=Sn, R =F	23
Cl	31, 43
Br	31, 43
I	43
Me	31, 41, 43
Et	31

TABLE 1.1. (Continued)

Compound	References
(n-Bu)	31, 43
Ph	43
(CH_2=CH)	43
(CH_3COO)	23
Four (-$Co(CO)_4$) Groups per Atom.	
$M^1\{Co(CO)_4\}_4$	
M^1 = Ge	27
M^1 = Sn	23, 45
M^1 = Pb	45

to a downward shift of bands, usually more marked than for M^1 replacement.

Unsymmetrically substituted $X_2YM^1Co(CO)_4$ compounds are of C_s symmetry. Splitting of the e mode of C_{3v} to $a^1 + a^{11}$ is reflected by the appearance of an extra band.

For silicon, poly -$Co(CO)_4$ substitution is known only in $H_2Si\{Co(CO)_4\}_2$ (36). Germanium, tin and lead all form polysubstituted compounds up to and including tetracobalt compounds. The bis-cobalt species with both substituents the same $\{X_2M^1\{Co(CO)_4\}_2\}$ are of C_{2v} molecular symmetry, with $3a_1 + 3b_1 + b_2$ infrared active modes predicted for the carbonyl stretching region. All these modes are usually observed with considerable mixing between modes (22). Where both substituents differ, symmetry is reduced to C_s with $4a^1 + 4a^{11}$ vibrations predicted. Graham (22) has used the relative absorbances of the two highest frequency bands in the spectra of the bis-cobalt compounds to calculate Co-M^1-Co bond angles.

Germanium and tin both form tris-cobalt derivatives, although considerably more tris-cobalt derivatives are known for tin than for germanium. The non-halogeno germanium derivatives readily lose CO to form bridged types of structure:

$$PhGe\{Co(CO)_4\}_3 \xrightarrow[h\nu]{\Delta} PhGe\{Co(CO)_4\}\{Co_2(CO)_7\} + CO \quad \text{(Ref.44)}$$

whereas attempts to induce the same decarbonylation in tin derivatives have failed.(43) There appears to be two factors controlling the decarbonylation, the size of M^1 and the size and nature of the substituent group.

Thus the smaller Ge atom is more favourable to forming condensed structures with greater Co-Co bonding than the larger Sn atom. (See next two sections).

The halogeno - Ge derivatives are however more stable to decarbonylation (27) than the corresponding alkyl or aryl derivatives. This is probably due to the electron withdrawing effect of the halogen, making Co-Co bonding less likely.

The tris $-Co(CO)_4$ molecules are usually of C_{3v} symmetry (R can usually be considered a sphere) with predicted $3a_1 + 4e$ infrared active modes in the carbonyl stretching region, generally being observed.

The tetrakis-cobalt compounds $M^1\{Co(CO)_4\}_4$ are known for Ge (27), Sn (23,45) and Pb (45). The Ge compound, like the Ge tris-cobalt compounds readily undergoes decarbonylation to form $GeCo_4(CO)_{14}$ (46).

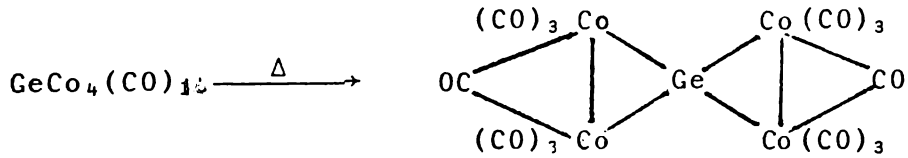

No such reaction has been observed for the Sn or Pb species (45).

These molecules are ideally of T_d molecular symmetry with $3t_2$ infrared active carbonyl stretching modes predicted. The spectra consist of two very strong bands plus two weak bands. This is best explained by a twisting of the $-Co(CO)_4$ groups about the M^1 - Co axis such that the molecule is of only T molecular symmetry, (with 4t infrared active modes in the carbonyl region predicted) (27).

1.2.3. COMPOUNDS IN WHICH A GROUP IVB ATOM BRIDGES A COBALT - COBALT BOND.

The known compounds are listed in Table 1.2. In this type, M^1 bridges a Co-Co bond in much the same manner as a bridging CO. Two simple types are found for Si, Ge and Sn, $(\mu\text{-}R_2M^1)\ Co_2(CO)_7$ and $(\mu\text{-}R_2M^1)_2\ Co_2(CO)_6$.

Of the first type, by far the greatest number of species are known for Ge. An interesting class of these derivatives is when one of the substituents on Ge is a $M(CO)_x$ species, (either $-Co(CO)_4$ or $-Mn(CO)_5$). Thus for the $-Co(CO)_4$ substituted Ge, we have a tricobalt species, $RGeCo_3(CO)_{11}$ (See Fig. 1.1b) The two known Sn derivatives are either extremely unstable, ($Me_2SnCo_2(CO)_7$ ref42) or involve 6 co ordinate Sn $\{(C_5H_7O_2)_2SnCo_2(CO)_7$ ref 35$\}$.

Of the second type of compound $(\mu\text{-}R_2M^1)_2Co_2(CO)_6$, the methyl substituted derivatives are known for Si(18), Ge(27,28,53,54,55) and Sn (42,55).

An NMR study on the Ge and Sn derivatives $(Me_2M')_2Co_2(CO)_6$(53,55) revealed the molecules to be fluxional in solution, with rapid site exchange of the axial and equatorial substituents on M^1.

There are three extended compounds of this type known. Both germanium compounds have been characterised crystallographically. $GeCo_4(CO)_{14}$ has two $-Co_2(CO)_7$ units (see Fig.1.2A) bonded to a central Ge, while $\{HgGeCo_5(CO)_{17}\}^-$ is similar, with a bridging CO replaced by a bridging $HgCo(CO)_4$ group (see Fig.1.2B).

TABLE 1.2. Compounds In Which M^1 Bridges a Co-Co Bond.

Compound	References
$(\mu\text{-}R_2M^1)(\mu\text{-}CO)Co_2(CO)_6$	
M^1=Si, R_2=Me_2	18
Ph_2	44
Ph and $Co(CO)_4$	44
M^1=Ge, R_2=Me_2	27, 38
Ph_2	48, 49
Me and $Co(CO)_4$	50, 52
Ph and $Co(CO)_4$	44
Me and $Mn(CO)_5$	51
Br and $Co(CO)_4$	52
M^1=Sn, R_2=Me_2	42
$(acac)_2$	35, 109
$(\mu\text{-}R_2M^1)_2Co_2(CO)_6$	
M^1=Si, R_2=Me_2	18
M^1=Ge, R_2=Me_2	27, 38, 53, 54, 55
M^1=Sn, R_2=Me_2	42, 55
Special Cases	
$(\mu\text{-}CO)Co_2(CO)_6SiCo_2(CO)_6(\mu\text{-}CO)$	56
$(\mu\text{-}CO)Co_2(CO)_6GeCo_2(CO)_6(\mu\text{-}CO)$	59
$\{(\mu\text{-}CO)Co_2(CO)_6Ge(Co_2(CO)_6)(\mu\text{-}HgCo(CO_4)\}$	58

FIGURE 1.2 SOME EXTENDED $GeCo_2$ LINKED STRUCTURES

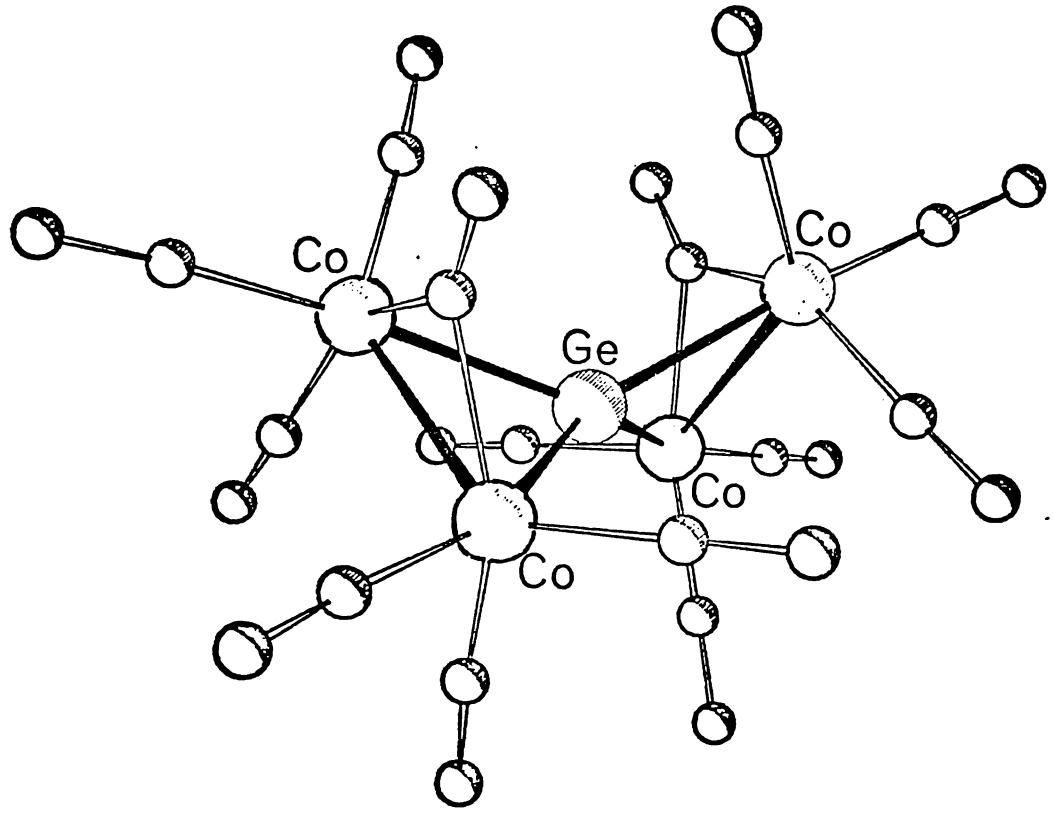

(A) $GeCo_4(CO)_{14}$ Ref.57

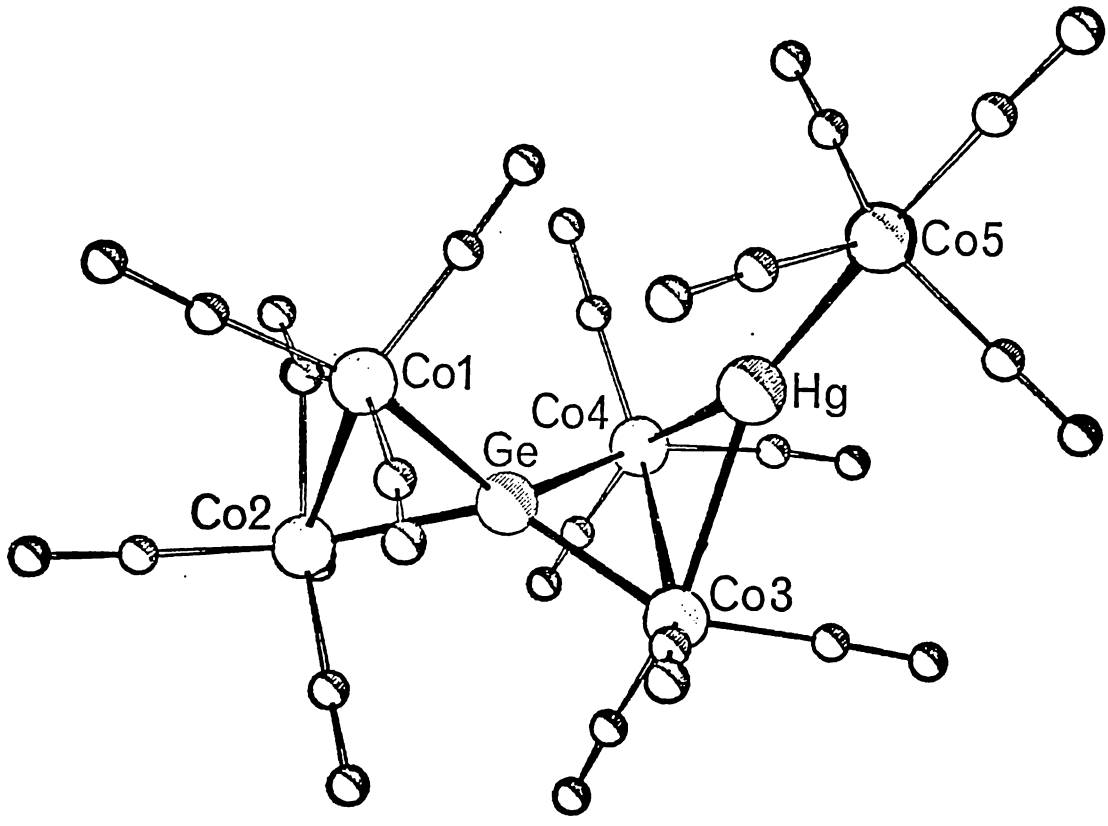

(B) $(GeCo_4(CO)_{13}[HgCo(CO)_4])^-$ Ref.58

$SiCo_4(CO)_{14}$ (56) has been characterised by its similar spectroscopic properties to $GeCo_4(CO)_{14}$.

The reluctance of Sn and Pb to bridge a Co-Co bond has been attributed by Curtis (42) to the increased sizes of the covalent radii making the required bond angle to bridge the Co-Co bond more strained. In the case of $(acac)_2SnCo_2(CO)_7$, the 6-coordination and resultant decrease in bond angle, makes bridging more acceptable (35).

This is further supported by the compound $Sn\{Fe(CO)_4\}_4$, where the bridging Sn is accommodated by two long Fe-Fe bonds of length $2{\cdot}87\mathring{A}$, (c.f.Fe-Fe bond in $(Me_2)_3\ Fe_2(CO)_6$ is $2{\cdot}74\mathring{A}$).

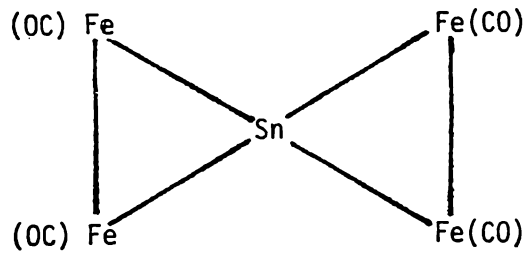

1.2.4. COMPOUNDS CONTAINING A GROUP IVB ATOM TRIPLY BRIDGING A COBALT TRIANGLE.

This type is directly analogous to the well-established methylidyne clusters which contain a carbon atom bridging a cobalt triangle of atoms. These clusters are known with a wide range of substituents on the bridging carbon and are generally extremely stable to thermal decomposition (61)

TABLE 1.3. Compounds in Which M^1 Bridges a Co_3 Triangle

Compound	References
$RM^1Co_3(CO)_9$	
M^1=Ge, R =CH_3	52
Ph	44
Br	64
$(CO)_xMM^1Co_3(CO)_9$	
M^1=Si, $M(CO)_x$=$Co(CO)_4$	62
M^1=Ge, $M(CO)_x$=$Co(CO)_4$	63, 64
$Mn(CO)_5$	51
Special Types	
$\{Co_3(CO)_9GeCo_2(CO)_7\}^-$	65
$\{Co_3(CO)_9GeCo\ (CO)_3GeCo_3(CO)_9\}^-$	66
$\{Co_3(CO)_9GeCo_4(CO)_{11}\}^-$	66

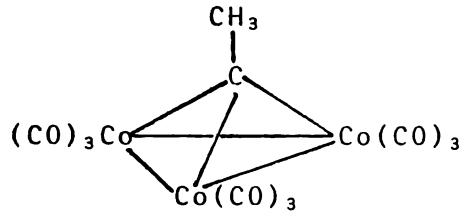

Ref(47)

Virtually all the silicon derivatives apparently of this type are methylidyne derivatives, $R_3Si\text{-}O\text{-}C\text{-}Co_3(CO)_9$(61), this presumably due to the strong Si-O bond. However recently Schmid (62) has established the existence of the true $SiCo_3$ cluster $(CO)_4Co\text{-}SiCo_3(CO)_9$ from the reaction of SiI_4 with $NaCo(CO)_4$ (See Fig.1.1C).

A considerable range of compounds containing $GeCo_3$ units are structurally established. Analogous to the Si compound is $(CO)_4Co\text{-}GeCo_3(CO)_9$ (63,64), while another metal carbonyl substituted compound, $Mn(CO)_5GeCo_3(CO)_9$ is also known (51). In this report there are also indications of further $M(CO)_X$ substituted species. $CH_3GeCo_3(CO)_9$(52) and $PhGeCo_3(CO)_9$ (44) can be formed by the decarbonylation of the parent compounds $RGe\{Co(CO)_4\}\{Co_2(CO)_7\}$ (See 1.4),

$$PhGeCo_3(CO)_{11} \xrightarrow{\Delta} PhGeCo_3(CO)_9 + 2CO \quad \text{(Ref.44)}$$

although their thermal stability is much less than their methylidyne analogues.

Nicholson and co-workers (See section 1.4) have reported one pentacobalt and two heptacobalt, (65,66) anionic Ge clusters, based on the $GeCo_3(CO)_9$ unit. $\{Co_3(CO)_9GeCo_2(CO)_7\}$ (See Fig.1.3A) contains a five coordinate Ge bonded to $-Co_3(CO)_9$ and $-Co_2(CO)_7$ groups. $\{Co_3(CO)_9GeCo(CO_3)GeCo_3(CO)_9\}$ (Fig. 1.3B) contains two $-GeCo_3(CO)_9$ units linked by a $Co(CO)_3$group, while the other heptacobalt cluster $\{Co_3(CO)_9GeCo_4(CO)_{11}\}$(Fig.1.3C) consists of a $-GeCo_3(CO)_9$ unit attached to a tetracobalt

FIGURE 1.3 HIGH NUCLEAR Ge-Co CLUSTERS

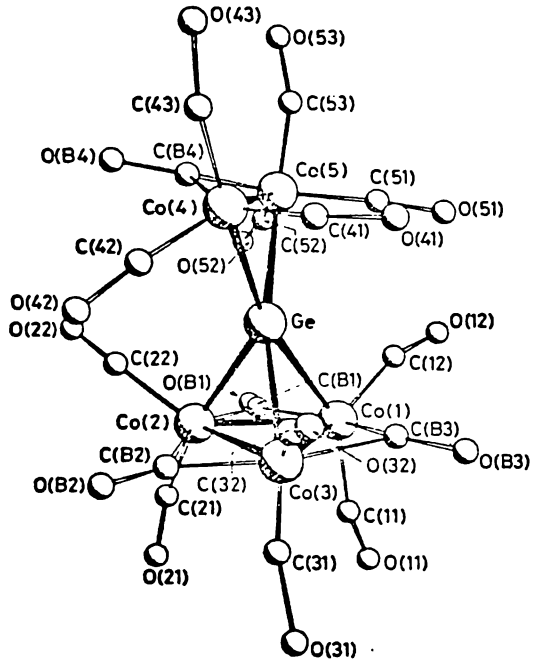

(A) $[GeCo_5(CO)_{16}]^-$ Ref. 65

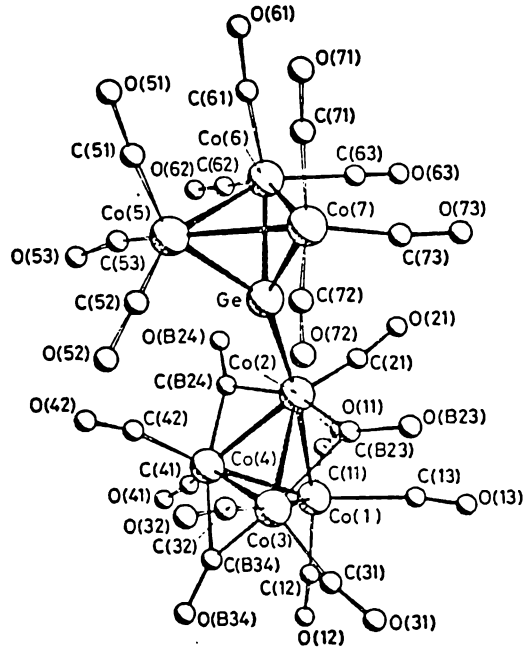

(C) $[GeCo_7(CO)_{20}]^-$ Ref. 66

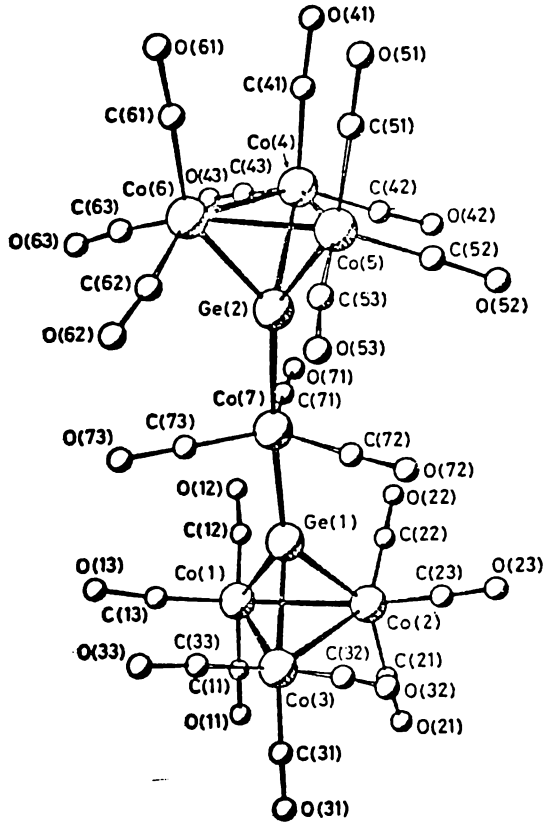

(B) $[Ge_2Co_7(CO)_{21}]^-$ Ref. 66

group (similar to $Co_4(CO)_{12}$).

The only Sn or Pb compound of this type reported, is $MeSnCo_3(CO)_9$ (17), from the reaction of Me_2SnCl_2 with $Co_2(CO)_8$. This report has been questioned however (6) and it appears likely that the reported compound is in fact a $Me_2SnCo_2(CO)_x$ derivative.

The trend for the smaller M^1 to occupy the triply bridging position has been explained by Schmid (68), who has observed amongst a range of clusters of the type MCo_3 (M=any atom) that there appears to be a maximum covalent radii for M to form the cluster, of about $1.30\overset{0}{A}$ (c.f. C=0.77, Si=1.11, Ge=1.22, Sn=1.41, Pb=$1.47\overset{0}{A}$) Thus only C, Si and Ge of the group IVB elements may occupy this position.

A summary of the structural behaviour of the different group IVB atom-cobalt carbonyls is best obtained by a comparison of the tetracobalt species they form:

TABLE 1.4. Tetracobalt Complexes of the Group IVB Elements.

$M^1\{Co(CO)_4\}_4$	-	Ge	Sn	Pb
$\{Co_2(CO)_7\}M^1\{Co_2(CO)_7\}$	Si	Ge	-	-
$Co(CO)_4M^1Co_3(CO)_9$	Si	Ge	-	-

Thus while Si favours bridging Co-Co bonds and Sn and Pb favour terminal $-Co(CO)_4$ substitution, Ge is intermediate in behaviour between these and forms all three types of compounds.

1.3 OTHER MAIN GROUP - COBALT CARBONYL CLUSTERS.

1.3.1. GENERAL.

It is useful at this stage to consider other main group-cobalt carbonyl clusters. Not only are many of these clusters isoelectronic with their Group IVB analogues, but they also provide a useful insight into possible extensions of the known Group IVB -Cobalt Carbonyl clusters.

1.3.2. CARBIDO CLUSTERS.

There are two main structural types of carbide clusters. The first type, the cage carbide is where the carbide carbon atom(s) is completely enclosed by the metal framework. The second less common type has the carbide carbon atom attached to the periphery of the metal structure.

TABLE 1.5. Cobalt Carbonyl Carbido Clusters.

Compound	Reference
$Co_6C(CO)_{14}^-$	69
$Co_6C(CO)_{15}^{2-}$	70
$Co_6C(CO)_{12}S_2$	71
$Co_8C(CO)_{18}^{2-}$	72
$Co_2Rh_4C(CO)_{15}^{2-}$	70

Chini (70) reported the first cobalt carbonyl-carbido cluster in 1974 (See Fig.1.4). Since then other reports (See table 1.5) have established this class of compound for cobalt. Although a fully encapsulated nitrogen cluster (73) and a partially

FIGURE 1.4 SOME CARBIDO CLUSTERS

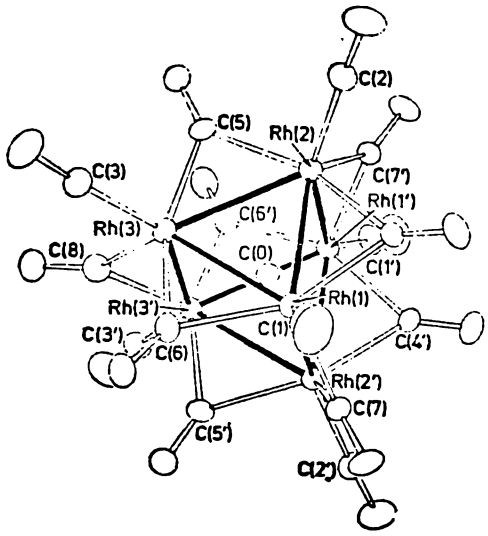

(A) $[Rh_6(CO)_{15}C]^{2-}$ Ref. 163

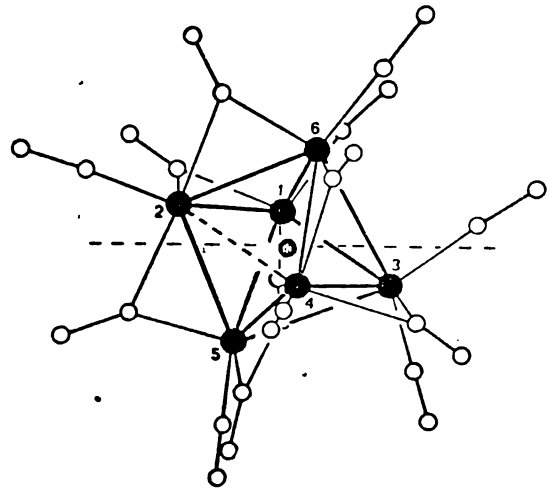

(B) $[Co_6(CO)_{14}C]^{-}$ Ref. 69

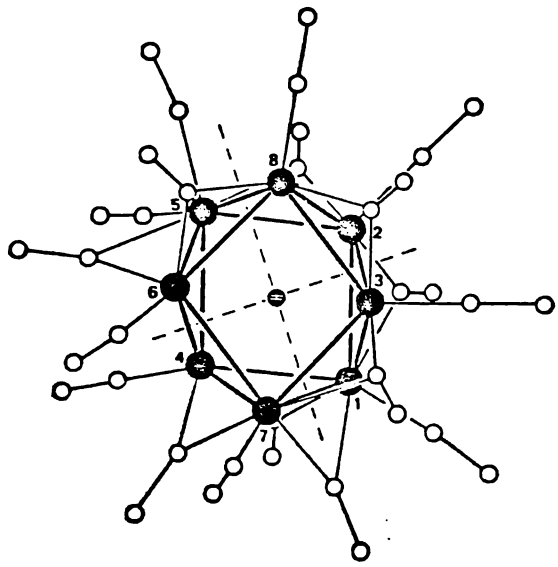

(A) $[Co_8(CO)_{18}C]^{2-}$ Ref. 69

encapsulated phosphorus cluster (74) (See section 1.3.4 have been reported, no cluster encapsulated Si,Ge,Sn or Pb have yet been reported. As van der Waal radii (69) preclude them from enclosure by a hexacobalt cluster, any group IVB compound of this type found in future structures must necessarily be of high-nuclearity.

1.3.3 GROUP III CLUSTERS.

Few compounds of this group are known, however boron (75) and aluminium (76) both form tricobalt clusters of the methylidyne type. In the reaction of the Group III trihalides with $Co_2(CO)_8$ (77) two classes of compounds are formed. Both boron and aluminium form adducts of the type indicated in the equation:

$$MX_3 + Co_2(CO)_8 \longrightarrow Co_2(CO)_8.MX_3$$

(M=B, X=Cl, Br,I; M=Al, X=Cl, Br)

Gallium and indium tribromide however both form compounds of composition $Ga(In)Co_2Br_4(CO)_6$.

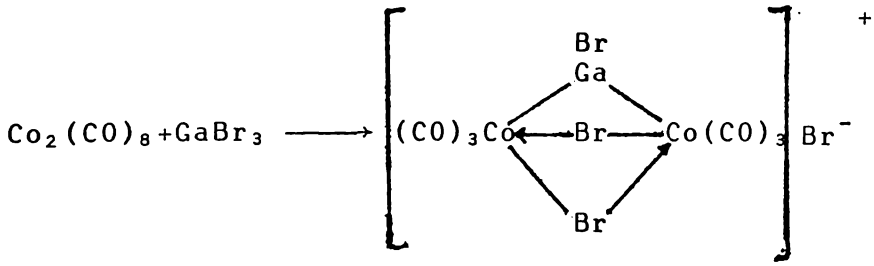

The reaction of BBr_3 with $Co_2(CO)_8$ (75) at 60°C, however yielded a compound of formula $Co_6(CO)_{18}B$, which was assigned a structure of the type $Ru_6(CO)_{17}C$.

1.3.4. GROUP V CLUSTERS

Because of the large number of transition metal nitrosyls and phosphines known (78), only compounds

where the group V atom is involved in the cluster, will be considered here. The group V atoms are isoelectronic with a $-Co(CO)_3$ group and their ability to replace a $Co(CO)_3$ group in a cluster is a feature of the chemistry of these compounds. This is best illustrated by the sequence of successive replacement of the $Co(CO)_3$ groups by arsenic in $Co_4(CO)_{12}$.

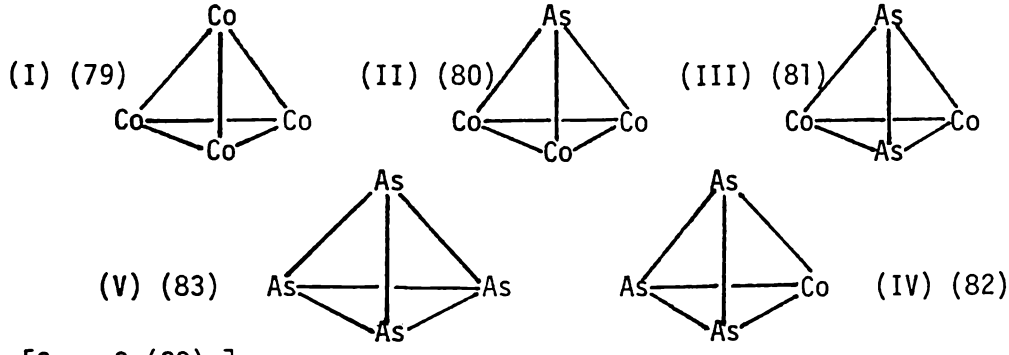

[Co = $Co(CO)_3$]

The above series is also known for phosphorus (ref.84,85). Compound II for P is however unstable (84), but is stabilised by the bonding of the P to a $Fe(CO)_4$ group or S atom (85)

Both P and As compounds of type II also form cyclic trimers of formula $M_3Co_9(CO)_{24}$ (80).

Other types of tetrahedral clusters are known. Seyferth has replaced a $-Co(CO)_3$ group in some methylidyne clusters with P (86) or As (87) (See Fig.1.5A), while Vahrenkamp has replaced a $Co(CO)_3$ group in a phosphide cluster (88,89) with other metal carbonyl moieties (Fig.1.5B) (Note the bridging Me_2As group)

One of the more interesting features of group V - cobalt carbonyls are the larger clusters. Vahrenkamp (90) has synthesized a pentacobalt cluster with three bridging phosphine groups (Fig.1.5C), from the reaction of η^3-$C_3H_5Co(CO)_3$ with $(CO)_3Ni$-PMe_2H. The reduction

FIGURE 1.5 SOME GROUP V-COBALT CARBONYL CLUSTERS (1)

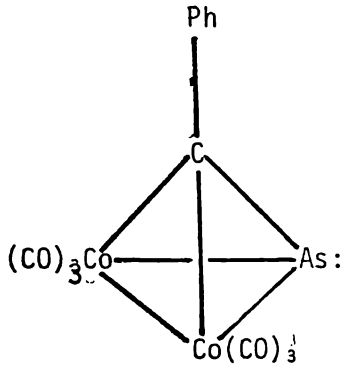

(A) $RC[Co_2(CO)_6]As$

Ref. 86

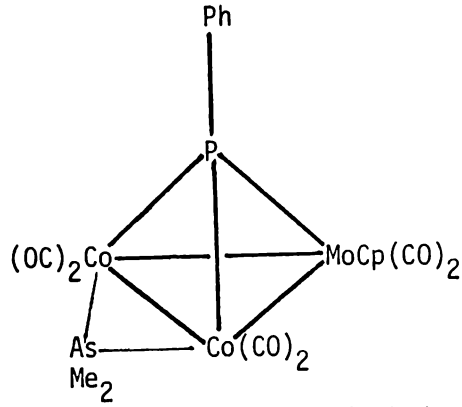

(B) $PhP[Co(CO)_2]_2MoCp(CO)_2(\mu\text{-}AsMe_2)$

Ref. 88

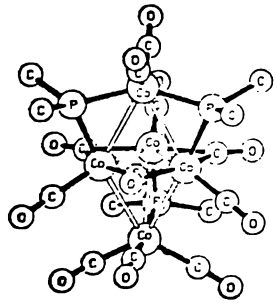

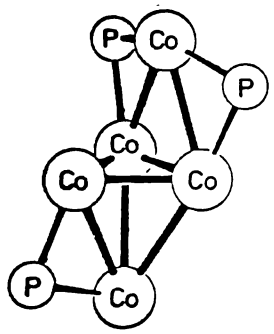

(C) $(Me_2P)_3Co_5(CO)_{11}$ Ref. 90

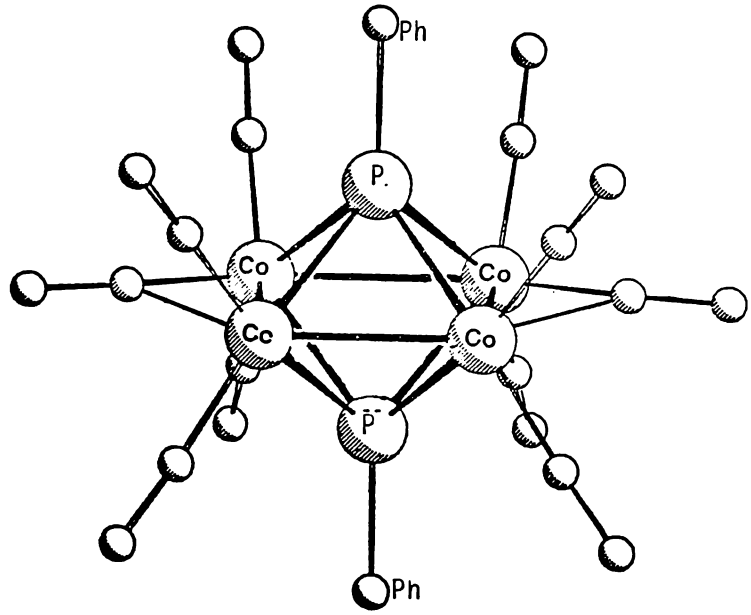

(D) $(PhP)_2Co_4(CO)_8(\mu\text{-}CO)_2$ Ref. 91

of $Co_2(CO)_8$ in toluene with ϕPCl_2 yields the novel tetracobalt diphosphorus cluster (91) (Fig.1.5D), where two P atoms cap a square planar array of four Co atoms to give a pseudo-octahedron. The reaction of $\{Fe(CO)_3PPhH\}_2$ with $Co_2(CO)_8$ yields a compound, isoelectronic and nearly isostructural with the diphosphorus tetracobalt cluster (92).

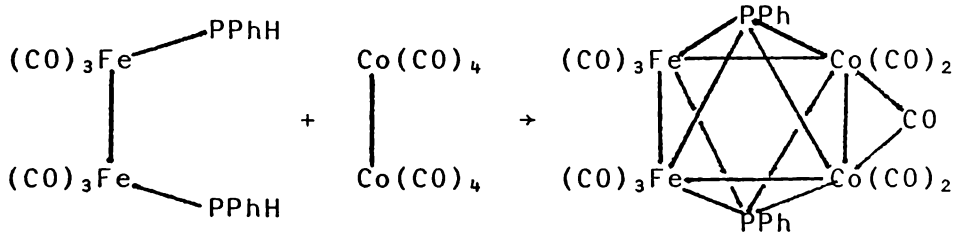

Other clusters known include; the hexacobalt cluster fully encapsulating a nitrogen atom (73)(Fig.1.6A) and "semi-interstitial phosphide" group bridging 6 cobalt atoms (74) (Fig.1.6B) mentioned previously, and an antimony cluster with a cubane-type structure (93) (Fig.1.6C).

1.3.5. GROUP VI - COBALT CARBONYL CLUSTERS

Most of the work on these compounds has been carried out using sulphur as the group VI atom. Many of the structures, especially those of the tetrahedral clusters, parallel those of phosphorus. Thus S (94) and Se (95) analogues of the methylidyne clusters are known, as well as clusters involving replacement of a $-Co(CO)_3$ group with another metal carbonyl moiety. The types of clusters and examples are summarised in Table 1.6.

There are a few examples of different structural types. These include a sulphur atom triply bridging a tetrahedral cluster of transition metal atoms (97),(Fig.1.7a)

FIGURE 1.6 SOME GROUP V-COBALT CARBONYL CLUSTERS (2)

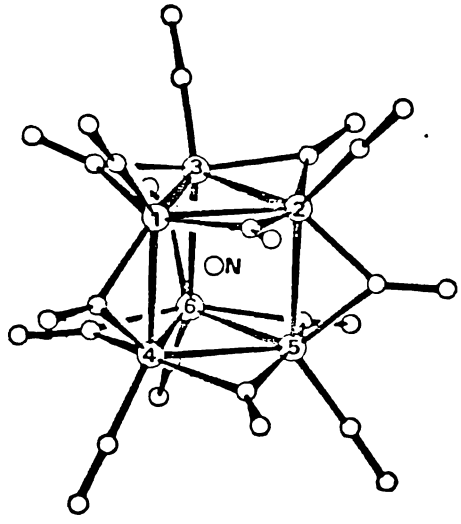

(A) $[Co_6N(\mu\text{-}CO)_9(CO)_6]^-$

Ref. 73

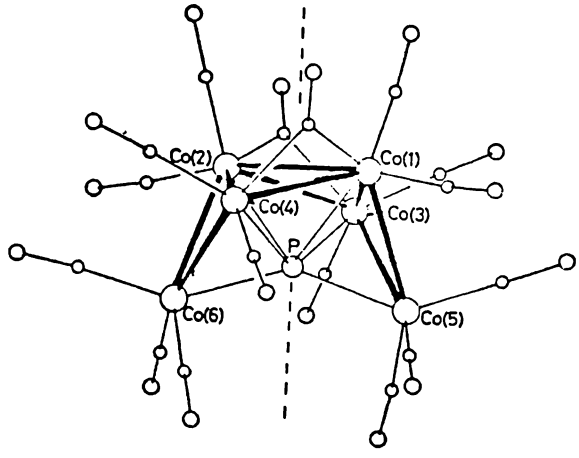

(B) $[Co_6(CO)_{14}(\mu\text{-}CO)_2P]^-$

Ref. 74

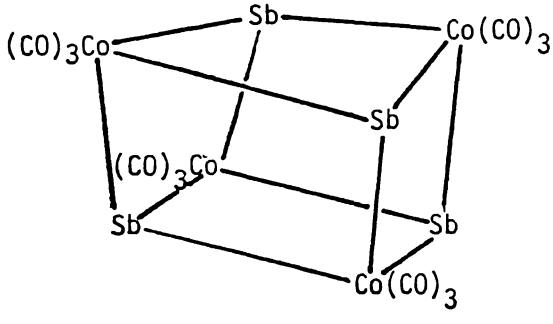

(C) $Co_4(CO)_{12}Sb_4$

Ref. 93

TABLE 1.6 Group VI-Cobalt Carbonyl Clusters

Tetrahedral Clusters	Reference
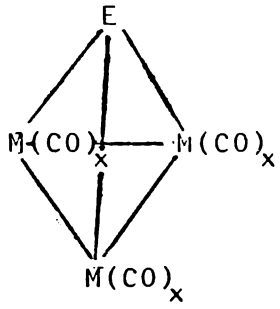	
$\{Co(CO)_3\}_3S$	94
$\{Co(CO)_3\}_3Se$	95
$\{Co(CO)_3\}_2Fe(CO)_3Se$	95
$\{Co(CO)_3\}_2Fe(CO)_3Te$	95
$\{Co(CO)_3\}_2Fe(CO)_3S$	96a
$\{Co(CO)_3\}\{Fe(CO)_3\}\{M(CO)_2Cp\}S$(M=Cr,Mo,W)	96,98
Trigonal Bipyramidal	
$FeCo_2MoS(AsMe_2)Cp(CO)_8$	97
$FeCoMoWS(AsMe_2)Cp_2(CO)_7$	
Octahedral	
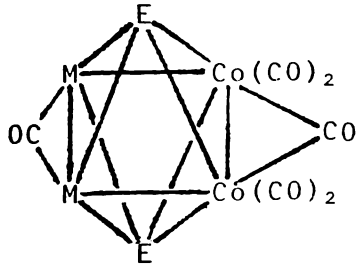	
M=$Co(CO)_2$, E=S,Te	91
M=$Fe(CO)_3$, E=S (no μ-CO between Fe-Fe)	92
Others	
$Co_3(CO)_4(SR_2)_5$ R=Et	99
(See Fig.1.7B) R=Ph	100
$(CO)_9Co_3SSCCo_3(CO)_9$	71
$Co_6C(CO)_{12}S_2$ (See Fig.1.7C)	71

in $FeCo_2MoS(AsMe_2)Cp(CO)_8$ and $FeCoMoWS(AsMe)_2Cp_2(CO)_7$. Also known are two compounds (99,100) in which a triangle of Co atoms is edge bridged by 5 organosulphur groups (Fig.1.7B).

From the reaction of CS_2 with $Co_2(CO)_8$, Bor et al.(71) have isolated the novel S clusters shown in Fig.1.7(c+d). Although $(CO)_9Co_3SSCCo_3(CO)_9$ is strictly a carbido cluster it is interesting in that a S-S bond links two methylidyne clusters. $Co_6C(CO)_{12}S_2$ has two S atoms each triply bridging a carbido-cluster.

1.4. SYNTHESES OF GROUP IVB-COBALT CARBONYLS

Two distinct types of syntheses of Group IVB-cobalt carbonyl compounds are known; those involving major changes in reactants (e.g. increase in number of metal atoms) and those involving relatively minor change(s) in the reactant(s) (e.g. increase in metal-metal bonding or substitution of a metal carbonyl moiety for another). The syntheses are summarised in Table 1.7.

Of the first type, the most widely used to date is the reaction of a Group IVB metal halide with $Co(CO)_4^-$. This reaction gives stepwise $-Co(CO)_4$ substitution on the Group IVB atom (27). The main limitation of this method is the range of starting halides generally being limited to one Group IVB atom per molecule. Halides with greater than one GroupIVB atom are generally too inaccessible or unstable to handle (28).

Potentially the most versatile of the syntheses for Si and Ge is the reaction of a hydride with $Co_2(CO)_8$. Si and Ge hydrides are known with chain lengths up to

FIGURE 1.7 SOME GROUP VI-COBALT CARBONYL CLUSTERS

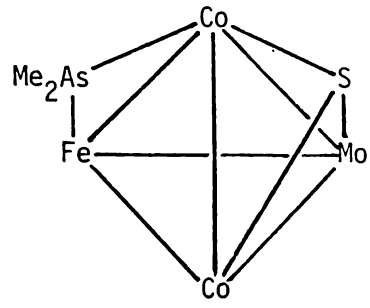

(A) $FeCo_2MoS(AsMe_2)Cp(CO)_8$

Ref. 97

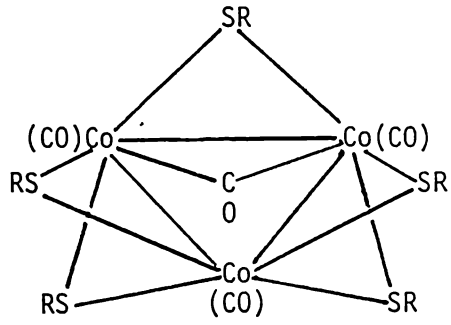

(B) $Co_3(CO)_4(SR)_5$

Ref. 100

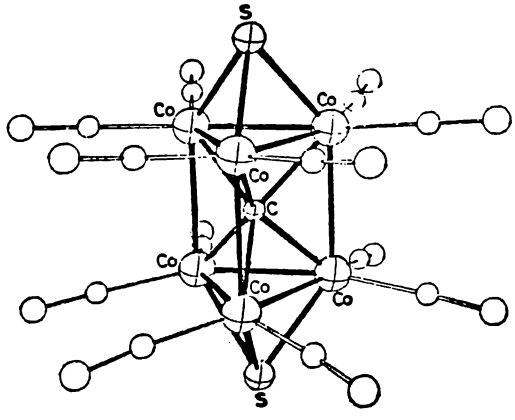

(C) $Co_6C(CO)_{12}S_2$ Ref. 71

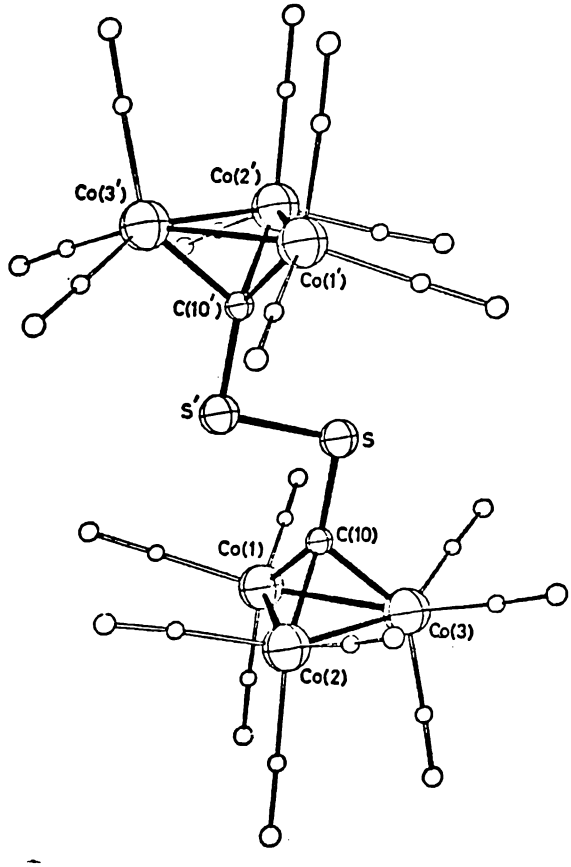

(D) $[(CO)_9Co_3CS]_2$ Ref. 71

TABLE 1.7 SYNTHESES OF GROUP IVB - COBALT CARBONYLS

A) Reactions involving major changes in reactants.

(i) Reaction of Group IVB metal halide with $Co(CO)_4^-$

e.g. $RGeCl_3+3NaCo(CO)_4 \longrightarrow RGeCl_{3-x}\{Co(CO)_4\}_x$

-M^1 halides generally limited to one Group IVB atom per molecule.

(ii) Reaction of group IVB halide with $Co_2(CO)_8$

(a) Reaction of metal (IV) Halide

e.g: $R_2SnCl_2+2Co_2(CO)_8 \longrightarrow R_2Sn\{Co(CO)_4\}_2+2ClCo(CO)_4$

- limited to reaction of diorganotin dihalides
- limited number of products.

(b) Reaction of M(II) Halide.

e.g: $GeI_2+Co_2(CO)_8 \longrightarrow I_2Ge\{Co(CO)_4\}_2$

- limited to atoms that form M(II) halides (ie:Ge,Sn,Pb)
- Limited number of products.

(iii) Reaction of Activated Group IVB Metal with $Co_2(CO)_8$

e.g: $Pb_{(act)}+2Co_2(CO)_8 \longrightarrow Pb\{Co(CO)_4\}_4$

- limited to tetracobalt products.

(iv) Reaction of Group IVB Hydride with $Co_2(CO)_8$

e.g: $MeGeH_3+3/2Co_2(CO)_8 \longrightarrow MeGeCo_3(CO)_{11}+Co+1\frac{1}{2}H_2$

- limited by formation of stable hydrides.

(v) Reaction of $Co(CO)_4^-$ with Group IVB -Cobalt Carbonyls

e.g: $Co(CO)_4^-+GeCo_4(CO)_{14} \longrightarrow GeCo_5(CO)_{16}^- +2CO$

- lack of specific control in reaction
- reaction influenced by impurities.

B) Reactions which involve limited Interconversion of species.

(i) Loss or Addition of CO from a Group IVB -Cobalt Carbonyl

TABLE 1.7 (Continued)

e.g: $Ph_2Ge\{Co(CO)_4\}_2 \xrightarrow{h\nu} Ph_2GeCo_2(CO)_7 + CO$

- product formed must be sufficiently stable.

(ii) Replacement of Metal Carbonyl Moiety by Another

e.g: $Co(CO)_4\text{-}GeCo_3(CO)_9 + Mn(CO)_5^- \longrightarrow Mn(CO)_5\text{-}GeCo_3(CO)_9 + Co(CO)_4^-$

- replacement follows series, $Mn(CO)_5^-$ replaces $Fe(CO)_4^{2-}$

replaces $Co(CO)_4^-$

10 metal atoms (101), and in addition, a range of substituents which limit reaction with $Co_2(CO)_8$ are known (102). This method is however, more limited for Sn and Pb. The only Sn hydrides sufficiently stable at room temperature are generally those containing one tin atom (103), whereas Pb hydrides are generally too unstable to use synthetically (101), unless highly organo-substituted.

In addition to these compounds, a range of mixed Group IVB metal hydrides are also known with chain lengths ranging up to 7 metal atoms (101).

So far the reactions of group IVB hydrides with cobalt carbonyls have been limited to the simple cases and only one reaction of a catenated group IVB hydride has so far been reported (See Table 1.8). Of note in these reactions are the differences in behaviour of Si and Ge, and the contradictions between different reports of the same reaction. Thus while Chalk and Harrod (12,13) obtained only $Ph_2HSiCo(CO)_4$ from their original reaction of Ph_2SiH_2 with $Co_2(CO)_8$, Graham (44) and

$$Ph_2SiH_2 + Co_2(CO)_8 \longrightarrow Ph_2HSiCo(CO)_4 + HCo(CO)_4$$

Fieldhouse (107) have since isolated $Ph_2SiCo_2(CO)_7$ and $Co(CO)_4CoPh_2SiOCCo_3(CO)_9$ respectively from the system.

Brooks and Graham (105) reported the reaction of Me_2GeH_2 with $Co_2(CO)_8$ yielded $MeGeCo_3(CO)_{11}$ as a product. However Cotton (53,55) and Gerlach (27) have found the only products resulting from the reaction are $\{Me_2Ge\}_2Co_2(CO)_6$ and $Me_2GeCo_2(CO)_7$. It is possible that the sample of Me_2GeH_2 Graham used was contaminated with $MeGeH_3$, as Ge-C bond cleavage is unlikely. No mention

TABLE 1.8. Reactions of M^1-Hydrides with $Co_2(CO)_8$(a) or $HCo(CO)_4$(b)

Hydride	Reaction Type	Product(s)	Reference
Cl_3SiH	(a)	$Cl_3SiCo(CO)_4$	12,13
$PhCl_2SiH$	(a)	$PhCl_2SiCo(CO)_4$	
Et_3SiH	(a)	$Et_3SiCo(CO)_4$	
Ph_3SiH	(a)	$Ph_3SiCo(CO)_4$	
Ph_2SiH_2	(a)	$Ph_2SiHCo(CO)_4$	
F_3SiH	(a)	$F_3SiCo(CO)_4$	11,15,104
Cl_3SiH	(b)	$Cl_3SiCo(CO)_4$	
Me_3SiH	(a) and (b)	$Me_3SiCo(CO)_4$	
$MeSiH_3$	(b)	$MeSiH_2Co(CO)_4$	
SiH_4	(b)	No reaction	
Ph_2SiH_2	(a)	$Ph_2SiCo_2(CO)_7$	44
$PhSiH_3$	(a)	$PhSiCo_3(CO)_{11}$	
R_2SiH_2(R =Ph or Et)	(a)	$(CO)_4Co\text{-}SiR_2\text{-}OCCo_3(CO)_9$	107
Me_3SiH	(a)	$Me_3SiCo(CO)_4$	20
$Me_2SiH\text{-}SiHMe_2$	(a)	$(Me_2Si)_2Co_2(CO)_6$	18
		$Me_2SiH\text{-}SiMe_2Co(CO)_4$	
		$Me_2SiCo(CO)_4\text{-}Me_2SiCo(CO)_4$*	
		$Me_2SiCo_2(CO)_7$*	
		$(OC)_4Co(SiMe_2)_yOCCo_3(CO)_9$* y=1or2	
		$Co_4(CO)_{12-x}(SiMe_2)_x$ **	
SiH_4	(a)	$SiCo_4(CO)_{14}$	56

TABLE 1.8. (Continued)

Hydride	Reaction Type	Product(s)	Reference
$PhGeH_3$	(a)	$PhGeCo_3(CO)_{11}$	44
Me_2GeH_2	(a)	$MeGeCo_3(CO)_{11}$ ***	105
Me_2GeH_2	(a)	$\{Me_2Ge\}_2Co_2(CO)_6$	53,55
R_3GeH (R=Me,Et)	(a)	$R_3GeCo(CO)_4$	20
$MeGeH_3$	(a)	$MeGeCo_3(CO)_{11}$	50
Me_2GeH_2		$\{Me_2Ge\}_2Co_2(CO)_6$	27,57
		$Me_2GeCo_2(CO)_7$	
GeH_4		$GeCo_4(CO)_{14}$	
$Me_2GeHCo(CO)_4$		$Me_2Ge\{Co(CO)_4\}_2$	
$Me_2GeHCo(CO)_4$	(b)	No Reaction	
$H_2MeGeMn(CO)_5$		$MeGe\{Mn(CO)_5\}\{Co_2(CO)_7\}$	51
$H_3GeMn(CO)_5$		$Mn(CO)_5GeCo_3(CO)_9$	
Me_3SnH		$Me_3Sn\text{-}Co(CO)_4$	20
Me_2SnH_2		$\{Me_2Sn\}_2Co_2(CO)_6$	55
Me_6Sn_2		$Me_3SnCo(CO)_4$†	106
		Me_4Sn and $Me_2Sn\{Co(CO)_4\}_2$#	

* Tentative assignment based on IR and NMR
** Speculative assignment
*** Report not confirmed in later paper
† Reaction in diethylether
# Reaction in T.H.F.

of this product was made in a later report (44).

A feature of the reactions of silanes with $Co_2(CO)_8$ appears to be incomplete reaction, with products isolable at a partially substituted stage (See Table 1.8). So far, no one has isolated partially substituted germanes from reaction with $Co_2(CO)_8$ although they have been observed (24).

The mechanism of the general reaction appears to be in dispute. Chalk and Harrod (13) proposed the following reaction scheme for the silane reactions.

$$R_3SiH + Co_2(CO)_8 \longrightarrow R_3SiCo(CO)_4 + HCo(CO)_4 \quad (1)$$

$$HCo(CO)_4 + R_3SiH \longrightarrow R_3SiCo(CO)_4 + H_2 \quad (2)$$

$$2HCo(CO)_4 \longrightarrow Co_2(CO)_8 + H_2 \quad (3)$$

Reaction (3) takes place readily at room temperature (108) and must therefore compete with reaction (2) for the consumption of the $HCo(CO)_4$, formed from (1). This proposal was confirmed by MacDiarmid (15,104) who reacted $MeSiH_3$ and Cl_3SiH directly with $HCo(CO)_4$.

Gerlach (27) has however questioned whether reaction (2) takes place. He found that $Me_2GeHCo(CO)_4$ and $HCo(CO)_4$ did not react together between -20^0C and 0^0C, and concluded that only reactions (1) and (3) in the above scheme occurred. MacDiarmid's (15,104) observation of reaction with $HCo(CO)_4$ could therefore be due to the reaction being carried out at room temperature with $HCo(CO)_4$ decomposing (reaction 3) before reaction with the hydride.

Mention should also be made of the reactions of $Co(CO)_4^-$ with a germanium cobalt carbonyl as a synthetic possibility. This has been explored by Nicholson and

co-workers, with several interesting products being isolated and characterised. Thus $\{GeCo_5(CO)_{16}\}^-$ (See Fig.1.3(a)) has resulted from the reaction;

$$GeCo_4(CO)_{14} + Co(CO)_4^- \longrightarrow GeCo_5(CO)_{16}^- + 2CO$$

Reaction of this anion with $Co_2(CO)_8$ (66) has yielded further clusters, $\{Ge_2Co_7(CO)_{21}\}^-$ and $\{GeCo_7(CO)_{20}\}^-$, (see Figs 1.3. b+c). The following reaction scheme for the formation of these clusters has been proposed.

$$\{GeCo_5(CO)_{16}\}^- \longrightarrow \{GeCo_3(CO)_9\}^- + Co_4(CO)_{12} + Co(CO)_4^-$$

$$\{GeCo_3(CO)_9\}^- + \{(CO)_4CoGeCo_3(CO)_9\} \longrightarrow \{Ge_2Co_7(CO)_{21}\}^-$$

$$\{GeCo_3(CO)_9\}^- + Co_4(CO)_{12} \longrightarrow \{GeCo_7(CO)_{20}\}^-$$

CHAPTER 2. EXPERIMENTAL TECHNIQUES.

2.1. GENERAL

As most of the compounds used or prepared in this work were either sensitive to hydrolysis and/or air oxidation, contact with air was avoided as far as possible. Thus volatile air-sensitive compounds were manipulated in a standard vacuum line and involatile compounds were handled and stored in nitrogen-flushed, glassware or gloveboxes. The higher molecular weight compounds prepared in this work were considerably less air-sensitive than the related lower molecular weight compounds and could be handled for relatively long periods in air with little appreciable decomposition.

All non-airsensitive compounds (solvents etc.) were handled according to their volatility and the reaction or conditions in which they were used. Incondensable gases were manipulated and measured on a Toepler pump fitted with a gas burette.

All glassware was rigorously acid-washed and thoroughly rinsed and dried before use, because of the risk of decomposition of compounds through exposure to alkaline impurities on the glass, (24).

2.2. SPECTROSCOPIC TECHNIQUES.

2.2.1 INFRARED SPECTROSCOPY

A Perkin-Elmer 180 was used to record general carbonyl spectra and also more definitive spectra. The wavenumber readout was calibrated with HCl/DCl for the νCO and νGe-H

region ($\simeq$ 2200 - 1800cm^{-1}) and found to be accurate within $\pm$0.2cm^{-1}.

Lower resolution spectra were recorded on either a Shimadzu I.R. 20A or a Perkin-Elmer 735B.

For involatile samples, spectra were recorded generally as hexane or dichloromethane solutions, in standard 0.1mm solution cells,with hexane being preferred where solubility permitted, due to the better resolved spectra it gave. For some less soluble samples which required dichloromethane as a solvent to obtain sufficiently concentrated solution, it was found thataddition of hexane to the solution significantly increased the resolution of the spectra without precipitating any solid.

More volatile samples could be recorded as a vapour in a 10cm or 20cm path length gas cell (depending on absorbance).

Both solution and gas cells were fitted with KBr windows which absorbed light below 400cm^{-1}.

2.2.2 NUCLEAR MAGNETIC RESONANCE.

Most spectra were recorded on a 60MHz J.E.O.L. C60HL high resolution NMR spectrometer, in evacuated tubes of 5mm o.d.. However in the latter half of this work a J.E.O.L. 90 MHz Multinuclear Fourier Transform spectrometer became available and was used to record the spectra of very dilute samples.

Spectra were recorded as either neat [illegible] or $SiCl_4$ or C_6H_6 solutions. For the first two cases, the

addition of 5 - 10% TMS was generally used for reference.

2.2.3 MASS SPECTROMETRY

Mass spectra were recorded by Mr. A. Brennan at Ruakura Agricultural Research Centre on a Varian CH5 mass spectrometer (range 30 - 1200 mass units). Volatile samples were introduced as gases through the reservoir, and solid samples through the probe, at the lowest possible temperature required to vaporise enough sample to obtain a spectrum.

Spectra were computer calibrated using polyfluoro-kerosine as a reference. Although this was reasonably accurate for low m/e values, higher mass values were sometimes found to differ by 1 or 2 mass units from known real values. Above m/e = 1000, spectra could not be computer calibrated and these were calibrated by comparison with a calibrated spectrum (below m/e = 1000) and the counting of CO units above m/e = 1000.

The analyses of mass spectra were considerably simplified by the recognition of the characteristic patterns of ions containing, 1 or 2 Ge atoms or a Sn atom. (See Fig. 2.1)

2.3. X-RAY CRYSTALLOGRAPHY

Crystals suitable for study, were grown from either CH_2Cl_2/C_6H_{14} solutions left to stand at 4^0C or -16^0C for several weeks, or hot CH_2Cl_2 solutions allowed to cool slowly to room temperature, and then to 4^0C (where stability permitted). Crystals were mounted with Araldite in either

FIGURE 2.1 MASS SPECTRAL INTENSITY PATTERNS

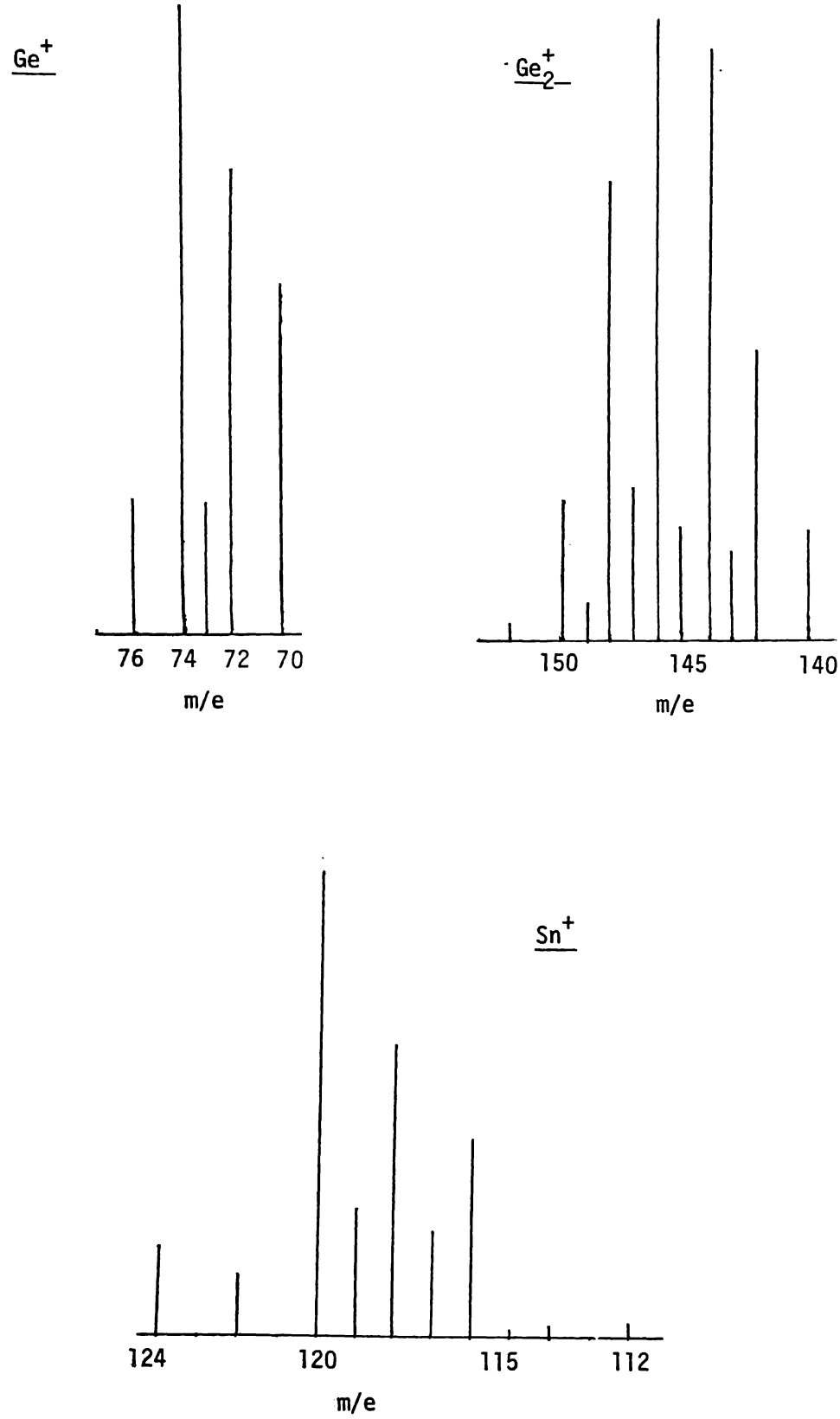

0.3mm or 0.5mm internal diameter glass capillaries.

The crystal quality and space group assignments were determined using Precession photography with a Cu-K_α x-ray source, which was Ni-filtered for zero and upper level photographs.

Data and accurate lattice parameters were obtained using the Enraf-Nonius CAD4 diffractometers of the Universities of Auckland and Adelaide, with graphite-monochromated Mo-K_α x-radiation (0.7107Å). Data were corrected for Lorentz and polarisation effects and for linear absorption.

Densities of the crystals were not determined experimentally but a rough density of ≈2g/ml based on related compounds (27) was used for calculation of the number of molecules in the unit cell.

Programs used for solution, refinement, calculation of dihedral angles and plotting are outlined in Appendix I.

2.4. STARTING MATERIALS.

2.4.1. SOLVENTS.

The organic solvents used in this work; hexane, benzene, dichloromethane, THF, diethyl ether and di-n-butyl ether were all dried over sodium wire before use. Deuterated solvents (C_6D_6, $CDCl_3$ and CD_2Cl_2) were all used straight from the bottle.

Liquid ammonia was dried over sodium two or three times before use.

2.4.2. GERMANIUM AND SILICON HALIDES

$MeGeCl_3$ was supplied by the Laramie Chemical Co. and

was found to be nearly 100% pure (byNMR spectroscopy), the contaminant being a trace of Me_2GeCl_2 which was removed by vacuum distillation. Me_2GeCl_2 and Me_3GeCl were both supplied by Alfa Chemicals. While the Me_3GeCl was found to be 100% pure, the Me_2GeCl_2 was contaminated with ca. 10% $MeGeCl_3$ which was removed on the vacuum line.

Me_2SiCl_2, Me_3SiCl and $SiCl_4$ were all supplied by Alfa Chemical Co. These were distilled away from siloxanes, and any contaminating HCl removed before use.

2.4.3. TIN HALIDES

Methyl tin halides were made by the scrambling reaction of $SnCl_4$ (supplied by B.D.H.) and Me_4Sn according to the method of Grant and Van Wazer (110). Typically Me_4Sn and $SnCl_4$ in a 1:1.3 molar ratio were refluxed at 150°C for 2-3 hours. The resultant solid mixture was distilled in micro distillation equipment fitted with an air condenser, to give modest yields of $MeSnCl_3$, Me_2SnCl_2 and Me_3SnCl (characterised by melting points (111) and subsequent conversions to the appropriate hydrides).

2.4.4. GROUP IVB HYDRIDES.

(i) GeH_4, Ge_2H_6 and Ge_3H_8 were prepared by the borohydride reduction of aqueous germanate (IV) ion (112).

$$Ge(IV)_{aq} \xrightarrow[H^+]{BH_4^-} GeH_4 + Ge_2H_6 + Ge_3H_8 + \ldots\ldots$$

(ii) $MeGeH_3$, Me_2GeH_2, Me_3GeH, Me_2SiH_2, Me_2SnH_2, $MeSnH_3$ and SnH_4 were all prepared by the lithium aluminium hydride reduction of the appropriate Group IVB halide.

$$\text{e.g. } Me_2SnCl_2 \xrightarrow[(n\text{-}Bu)_2O]{LiAlH} Me_2SnH_2.$$

Of note here is the difficulty experienced in preparing SnH_4. This preparation had to be carried out at low temperature (-63.5°C) and allowed to warm to room temperature slowly. $LiAlH_4$ had to be purified by Soxhlet extraction before use.

(iii) Me_3SiGeH_3, Me_3GeGeH_3 and $Me_2Si\{GeH_3\}_2$ were prepared in good yield by the coupling reaction of a Group IVB halide with GeH_3Na in the absence of a solvent (113).

e.g. $Me_2SiCl_2 + 2GeH_3Na \longrightarrow (GeH_3)_2SiMe_2 + 2NaCl$

GeH_3Na was prepared by the low temperature reaction of GeH_4 with Na in liquid ammonia (113).

$GeH_4 + Na \xrightarrow[-63.5^0C]{NH_3} GeH_3Na + \frac{1}{2}H_2$.

2.4.5. CARBON MONOXIDE

CO was prepared by the addition of 80% formic acid to concentrated sulphuric acid (114). The CO produced was slowly passed through two traps immersed in liquid nitrogen to remove, CO_2, H_2O or volatile acid(s), before use.

2.4.6. METAL CARBONYLS.

(i) $Co_2(CO)_8$

This was supplied by Pressure Chemical Co. and stored under a nitrogen atmosphere at -16°C. It was found to be pure enough for most uses but where purity was critical, it was sublimed under vacuum before use.

(ii) $Mn_2(CO)_{10}$

This was also supplied by Pressure Chemical Co. and stored under nitrogen at 4°C. It was used straight from the bottle.

2.4.7. PREPARATION OF $Co(CO)_4^- Na^+$ and $Mn(CO)_5^- Na^+$.

These were prepared by the reduction of the appropriate metal carbonyl dimer by a 1% sodium amalgam in diethyl ether or THF. When the colour of the parent dimer was discharged, the solution was allowed to settle and then decanted away from the remaining mercury/amalgam, ready to use for reaction.

2.5. GENERAL REACTION OF A GROUP IVB HYDRIDE WITH A COBALT CARBONYL.

The method used for this type of reaction was essentially the same throughout this work:

The hydride (weighed under vacuum) was condensed onto a frozen, thoroughly degassed, saturated hexane solution (usually 5-10ml) of the appropriate cobalt carbonyl. ($Co_2(CO)_8$, $GeCo_4(CO)_{14}$ etc) inside a glass tube of ca.50ml volume and of sufficient thickness to withstand medium gas pressures, attached to a vacuum line. The tube was then sealed and wrapped in aluminium foil to prevent exposure to light, and the mixture allowed to react for a period at room temperature.

The tube was opened by the use of a flexible rubber sleeve fitted with a tap adaptor with which the top part of the glass tube could be broken without leakage of any gases.

Reaction mixtures were worked up by the removal of incondensable and volatile gases. The condensable, volatile gases were stored on the vacuum line and the most volatile, least volatile and middle, fractions examined by infrared spectroscopy.

The involatile products remaining in the reaction tube were immersed in a nitrogen atmosphere and extracted with hexane and/or dichloromethane depending upon their solubility.

If the reaction was to be sampled periodically, then a 250ml glass flask fitted with a Kontes greaseless tap was used instead of the sealed tube. After a period of reaction, volatile gases were removed and the condensable fraction of this was stored on the vacuum line as above. An infrared spectrum of the non-volatile products in solution was run and the volatile components returned and the reaction mixture resealed.

The Kontes greaseless tap was found to keep a good vacuum for periods of up to 3 months.

2.6. DETERMINATION OF H_2/CO

The amounts of H_2 and CO present in a mixture of the two were determined by an average molecular weight method. Firstly the total amount of gas was measured using a Toepler pump fitted with a gas burette. Then, a known pressure of gas was admitted into a bulb of known volume and weighed, from which an average molecular weight was determined. The total quantities of H_2 and CO could thus be determined by relating this back to the initial measurement of total gas volume.

CHAPTER 3. REACTIONS OF SOME METHYL-SUBSTITUTED GROUP IVB HYDRIDES WITH $Co_2(CO)_8$.

3.1. Reaction of Me_2GeH_2 With $Co_2(CO)_8$.

3.1.1. General.

It was of interest to thoroughly study the reaction of a Group IVB hydride with $Co_2(CO)_8$, to determine whether reaction conditions influenced the products obtained. The reaction of Me_2GeH_2 with $Co_2(CO)_8$ is an ideal system; the number of functional hydrogens on the Ge is two, therefore limiting the number of partially substituted hydrides possible, while still sufficient to completely replace a bridging CO group in $Co_2(CO)_8$ and enabling the Ge to bridge a Co-Co bond.

Further, three dimethylgermyldicobalt species are known; $Me_2Ge\{Co(CO)_4\}_2$(22), $Me_2GeCo_2(CO)_7$(38), and $(Me_2Ge)_2Co_2(CO)_6$(53), the latter two compounds previously being isolated from this reaction system (27).

As the three dimethylgermyldicobalt species generally could not be separated from each other (except for $(Me_2Ge)_2Co_2(CO)_6$), absolute yields were not obtained. Instead, relative yields from reaction to reaction were determined by comparison of the infrared spectra of products of each reaction. Each of the three compounds has one sharp band, fairly free of absorptions of the other species. Thus the relative intensities of the 2088 cm^{-1} band of $Me_2Ge\{Co(CO)_4\}_2$, the 2081 cm^{-1} band of $Me_2GeCo_2(CO)_7$ and the 2066 cm^{-1} band of $(Me_2Ge)_2Co_2(CO)_6$ were used to determine relative yields (from reaction to reaction)of the three species . The infrared spectra of the three species are listed in Tables 3.1 (a), (b), (c) and shown in Figs. 3.1 (a), (b), (c).

TABLE 3.1 INFRARED SPECTRA OF DIMETHYLGERMYLDICOBALT SPECIES

(A) $Me_2Ge[Co(CO)_4]_2$	(B) $Me_2GeCo_2(CO)_7$	(C) $(Me_2Ge)_2Co_2(CO)_6$
2099 w	2088 s	2066 s
2081 vs	2048 vs	2048 vs
2027 vs	2026 vs	2028 vs
2006 vs	2008 vs	1990 vs
1996 m	1998 sh w	1981 m
	1965 sh vw	
	1841 m-s	

ALL HEXANE SOLUTIONS

FIGURE 3.1 INFRARED SPECTRA OF DIMETHYLGERMYLDICOBALT SPECIES

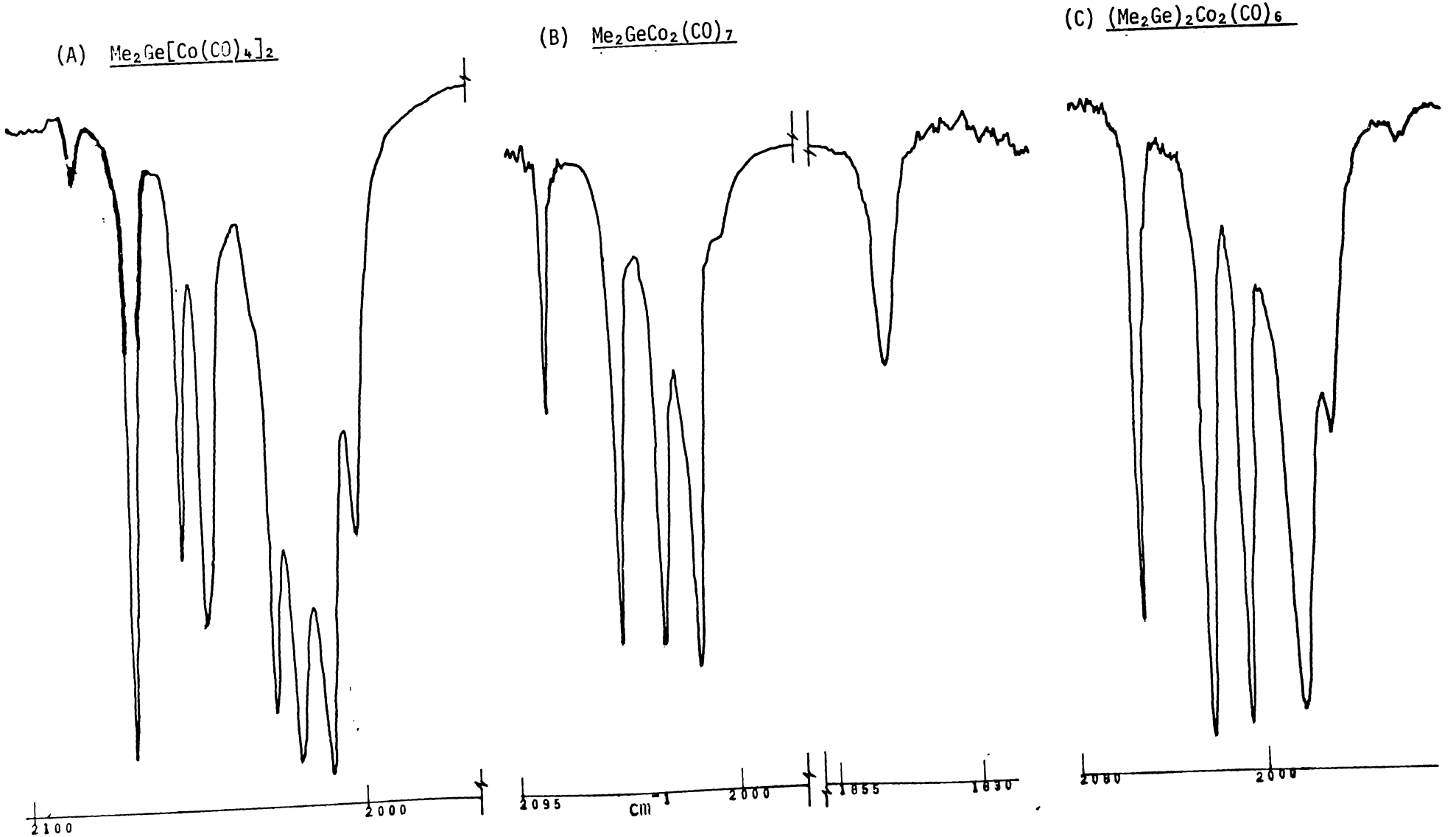

3.1.2. Experimental

Run 1:

Typically, Me_2GeH_2 (212mg, 2.03mmoles) and $Co_2(CO)_8$ (693mg, 2.03mmoles) were left to react for 7 days and worked up as described in section 2.5 . The yellow-brown, relatively involatile products were extracted with hexane and their infrared spectrum run (see Fig.3.2, Table 3.2). It is of use to note (for later comparison), that in this reaction the 2088 cm^{-1} band (of $Me_2Ge\{Co(CO)_4\}_2$ was slightly more intense than the 2081 cm^{-1} band (of $Me_2GeCo_2(CO)_7$). No bands due to $(Me_2Ge)_2Co_2(CO)_6$ could be detected.

From the volatile fraction, unreacted $Co_2(CO)_8$ (4mg, 0.01 mmoles) was recovered, while a small quantity of Me_2GeH_2 (observed in gas phase infrared spectrum) could not be separated from the bulk hexane.

In a further run of this reaction using similar conditions and reactant ratios, identical products and yields (except for $Co_4(CO)_{12}$), (from infrared spectra) were observed, (see Table 3.3)

Further runs were carried out to explore the following aspects of the reaction:

(i) the effect of exposure to sunlight on the reaction (run 3)

(ii) to measure the incondensable gases produced during reaction and observe the effect of adding or removing CO (runs 4,5,6)

(iii) the effect of using an excess of Me_2GeH_2 (run 7)

(iv) whether $Me_2GeCo_2(CO)_7$ or $Me_2Ge\{Co(CO)_4\}_2$ react directly with Me_2GeH_2 (run 8)

The details of these runs are tabulated in Table 3.3 while further points of interest that require more detail,

FIGURE 3.2 INFRARED SPECTRUM OF THE PRODUCTS FROM $Me_2GeH_2/Co_2(CO)_8$, Run 1.

TABLE 3.2 INFRARED SPECTRUM OF THE PRODUCTS FROM $Me_2GeH_2/Co_2(CO)_8$, Run 1.

2088	s	2027	vs	1966	sh w
2081	s-vs	2017	m	1866	m
2062	s	2008	vs	1841	s
2051	vs	1996	m		

Hexane Solution For Assignments See Table 3.1.

Table 3.3 The Reactions of Me_2GeH_2 With $Co_2(CO)_8$

Run	Me_2GeH_2 mmole (recovered)	$Co_2(CO)_8$ mmole	Time	Comments.
1	2.03 (*)	2.03	7 days	$Me_2Ge\{Co(CO)_4\}_2$, $Me_2GeCo_2(CO)_7$ main products. Trace $Co_4(CO)_{12}$ observed. See Fig. 3.2 and Table 3.2.
2	0.77 (*)	0.77 (*)	15 days	Same products and relative yields as for Run 1. See Fig. 3.2 and Table 3.2.
3	2.23 (*)	2.23 (*)	7 days	After 3 days, tube exposed to sunlight for remainder of reaction. Products and relative yields as for runs 1 and 2.
4	4.00 (*)	4.00 (*)		Incondensable gases removed and measured throughout reaction (See Table 3.5). Spectrum of final products showed much more $Me_2GeCo_2(CO)_7$ relative to $Me_2Ge\{Co(CO)_4\}_2$. See Fig. 3.3 and Table 3.4
5	3.80 (*)	3.80 (*)		Repeat of Run 4. Same products and relative yields. See Table 3.5 for incondensable production.
6	1.27 (*)	1.27 (*)	11 days	Ca.1Atm. pressure CO added at start of reaction. Product virtually pure $Me_2Ge\{Co(CO)_4\}_2$ (trace of $Me_2GeCo_2(CO)_7$).

(*) unreacted reagent, observed but not measured.

over/

Table 3.3 (Continued)

Run	Me_2GeH_2 mmole (recovered)	$Co_2(CO)_8$ mmole	Time	Comments
7	4.35	0.77	75 days	Excess Me_2GeH_2 added to $Co_2(CO)_8$ and reaction products sampled periodically (see 2.5). See Fig. 3.4. Small quantity of $Me_2GeHCo(CO)_4$ appeared late in reaction.
8		-	76 days	Me_2GeH_2 added to products from Run 2 and reaction sampled periodically. See Fig. 3.5. Small quantity of $Me_2GeHCo(CO)_4$ appeared late in reaction.

FIGURE 3.3 INFRARED SPECTRUM OF THE PRODUCTS FROM RUN 4.

TABLE 3.4 INFRARED SPECTRUM OF THE PRODUCTS FROM RUN 4.

2088 s-vs	2050 vs	1994 m
2081 m	2026 vs	1866 w
2062 m-s	2012 sh	1842 s-vs
2054 sh m	2007 vs	

Hexane Solution For Assignments See Table 3.1.

(as well as further experiments), are given below.

Runs 4, 5, 6.

Table 3.5. Measurement of Incondensable Gases Produced During Reaction of Me_2GeH_2 With $Co_2(CO)_8$.

Run 4.

Time	mmoles of H_2	mmoles of CO
1 hr	2.4	2.8
16 hrs	3.0	2.9
48 hrs	3.3	2.9
200 hrs	3.6	3.0

Run 5.

15 min	1.6	2.0
53 min	2.6	2.9
150 hrs	3.5	3.0
240 hrs	3.7	3.1

We may calculate the respective yields of $Me_2GeCo_2(CO)_7$ and $Me_2Ge\{Co(CO)_4\}_2$ based on the consumed Me_2GeH_2, from these results thus:

for run 4:

3.6mmoles of H_2 produced => 3.6mmoles of Me_2GeH_2 reacted

3.0mmoles CO produced = no. of mmoles of $Me_2GeCo_2(CO)_7$ produced (83% yield)

(ie assuming amount of CO evolved from $Co_4(CO)_{12}$ is negligible)

$\therefore$ no. of mmoles of $Me_2Ge\{Co(CO)_4\}_2$ = mmoles (Me_2GeH_2 reacted) - mmoles ($Me_2GeCo_2(CO)_7$)

= 3.6 - 3.0

= 0.6 (17% yield)

Thus 83% of the consumed Me_2GeH_2 ends up as $Me_2GeCo_2(CO)_7$

and 17% as $Me_2Ge\{Co(CO)_4\}_2$.

For run 5, calculation of the yields of $Me_2GeCo_2(CO)_7$ and $Me_2Ge\{Co(CO)_4\}_2$, based on the consumed Me_2GeH_2, using the above method gives, 83% and 17% respectively, in excellent agreement with run 4.

In addition to these experiments (runs 4,5,6), two further experiments were carried out. Firstly, a hexane solution of the products from run 1 (mixture of $Me_2GeCo_2(CO)_7$ and $Me_2Ge\{Co(CO)_4\}_2$) had any incondensable gases present, removed daily for 3 weeks. At the end of this period an infrared spectrum of the solution showed absorptions due only to $Me_2GeCo_2(CO)_7$ and $Co_4(CO)_{12}$ (weak).

Approximately $\frac{1}{2}$ Atmosphere pressure of CO was added to this solution. An infrared spectrum of the solution after four weeks showed the product was virtually pure $Me_2Ge\{Co(CO)_4\}_2$ with only traces of $Me_2GeCo_2(CO)_7$ and $Co_4(CO)_{12}$ present.

Run 7:

Sampling after four days showed the major product to be $Me_2GeCo_2(CO)_7$, along with small quantities of $(Me_2Ge)_2Co_2(CO)_6$, $Me_2Ge\{Co(CO)_4\}_2$ and $Co_4(CO)_{12}$. The second sample (8 days) showed a slight increase in concentration of $(Me_2Ge)_2Co_2(CO)_6$ relative to the two other dimethylgermyl-dicobalt species. After this, a further 290mg (2.77mmoles) of Me_2GeH_2 were added to the reaction mixture. Subsequent samples showed a slow increase in the concentration of $(Me_2Ge)_2Co_2(CO)_6$. Later samples also showed traces of $Me_2GeHCo(CO)_4$.

To check that the formation of $(Me_2Ge)_2Co_2(CO)_6$ was not due to condensation of either $Me_2GeCo_2(CO)_7$ or

FIGURE 3.4 RELATIVE INFRARED BAND INTENSITIES DURING REACTION OF EXCESS $Me_2GeH_2/Co_2(CO)_8$.

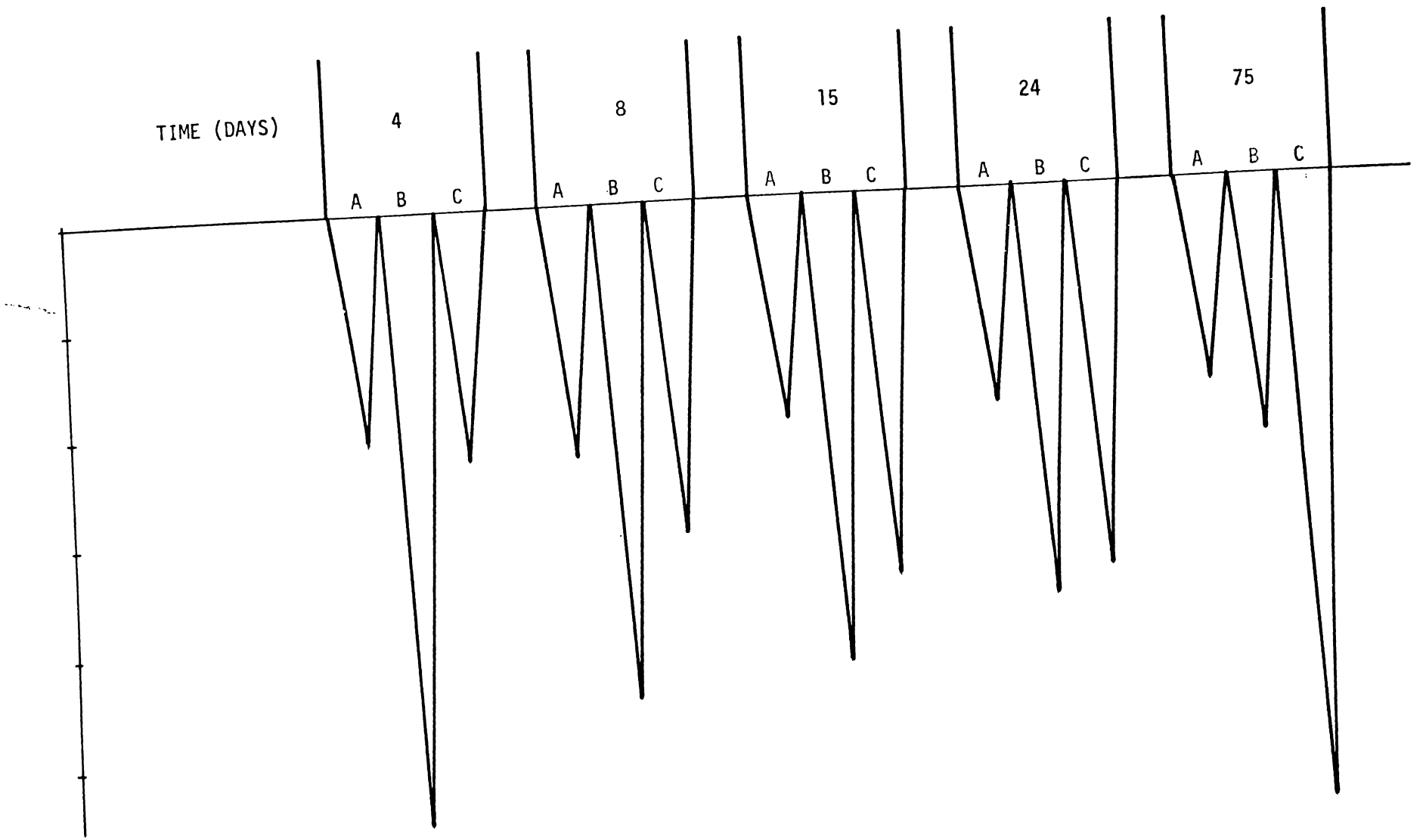

A = $Me_2Ge[Co(CO)_4]_2$, B = $Me_2GeCo_2(CO)_7$, C = $(Me_2Ge)_2Co_2(CO)_6$.

FIGURE 3.5

RELATIVE INFRARED BAND INTENSITIES DURING REACTION OF $Me_2GeH_2/Me_2GeCo_2(CO)_7/Me_2Ge[Co(CO)_4]_2$.

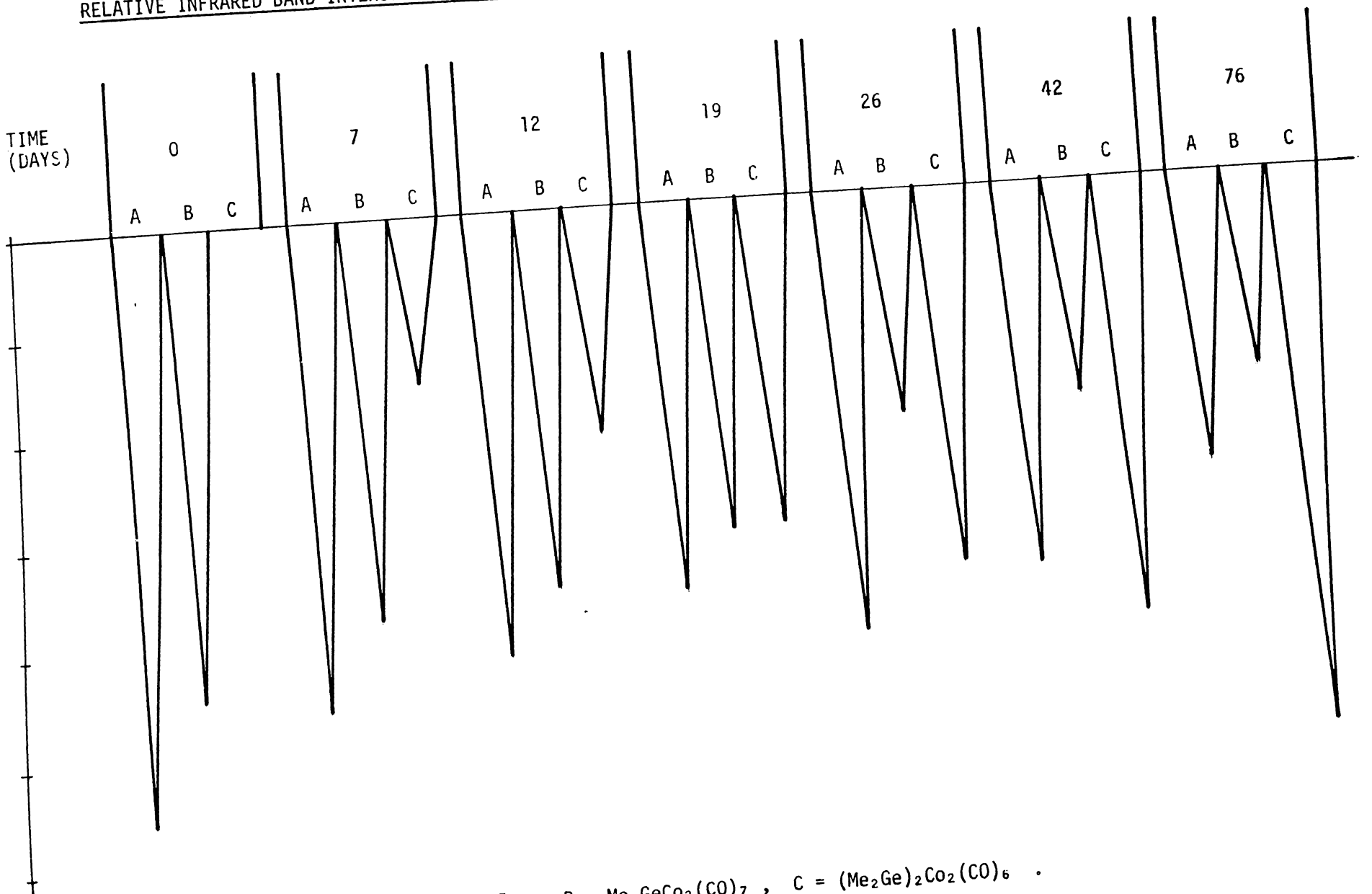

A = $Me_2Ge[Co(CO)_4]_2$, B = $Me_2GeCo_2(CO)_7$, C = $(Me_2Ge)_2Co_2(CO)_6$.

$Me_2Ge\{Co(CO)_4\}_2$, a hexane solution of the products from run 3 were left sealed under the same conditions as run 7 for 20 weeks. The infrared spectrum of the solution showed no change in composition other than a slight increase in $Me_2GeCo_2(CO)_7$ relative to $Me_2Ge\{Co(CO)_4\}_2$.

3.1.3 Discussion

The reaction of Me_2GeH_2 with $Co_2(CO)_8$ has been studied more thoroughly than previous reports (27,55). Three different, fully substituted products can be obtained by careful control of the reaction conditions. Controlling the reactant ratios at 1:1 results in $Me_2GeCo_2(CO)_7$ and $Me_2Ge\{Co(CO)_4\}_2$ as the only products of reaction (given sufficient reaction time).

$$Me_2GeH_2 + Co_2(CO)_8 \longrightarrow Me_2GeCo_2(CO)_7 + Me_2Ge\{Co(CO)_4\}_2$$

The yields of these two products depend upon the concentration of CO present during reaction. The reactions in a sealed tube (runs 1,2 and 3) thus produce both $Me_2GeCo_2(CO)_7$ and $Me_2Ge\{Co(CO)_4\}_2$ in good yield. The CO in these reactions arises from the formation of $Me_2GeCo_2(CO)_7$ and thus cannot exceed 1 or 2 mmoles, (approximately 0.5 - 1.0 Atmosphere pressure). The removal of this CO, produced during reaction (runs 4 and 5), leads to $Me_2GeCo_2(CO)_7$ as virtually the only product. Conversely, the addition of extra CO ($\simeq$1 Atmosphere pressure) prior to reaction results in almost exclusive formation of $Me_2Ge\{Co(CO)_4\}_2$.

That this effect of CO is on the products was confirmed by the removal and addition of quantities of CO from (or to) solutions of $Me_2Ge\{Co(CO)_4\}_2$ and $Me_2GeCo_2(CO)_7$ to give the lesser or higher carbonylated species, respectively.

Thus the equilibrium:

$Me_2GeCo_2(CO)_7 + CO \rightleftarrows Me_2Ge\{Co(CO)_4\}_2$

must exist with only relatively small pressures of CO influencing the equilibrium at room temperature. The small quantity of CO produced by initial $Me_2GeCo_2(CO)_7$ formation in the sealed tube reactions (runs 1,2,3) thus significantly affects the final composition of the two products.

Increasing the ratio of Me_2GeH_2 to $Co_2(CO)_8$ over 1:1 leads to formation of $\{Me_2Ge\}_2Co_2(CO)_6$. This has been shown to arise from reaction of the excess Me_2GeH_2 with either $Me_2GeCo_2(CO)_7$ or $Me_2Ge\{Co(CO)_4\}_2$, rather than condensation of these latter two species. The more likely reactant is $Me_2GeCo_2(CO)_7$ as it more closely resembles $Co_2(CO)_8$, having one bridging CO group.

$Me_2GeH_2 + Me_2GeCo_2(CO)_7 \longrightarrow \{Me_2Ge\}_2Co_2(CO)_6 + CO$

This is the first definite proof of the reaction of a group IVB hydride with a group IVB cobalt carbonyl.

While reaction of Me_2GeH_2 with $Co_2(CO)_8$ is virtually complete within a week (see Table 3.5), the reaction of Me_2GeH_2 with $Me_2GeCo_2(CO)_7$ (or $Me_2Ge\{Co(CO)_4\}_2$) is considerably slower under the same reaction conditions, otherwise the 1:1 reaction would also form $(Me_2Ge)_2Co_2(CO)_6$.

Two possible explanations may be formulated for this slow reaction. Firstly it is likely that $Me_2GeCo_2(CO)_7$ is inherently less reactive towards group IVB hydrides, because of increased steric crowding around the cobalt atom, the change in electron density on the cobalts (by the substitution of a bridging CO group by a Me_2Ge group) and (if the reaction proceeds via some interaction with a bridging CO group),

because of the reduced number of bridging CO groups (in $Me_2GeCo_2(CO)_7$).

A second possible explanation for slow reaction may be the effect of the free CO. The products formed in the reaction of $Fe_2(CO)_9$ with THF are influenced by whether CO is present or not (115). Therefore in this reaction system, CO may hinder reaction of Me_2GeH_2 with $Me_2GeCo_2(CO)_7$, possibly by control of the $Me_2GeCo_2(CO)_7/Me_2Ge\{Co(CO)_4\}_2$ equilibrium.

Increasing the hydride concentration in this reaction (runs 7 and 8) appeared to have little effect on increasing the reaction rate. Unless the effect is concealed by CO-retardation, it would seem that the rate of reaction is independent of the concentration of the hydride (i.e. Zero order in Me_2GeH_2).

There remain three further observations of interest in this reaction system. In the reaction of excess Me_2GeH_2 with $Co_2(CO)_8$ (run 7), the initial sampling indicated an increased yield of $Me_2GeCo_2(CO)_7$ relative to runs 1,2,3, despite the reaction being carried out in a sealed environment. This may be explained if the excess hydride aids decarbonylation of $Me_2Ge\{Co(CO)_4\}_2$. There is some evidence for this effect in the $Me_2SiH_2/Me_2GeCo_2(CO)_7/Me_2Ge\{Co(CO)_4\}_2$ reaction (see section 6.9).

The observation of small amounts of $Me_2GeHCo(CO)_4$ late in the reactions of Me_2GeH_2 with $Me_2GeCo_2(CO)_7$ and $Me_2Ge\{Co(CO)_4\}_2$ may arise from a minor side reaction involving Me_2GeH_2. This is consistent with observations from other reactions involving excess hydride and cobalt carbonyl species unreactive towards hydride substitution (see Chapter 6).

A possible formation is from attack of Me_2GeH_2 on $Me_2Ge\{Co(CO)_4\}_2$:

$Me_2GeH_2 + Me_2Ge\{Co(CO)_4\}_2 \longrightarrow 2Me_2GeHCo(CO)_4$.

The appearance of small quantities of $Co_4(CO)_{12}$ in these (and later) reactions appears to be a minor unavoidable side reaction involving either $Co_2(CO)_8$ or a partially-substituted hydride. No $Co_4(CO)_{12}$ was observed to result from mixtures of group IVB hydrides and group IVB-cobalt carbonyls left to react under the same conditions for long periods (see chapter 6). $Co_4(CO)_{12}$ has been observed as a minor product from other reaction systems (27).

A comparison of products obtained from this study with other reports is useful. Graham reported (105) that $MeGeCo_3(CO)_{11}$ resulted in this reaction (of Me_2GeH_2 and $Co_2(CO)_8$) and commented that Ge-C cleavage must be involved. Unfortunately no experimental detail was given, although we note his studies of the related reaction of $PhGeH_3$ with $Co_2(CO)_8$ (44) used similar experimental conditions to this work. No Ge-C cleavage was observed in this reaction in this work. It seems likely that the sample of Me_2GeH_2 he used was contaminated at least in part by $MeGeH_3$ (from which reaction with $Co_2(CO)_8$ yields $MeGeCo_3(CO)_{11}$ - ref. 24). Note that in our experience, all commercial samples of Me_2GeCl_2 contain $MeGeCl_3$ which is difficult to separate.

Cotton (55) and Gerlach (27) have previously obtained $(Me_2Ge)_2Co_2(CO)_6$ and $Me_2GeCo_2(CO)_7$ from this system by the dropwise addition of a toluene solution of excess Me_2GeH_2 to a toluene solution of $Co_2(CO)_8$. They did not observe $Me_2Ge\{Co(CO)_4\}_2$, but this is readily explained as their reactions were carried out in an open system. The isolation of $(Me_2Ge)_2Co_2(CO)_6$ after a comparatively short reaction time

(3 hours) may also be due to this (if CO hinders the reaction of Me_2GeH_2 with $Me_2GeCo_2(CO)_7$) although the effect of change of solvent cannot be excluded.

3.2. Reaction of $MeGeH_3$ With $Co_2(CO)_8$.

3.2.1. Experimental

Run 1:

$MeGeH_3$ (209mg, 2.36 mmoles) and $Co_2(CO)_8$ (1210mg, 3.54 mmoles) were left to react together for 1 week and worked up as described in section 2.5. The infrared spectrum of the involatile products is listed in Table 3.6. This shows mainly $MeGeCo_3(CO)_{11}$ plus small amounts of $Co_4(CO)_{12}$ and another species assigned as $MeGe\{Co(CO)_4\}_3$ (see section 3.2.2.)

Successive recrystallisations in reduced volumes of hexane at 0^oC, -15^oC and -83.5^oC, gave enriched solutions of $MeGe\{Co(CO)_4\}_3$. 1031mg (1.80mmoles) of pure $MeGeCo_3(CO)_{11}$ (76% yield based on $MeGeH_3$) were recovered, although there was still more present in a mixture of the three components.

Run 2:

This was essentially a repeat of run 1. $MeGeH_3$ (220mg, 2.43mmoles) and $Co_2(CO)_8$ (1250mg, 3.64mmoles) were left to react for 6 days and worked up as in section 2.5. The involatile products gave a virtually identical infrared spectrum as for run 1 (see Table 3.6), except the relative intensities of the $Co_4(CO)_{12}$ bands were weaker. 1140mg (1.99mmoles of $MeGeCo_3(CO)_{11}$ (82% yield based on $MeGeH_3$) were recovered.

Run 3:

CO (ca. 1 Atmosphere pressure) was added to $MeGeH_3$

Table 3.6 Infrared Spectrum* of the Involatile Products From the $MeGeH_3/Co_2(CO)_8$ Reaction

Peak (cm^{-1})	Rel.Int.	Assignment
2102	w	$MeGeCo_3(CO)_{11}$ + $MeGe\{Co(CO)_4\}_3$
2083 sh	m	$MeGe\{Co(CO)_4\}_3$
2080	vs	$MeGeCo_3(CO)_{11}$
2062	w-m	$Co_4(CO)_{12}$
2054	vs	$MeGeCo_3(CO)_{11}$ + $Co_4(CO)_{12}$
2042 sh	vvw	$MeGeCo_3(CO)_{11}$ + $MeGe\{Co(CO)_4\}_3$
2028	s	$MeGeCo_3(CO)_{11}$ + $MeGe\{Co(CO)_4\}_3$
2022 sh	w	$MeGeCo_3(CO)_{11}$ + $MeGe\{Co(CO)_4\}_3$
2018 sh	w	$MeGeCo_3(CO)_{11}$
2013	s	$MeGeCo_3(CO)_{11}$ + $MeGe\{Co(CO)_4\}_3$
2005 sh	w	$MeGeCo_3(CO)_{11}$
1994 sh	w	$MeGeCo_3(CO)_{11}$ + $MeGe\{Co(CO)_4\}_3$
1865	w	$Co_4(CO)_{12}$
1848	w-m	$MeGeCo_3(CO)_{11}$
1835	w	$MeGeCo_3(CO)_{11}$

* Hexane solution.

(123mg, 1.36mmoles) and $Co_2(CO)_8$ (700mg, 2.04mmoles) and the mixture allowed to react for 12 days and worked up as in section 2.5. An infrared spectrum of the involatile products was similar to that obtained in runs 1 and 2 with no appreciable change in the relative band intensities of $MeGeCo_3(CO)_{11}$ and $MeGe\{Co(CO)_4\}_3$.

3.2.2. Characterisation of $MeGe\{Co(CO)_4\}_3$.

3.2.2.1 Handling

$MeGe\{Co(CO)_4\}_3$ is an orange solid, very soluble in hexane. A hexane solution of $MeGe\{Co(CO)_4\}_3$ contaminated with some $MeGeCo_3(CO)_{11}$ stored at 4^0C in the absence of light was found to have almost completely converted to $MeGeCo_3(CO)_{11}$ and CO after only 3 days.

3.2.2.2 Mass Spectrum

The mass spectra of a sample of pure $MeGeCo_3(CO)_{11}$ and a sample containing primarily $MeGe\{Co(CO)_4\}_3$ (contaminated with some $MeGeCo_3(CO)_{11}$), were obtained under identical conditions. These gave identical spectra with a parent ion corresponding to $MeGeCo_3(CO)_{11}^+$. The discussion and assignment of this spectrum (of $MeGeCo_3(CO)_{11}$) has been carried out elsewhere (24) and will not be repeated here.

The most likely explanation for seeing the same spectrum in both cases is, that the temperature required to vaporise the latter sample resulted in the rapid decarbonylation of $MeGe\{Co(CO)_4\}_3$ as witnessed experimentally (see preceding section).

A similar phenomenom has been reported for other species

that readily lose CO. Thus the observed mass spectra of $\{R_2GeFe(CO)_4\}_2$ species is very similar to that of $(R_2Ge)_2Fe_2(CO)_7$,

i.e. $\{R_2FeGe(CO)_4\}_2 \xrightarrow{\Delta} (R_2Ge)_2Fe_2(CO)_7 + CO$ Ref. 172

3.2.2.3 Infrared Spectrum

Although $MeGe\{Co(CO)_4\}_3$ could not be freed of traces of $MeGeCo_3(CO)_{11}$, an infrared spectrum of a sample considerably enriched in $MeGe\{Co(CO)_4\}_3$ was obtained. This spectrum is shown in Fig.3.6 and listed and assigned in Table 3.7 along with the spectrum of the analogous $MeSn\{Co(CO)_4\}_3$.

There is considerable overlap of bands from $MeGe\{Co(CO)_4\}_3$ with those from $MeGeCo_3(CO)_{11}$, but the $MeSn\{Co(CO)_4\}_3$ bands can clearly be paralleled by resolved absorptions or $MeGeCo_3(CO)_{11}$ absorptions of anomalous intensity. Slight shifts to lower frequency observed are consistent with the change of the group IVB atom from Sn to Ge (22).

Assuming C_{3v} symmetry for $MeGe\{Co(CO)_4\}_3$, group theory predicts 7 infrared active carbonyl stretching modes, represented by $3a_1 + 4e$. All these are observed as well as a ^{13}CO band.

3.2.3. Discussion

The reaction of $MeGeH_3$ with $Co_2(CO)_8$ has been re-examined and $MeGe\{Co(CO)_4\}_3$ has been isolated and characterised in addition to $MeGeCo_3(CO)_{11}$, previously reported (24). This compound has not previously been isolated or characterised, although Gerlach (27) obtained indications that it occurs

FIGURE 3.6 INFRARED SPECTRUM OF A $MeGe[Co(CO)_4]_3$ MIXTURE.

TABLE 3.7 INFRARED SPECTRUM OF A $MeGe[Co(CO)_4]_3$ MIXTURE.

Peak (cm^{-1})	Assignment	$MeSn[Co(CO)_4]_3$[a]
2102 w		2101 w
2094 vvw	?	
2084 s-vs		2079 s
2080 sh m	$MeGeCo_3(CO)_{11}$	
2066 sh vw	$Co_4(CO)_{12}$	
2054 w	$MeGeCo_3(CO)_{11}$ + $Co_4(CO)_{12}$	
2038 sh w-m		2040 sh w
2030 sh m		2028 sh w
2020 vs		2020 s
2012 vs		2010 s
2004 sh w-m		
1997 sh w		1992 sh w
		1961 vw
1866 vvw	$Co_4(CO)_{12}$	
1848 vw	$MeGeCo_3(CO)_{11}$	
1835 vvw	$MeGeCo_3(CO)_{11}$	

HEXANE SOLUTION

a) Reference 41.

in the reaction of $MeGeBr\{Co(CO)_4\}_2$ with $NaCo(CO)_4$.

$MeGe\{Co(CO)_4\}_3$ is unstable thermally, losing CO to form $MeGeCo_3(CO)_{11}$, even at 4°C in the absence of light.

$$MeGe\{Co(CO)_4\}_3 \longrightarrow MeGeCo_3(CO)_{11} + CO$$

Whether this process is reversible was not established, although the appearance of both $MeGeCo_3(CO)_{11}$ and $MeGe\{Co(CO)_4\}_3$ in the reaction products suggest this to be so. An attempt to increase yields of $MeGe\{Co(CO)_4\}_3$ by the addition of ca. 1 Atmosphere of CO to the reaction mixture, gave little, if any, change in the relative yields of $MeGeCo_3(CO)_{11}$ and $MeGe\{Co(CO)_4\}_3$. The amount of CO added would have effectively doubled the total pressure of CO (assuming 2.4 mmoles of $MeGeH_3$, yields 2.4 mmoles of CO during the formation of $MeGeCo_3(CO)_{11}$). This was equivalent to ca. 2 Atmospheres pressure of CO in the 50ml reaction vessel. Thus the equilibrium between the two species must favour the lesser carbonylated species ($MeGeCo_3(CO)_{11}$), more so than for the corresponding equilibrium for the dimethylgermyldicobalt species:

$$Me_2Ge\{Co(CO)_4\}_2 \rightleftharpoons Me_2GeCo_2(CO)_7 + CO$$

This is presumably due to the greater steric and electron withdrawing effects of the $-Co(CO)_4$ group relative to Methyl, making CO elimination and consequently increased Co-Co bonding more favourable. This trend is also observed for the $GeH_4/Co_2(CO)_8$ reaction, where no $Ge\{Co(CO)_4\}_4$ is observed as a reaction product (see chapter 5).

3.3. Reaction of Me_2SiH_2 With $Co_2(CO)_8$.

3.3.1. General

The reaction of Ph_2SiH_2 with $Co_2(CO)_8$ has been the subject of several reports, with a different product identified in each; $Ph_2SiHCo(CO)_4$, (13), $Ph_2Co_2(CO)_7$, (49), and $Co(CO)_4Ph_2SiOCCo_3(CO)_9$, (107). The analogous reaction of Me_2SiH_2 with $Co_2(CO)_8$ has not yet been reported, although the related reaction involving $Me_2HSi\text{-}SiHMe_2$ (18) has yielded a number of products (see Table 1.7). It was therefore of interest to study the Me_2SiH_2 reaction, to compare it with the above silanes and also for comparison with the analogous germanium and tin reactions.

3.3.2. Experimental

Run 1:

Me_2SiH_2 (140mg, 2.33 mmoles) and $Co_2(CO)_8$ (798mg, 2.33 mmoles) were left to react for 10 days and worked up as described in section 2.5. The infrared spectrum of the relatively involatile products is listed in Table 3.8.

The products from this reaction proved impossible to obtain pure, due to the large quantity of $Co_2(CO)_8$ present, which was of similar solubility and volatility. However the major fate of the Me_2SiH_2 appears to be as the new compound, $Me_2SiHCo(CO)_4$. An infrared spectrum of a more pure sample is reported below. There appears to be another minor product with a peak at 2084cm^{-1}, however this compound remains unidentified.

From the volatile fraction, no Me_2SiH_2 was recovered, however some $Co_2(CO)_8$, $HCo(CO)_4$ and $Me_2SiHCo(CO)_4$ were observed.

Table 3.8 Infrared Spectrum* of The Less Volatile Products From the Reaction of $Me_2SiH_2/Co_2(CO)_8$ (Run 1)

Peak (cm^{-1})	Rel.Int.	Assignment
2092	w	$Me_2SiHCo(CO)_4$
2084	vw	?
2068	s	$Co_2(CO)_8$
2062	s	$Co_4(CO)_{12}$
2053	s	$Co_4(CO)_{12}$
2041	s	$Co_2(CO)_8$
2029	s	$Me_2SiHCo(CO)_4$
2022	m	$Co_2(CO)_8$
2006	w	$Me_2SiHCo(CO)_4$
1995	m	$Me_2SiHCo(CO)_4$
1865	m	$Co_4(CO)_{12}$ + $Co_2(CO)_8$
1855	w-m	$Co_2(CO)_8$

* Hexane solution

Run 2:

Me_2SiH_2 (96mg, 1.60 mmoles) and $Co_2(CO)_8$ (650mg, 1.90 mmoles) were left to react together, and the incondensable gases evolved during reaction measured, for 8 days, as described in section 2.6. (Table 3.9). The infrared spectrum of the relatively involatile products (after workup) is listed in Table 3.10. It shows a mixture of unreacted $Co_2(CO)_8$, $Co_4(CO)_{12}$ and two dimethylsilyl products; $Me_2SiHCo(CO)_4$ and $Co(CO)_4Me_2SiOCCo_3(CO)_9$, both identified by their infrared spectra and volatility (see below).

Pure samples of the components could not be obtained however they could be considerably purified (with difficulty). The crystals obtained from a hexane recrystallisation of the extract at -16°C were found to be enriched in $Co_4(CO)_{12}$ and $Co(CO)_4Me_2SiOCCo_3(CO)_9$.

The crystals were redissolved in hexane and re-crystallised at -16°C. A further recrystallisation at -45°C greatly enriched the mother liquor in $Co(CO)_4Me_2SiOCCo_3(CO)_9$. (see below).

The hexane was removed slowly under vacuum, from the original mother liquor. Successive vacuum sublimations enriched the sublimate in $Me_2SiHCo(CO)_4$ (see below).

2mg (0.03 mmole) of Me_2SiH_2 was recovered from the volatile fraction. Some $Me_2SiHCo(CO)_4$ was also observed.

Table 3.9 Incondensable Gases Produced During Reaction of Me_2SiH_2 and $Co_2(CO)_8$.

Time	mmoles H_2	mmoles CO
15 min.	0.18	0.63
80 min.	0.63	1.18

Table 3.9 Continued.

Time	mmoles H_2	mmoles CO
18 hrs.	0.89	1.30
40 hrs.	0.98	1.36
65 hrs.	1.06	1.31
180 hrs.	1.11	1.32

The incondensable gases measurements allow us to calculate rough yields from this reaction:

1.11 mmoles H_2 produced ==>0.45 mmoles H_2 remains bound (2mg Me_2SiH_2 recovered)

==>0.90 mmoles SiH

==>0.90 mmoles $Me_2SiHCo(CO)_4$ (58% yield)

and mmoles of $Me_2SiCo_4(CO)_{14}$ = 1.56 - 0.90

= 0.66 (42% yield)

Alternatively we can calculate yield from CO production:

mmoles of CO = 2x (mmoles of $Me_2SiCo_4(CO)_{14}$)

$\therefore$ mmoles of $Me_2SiCo_4(CO)_{14}$ = 1.36 ÷ 2

= 0.68 (44%)

and mmoles of $Me_2SiHCo(CO)_4$ = 1.56 - o.68

= 0.88 (56%)

(this assumes $Co_4(CO)_{12}$ is produced in negligible yield)

The two figures are in good agreement and give yields of $Me_2SiHCo(CO)_4$ and $Me_2SiCo_4(CO)_{14}$ of ca. 60% and 40% respectively (this implies 1.7 mmoles $Co_2(CO)_8$ are consumed, which is ≃90% of the available).

3.3.3 Characterisation of Products.

3.3.3.1 Handling

$Me_2SiHCo(CO)_4$ is a white volatile solid (at room

Table 3.10 Infrared Spectrum* of The Less Volatile Products From the $Me_2SiH_2/Co_2(CO)_8$ Reaction (Run 2).

Peak (cm^{-1})	Rel.Int	Assignment
2103 sh	vw	$Me_2SiCo_4(CO)_{14}$
2097 sh	vw	$Me_2SiCo_4(CO)_{14}$
2092	w	$Me_2SiHCo(CO)_4$
2068	s	$Co_2(CO)_8$
2062	s	$Co_4(CO)_{12}$
2053	s	$Co_4(CO)_{12}$
2041	vs	$Co_2(CO)_8$
2028	s	$Me_2SiHCo(CO)_4 + Me_2SiCo_4(CO)_{14}$
2021	m	$Co_2(CO)_8$
2005	s	$Me_2SiHCo(CO)_4$
2002 sh	w	$Me_2SiCo_4(CO)_{14}$
1994	s	$Me_2SiHCo(CO)_4$
1865	m	$Co_2(CO)_8 + Co_4(CO)_{12}$
1855	w-m	$Co_2(CO)_8$

* Hexane solution.

temperature), which is extremely soluble in hexane and very sensitive to decomposition by air. $Co(CO)_4Me_2SiOCCo_3(CO)_9$ is a dark purple involatile solid, which is reasonably soluble in hexanc. It is sensitive to air decomposition, although solutions free of air have been stored for months at 4^0C without appreciable decomposition.

3.3.3.2 Infrared Spectrum of $Me_2SiHCo(CO)_4$.

Although this compound was never obtained pure, subtraction of the contaminating $Co_2(CO)_8$ bands could easily be made. The best spectrum obtained is shown in Fig. 3.7 and listed and assigned in Table 3.11.

Molecules of the general type $X_2YM^1Co(CO)_4$ have C_s symmetry from which we predict 4 infrared active modes for the carbonyl stretches (3a' + a"). Four bands are observed in this spectrum and these may be assigned according to Graham (22). Thus the two bands at low frequency ($2003cm^{-1}$ and $1995cm^{-1}$) can be assigned as a' and a" modes resulting from the splitting of the e mode of C_{3v} symmetry. The remaining 2 bands are best treated as a mixture of equatorial and axial carbonyl stretches, resulting from strong coupling between these actual modes, because both modes are relatively strong, while the symmetric equatorial carbonyl stretch would be expected to produce only a weak dipole change.

3.3.3.3 Infrared Spectrum of $Co(CO)_4Me_2SiOCCo_3(CO)_9$

Again, this compound could not be obtained pure, however subtraction of the contaminating bands in the

TABLE 3.12 INFRARED SPECTRUM OF $Me_2SiCo_4(CO)_{14}$ MIXTURE

2103	w	(2104 w)	
2098	w-m	(2099 w-m)	
2067	w-m		$Co_2(CO)_8$
2062	m		$Co_4(CO)_{12}$
2052	sh m		$Co_4(CO)_{12}$
2048	vs	(2051 vs)	
2042	sh m	(2044 s)	$Co_2(CO)_8$
2034	s	(2035 s)	
2022	sh w		$Co_2(CO)_8$
2013	w	(2010 m)	
2002	m	(2003 m)	
1866	w-m		$Co_4(CO)_{12}$
1855	w		$Co_2(CO)_8$

(Spectrum of $Ph_2SiCo_4(CO)_{14}$ is in brackets. Ref 107.)

TABLE 3.11 INFRARED SPECTRUM OF $Me_2SiHCo(CO)_4$ MIXTURE

2093	m-s	
2068	m-s	$Co_2(CO)_8$
2062	m-s	$Co_4(CO)_{12}$
2053	sh m	$Co_4(CO)_{12}$
2048	s	$Me_2SiCo_4(CO)_{14}$
2041	s	$Co_2(CO)_8$
2034	sh m	$Me_2SiCo_4(CO)_{14}$
2029	s	
2022	sh m	$Co_2(CO)_8$
2014	sh w	$Me_2SiCo_4(CO)_{14}$
2006	sh s	
1994	vs	
1865	m	$Co_4(CO)_{12}$
1855	w	$Co_2(CO)_8$

BOTH HEXANE SOLUTIONS

FIGURE 3.8 INFRARED SPECTRUM OF $Me_2SiCo_4(CO)_{14}$.

FIGURE 3.7 INFRARED SPECTRUM OF $Me_2SiHCo(CO)_4$.

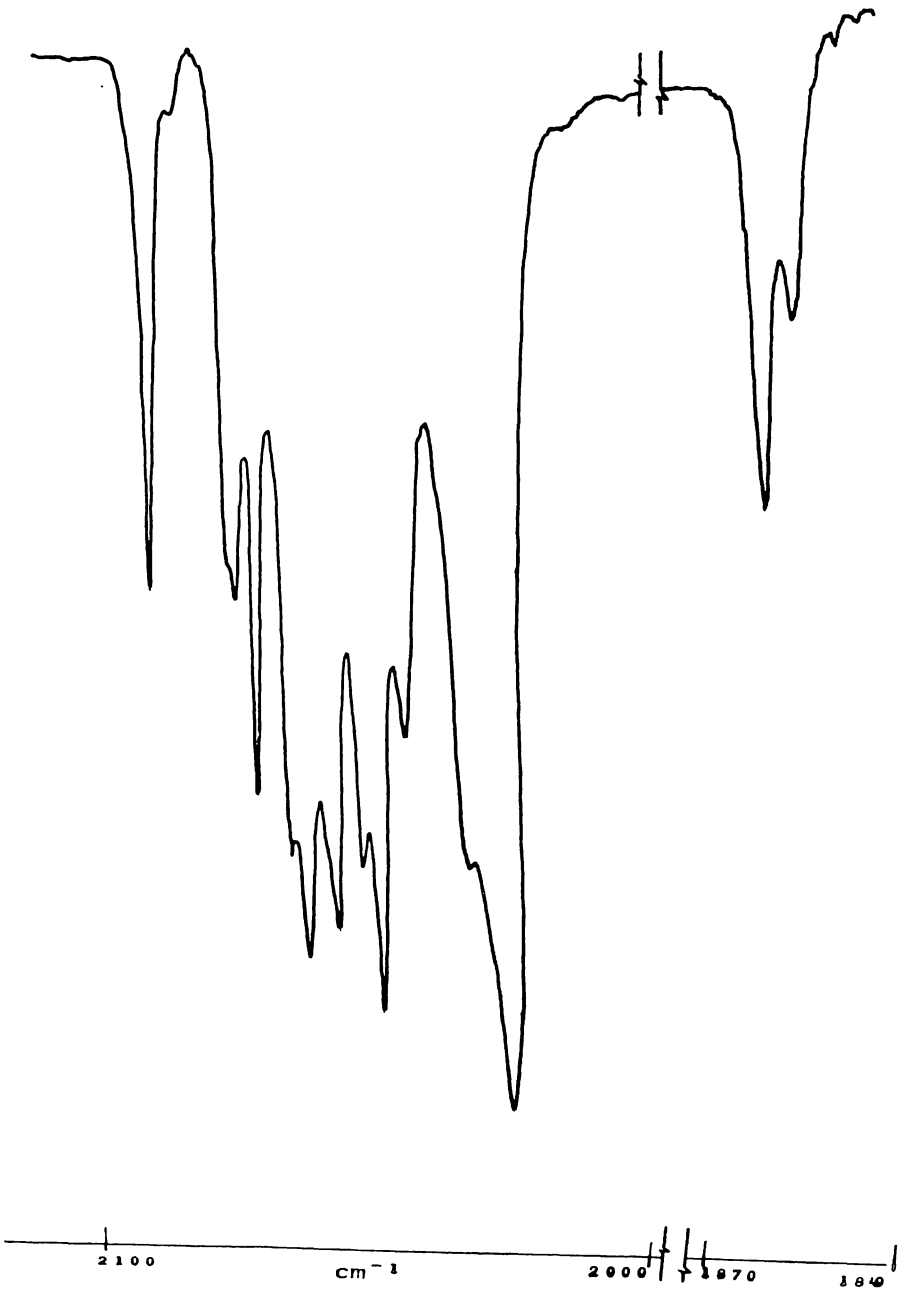

infrared spectrum is easily made. The infrared spectrum of the most enriched mixture is shown in Fig.3.8 and listed along with the spectrum of the analogous $Co(CO)_4 Ph_2SiOCCo_3(CO)_9$, (107), in Table 3.12. The spectrum can be assigned as the superposition of the spectra of a $R\text{-}Co(CO)_4$ species and a $ROCCo_3(CO)_9$ species. From the infrared spectra of $Me_3SiOCCo_3(CO)_9$, (116) and $Et_3NH_2BOCCo_3(CO)_9$, (117), we may assign bands due to the $-OCCo_3(CO)_9$ group (2103, 2048, 2034 and 2013 cm^{-1}). These bands appear to change little in position and relative intensity upon changing the substituent on the oxygen. This leaves 3 unassigned bands (at 2098, 2044 and 2002 cm^{-1}). If we approximate site symmetry of C_{3v} (i.e. point mass substituent on $-Co(CO)_4$ group), we would predict 3 infrared active modes for the carbonyl stretches ($2a_1 + e$). We may assign the strong band at 2002 cm^{-1} as the e mode and the two remaining bands as the $2a_1$ modes (see 3.3.3.2). Alternatively we can assume C_s site (and overall) symmetry, from which we predict 4 infrared active modes (3a' + a"). As the e mode (of C_{3v}) splits into a' + a" (for C_s), the remaining band of this pair may accidentally overlap with an $-OCCo_3(CO)_9$ mode or alternatively the splitting may be too small to be resolved (c.f. spectrum of $MeGeH_2Co(CO)_4$, ref. 24).

As is apparent from this assignment, there is little coupling of carbonyl modes between the $-Co(CO)_4$ and $-OCCo_3(CO)_9$ groups across the silicon.

3.3.4 Discussion

The reaction of Me_2SiH_2 with $Co_2(CO)_8$ has been examined and two new products identified, a partially-substituted

hydride, $Me_2SiHCo(CO)_4$ and a methylidyne cluster, $Co(CO)_4Me_2SiOCCo_3(CO)_9$. Although definitive assignments of these products cannot be made without further spectroscopic evidence (e.g. mass spectral, nmr), their infrared spectra combined with the knowledge of the reaction and the unlikelihood of Si-Si bond formation (see section 3.5), strongly support the above formulations. Further, the phenyl analogues of both these compounds have previously been obtained from the analogous reaction of Ph_2SiH_2 with $Co_2(CO)_8$. (13, 107).

The reaction of Me_2SiH_2 with $Co_2(CO)_8$ appears to be sensitive to the presence of CO. Thus when CO is present, the major product appears to be $Me_2SiHCo(CO)_4$ with no $Co(CO)_4Me_2SiOCCo_3(CO)_9$ observed, (a further minor product with an infrared band at $2084cm^{-1}$ was observed, however this has not been identified). If CO (and H_2) is removed during reaction, the products of the reaction are $Me_2SiHCo(CO)_4$ and $Co(CO)_4Me_2SiOCCo_3(CO)_9$ (both obtained in roughly equal yield).

The measurement of a large volume of CO after only 15 minutes reaction time (see Table 3.9) suggests the formation of species (other than $Me_2SiHCo(CO)_4$) at this stage of the reaction. After 8 days in the presence of CO (and/or H_2), $Me_2SiHCo(CO)_4$ is observed as the major product of the reaction, which cannot explain this large volume of CO observed initially. It appears then that the species resulting from this CO evolution is not surviving in the presence of CO (and/or H_2).

A possible explanation for this assumes that a major product formed initially is $Me_2SiCo_2(CO)_7$. This product

$$Me_2SiH_2 + Co_2(CO)_8 \longrightarrow Me_2SiCo_2(CO)_7 + CO$$

was not observed to arise from the reaction, but we should note that there are few species of type $R_2SiCo_2(CO)_7$ known (see Table 1.2). If we assume $Me_2SiCo_2(CO)_7$ formation then we can imagine it reacting in a number of ways:

(i) $Me_2SiCo_2(CO)_7 + Co_2(CO)_8 \longrightarrow Co(CO)_4Me_2SiOCCo_3(CO)_9 + CO$

or

(ii) $Me_2SiCo_2(CO)_7 \xrightarrow[Co_2(CO)_8]{Me_2SiH_2} Me_2SiHCo(CO)_4 + Co(CO)_4Me_2SiOCCo_3(CO)_9$.

In both cases the formation of $Co(CO)_4Me_2SiOCCo_3(CO)_9$ can be explained by silicon's strong affinity towards forming Si-O bonds (118). As $Me_2SiHCo(CO)_4$ is the major product observed in run 1 (i.e. presence of CO) this suggests two possibilities. Either CO (or H_2) decomposes $Me_2SiCo_2(CO)_7$, $Me_2SiCo_4(CO)_{14}$ or some other species, or the above reactions (and others) are sensitive to the presence of CO.

3.4. Reactions of Tin Hydrides With $Co_2(CO)_8$.

3.4.1 Reaction of SnH_4.

SnH_4 (119mg, 1.03mmoles) and $Co_2(CO)_8$ (658mg, 1.92mmoles) were left to react together as described in 2.5 for 12 weeks at 4^0C, (in order to slow down decomposition of SnH_4). The infrared spectrum of the involatile products showed them to be a mixture of $Sn\{Co(CO)_4\}_4$ and $Co_4(CO)_{12}$. 477mg (0.593mmoles) of pure $Sn\{Co(CO)_4\}_4$ were recovered by recrystallisation from CH_2Cl_2/C_6H_{14} (58% yield based on available Sn).

The volatile fraction showed traces of excess $Co_2(CO)_8$ but no tin-hydride was observed.

3.4.2 Reaction of $MeSnH_3$.

$MeSnH_3$ (149mg, 109mmoles) and $Co_2(CO)_8$ (716mg, 2.09mmoles) were left to react together for 5 weeks as described in 2.5. Two extracts of the involatile products were taken. The initial hexane extract consisted of $MeSn\{Co(CO)_4\}_3$ (480mg, 0.745mmoles, 68% yield based on Sn) identified by its infrared spectrum (43), and a trace of $Co_4(CO)_{12}$. The CH_2Cl_2 extract yielded 244mg (0.304mmoles) of pure $Sn\{Co(CO)_4\}_4$, (28% yield).

In the volatile fraction, no νSn-H or νSn-C were identified by infrared spectroscopy.

3.4.3 Reaction of Me_2SnH_2.

Me_2SnH_2 (65mg, 0.430mmoles) and $Co_2(CO)_8$ (170mg, 0.50mmoles) were left to react for 2 weeks as in 2.5. Virtually all the involatile solid product was soluble in 5ml hexane. The small quantity of solid remaining gave an infrared spectrum

showing a mixture of $MeSn\{Co(CO)_4\}_3$, $Me_2Sn\{Co(CO)_4\}_2$, (22) and $Co_4(CO)_{12}$. Recrystallisation from the hexane extract yielded 202mg (0.411mmoles) of pure $Me_2Sn\{Co(CO)_4\}_2$, (96% yield).

In the volatile fraction were identified excess $Co_2(CO)_8$ and a trace of $Me_3SnCo(CO)_4$, (22).

3.4.4. Discussion

The tin hydrides reacted in this work all gave exclusively terminal $-Co(CO)_4$ substituted products. A few points of interest arise from this work. In the SnH_4 reaction, a relatively low yield of $Sn\{Co(CO)_4\}_4$ was obtained. This is most likely explained by the thermal instability of SnH_4 (119) which decomposes readily at room temperature, to its elements.

$$SnH_4 \longrightarrow Sn + 2H_2$$

Even though the reaction was carried out at 4^0C to minimise decomposition, it appears that this is still significant. Although $Sn\{Co(CO)_4\}_4$ can be prepared from the reaction of tin and $Co_2(CO)_8$ (45) yields are low (14%) and this process

$$Sn_{(act)} + 2Co_2(CO)_8 \xrightarrow{Ether} Sn\{Co(CO)_4\}_4$$

would not be expected to significantly increase the yield of $Sn\{Co(CO)_4\}_4$ in this reaction. Unfortunately, involatile, non-carbonyl containing products were not looked for in this reaction.

The $MeSnH_3$ reaction, in addition to yielding the expected $MeSn\{Co(CO)_4\}_3$ also afforded $Sn\{Co(CO)_4\}_4$ in relatively high yield (28%). The Sn-C cleavage in this reaction arises from relatively mild reaction conditions. As no M^1-C cleavage was observed in any of the

preceding Ge or Si reactions, it must be due to the relatively weak Sn-C bond (Si-C, ≃300 $kJmol^{-1}$, Ge-C 255 $kJmol^{-1}$, Sn-C 193 $kJmol^{-1}$, ref. 143). The fate of the cleaved methyl group was not determined but its most likely fate would appear to be as CH_4 or C_2H_6.

The $Me_2SnH_2/Co_2(CO)_8$ reaction has been studied previously with surprisingly (in the context of this work) only $(Me_2Sn)_2Co_2(CO)_6$ found as a product (55). The differences in products may be explained by the use of an open system to obtain $(Me_2Sn)_2Co_2(CO)_6$, (see section 3.1). However it should be noted that pressures of CO in the closed system used in this work must be very small (arising only from $Co_4(CO)_{12}$ formation) and no bridged species were observed (neither $(Me_2Sn)_2Co_2(CO)_6$ nor $Me_2SnCo_2(CO)_7$).

The detection of small quantities of $MeSn\{Co(CO)_4\}_3$ and $Me_3SnCo(CO)_4$ as products from this reaction, may indicate some Sn-C cleavage and bond formation (as for $MeSnH_3$ reaction) although it is also possible that the sample of Me_2SnH_2 used may have been contaminated with the respective hydrides.

3.5 The Reactions of Me_3GeGeH_3 and Me_3SiGeH_3 With $Co_2(CO)_8$.

3.5.1 General

As $MeGeH_3$ reacts with $Co_2(CO)_8$ to give $MeGeCo_3(CO)_{11}$ (see section 3.2) and this product can be induced to undergo decarbonylation to form an unstable $M^1Co_3(CO)_9$ cluster (52) by heating, it was hoped that the addition of a larger group

$$MeGeCo_3(CO)_{11} \xrightarrow{\Delta} MeGeCo_3(CO)_9$$

on the $-GeH_3$ group would enable decarbonylation to occur more smoothly (see section 1.2.4) and form a more stable $-GeCo_3(CO)_9$ cluster:

$$Me_3M^1GeH_3 + 1\tfrac{1}{2}Co_2(CO)_8 \longrightarrow Me_3GeGeCo_3(CO)_9 + 3CO + 1\tfrac{1}{2}H_2$$

3.5.2 Reaction of Me_3GeGeH_3

Run 1:

Me_3GeGeH_3 (95mg, 0.492mmoles) and $Co_2(CO)_8$ (294mg, 0.861mmoles) were left to react (reactant ratio 1:1.8) as described in 2.5 for 4 days. To the involatile products were added 10ml of hexane, which extracted a small proportion of the solid. The infrared spectrum of this extract (see Table 3.13) showed it to consist mainly of $GeCo_4(CO)_{14}$, with some $Me_3GeCo(CO)_4$, $Co_4(CO)_{12}$ and another species with a prominent band at $2087cm^{-1}$ (the isolation and characterisation of this species is dealt with in Chapter 4).

The remaining bulk, solid products were extracted from the reaction vessel with 10ml CH_2Cl_2 to give an infrared spectrum showing virtually pure $GeCo_4(CO)_{14}$, contaminated with some $Co_4(CO)_{12}$ and the $2087cm^{-1}$ species.

Recrystallisation of the combined extracts yielded 209mg (0.298mmoles) of $GeCo_4(CO)_{14}$ (61% yield based on

Table 3.13 Infrared Spectrum* of the Initial Extract From the $Me_3GeGeH_3/Co_2(CO)_8$ Reaction (1:2)

Peak (cm^{-1})	Rel.Int.	Assignment
2094 sh	vw	$Me_3GeCo(CO)_4$
2087	w	$Ge_2Co_6(CO)_{20}$
2079	s	$GeCo_4(CO)_{14}$
2068 sh	w-m	$Ge_2Co_6(CO)_{20}$
2062	vs	$GeCo_4(CO)_{14}$ + $Co_4(CO)_{12}$
2054	m-s	$Ge_2Co_6(CO)_{20}$ + $Co_4(CO)_{12}$
2043	vw	$Me_3GeCo(CO)_4$
2040	w	$GeCo_4(CO)_{14}$
2032	w-m	$GeCo_4(CO)_{14}$
2004	vw	$GeCo_4(CO)_{14}$
1994	m	$Me_3GeCo(CO)_4$
1866	w	$Co_4(CO)_{12}$
1848	w-m	$GeCo_4(CO)_{14}$
1844 sh	vw	$Ge_2Co_6(CO)_{20}$

* Hexane solution.

available Me_3GeGeH_3). From the volatile fraction and the initial hexane extract were recovered 87mg (0.301mmoles) of $Me_3GeCo(CO)_4$ (61% yield based on available Me_3GeGeH_3).

Although the presence of considerable unreacted Me_3GeGeH_3 in the volatile fraction was detected (by infrared spectroscopy) quantitative separation of this from the bulk hexane could not be effected due to their very similar volatilities.

Run 2:

This was essentially a repeat of run 1. Me_3GeGeH_3 (182mg, 0.942mmoles) and $Co_2(CO)_8$ (612mg, 1.79mmoles) were left to react (reactant ratio 1:1.9) for 4 weeks and worked up as described in 2.5. Extraction and separation of the products as in run 1, gave similar infrared spectra, indicating the same products and relative yields. Recovered were; 436mg (0.622mmoles) of $GeCo_4(CO)_{14}$ (66% yield based on available Me_3GeGeH_3) and 157mg (0.544mmoles) of $Me_3GeCo(CO)_4$ (58% yield based on available Me_3GeGeH_3). Again, the unreacted Me_3GeGeH_3 could not be separated from the hexane solvent.

Run 3:

Me_3GeGeH_3 (97mg, 0.50mmoles) and $Co_2(CO)_8$ (91mg, 0.27 mmoles) were left to react (reactant ratio 1.9:1) for 14 weeks as described in 2.5. The relatively involatile products were largely insoluble in hexane and were thus extracted with CH_2Cl_2 to give an infrared spectrum (listed in Table 3.14) which consisted of broad poorly resolved bands arising from a complex mixture of unidentified components. Solvent

Table 3.14 Infrared Spectrum* of the Less Volatile Products From the $Me_3GeGeH_3/Co_2(CO)_8$ Reaction (2:1)

Peak (cm^{-1})	Rel.Int.	Assignment
2093 sh	w	$Me_3GeCo(CO)_4$
2089 sh	w	
2085 sh	w	
2083	m	
2080 sh	vw	
2068 sh	m	
2062 sh	vw	
2056	s	
2041 sh	w	
> br		
2038	vs	$Me_3GeCo(CO)_4$?
2032	w	
2025 sh		
2018		
2012 > br	vs	
2006		
1994	vs	$Me_3GeCo(CO)_4$
1980 sh	m	

* CH_2Cl_2 solution.

extractions and recrystallisations did little to resolve the mixture.

From the volatile fraction were recovered 28mg (0.10 mmoles) of $Me_3GeCo(CO)_4$ (20% yield based on available Me_3GeGeH_3), while a large amount of Me_3GeGeH_3 could not be quantitatively separated from the hexane.

3.5.3. Reaction of Me_3SiGeH_3.

Me_3SiGeH_3 (115mg, 0.774mmoles) and $Co_2(CO)_8$ (530mg, 1.55 mmoles) were left to react (reactant ratio 1:2) for $2\frac{1}{2}$ weeks and worked up as in 2.5. The hexane soluble products, gave an infrared spectrum consisting of peaks due to $GeCo_4(CO)_{14}$ and $Co_4(CO)_{12}$. The rest of the involatile products were extracted with CH_2Cl_2 to give an infrared spectrum similar to the one obtained in the Me_3GeGeH_3 reaction (runs 1 and 2), showing mainly $GeCo_4(CO)_{14}$ with traces of $Co_4(CO)_{12}$ and the 2087cm^{-1} species. Recrystallisation of the combined extracts yielded 453mg (0.646mmoles) of $GeCo_4(CO)_{14}$ (83% yield based on available Me_3SiGeH_3).

In the volatile fraction, excess hydride, $Me_3SiCo(CO)_4$ (20), and $HCo(CO)_4$ (108), were identified by their infrared spectra, however overnight fractional separation, resulted in decomposition (probably due to an air leak).

3.5.4 Discussion

As pointed out in 3.5.1, these reactions were carried out to try to prepare a M^1-$GeCo_3$ cluster (M^1=Si,Ge) by Ge-H substitution. Thus reactions of $Me_3M^1GeH_3$ were carried out

in a reaction ratio of roughly one Ge-H to one $-Co(CO)_4$. It was found however that the main feature of these reactions was the cleavage of M^1-Ge by $Co_2(CO)_8$ (presumably), to give $GeCo_4(CO)_{14}$ and $Me_3M^1Co(CO)_4$. As we now see (in hindsight) that a deficit of $Co_2(CO)_8$ was effectively used in these reactions, in view of the roughly equimolar quantities of $Me_3GeCo(CO)_4$ and $GeCo_4(CO)_{14}$ obtained as products from the Me_3GeGeH_3 reaction, it seems probable that using sufficient quantities of $Co_2(CO)_8$ would effect quantitative cleavage of Ge-Ge. This is further supported by the complete consumption of $Co_2(CO)_8$ in these reactions (virtually 100% of $Co_2(CO)_8$ can be accounted for in the products).

$$Me_3GeGeH_3 + 5/2Co_2(CO)_8 \longrightarrow Me_3GeCo(CO)_4 + GeCo_4(CO)_{14} + 2CO + 3/2H_2$$

In the reaction of Me_3SiGeH_3, the quantity of $GeCo_4(CO)_{14}$ obtained (0.645mmoles) means that only 0.26mmoles of $Co_2(CO)_8$ remained which is insufficient to react with all the cleaved Me_3Si- to form $Me_3SiCo(CO)_4$. Unfortunately a full characterisation of products was not carried out (due to decomposition). The differences in behaviour between Me_3SiGeH_3 and Me_3GeGeH_3 (Me_3GeGeH_3, gives roughly equimolar yields of $Me_3GeCo(CO)_4$ and $GeCo_4(CO)_{14}$) may be explained either by the stronger Si-Ge bond (thermochemical bond energies; 182kJmol^{-1} for Si-Ge, and 163kJmol^{-1} for Ge-Ge, ref.146) not being cleaved until Ge-H substitution is virtually complete (thus consuming a greater proportion of the $-Co(CO)_4$ and leaving the Me_3Si-group short of $Co_2(CO)_8$), or if the Ge species formed from Si-Ge cleavage reacts more quickly with $Co_2(CO)_8$ (or $HCo(CO)_4$) than the Si species. As $Me_3Si^{\bullet}$ radicals would be expected to be very reactive, a possibility is that the Si is expelled as Me_3SiH:

$Me_3SiGeH_3 + Co_2(CO)_8 \longrightarrow GeH_2Co_2(CO)_x + Me_3SiH$

There have previously been only two reports of the reaction of a compound containing a M^1-M^1 bond reacting with $Co_2(CO)_8$. Bulten and Budden (106) have observed quantitative cleavage of the Sn-Sn bond in Me_6Sn_2 by $Co_2(CO)_8$.

$Me_6Sn_2 + Co_2(CO)_8 \xrightarrow{Et_2O} 2Me_3SnCo(CO)_4$

The reaction of $(Me_2HSi)_2$ with $Co_2(CO)_8$ (18) gave products with no Si-Si cleavage in addition to a product necessarily involving cleavage, $(Me_2Si)_2Co_2(CO)_6$, (see Table 1.7).

The reaction using a considerable excess of Me_3GeGeH_3 (run 3) was carried out with the aim of obtaining a partially substituted hydride:

$Me_3GeGeH_3 + \frac{1}{2}Co_2(CO)_8 \longrightarrow Me_3GeGeH_2Co(CO)_4 + \frac{1}{2}H_2$

If this was obtained as a product, it was not identified, and it was one component of a complex mixture. The low solubility of the products and the broad poorly resolved infrared spectrum suggests that in addition to partially substituted hydrides there were possibly some polymeric species, possibly arising through reaction of partially substituted hydrides with each other. The isolation of a quantity of $Me_3GeCo(CO)_4$ shows that some (at least) Ge-Ge cleavage had been effected.

CHAPTER 4.

Preparation and Characterisation of $Ge_2Co_6(CO)_{20}$

4.1 General

The reactions in the previous chapter involved controlled substitution on the group IVB atom. It was of interest to study the reactions of more complex hydrides with $Co_2(CO)_8$ in order to see if more complex products could be formed. Although the reactions of $Me_3M^1GeH_3$ indicated that cleavage of the M^1-M^1 bond may be a significant feature of these reactions, Ge_2H_6 as a reactant, offered a polygermane in which both Ge atoms were functional and equivalent.

4.2 Experimental

4.2.1 Reactions of Ge_2H_6 with $Co_2(CO)_8$ in a 1:3 ratio.

Run 1.

Ge_2H_6 (97mg, 0.64mmoles) and $Co_2(CO)_8$ (660mg, 1.92mmoles) were left to react together (reactant ratio 1:3) for 4 weeks and worked up as described in 2.5. All of the dark involatile products were dissolved in 30ml CH_2Cl_2. The infrared spectrum of this solution (see Table 4.1) showed as major products, $GeCo_4(CO)_{14}$ and the 2087cm^{-1} species (observed in the $Me_3M^1GeH_3$ reactions). Also present are minor quantities of $Co_4(CO)_{12}$ and another species with a strong infrared adsorption at 2094cm^{-1}.

From the volatile fraction, 7mg (0.05mmoles) of unreacted Ge_2H_6 were recovered and a trace of unreacted $Co_2(CO)_8$ observed.

The solvent was removed from the involatile products and a further 15ml CH_2Cl_2 added and shaken to dissolve as much solid as possible. This was filtered under vacuum. The insoluble component was a virtually pure product with a strong infrared band at 2087cm^{-1}. This was freed of traces of $GeCo_4(CO)_{14}$, $Co_4(CO)_{12}$ and the 2094cm^{-1} species by recrystallisation from a CH_2Cl_2/C_6H_{14} mixture at -16°C: yield 240mg. Since this product is of formula $Ge_2Co_6(CO)_{20}$ (see next sections) this represents 0.222mmoles (36% yield based on consumed Ge_2H_6).

Although further quantities of this product remained as a mixture with $GeCo_4(CO)_{14}$ and $Co_4(CO)_{12}$, it could not be separated by the above method or by solvent extraction or recrystallisation. These latter two methods were also found to be unsuitable for obtaining pure quantities of this product from the initial bulk extract.

Table 4.1 Infrared Spectrum* of the Involatile Products From the $Ge_2H_6/Co_2(CO)_8$ Reaction (1:3).

Peak (cm^{-1})	Rel.Int.	Assignment
2094	vw	2094 Species
2087	s	$Ge_2Co_6(CO)_{20}$
2079	s	$GeCo_4(CO)_{14}$
2068	vs	$Ge_2Co_6(CO)_{20}$
2061	vs	$GeCo_4(CO)_{14}$ + $Co_4(CO)_{12}$
2055	vs	$Ge_2Co_6(CO)_{20}$ + $Co_4(CO)_{12}$
2040	w	$GeCo_4(CO)_{14}$
2035	w	$Ge_2Co_6(CO)_{20}$
2032	w-m	$Ge_2Co_6(CO)_{20}$ + $GeCo_4(CO)_{14}$
2027	w-m	$Ge_2Co_6(CO)_{20}$
2022 sh	w	$GeCo_4(CO)_{14}$
2004	w	$Ge_2Co_6(CO)_{20}$ + $GeCo_4(CO)_{14}$
1866	w-m	$Co_4(CO)_{12}$
1848	w-m	$Ge_2Co_6(CO)_{20}$ + $GeCo_4(CO)_{14}$
1844	w-m	$Ge_2Co_6(CO)_{20}$

* CH_2Cl_2/C_6H_{14} solution

The approximate percentage composition of solutions was calculated by measuring the relative intensities of the infrared bands at 2079cm^{-1}($GeCo_4(CO)_{14}$) and 2087cm^{-1} (of this new species) of prepared standard mixtures of these two species in relative molar ratios of 80:20, 60:40 and 40:60 respectively. The spectrum of the initial product mixture (Table 4.1) was found to be close to a 50:50 molar mixture.

Run 2.

Ge_2H_6 (131mg, 0.866mmoles) and $Co_2(CO)_8$ (920mg, 2.7mmoles) were left to react (reactant ratio 1:3) for 5 weeks and worked up as in run 1. The infrared spectrum of the involatile products was similar to that obtained in run 1, indicating similar products and relative yields.

Run 3.

Ge_2H_6 (330mg, 2.17mmoles) and $Co_2(CO)_8$ (2230mg, 6.51mmoles) were left to react (reactant ratio 1:3) for 5 weeks as in run 1. The infrared spectrum indicated similar products and relative yields as for runs 1 and 2.

Run 4.

The incondensable gases produced during reaction of Ge_2H_6 (276mg, 1.84mmoles) and $Co_2(CO)_8$ (1890mg, 5.51mmoles) were removed and measured over 14½ days as described in 2.5 (see table 4.2).

Table 4.2 Incondensable Gas Evolution During Reaction of $Ge_2H_6/Co_2(CO)_8$

Time	mmoles H_2	mmoles CO
23 minutes.	1.49	3.42
93 minutes	2.52	5.10
19½ hours	3.26	3.72
3 days	4.52	6.46
10½ days	5.74	6.66
14½ days	5.89	6.86

The amount of H_2 evolved corresponds to 106% of the total available. In the determination of H_2 and CO quantities, the greatest error arises from the weighing of the small quantities of gas in the calibrated bulb. In some determinations, this error was as high as 3-4%. Thus the discrepancy in the total evolved H_2 figure can be accounted for. The figures indicate a relative ratio of 1 mole H_2 evolved to 1.2 moles CO evolved.

The infrared spectrum of the involatile products was similar to that obtained in runs 1,2 and 3, indicating similar products and yield.

4.2.2 Handling

The 2087cm^{-1} species is an orange solid which is stable for months when stored at 4°C in the absence of light. It may be handled for short periods in air but prolonged exposure leads to decomposition. It decomposes slowly (see 4.3.4) in hexane at 60°C, losing CO.

It is just soluble in hexane and considerably more so in CH_2Cl_2.

Attempts to obtain a single crystal of suitable dimensions for an x-ray study, met with no success. Recrystallisation from hexane, dichloromethane and toluene yielded small twinned needles. Recrystallisation from more basic oxygenated solvents such as diethylether and acetone led to decomposition of the 2087cm^{-1} species.

4.3 Characterisation of $Ge_2Co_6(CO)_{20}$

4.3.1 Mass Spectrum.

The mass spectrum of the 2087cm^{-1} species is listed in table 4.3. The relative involatility of the compound, meant a moderately high temperature (≃80°C) was needed to vaporise enough sample to obtain a spectrum, however the spectrum showed only one species of high molecular weight.

The spectrum showed a parent ion corresponding to $Ge_2Co_6(CO)_{20}^+$, and the loss of twenty CO groups from this ion. This series of ions is of relatively high intensity, carrying 79% of the total ion current (cf. for $GeCo_4(CO)_{14}$, ions containing $GeCo_4^+$ carry 73% of total ion current, ref.57).

Other prominent ions are the $Ge_2Co_4^+$, $Ge_2Co_2^+$ and $GeCo_2^+$ ions. The number of Ge and Co atoms in these ions suggest a structure based upon the $GeCo_2^+$ triangle (see ref. 6). The $Ge_2Co_3^+$ or $GeCo_3^+$ ions are not especially intense, unlike those observed in the compounds of type $RGeCo_3(CO)_9$ (64) and no Ge_2^+ ion is observed, suggesting no Ge-Ge bond.

Table 4.3 Mass Spectrum of $Ge_2Co_6(CO)_{20}$

m/e	rel. int	Assignment
1054-1066	26	$Ge_2Co_6(CO)_x^+$, x = 20
1026-1038	19	x = 19
998-1010	39	x = 18
970-982	100	x = 17
942-954	14	x = 16
914-926	17	x = 15
886-898	31	x = 14
858-870	76	x = 13
830-842	97	x = 12
802-814	61	x = 11
774-786	70	x = 10
746-758	63	x = 9
718-730	82	x = 8
690-702	66	x = 7
662-674	58	x = 6
634-646	62	x = 5
606-618	60	x = 4
578-590	43	x = 3
550-562	40	x = 2
522-534	41	x = 1
494-506	61	x = 0

Table 4.3 Cont'd ...

463-475	18	$Ge_2Co_5(CO)^+$
433-447	36	$Ge_2Co_5^+$
404-416	9	$Ge_2Co_4(CO)^+$
376-388	29	$Ge_2Co_4^+$
345-357	14	$Ge_2Co_3(CO)^+$
329-341	8	$Ge_2Co_3C^+$
317-329	24	$Ge_2Co_3^+$
306-312	10	$GeCo_4^+$
286-298	12	$Ge_2Co_2(CO)^+$
258-270	24	$Ge_2Co_2^+$
272-278	15	$GeCo_2(CO)_3^+$
244-250	21	$GeCo_2(CO)_2^+$
216-228	22	$GeCo_2(CO)^+$
188-194	46	$GeCo_2^+$

4.3.2 Infrared Spectrum

The infrared spectrum of the 2087cm^{-1} species in the carbonyl stretching region bears a striking resemblance to the spectrum of $GeCo_4(CO)_{14}$ (see Fig.4.1 and Table 4.4). The spectrum also shows no features characteristic of terminal $-Co(CO)_4$ groups (see section 3.2.2.3) or of the methylidyne analogue clusters, $RGeCo_3(CO)_9$ (64).

This similarity between the two spectra suggests a related structure for the 2087cm^{-1} species. Thus assuming the formula of $Ge_2Co_6(CO)_{20}$ obtained from the mass spectrum to be correct, a likely structure is the $GeCo_2$ linked structure shown in Fig. 4.2.

If the $GeCo_2$ and $Co_2(\mu\text{-}CO)$ units are asymmetric, as found for $GeCo_4(CO)_{14}$ (57), the molecule has no symmetry and 18 infrared bands are expected in the terminal νCO region, together with 2 bridging frequencies. However, if the asymmetries and the presence of the bridging carbonyls are neglected, the molecule would be of C_{2v} symmetry and $5a_1+4a_2+4b_1+5b_2$ modes would be expected for the CO stretching region, with 14 of these infrared active. That this is a reasonable approximation is indicated by the close relation of the $GeCo_4(CO)_{14}$ modes to those predicted by its idealised symmetry of D_2d (57).

The observed spectrum (Fig.4.1) has 8 clearly resolved bands, including the 2004cm^{-1} one which may be a ^{13}CO mode. However there are weakly-marked inflexions on the high frequency edges of the three strongest bands and a clear inflexion about 2050cm^{-1}, which all show relative solvent shifts (see CH_2Cl_2 spectrum) and are therefore probably not ^{13}CO modes.

TABLE 4.4 INFRARED SPECTRA OF $Ge_2Co_6(CO)_{20}$ and $GeCo_4(CO)_{14}$.

$Ge_2Co_6(CO)_{20}$

2087	s	2090	sh
2068	vs	2088	s
2054	s	2074	sh
2050	sh	2068	vs
2040	w	2061	sh
2033	w-m	2057	s
2027	m	2050	sh
2021	w-m	2041	w
2003	w	2031	w-m
		2027	m
1848	sh	2018	w-m
1844	w-m	2004	vw
HEXANE SOLUTION		1844	w-m
		DICHLOROMETHANE SOLUTION	

$GeCo_4(CO)_{14}$

2079	s
2061	vs
2040	w-m
2032	m
2023	w-m
2005	w
1848	m
HEXANE SOLUTION	

FIGURE 4.1 INFRARED SPECTRA OF $Ge_2Co_6(CO)_{20}$ and $GeCo_4(CO)_{14}$.

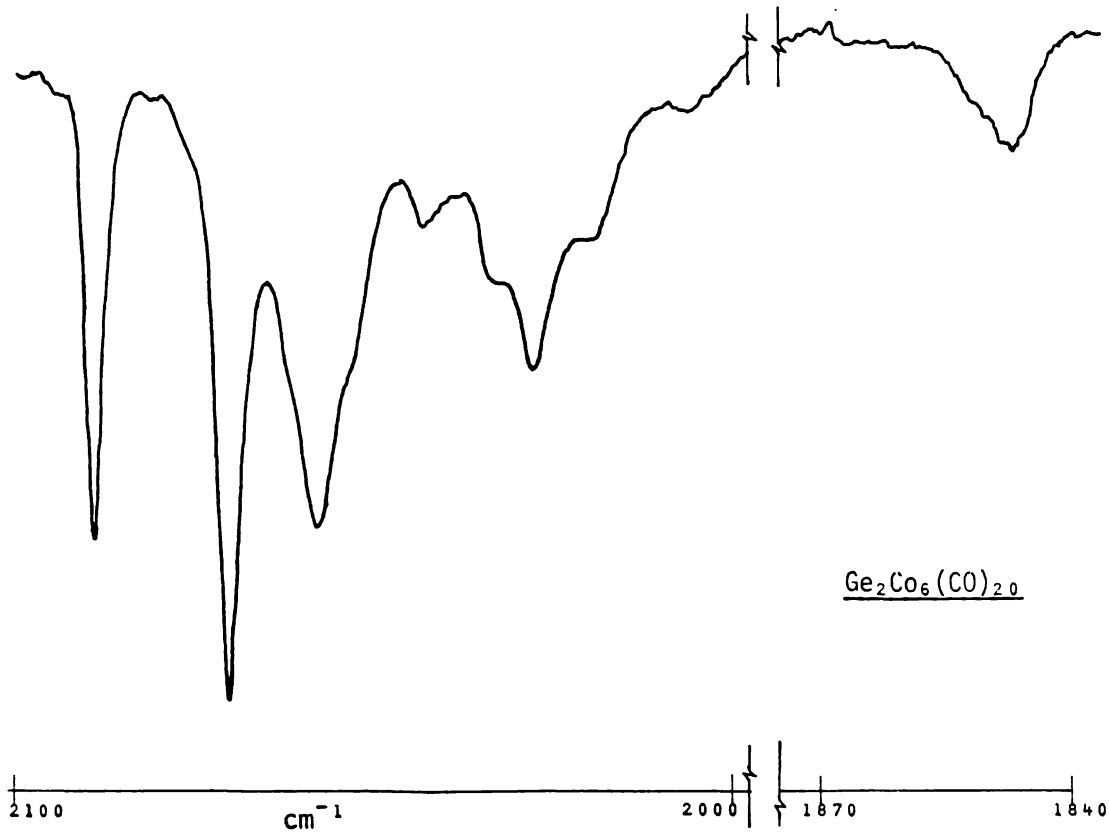

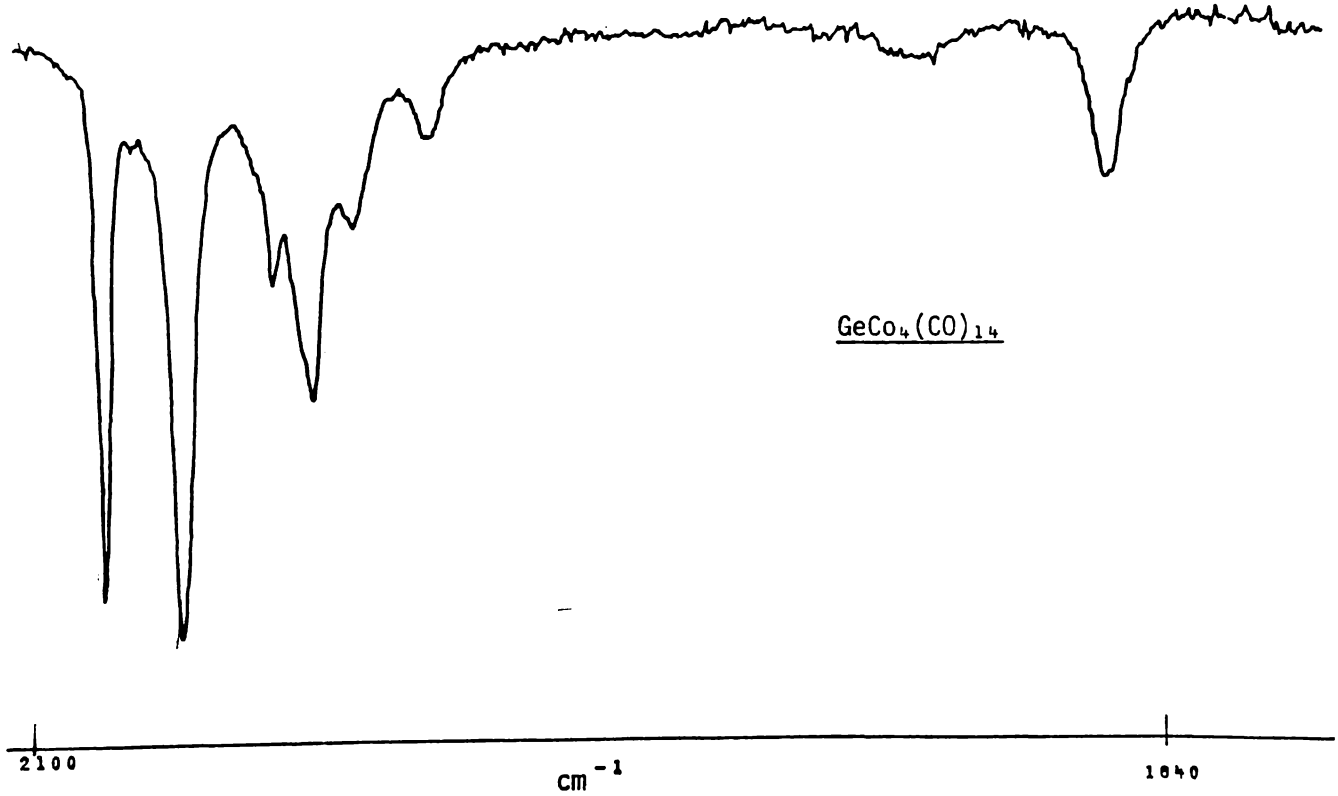

FIGURE 4.2 PROPOSED STRUCTURE OF $Ge_2Co_6(CO)_{20}$.

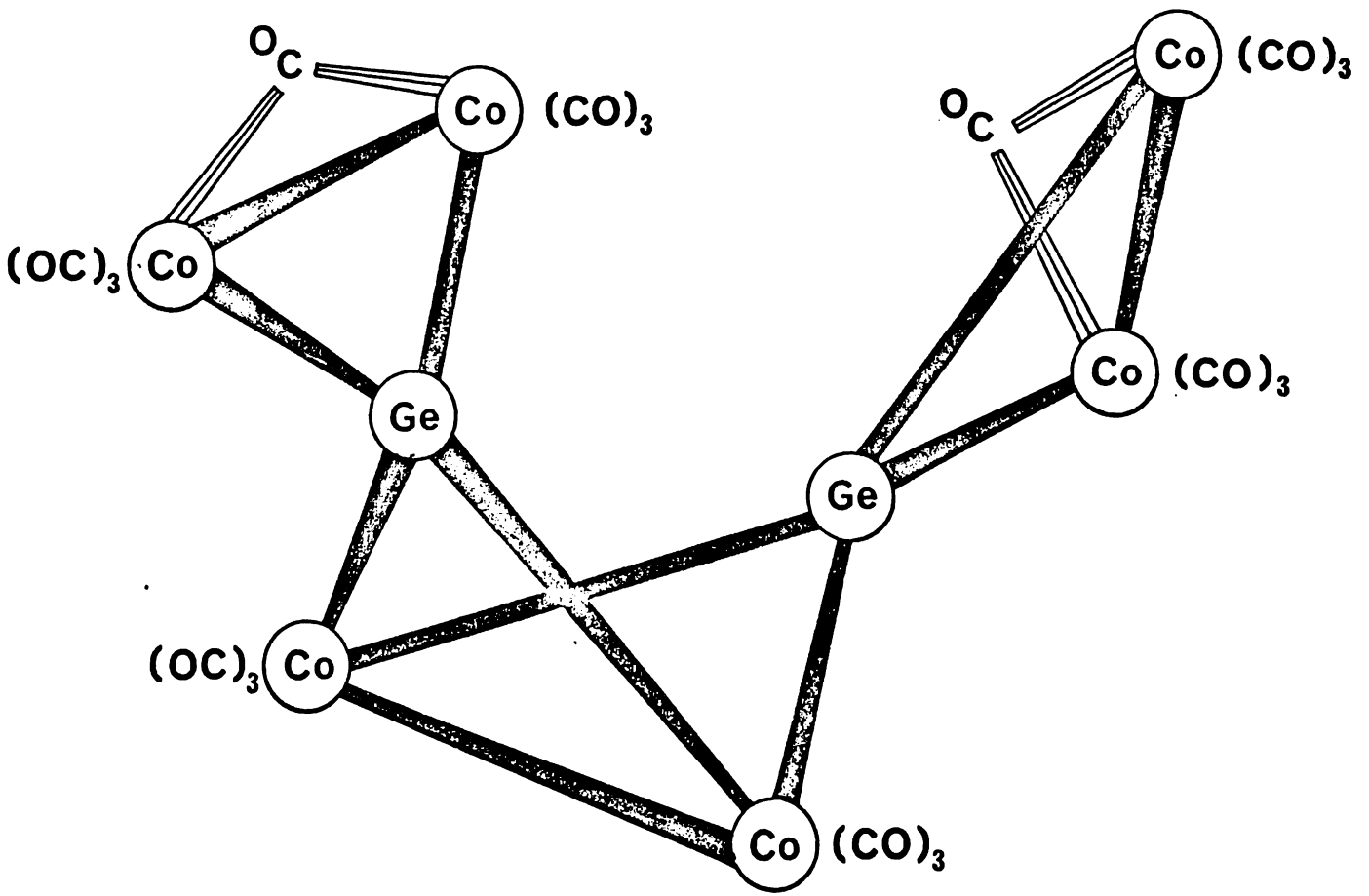

While these observations do not prove the pseudo-C_{2v} structure, they are compatible with it.

An alternative approach is to regard the molecule as three $Co_2(CO)_6$ $(\mu\text{-}X)_2$ units (X=Ge or CO). Bör has analysed the basic $M_2(CO)_6(\mu\text{-}X)_2$ spectrum (120) and shown that four strong bands are expected, together with a much weaker band and an inactive mode. This pattern is seen for $(Me_2Ge)_2Co_2(CO)_6$ and $Me_2GeCo_2(CO)_6(\mu\text{-}CO)$. (see Fig. 3.1) This suggests no more than 12 strong bands for the three units in combination in $Ge_2Co_6(CO)_{20}$, although it is unlikely that all combinations will result in large dipole moments. Thus a spectrum with 8-10 strong bands is reasonable.

One band of note in the $Ge_2Co_6(CO)_{20}$ and $GeCo_4(CO)_{14}$ spectra, is the band at highest frequency. In $GeCo_4(CO)_{14}$ this band is at $2079cm^{-1}$, while in $Ge_2Co_6(CO)_{20}$ it is at $2087cm^{-1}$. This mode is probably the in-phase symmetric stretch and the shift to higher frequency probably reflects increased coupling of modes (in the more complex homologue) rather than an increased energy of the mode. This increased coupling is consistent with previous observations of coupling of $-Co(CO)_x$ modes across Ge, (22), and across a Co-Co bond,(120).

4.3.3 Total Pyrolysis.

The total thermal pyrolysis of the $2087cm^{-1}$ species was carried out to determine the total CO content:
A sample of the $2087cm^{-1}$ species was heated slowly in a glass tube to $\simeq 200^0C$ until evolution of gas slowed. At this stage the sample was heated to $\simeq 500^0C$ until gas evolution ceased, leaving a solid film with a metallic lustre. The evolved gases were measured on a Toepler pump.

Run 1.

Weight of sample: 151 mg.

Amount of gas evolved: 2.44 mmoles

Weight of equivalent CO: 68.5mg

% weight that is CO: 45.4

Run 2.

Weight of sample: 84.3 mg.

Amount of gas evolved: 1.31mmoles

Weight of equivalent CO: 36.7 mg

% weight that is CO: 43.5

4.3.4 Decarbonylation.

Run 1.

A hexane solution of the 2087cm^{-1} species (63mg) was heated at 60^{0}C, and incondensable gas evolution measured over a period of ca. 19 days. The results are summarised in Table 4.5 and Fig. 4.3.

After this period, the hexane was removed from the reaction vessel, and ca. 2ml CH_2Cl_2 was added to the dark black solid and an infrared spectrum run. The spectrum was that of the new compound $\{Co(CO)_4Ge\}_2Co_4(CO)_{11}$ (characterised in Ch.7) contaminated with a trace of $GeCo_4(CO)_{13}$, (62). The $GeCo_4(CO)_{13}$ was easily removed by extraction with CH_2Cl_2.

Run 2.

This was a repeat of run 1. Thus 363 mg of $Ge_2Co_6(CO)_{20}$

FIGURE 4.3 DECARBONYLATION OF $Ge_2Co_6(CO)_{20}$,(RUN 1)

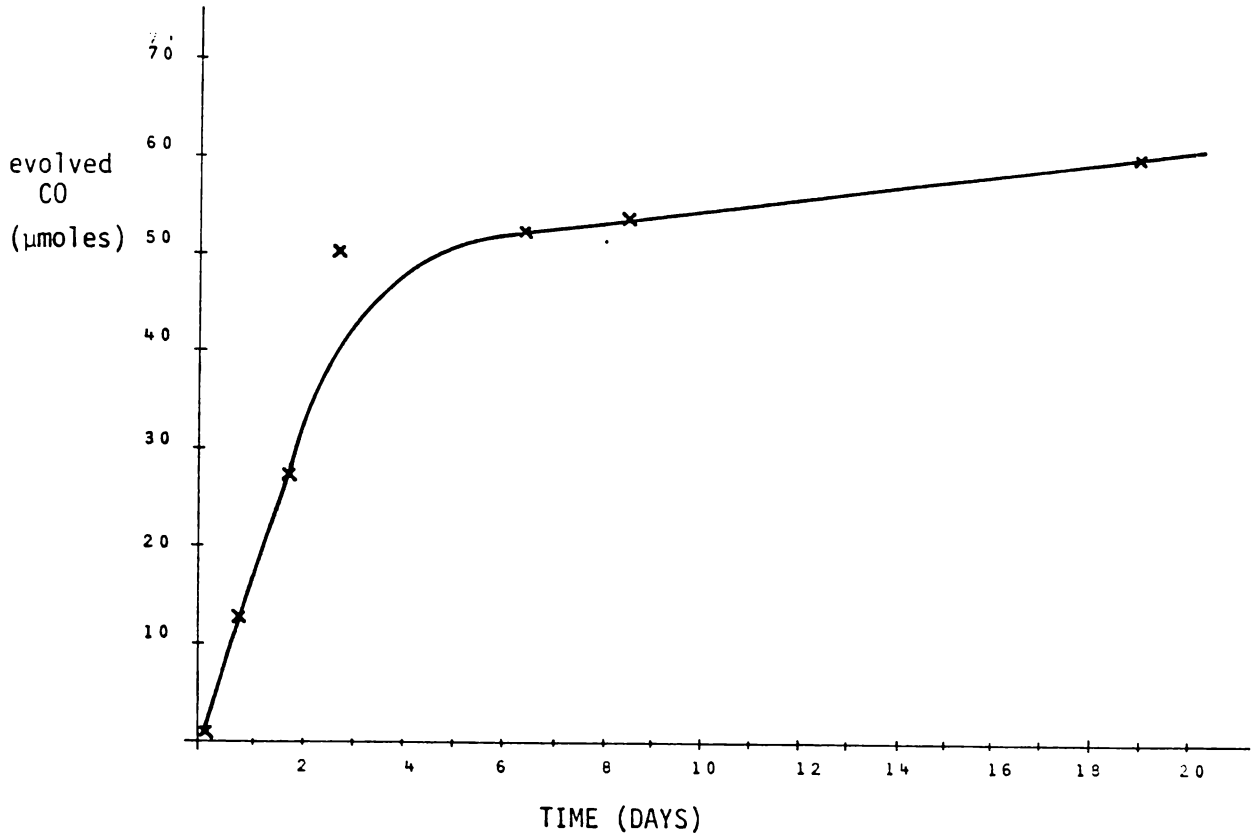

TABLE 4.5 DECARBONYLATION OF $Ge_2Co_6(CO)_{20}$, (60 °C).

RUN 1: 63 mg,(59.5μmole).		RUN 2: 363 mg,(0.343mmole)	
Time(days)	Evolved CO(μmole)	Time(days)	Evolved CO(mmole)
0.08	1	4	0.265
0.75	12.5	6	0.275
1.71	27.3	11	0.328
2.61	50.8	14	0.373
6.46	52.8		
8.43	53.8		
19	60.7		

in hexane, was heated at 60°C for 14 days, and evolved incondensable gases measured (see table 4.5).
An infrared spectrum of the products was similar to that obtained in run 1.

4.4. Discussion.

It has been shown (57), that GeH_4 reacts with $Co_2(CO)_8$ thus:

$$GeH_4 + 2Co_2(CO)_8 \longrightarrow GeCo_4(CO)_{14} + 2CO + 2H_2 \qquad (1)$$

The parallel reaction with Ge_2H_6 proceeds largely according to equation (2) with a good yield of the new compound.

$$1.5\ Ge_2H_6 + 5Co_2(CO)_8 \longrightarrow Ge_2Co_6(CO)_{20} + GeCo_4(CO)_{14} + 4.5H_2 + 6CO \qquad (2)$$

This stoichiometry has been confirmed by spectroscopic methods and also by the measurement of the evolved incondensable gases which gave a relative ratio of H_2:CO of 1:1.2 (cf. from equation 2, expected 1:1.3). Note that in the reactions in this chapter, a slight deficit of $Co_2(CO)_8$ was used, (relative to the stoichiometry in equation 2).

The accumulated evidence strongly supports the formulation of the new compound as $Ge_2Co_6(CO)_{20}$, a species closely related to $GeCo_4(CO)_{14}$. Mass spectroscopic evidence clearly shows this compound to have 2 Ge atoms per molecule. In addition there is a highest observed mass envelope corresponding to $Ge_2Co_6(CO)_{20}$ and also ions resulting from the successive loss of 20 carbonyls from the Ge_2Co_6 skeleton.

This formula is also supported by the quantitative decarbonylation of this product at 60°C to $\{Co(CO)_4Ge\}_2Co_4(CO)_{11}$ (see chapter 7 for characterisation).

$$Ge_2Co_6(CO)_{20} \xrightarrow[hexane]{60^0C} \{Co(CO)_4Ge\}_2Co_4(CO)_{11} + CO$$

The total pyrolysis gives figures which indicate considerably less CO evolved than expected for a molecule of $Ge_2Co_6(CO)_{20}$. Aylett (121) has found that static pyrolyses of silicon metal carbonyl species, do not release all of the available C and O as CO but some remains as silicon carbides and oxides. We must assume that some C and/or O remained as part of the residues after gas evolution had ceased. This method appears to be unsuitable for CO determinations.

Having established the formula, we are left with the problem of the structure. The relatively strong $Ge_2Co_4^+$, $Ge_2Co_2^+$ and $GeCo_2^+$ envelopes in the mass spectrum suggests the compound consists of linked $GeCo_2$ triangles. This is further supported by the carbonyl infrared spectrum which is remarkably similar to that of $GeCo_4(CO)_{14}$ (57). Although we cannot fully assign the spectrum, the appearance of two peaks at ca.1840cm^{-1}, is consistent with the molecule having two bridging CO groups.

The mass spectrum shows no Ge_2^+ ion, suggesting no Ge-Ge bond in the molecule. This is strongly supported by the M^1-M^1 cleaving nature of $Co_2(CO)_8$ (see section 3.5) and also by the appearance of $Ge_2Co_6(CO)_{20}$ as a minor product from the reactions of $Me_3M^1GeH_3$ (M^1=Si,Ge) (see section 3.5) and GeH_4 (see Chapter 5) with $Co_2(CO)_8$, in which the formation of a Ge-Ge bond would appear to be unlikely (considering the nature of $Co_2(CO)_8$).

Thus the structure most consistent with the above evidence is that of the higher homologue of $GeCo_4(CO)_{14}$ shown in Fig.4.2,

of two $-GeCo_2(CO)_7$ units linked by a central $-Co_2(CO)_6$ group. Although other structures of formula $Ge_2Co_6(CO)_{20}$ can be envisaged, the spectroscopic evidence is inconsistent with $-GeCo_3(CO)_9$ or $-GeCo(CO)_4$ groups being present in the molecule.

As added support we note, (a) the following Chapters show that molecules of similar structure can be built up by the addition reactions of Ge-H bonds to $GeCo_4(CO)_{14}$;

e.g. 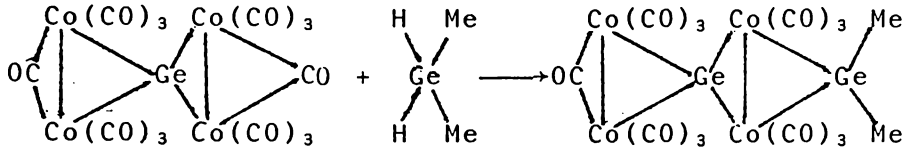

(See Chapter 6)

and (b) that the condensation of the extended $Ge_2Co_6(CO)_{20}$ structure to the $\{Co(CO)_4Ge\}_2Co_4(CO)_{11}$ cluster is a close parallel to the known condensation of $GeCo_4(CO)_{14}$, (57), to the pyramidal $\{(CO)_4Co\}GeCo_3(CO)_9$ cluster.

CHAPTER 5. The Reactions of GeH_4 and Some Polygermanes With $Co_2(CO)_8$.

5.1. General.

The reactions of GeH_4, Ge_2H_6, Ge_3H_8 and $(GeH_3)_2SiMe_2$ with $Co_2(CO)_8$ are reported in this chapter. Further aspects of these reactions (of those previously studied) have been explored, in particular the effect of varying reactant ratios and the identification of further products arising from the reactions.

5.2 The Reactions of GeH_4

5.2.1 Experimental.

Run 1.

GeH_4 (136mg, 1.78mmoles) and $Co_2(CO)_8$ (1240mg, 3.63 mmoles) were left to react for 10 days and worked up as in 2.5. The involatile products were dissolved in ca. 10 ml CH_2Cl_2 and gave an infrared spectrum as in Table 5.1. The spectrum consists of bands due mainly to $GeCo_4(CO)_{14}$ (57), some $Co_4(CO)_{12}$ (122) and a small quantity of $Ge_2Co_6(CO)_{20}$.

Recrystallisation of these products from a C_6H_{14} /CH_2Cl_2 mixture yielded 1131mg (1.61mmoles) of $GeCo_4(CO)_{14}$ (93% yield based on consumed GeH_4).

From the volatile fraction were observed, traces of unreacted GeH_4 (3mg, 0.04 mmoles) and $Co_2(CO)_8$.

Further runs of this reaction were carried out to explore various aspects of the reaction such as:

(i) Reproducibility of the reaction ($1GeH_4$: $2Co_2(CO)_8$) (run 2)

(ii) Measurement of the incondensable gases produced during the $1GeH_4$: $2Co_2(CO)_8$ reaction. (runs 3,4)

(iii) To observe whether added CO influenced the reaction (run 5)

(iv) To observe the effect of reduced temperature (run 6)

(v) The effect of using an excess of GeH_4 (molar ratio 1:1) (runs 7,8).

(vi) Measurement of incondensable gases produced in the 1:1 reaction (run 9).

The details are tabulated in Table 5.2, while further details and results of some of the reactions are listed below.

Table 5.1 Infrared Spectrum* of Products From the $GeH_4/Co_2(CO)_8$ Reaction, Run 1. (1:2).

Peak (cm^{-1})	Rel.Int.	Assignment
2094 sh	vvw	2094 Species
2087 sh	vw	$Ge_2Co_6(CO)_{20}$
2079	s	$GeCo_4(CO)_{14}$
2068 sh	w	$Ge_2Co_6(CO)_{20}$
2061	vs	$GeCo_4(CO)_{14}$ + $Co_4(CO)_{12}$
2053 sh	w-m	$Ge_2Co_6(CO)_{20}$ + $Co_4(CO)_{12}$
2040	w	$GeCo_4(CO)_{14}$
2031	m	$Ge_2Co_6(CO)_{20}$ + $GeCo_4(CO)_{14}$
2021 sh	w-m	$GeCo_4(CO)_{14}$
2004	vw	$Ge_2Co_6(CO)_{20}$ + $GeCo_4(CO)_{14}$
1863	w	$Co_4(CO)_{12}$
1848	w-m	$GeCo_4(CO)_{14}$
1844	vvw	$Ge_2Co_6(CO)_{20}$

* CH_2Cl_2/C_6H_{14} solution

Table 5.2 The Reactions of GeH_4 With $Co_2(CO)_8$.

Run	GeH_4 mmole (recovered)	$Co_2(CO)_8$	Time	Yield of $GeCo_4(CO)_{14}$ %	Comments
1	1.78 (0.04)	3.63	10 days	1131mg, 93	See Table 5.1; $Co_4(CO)_{12}$, $Ge_2Co_6(CO)_{20}$ and 2094cm^{-1} product observed in small amounts.
2	2.91 (*)	5.82	18 days	*	Infrared spectrum of products same as in Run 1. (see Table 5.1)
3	3.32 (0.07)	6.33	16 days	*	Incondensable gases measured, see Table 5.3. Spectrum of products similar to Table 5.1.
4	1.14 (0.05)	2.27	22 days	*	Incondensable gases measured, see Table 5.3. Spectrum of products similar to Table 5.1.
5	1.10	2.20	11 days	*	CO (ca.1Atm) added at start of reaction. Spectrum of products similar to Table 5.1.
6	1.22 (0.10)	2.43 (0.24)	74 days	*	Reaction carried out between -4°C and 0°C. Incondensable gases measured, See Table 5.4. IR Spectrum of products similar to Table 5.1. 0.24mmoles $HCo(CO)_4$ and 0.02mmoles $GeH_3Co(CO)_4$ recovered.
7	1.45 (0.67)	1.45	21 days	0.656mmoles 95% yield	Excess GeH_4 used. IR of products similar to Table 5.1.

over/

Table 5.2 (Continued)

Run	GeH_4 mmole (recovered)	$Co_2(CO)_8$	Time	Yield of $GeCo_4(CO)_{14}$ %	Comments.
8	2.78	2.78	14 weeks		Excess GeH_4 used. IR of products indicated greater relative yield of $Ge_2Co_6(CO)_{20}$. (See Table 5.5).
9	1.34	1.34	3 days		Excess GeH_4 used. Incondensable gases, measured during reaction. (See Table 5.6).

* Not measured.

Runs 3 and 4.

Table 5.3 Incondensable Gases Produced During Reaction of GeH_4 and $Co_2(CO)_8$ (1:2).

Run 3

Time	mmoles H_2	mmoles CO
1½ hours	1.33	3.58
45 hours	3.23	4.96
9 days	5.08	5.51
16 days	5.82	5.82

Run 4.

Time	mmoles H_2	mmoles CO
1½ hrs	0.53	1.12
1 day	1.09	1.49
9 days	1.84	1.93
22 days	2.15	2.18

Run 6.

Table 5.4 Incondensable Gases Produced During Low Temperature Reaction of $GeH_4/Co_2(CO)_8$ (1:2).

Time	mmoles H_2	mmoles CO
3 hours 40 mins.	0.13	0.26
21 hours	0.61	1.07
47 hours	1.06	1.70
88 hours	1.22	1.80
9 days	1.32	1.84
14 days	1.39	1.92
74 days	1.53	2.33

The infrared spectrum of the involatile products was

similar to that shown in Table 5.1, however from the volatile fraction were recovered (in addition to unreacted GeH_4 and $Co_2(CO)_8$); 41mg (0.24mmoles of $HCo(CO)_4$ and 6mg (0.02mmoles) of $GeH_3Co(CO)_4$. (19)

Runs 7 and 8

These were reactions of excess GeH_4 with $Co_2(CO)_8$ (1:1 reactant ratio) with relatively short (run 7) and long (run 8) reaction times. Run 7 gave essentially the same infrared spectrum of the involatile products as for the previous runs, with $GeCo_4(CO)_{14}$ as the major product (yield; 460mg, 0.656mmoles, 95% yield based on consumed GeH_4) and $Co_4(CO)_{12}$ and $Ge_2Co_6(CO)_{20}$ in relatively minor yields. From the volatile fraction, 51mg (0.67mmoles) of unreacted GeH_4 were recovered (thus 94% of total Ge can be accounted for).

In run 8, the infrared spectrum of the involatile products (see Table 5.5) indicated a considerably higher yield of $Ge_2Co_6(CO)_{20}$ (relative to $GeCo_4(CO)_{14}$) was obtained. Infrared absorbances (see section 4.2.1) indicated the approximate constitution of the solution to be 80% $GeCo_4(CO)_{14}$ to 20% $Ge_2Co_6(CO)_{20}$ (by molar quantities). Also present were small quantities of the 2094cm^{-1} species and a species with a prominent absorption at 2090cm^{-1}. This species was separated from the other components by vacuum sublimation. The infrared spectrum of this species and discussion of its characterisation, is dealt with in the following section. Overnight vacuum sublimation of the mixture resulted in decomposition due to an air leak in the apparatus.

From the volatile fraction were recovered, a quantity of unreacted GeH_4 (25mg, 0.33mmoles) and a small quantity

Table 5.5 Infrared Spectrum* of Products From $GeH_4/Co_2(CO)_8$ Reaction, Run 8, (1:1)

Peak (cm^{-1})	Rel.Int.	Assignment
2106	vw	$HGe\{Co(CO)_4\}_3$
2094	w	2094 species
2090 sh	w	$HGe\{Co(CO)_4\}_3$
2087	m	$Ge_2Co_6(CO)_{20}$
2079	s	$GeCo_4(CO)_{14}$
2068 sh	m	$Ge_2Co_6(CO)_{20}$
2060	vs	$GeCo_4(CO)_{14}$
2055 sh	m	$Ge_2Co_6(CO)_{20}$
2049 sh	w	?
2040	w	$GeCo_4(CO)_{14}$
2026 sh	w	$Ge_2Co_6(CO)_{20}$
2023	s	$GeCo_4(CO)_{14}$ + $Ge_2Co_6(CO)_{20}$
2019 sh	m	$HGe\{Co(CO)_4\}_3$
2006 sh	w	$GeCo_4(CO)_{14}$ + $Ge_2Co_6(CO)_{20}$
1848	w-m	$GeCo_4(CO)_{14}$
1844 sh	w	$Ge_2Co_6(CO)_{20}$

* CH_2Cl_2/C_6H_{14} solution.

of $GeH_3Co(CO)_4$ (6mg, 0.02mmoles).

Run 9.

Table 5.6 Incondensable Gases Produced During Reaction of Excess GeH_4 with $Co_2(CO)_8$.

Time (hours)	mmoles H_2	mmoles CO
$1\frac{1}{2}$	0.57	0.57
$24\frac{1}{2}$	0.84	0.74
73	1.18	0.92

5.2.2 Infrared Spectrum of Product Sublimed from Run 8.

The infrared spectrum of this species (see Fig. 5.1, Table 5.7) is consistent with assignment as a $XM^1\{Co(CO)_4\}_3$ species (43), (refer also to the spectra of $MeGe\{Co(CO)_4\}_3$ and $MeSn\{Co(CO)_4\}_3$ section 3.2.2.3). The number of, contours and positions of bands of the spectra of $MeGe\{Co(CO)_4\}_3$, $MeSn\{Co(CO)_4\}_3$ and this new compound match closely. The $3a_1 + 4e$ infrared active modes for the carbonyl stretches, are all observed, with a further two $\nu^{13}CO$ also observed.

The slight shift in position of the bands to higher frequency in the spectrum of the unknown compound compared to that of $MeGe\{Co(CO)_4\}_3$, is consistent with the replacement of a methyl group by a hydrogen (25). Thus the composition of the reactants, volatility, solubility and infrared spectrum of this compound is consistent with its tentative assignment as $HGe\{Co(CO)_4\}_3$.

5.2.3 Discussion.

In Gerlach's earlier experiment (27), $GeCo_4(CO)_{14}$ was

FIGURE 5.1 INFRARED SPECTRUM OF $HGe[Co(CO)_4]_3$.

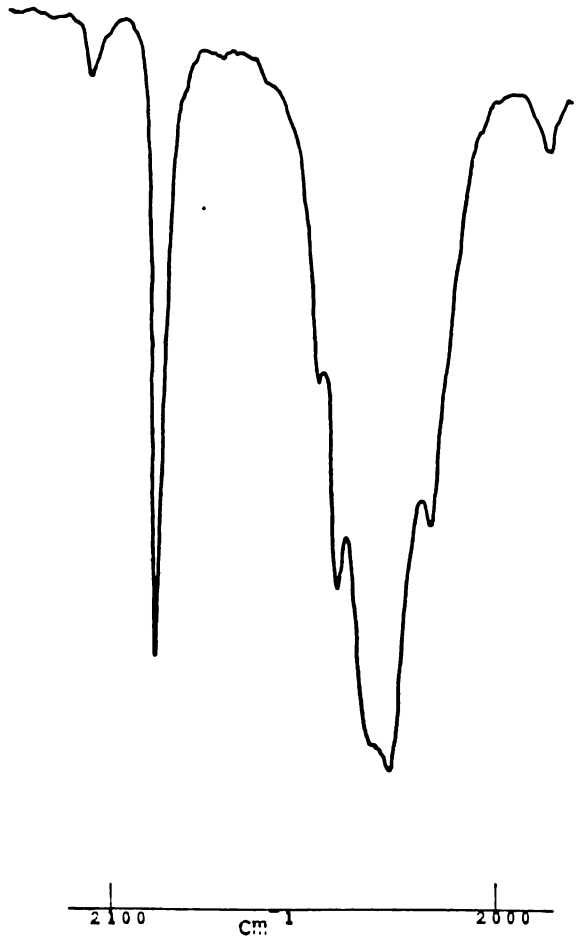

TABLE 5.7 INFRARED SPECTRUM OF $HGe[Co(CO)_4]_3$

2106 w	2019.5 vs
2088 s	2008 sh w
2040.5 sh m	2002 sh vw
2033.5 sh m-s	1971 vw
2024 sh s	

HEXANE SOLUTION

the only new product identified from the reaction of GeH_4 with $Co_2(CO)_8$ under the conditions used in this work. Small amounts of $Co_4(CO)_{12}$ were also observed. The experiments reported here confirm that $GeCo_4(CO)_{14}$ is the dominant product when the reaction ratio is $1GeH_4:2Co_2(CO)_8$, with yields of over 90% of purified product and only minor quantities of $Co_4(CO)_{12}$ observed. Other minor products have now been identified in this system and their proportions rise, especially when excess GeH_4 and long reaction times are used. However, $GeCo_4(CO)_{14}$ was always the major product.

The major reaction conforms to the stoichiometry of equation (1), and the

$$GeH_4 + 2Co_2(CO)_8 \longrightarrow GeCo_4(CO)_{14} + 2H_2 + 2CO \qquad (1)$$

small amounts of $Co_4(CO)_{12}$ can be dismissed as due to a minor side reaction. When the reactant ratio was 1 GeH_4 to 2 $Co_2(CO)_8$, the consumption of both reagents was very similar, although most reactions did not go absolutely to completion, with 2 - 8 % of the GeH_4 recovered and a little unreacted $Co_2(CO)_8$ observed. However, equation (1) does not appear to be an equilibrium, since the course of the reaction was not altered by removal of H_2 and CO (runs 3 and 4), nor by addition of CO at the beginning (run 5).

It has also been shown (46) that:

$$Ge\{Co(CO)_4\}_4 \longrightarrow GeCo_4(CO)_{14} + 2CO \qquad (2)$$

$\left\{\text{with no sign of the intermediate } \{(CO)_7Co_2\}Ge\{Co(CO)_4\}_2\right\}$ proceeds smoothly at room temperature. As no $Ge\{Co(CO)_4\}_4$ was identified as a product in these reactions, even when ca. 1 Atmosphere of CO was added (run 5), it appears that any equilibrium (in equation 2) must be much more in favour

of $GeCo_4(CO)_{14}$ than was the corresponding equilibrium for the methyl (or dimethyl) germane analogues (see sections 3.1.3 and 3.2.3) This is expected following the same arguments outlined in section 3.2.3 for methylgermanium - tricobalt species, i.e. increased steric crowding coupled with the large size of the Ge covalent radius, making increased Co-Co bonding favourable in the tetracobalt species.

The related reaction;

$$GeCo_4(CO)_{14} \longrightarrow GeCo_4(CO)_{13} + CO \qquad (3)$$

is also established (27), occuring slowly at 40°C in the absence of a solvent and more quickly in solution. No $GeCo_4(CO)_{13}$ was observed in this work under the conditions used (at room temperature) although it appears that the reaction (equation3) occurs very slowly at room temperature, as Gerlach, in his original report (27) observed a small quantity of $GeCo_4(CO)_{13}$ from the reaction of GeH_4 with $Co_2(CO)_8$ over a period of 16 weeks.

A new product, $Ge_2Co_6(CO)_{20}$, has been identified from the $GeH_4/Co_2(CO)_8$ reaction. This product was a minor component when the ratio of GeH_4:$Co_2(CO)_8$ was 1:2, but its yield increased when the reactant ratio was raised to 1:1 (i.e. excess of GeH_4) and the reaction time extended. Thus when a reaction time of 3 weeks was used, the 1:1 and the 1:2 reaction mixtures gave similar relative yields of $GeCo_4(CO)_{14}$ and $Ge_2Co_6(CO)_{20}$ (≃95% yield of $GeCo_4(CO)_{14}$ based on consumed GeH_4) and the excess GeH_4 remained unreacted. However when the reaction time was extended to 14 weeks a significantly increased yield of $Ge_2Co_6(CO)_{20}$ was observed. The possible formation of this species in this (and other reactions) is dealt with in chapter 8.

Further products have been identified in this reaction system. Thus $GeH_3Co(CO)_4$ and $HGe\{Co(CO)_4\}_3$ (if the assignment is accepted) have been isolated from the reaction of excess GeH_4 (1:1 reactant ratio, runs 7 and 8) with $Co_2(CO)_8$. These reactions must favour the formation of these partially substituted germanes, especially in the later stages as $Co_2(CO)_8$ is consumed and the proportion of hydride to $Co_2(CO)_8$ increases. The other product identified in these reactions was the $2094cm^{-1}$ species which remains uncharacterised although a possible structure is discussed in section 5.4.

5.3 Further Reactions of Ge_2H_6 with $Co_2(CO)_8$

5.3.1. Reaction in a 1:4 Ratio.

Ge_2H_6 (217mg, 1.44mmoles) and $Co_2(CO)_8$ (1960mg, 5.74mmoles) were allowed to react for 4 weeks and worked up as described in 2.5. The infrared spectrum of the involatile products (see Table 5.8) indicated the same products as for the 1:3 ratio reactions (see Chapter 4), however with a slightly lower relative yield of $Ge_2Co_6(CO)_{20}$ (relative to $GeCo_4(CO)_{14}$), such that the approximate composition of the solution was a 60:40 percent mixture (by molar ratios of $GeCo_4(CO)_{14}$: $Ge_2Co_6(CO)_{20}$).

From the volatile fraction, no Ge_2H_6 was observed but, 182mg (0.532mmoles) of unreacted $Co_2(CO)_8$ were recovered.

5.3.2 Reaction in a 1:2 Ratio.

Ge_2H_6 (262mg, 1.73mmoles) and $Co_2(CO)_8$ (1180mg, 3.47mmoles) were left to react (reaction ratio 1:2) for 6 weeks and worked up as described in 2.5. The infrared spectrum (see Table 5.9) of the involatile products showed considerably more $Ge_2Co_6(CO)_{20}$

Table 5.8 Infrared Spectrum* of the Involatile Products From the $Ge_2H_6/Co_2(CO)_8$ Reaction (1:4).

Peak (cm^{-1})	Rel.Int	Assignment
2094	vw	2094 species
2088	m	$Ge_2Co_6(CO)_{20}$
2080	s	$GeCo_4(CO)_{14}$
2069	s	$Ge_2Co_6(CO)_{20}$
2062	vs	$GeCo_4(CO)_{14}$ + $Co_4(CO)_{12}$
2054	s	$Ge_2Co_6(CO)_{20}$ + $Co_4(CO)_{12}$
2040	m-s	$GeCo_4(CO)_{14}$ + $Co_2(CO)_8$
2031	m-s	$Ge_2Co_6(CO)_{20}$ + $GeCo_4(CO)_{14}$
2028	w	$Ge_2Co_6(CO)_{20}$
2022	w-m	$GeCo_4(CO)_{14}$
2004	w	$Ge_2Co_6(CO)_{20}$ + $GeCo_4(CO)_{14}$
1865	w-m	$Co_4(CO)_{12}$ + $Co_2(CO)_8$
1854	w	$Co_2(CO)_8$
1848	w-m	$GeCo_4(CO)_{14}$ + $Ge_2Co_6(CO)_{20}$
1843 sh	w	$Ge_2Co_6(CO)_{20}$

* CH_2Cl_2/C_6H_{14} solution.

Table 5.9 Infrared Spectrum* of the Less Volatile Products From the $Ge_2H_6/Co_2(CO)_8$ Reaction (1:2)

Peak (cm^{-1})	Rel.Int.	Assignment
2110 sh		
2106 sh		$HGe\{Co(CO)_4\}_3$
2094 sh	s	2094 species
2090 sh		$HGe\{Co(CO)_4\}_3$
2087		$Ge_2Co_6(CO)_{20}$
2079	w	$Ge_2Co_6(CO)_{20}$
2069	vs	$Ge_2Co_6(CO)_{20}$
2063 sh		$GeCo_4(CO)_{14}$ + $Co_4(CO)_{12}$
2056 sh	s	$Ge_2Co_6(CO)_{20}$
2052		$Co_4(CO)_{12}$
2035		$Ge_2Co_6(CO)_{20}$
2026 sh br	m-s	+
2019 sh		$HGe\{Co(CO)_4\}_3$
2009 sh		$HGe\{Co(CO)_4\}_3$
2004 br	w	$Ge_2Co_6(CO)_{20}$
1865	vw	$Co_4(CO)_{12}$
1848 sh	vw	$GeCo_4(CO)_{14}$
1842	w	$Ge_2Co_6(CO)_{20}$
1835 sh	w	?

* CH_2Cl_2 solution

than $GeCo_4(CO)_{14}$, however there were also a relatively high quantity of $HGe\{Co(CO)_4\}_3$, and small quantities of the $2094cm^{-1}$ species, $Co_4(CO)_{12}$ and another species with a bridging carbonyl mode at $1835cm^{-1}$.

From the volatile fraction were identified a trace of $HCo(CO)_4$ and a quantity of $GeH_3Co(CO)_4$ (15mg, 0.06mmoles)

5.3.3 Effect of Added CO

Ge_2H_6 (215mg, 1.41mmoles), $Co_2(CO)_8$ (1450mg, 4.23mmoles) and ca. 1 Atmosphere pressure of added CO were left to react for $2\frac{1}{2}$ weeks and worked up as in 2.5. The infrared spectrum of the relatively involatile products, showed absorptions due to $GeCo_4(CO)_{14}$, $Ge_2Co_6(CO)_{20}$, $Co_4(CO)_{12}$ and the $2094cm^{-1}$ species in similar ratios as for the spectrum listed in Table 4.1 (for the Ge_2H_6:$Co_2(CO)_8$, 1:3 reaction). Also present are medium intensity absorptions attributed to $HGe\{Co(CO)_4\}_3$.

5.3.4 Sampling of the Reaction Mixture.

Ge_2H_6 (297mg, 1.96mmoles) and $Co_2(CO)_8$ (2020mg, 5.89mmoles) were allowed to react and the infrared spectrum of the reaction mixture run after 1, 9 and 20 days (see Table 5.10)

After 1 day the spectrum showed absorptions due to some $Ge_2Co_6(CO)_{20}$, little $GeCo_4(CO)_{14}$ and $HGe\{Co(CO)_4\}_3$ and a considerable quantity of $Co_4(CO)_{12}$. After 9 days, there was a considerable increase in $GeCo_4(CO)_{14}$ (relative to $Ge_2Co_6(CO)_{20}$ The final reaction mixture (after 20 days) can be compared with those obtained in Chapter 4 (see Table 4.1). It shows

Table 5.10 Infrared Spectra of Products From Reaction of $Ge_2H_6/Co_2(CO)_8$ at 1 Day, 9 Days and 20 Days.

1 day	9 days	20 days	Assignment
2105 vw	-	2104 vw	$HGe\{Co(CO)_4\}_3$
-	2094 w	2094 vw	2094 species
2090 w	-	2090 w	$HGe\{Co(CO)_4\}_3$
2087 m	2087 m	2087 w	$Ge_2Co_6(CO)_{20}$
2079 w	2079 m-s	2079 s	$GeCo_4(CO)_{14}$
2068 sh s	2068 sh m-s	2068 sh m-s	$Ge_2Co_6(CO)_{20} + Co_2(CO)_8$
2063 vs	2062 vs	2063 vs	$GeCo_4(CO)_{14} + Co_4(CO)_{12}$
2053 vs	2053 vs	2053 vs	$Ge_2Co_6(CO)_{20} + Co_4(CO)_{12}$
-	2038 sh m	2041 m-s	$GeCo_4(CO)_{14} + Co_2(CO)_8$
2026 s	2028 sh m	2028 m	$Ge_2Co_6(CO)_{20} + GeCo_4(CO)_{14}$
2022	2022 sh w	2022 sh w	$HGe\{Co(CO)_4\}_3$
2010 sh w	2010 sh w	2010 sh w	$HGe\{Co(CO)_4\}_3$
2004 sh w	2004 w	2004 w	$Ge_2Co_6(CO)_{20} + GeCo_4(CO)_{14}$
1866 m	1865 m	1865 s	$Co_4(CO)_{12} + Co_2(CO)_8$
1855 m			$Co_2(CO)_8$
1848 w-m	1848 w-m	1848 w-m	$GeCo_4(CO)_{14}$
1844 w-m	1844 w-m	1844 sh w	$Ge_2Co_6(CO)_{20}$

much less $Ge_2Co_6(CO)_{20}$ (relative to $GeCo_4(CO)_{14}$) and considerably more $Co_4(CO)_{12}$.

5.3.5 Discussion.

The reaction of Ge_2H_6 with $Co_2(CO)_8$ has been re-examined with certain aspects of the reaction studied.

It appears that a certain amount of control of the reaction can be exercised by changing the reactant ratios. Thus changing the reactant ratio from 1:3 to 1:4 (Ge_2H_6:$Co_2(CO)_8$) appeared to give a slightly increased yield of $GeCo_4(CO)_{14}$ (which is stoichiometrically more favoured by this reactant ratio) and by lowering the reactant ratio to 1:2 appeared to increase the yield of $Ge_2Co_6(CO)_{20}$ relative to $GeCo_4(CO)_{14}$, although in this latter case other products resulting from partial substitution (due to the overall deficit of $Co_2(CO)_8$ used) were also observed. Further work on these reactions using more varied reactant ratios, to study more aspects of this control, in particular the quantitative determination of the product yields, is needed.

Changes in the partial pressure of CO, either by removing (see section 4.2.1, run 4) or adding CO had little effect on the reaction of Ge_2H_6 with $Co_2(CO)_8$, although $HGe\{Co(CO)_4\}_3$ was observed as a product when the reaction was carried out in increased CO concentration. This probably arises due to incomplete reaction. This may be due to the relatively short reaction time (of $2\frac{1}{2}$ weeks) or possibly due to CO retardation of the reaction. CO retardation is consistent with the measurement of the incondensable gases (see Table 4.2) which indicated all the Ge-H had reacted

after 14 days. Note that in this case the quantity of CO present was considerably smaller due to the periodic removal and measurement of the incondensable gases.

The sampling of the reaction mixture after 24 hours reaction time ultimately led to the formation of a considerable quantity of $Co_4(CO)_{12}$ and only relatively small quantities of $Ge_2Co_6(CO)_{20}$ and $GeCo_4(CO)_{14}$ as final products. The most likely explanation for this is, at this stage of the reaction, extremely air-sensitive species are present, which upon exposure to only very low levels of air, oxidise rapidly forming $Co_4(CO)_{12}$.

5.4 Reactions of Other Polygermanes

5.4.1 Reaction of Ge_3H_8

Ge_3H_8 (42mg, 0.19mmoles) and $Co_2(CO)_8$ (315mg, 0.921mmoles) were left to react (reactant ratio 1:4.8) for 3 weeks and worked up as in 2.5. The infrared spectrum of the involatile products (see Table 5.11) shows $GeCo_4(CO)_{14}$ and $Ge_2Co_6(CO)_{20}$ in approximately the same ratios as for the $Ge_2H_6/Co_2(CO)_8$ (1:3) reaction (see Section 4.2.1) i.e. roughly 50/50 molar ratio solution. Also present are, a slightly increased yield (relative to Ge_2H_6 reaction) of the $2094cm^{-1}$, some unreacted $Co_2(CO)_8$ and some $Co_4(CO)_{12}$.

Recrystallisation of these products at 4^0C from a CH_2Cl_2 solution, gave a small quantity (ca. 5-10mg) of a pure sample of the $2094cm^{-1}$ species.

Table 5.11 Infrared Spectrum* of Involatile Products From $Ge_3H_8/Co_2(CO)_8$ Reaction.

Peak (cm^{-1})	Rel.Int.	Assignment
2094	w	2094 species
2088	m	$Ge_2Co_6(CO)_{20}$
2079	m	$GeCo_4(CO)_{14}$
2068	vs	$Ge_2Co_6(CO)_{20}$ + $Co_2(CO)_8$
2063	vs	$GeCo_4(CO)_{14}$ + $Co_4(CO)_{12}$
2054	vs	$Ge_2Co_6(CO)_{20}$ + $Co_4(CO)_{12}$
2041	vs	$GeCo_4(CO)_{14}$ + $Co_2(CO)_8$
2027 sh	sm	$Ge_2Co_6(CO)_{20}$ + $GeCo_4(CO)_{14}$
2021	s	$Ge_2Co_6(CO)_{20}$ + $Co_2(CO)_8$
2003	vw	$Ge_2Co_6(CO)_{20}$ + $GeCo_4(CO)_{14}$
1816	m-s	$Co_4(CO)_{12}$ + $Co_2(CO)_8$
1855	m-s	$Co_2(CO)_8$
1848	m	$GeCo_4(CO)_{14}$
1843	m	$Ge_2Co_6(CO)_{20}$

* C_6H_{14}/CH_2Cl_2 solution.

5.4.2. Handling and Infrared Spectrum of the 2094cm^{-1} Species.

The 2094cm^{-1} species is a dark moderately air-sensitive solid barely soluble in hexane or dichloromethane. Its infrared spectrum is shown in Fig. 5.2 and listed in Table 5.12. This spectrum is similar to the spectra of $Ge_2Co_6(CO)_{20}$ and $GeCo_4(CO)_{14}$ (see Section 4.3.2) in contours and positions of bands.

5.4.3 Reaction of $(GeH_3)_2SiMe_2$

Run 1:

$(GeH_3)_2SiMe_2$ (188mg, 0.90mmoles) and $Co_2(CO)_8$ (1080mg, 3.15mmoles) were left to react (ratio 1:3.5) for 2½weeks as described in 2.5. To the relatively involatile products were added 10ml of hexane. The infrared spectrum of the dissolved solids (Table 5.13), shows bands due to $GeCo_4(CO)_{14}$, $Ge_2Co_6(CO)_{20}$, $Me_2SiHCo(CO)_4$, $Me_2SiCo_4(CO)_{14}$ and $Co_4(CO)_{12}$.

The remaining bulk of the solid was dissolved in 10ml of CH_2Cl_2 to give an infrared spectrum showing it to be virtually pure $Ge_2Co_6(CO)_{20}$, contaminated with traces of $GeCo_4(CO)_{14}$ and $Co_4(CO)_{12}$.

Recrystallisations from CH_2Cl_2/C_6H_{14}, yielded; 863mg (0.815mmoles) of $Ge_2Co_6(CO)_{20}$ (91% yield based on $(GeH_3)_2SiMe_2$) and 58mg (0.083mmoles) of $GeCo_4(CO)_{14}$ (4.6% yield).

Run 2.

$(GeH_3)_2SiMe_2$ (125mg, 0.598mmoles) and $Co_2(CO)_8$ (1020mg, 2.99mmoles) were left to react (ratio 1:5) in hexane for 5 weeks and worked up as in 2.5. The infrared spectra of

FIGURE 5.2 INFRARED SPECTRUM OF THE 2094 cm^{-1} SPECIES.

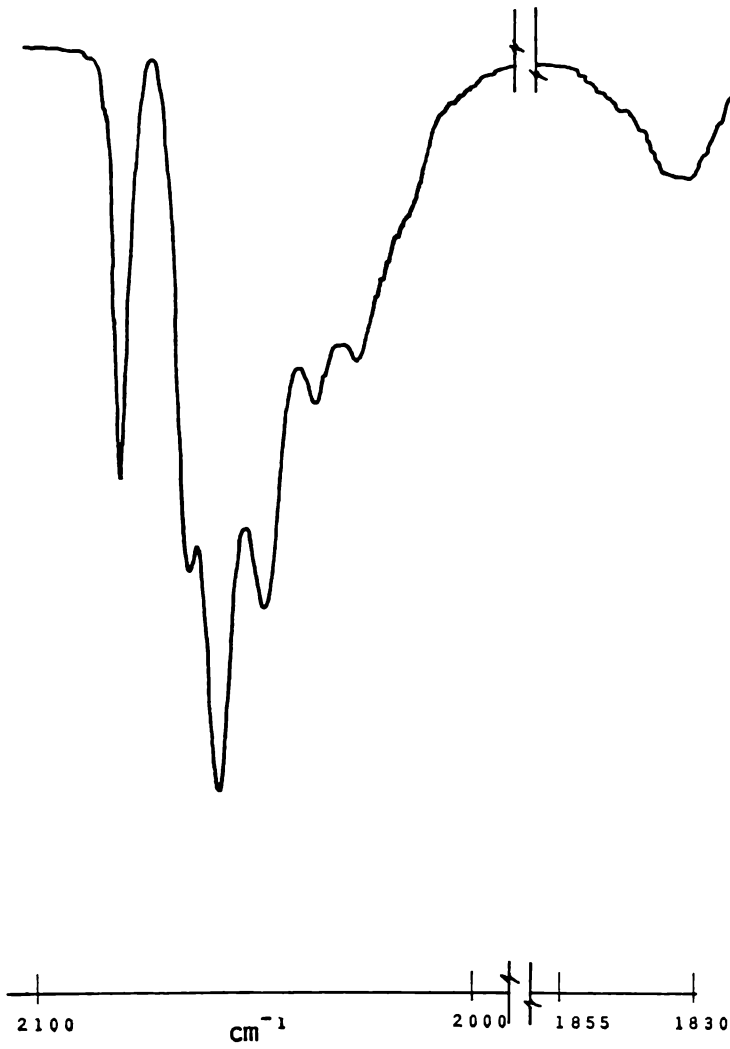

TABLE 5.12 INFRARED SPECTRUM OF THE 2094 cm^{-1} SPECIES.

2094 s	2038 m
2073 s	2027 m
2065 vs	2011 sh w
2052.5 s	1833 br w

DICHLOROMETHANE SOLUTION

Table 5.13 Infrared Spectrum* of Hexane Soluble Products From $(GeH_3)_2SiMe_2/Co_2(CO)_8$ Reaction.

Peak (cm^{-1})	Rel.Int	Assignment
2104 sh	vw	$Me_2SiCo_4(CO)_{14}$
2096 sh	vw	$Me_2SiCo_4(CO)_{14}$
2092	w	$Me_2SiHCo(CO)_4$
2087	m	$Ge_2Co_6(CO)_{20}$
2079	s	$GeCo_4(CO)_{14}$
2068	s	$Ge_2Co_6(CO)_{20} + Co_2(CO)_8$
2062	vs	$GeCo_4(CO)_{14} + Co_4(CO)_{12}$
2054	vs	$Ge_2Co_6(CO)_{20} + Co_4(CO)_{12}$
2041	s	$GeCo_4(CO)_{14} + Co_2(CO)_8$
2033 sh	w	$Ge_2Co_6(CO)_{20} + GeCo_4(CO)_{14}$
2030	m	$Me_2SiHCo(CO)_4 + Me_2SiCo_4(CO)_{14}$
2022	w-m	$GeCo_4(CO)_{14} + Co_2(CO)_8$
2006	m	$Me_2SiHCo(CO)_4$
2004 sh	vw	$Ge_2Co_6(CO)_{20} + GeCo_4(CO)_{14}$
1995	s	$Me_2SiHCo(CO)_4$
1866	s	$Co_4(CO)_{12} + Co_2(CO)_8$
1854	w-m	$Co_2(CO)_8$
1848	w-m	$GeCo_4(CO)_{14}$
1844 sh	w	$Ge_2Co_6(CO)_{20}$

* Hexane solution.

the hexane and dichloromethane solutions (as in Run 1) were similar to those obtained in Run 1, indicating similar products and relative yields.

5.4.4 Discussion.

The reaction of $(GeH_3)_2SiMe_2$ with $Co_2(CO)_8$ has been shown to be a good synthetic method for obtaining near quantitative yields of $Ge_2Co_6(CO)_{20}$, as an easily separable component from the other products of reaction, $GeCo_4(CO)_{14}$, $Me_2SiCo_4(CO)_{14}$ and $Me_2SiHCo(CO)_4$.

The reaction of Ge_3H_8 with $Co_2(CO)_8$ yields $GeCo_4(CO)_{14}$ and $Ge_2Co_6(CO)_{20}$ in a roughly 50/50 percent molar mixture (by infrared absorbances), similar to that obtained from the $Ge_2H_6/Co_2(CO)_8$ (1:3) reaction (see Chapter 4).

The major products and yields from these reactions can be rationalised using the following argument: Initial reaction of $Co_2(CO)_8$ with the hydride leads to the formation of a pentametallic ring species.

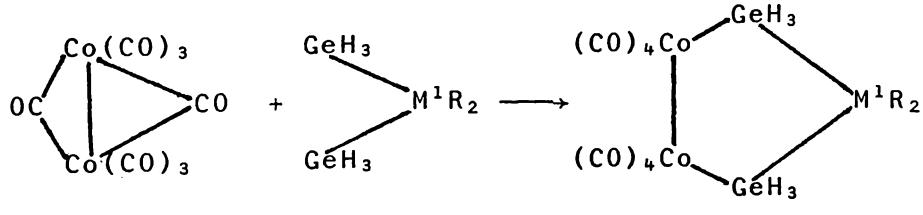

This species can then expel the M^1R_2 central group, and the $GeCo_2Ge$ linked species can condense to ultimately form $Ge_2Co_6(CO)_{20}$.

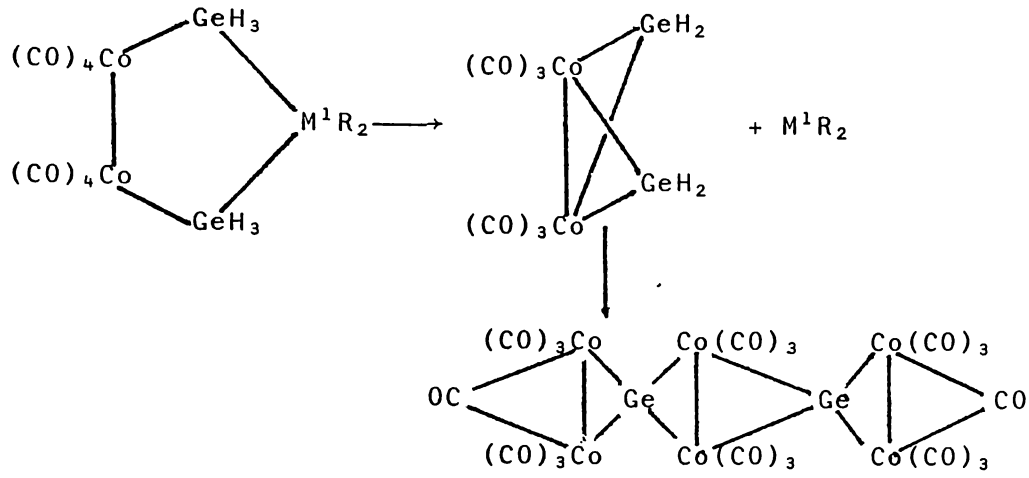

Thus for the Ge_3H_8 reaction, while one mole of Ge_3H_8 would be expected to give one mole of $Ge_2Co_6(CO)_{20}$, it would also give one mole of $GeCo_4(CO)_{14}$ from expulsion of the central GeH_2 group. Experimentally this is observed with a 50/50 percent molar mixture of the two products observed.

The observation of $Me_2SiHCo(CO)_4$ as a product in the $(GeH_3)_2SiMe_2$ reaction suggests that in this reaction (at least) the central group is expelled as Me_2SiH_2, thus the mechanism is likely to be more complex than the above simplistic one.

Competing with this major process must be other minor processes. The apparently higher yield of the $2094cm^{-1}$ species in the Ge_3H_8 reaction (relative to the $Ge_2H_6$and GeH_4 reactions) parallels the higher yield of $Ge_2Co_6(CO)_{20}$ from the Ge_2H_6 reaction (relative to the GeH_4 reaction). Although we could not characterise the $2094cm^{-1}$ species, it is useful to speculate on a possible structure. The above parallel, combined with the similarity between the infrared spectra of this species, $Ge_2Co_6(CO)_{20}$ and $GeCo_4(CO)_{14}$ and its relative insolubility, suggest the $2094cm^{-1}$ species may be the higher homologue of the $Ge_2Co_6(CO)_{20}$ and $GeCo_4(CO)_{14}$ series, $Ge_3Co_8(CO)_{26}$, with an additional $GeCo_2(CO)_6$ unit (to $Ge_2Co_6(CO)_{20}$).

CHAPTER 6 The Reactions of Group IVB Hydrides With Germanium Cobalt Carbonyls.

6.1 General

The evidence from previous chapters suggested that germanium hydrides react with species in the reaction system other than $Co_2(CO)_8$. This chapter is concerned with the reactions of some Si, Ge and Sn hydrides with species related to $Co_2(CO)_8$, namely $GeCo_4(CO)_{14}$, $MeGeCo_3(CO)_{11}$ and $Me_2GeCo_2(CO)_7/Me_2Ge\{Co(CO)_4\}_2$.

All new species resulting from these reactions are discussed in this chapter, except $(Me\ Ge)_2Co_4(CO)_{11}$ which was characterised by x-ray crystallography and is discussed in chapter 7. Discussion of the reactions (including possible mechanisms) is dealt with in chapter 8.

6.2 The Reaction of GeH_4 With $GeCo_4(CO)_{14}$

$GeCo_4(CO)_{14}$ (200mg, 0.28mmoles) and GeH_4 (82mg, 1.07 mmoles) were left to react for 6 weeks and worked up as in section 2.5. The infrared spectrum of the involatile products (see Table 6.1) shows absorptions due mainly to unreacted $GeCo_4(CO)_{14}$, with some $Ge_2Co_6(CO)_{20}$, a noticeably higher yield of the $2094cm^{-1}$ species, some $HGe\{Co(CO)_4\}_3$ (see section 5.2.2) and an unidentified species with a prominent infrared band at $2102cm^{-1}$. From this, 172mg (0.245 mmoles) of $GeCo_4(CO)_{14}$ were recovered.

From the volatile fraction were recovered 76mg (0.99 mmoles) of unreacted GeH_4.

Table 6.1 Infrared Spectrum* of the Involatile Products From the $GeH_4/GeCo_4(CO)_{14}$ Reaction.

Peak (cm^{-1})	Rel.Int	Assignment
2102	vw	?
2094	w	2094 species
2087	w-m	$Ge_2Co_6(CO)_{20}$
2079	s	$GeCo_4(CO)_{14}$
2068 sh	m	$Ge_2Co_6(CO)_{20}$
2061	vs	$GeCo_4(CO)_{14}$
2040	m-s	$GeCo_4(CO)_{14}$
2032	s	$GeCo_4(CO)_{14}$ + $Ge_2Co_6(CO)_{20}$
2023	m	$GeCo_4(CO)_{14}$
2004	w	$GeCo_4(CO)_{14}$ + $Ge_2Co_6(CO)_{20}$
1848	m	$GeCo_4(CO)_{14}$
1844 sh	vw	$Ge_2Co_6(CO)_{20}$

* C_6H_{14}/CH_2Cl_2 solution.

6.3 The Reaction of Me_2GeH_2 With $GeCo_4(CO)_{14}$

6.3.1 Experimental

Run 1:

$GeCo_4(CO)_{14}$ (322mg, 0.459mmoles) and Me_2GeH_2 (72mg, 0.69mmoles) were left to react for 7 weeks and worked up as in 2.5. The infrared spectrum of the involatile products (Table 6.2) shows a spectrum of virtually pure $Me_2Ge_2Co_4(CO)_{13}$ (see next section for characterisation), contaminated with a trace of unreacted $GeCo_4(CO)_{14}$.

23mg (0.22mmoles) of unreacted Me_2GeH_2 were recovered from the volatile fraction.

Run 2.

$GeCo_4(CO)_{14}$ (535mg, 0.763mmoles) and excess Me_2GeH_2 (180mg, 1.72mmoles) were left to react for 12 weeks and worked up as in 2.5. The infrared spectrum of the involatile products was similar to that obtained in run 1, i.e. consisting of virtually pure $Me_2Ge_2Co_4(CO)_{13}$ with a trace of unreacted $GeCo_4(CO)_{14}$.

From the volatile fraction were recovered ≃110mg (≃1.05mmoles) of Me_2GeH_2 (contaminated with a trace of Hexane).

6.3.2 Handling of $Me_2Ge_2Co_4(CO)_{13}$

$Me_2Ge_2Co_4(CO)_{13}$ is an orange solid which is stable at room temperature in the absence of air. $Me_2Ge_2Co_4(CO)_{13}$ decomposes in air, however it may be handled for short periods in air with little appreciable decomposition. Its solubility

Table 6.2 Infrared Spectrum* of Products From the $Me_2GeH_2/GeCo_4(CO)_{14}$ Reaction.

Peak (cm^{-1})	Rel.Int	Assignment
2096	m	$Me_2Ge_2Co_4(CO)_{13}$
2080	w	$GeCo_4(CO)_{14}$
2064	vs	$Me_2Ge_2Co_4(CO)_{13}$
2053	vs	$Me_2Ge_2Co_4(CO)_{13}$
2042	vs	$Me_2Ge_2Co_4(CO)_{13}$
2040	w	$GeCo_4(CO)_{14}$
2027	m	$Me_2Ge_2Co_4(CO)_{13}$
2020 sh	w	$Me_2Ge_2Co_4(CO)_{13}$
2014	s	$Me_2Ge_2Co_4(CO)_{13}$
2006	vvw	$GeCo_4(CO)_{14}$
2002	w	$Me_2Ge_2Co_4(CO)_{13}$
1987	w	$Me_2Ge_2Co_4(CO)_{13}$
1842	m	$Me_2Ge_2Co_4(CO)_{13}$

* C_6H_{14}/CH_2Cl_2 solution.

in organic solvents appears to be similar to that of $GeCo_4(CO)_{14}$, i.e. it is moderately soluble in non-polar solvents such as hexane and significantly more so in more polar solvents such as dichloromethane.

6.3.3 Mass Spectrum of $Me_2Ge_2Co_4(CO)_{13}$

The mass spectrum of $Me_2Ge_2Co_4(CO)_{13}$ (Table 6.3) shows a parent ion at m/e = 770-782, $\{C_{15}H_6O_{13}Co_4Ge_2\}$ and an intense series of ions corresponding to the stepwise loss of 13 CO groups from a $Me_2Ge_2Co_4$ skeleton (59% of the total ion current is carried by this series). Ions resulting from the loss of one methyl and of two methyl groups from the Ge_2Co_4 metal skeleton are only of significant intensity when most of the CO has been lost, (note however that peaks arising from loss of 2 Me groups overlap with those from CO loss from the skeleton). Ions retaining the Ge_2Co_4 metal skeleton carry 80% of the total ion current, which is a similar proportion to that observed for $Ge_2Co_6(CO)_{20}$ (see section 4.3.1). Ge loss is common only when Co has also been lost.

6.3.4 Infrared Spectrum

The replacement of a bridging CO group in $Ge\{Co_2(CO)_7\}_2$ by a Me_2Ge group, reduces the symmetry to C_s. Although $GeCo_4(CO)_{14}$ has C_2 symmetry in the solid phase (57), the observed terminal carbonyl stretching frequencies match those expected for the idealised D_{2d} symmetry of the unit, ignoring the bridging CO groups. Thus only 5 terminal CO stretching bands were observed. In $Me_2Ge_2Co_4(CO)_{13}$, considerably more

Table 6.3 Mass Spectrum of $Me_2Ge_2Co_4(CO)_{13}$

m/e	rel. int	Assignment
770-782	17	$Me_2Ge_2Co_4(CO)_x$, x = 13
742-754	14	x = 12
714-726	17	x = 11
686-698	25	x = 10
658-670	23	x = 9
630-642	34	x = 8
602-614	100	x = 7
574-586	93	x = 6
546-558	57	x = 5
518-530	23	x = 4
490-502	42	x = 3
462-474	51	x = 2
434-446	39	x = 1
400-418	77	x = 0
755-767	1	$MeGe_2Co_4(CO)_x$, x = 13
727-739	1	x = 12
699-711	0	x = 11
671-683	2	x = 10
643-655	2	x = 9
615-627	2	x = 8
587-599	1	x = 7
559-571	2	x = 6
531-543	3	x = 5
503-515	10	x = 4
475-487	18	x = 3
447-459	21	x = 2
419-431	8	x = 1
391-403	73	x = 0
376-388	71	$Ge_2Co_4^+$

Table 6.3 Cont'd ...

347-359	15	$Me_2Ge_2Co_3^+$
332-344	24	$MeGe_2Co_3^+$
317-329	27	$Ge_2Co_3^+$
306-312	7	$GeCo_4^+$
288-300	3	$Me_2Ge_2Co_2^+$
273-285	20	$MeGe_2Co_2^+$
258-270	23	$Ge_2Co_2^+$
247-259	3	$GeCo_3^+$
229-241	2	$Me_2Ge_2Co^+$
214-226	7	$MeGe_2Co^+$
199-211	19	Ge_2Co^+
188-194	8	$GeCo_2^+$
100-106	19	Me_2Ge^+
85-91	31	$MeGe^+$
70-76	12	Ge^+

bands were observed (see Fig. 6.1 and Table 6.4) due to the lowering of symmetry.

For C_s symmetry are predicted, 12 infrared active modes for the terminal CO stretches ($6a^1 + 6a^{11}$) and of these at least 9 are observed, with the possibility of a further band (if this is not regarded as a ^{13}CO band).

Alternatively, if the spectrum is regarded as a combination of the spectra of $(Me_2Ge)_2Co_2(CO)_6$ and $Me_2GeCo_2(CO)_7$ (see Fig. 3.1 and Table 3.1), then 9 terminal CO stretching bands would be found if overlap of bands within 2-3cm^{-1} resulted in one observed band. This treatment appears to give a good assignment.

One point to note here is that the highest observed band for $Me_2Ge_2Co_4(CO)_{13}$ is considerably higher (at 2096cm^{-1}) than for $Me_2GeCo_2(CO)_7$ (at 2087cm^{-1}), (both molecules are of C_s symmetry and thus there should be no infrared inactive modes). This indicates the coupling of CO modes across the central Ge in $Me_2Ge_2Co_4(CO)_{13}$ and shows the molecule is best treated as a whole.

The spectrum of $Me_2Ge_2Co_4(CO)_{13}$ also supports the suggestion that the simple observed spectrum of $GeCo_4(CO)_{14}$ (57), results from idealised D_{2d} symmetry in solution rather than having no coupling of CO group vibrations across the central Ge.

6.3.5 X-Ray Crystallography Study.

Crystals of $Me_2Ge_2Co_4(CO)_{13}$ were grown as described in section 2.3. Preliminary precession photography using Ni-filtered Cu-Kα X-radiation indicated the crystal to be tetragonal with space group either $P4_12_12$ or $P4_32_12$, with Z=8.

FIGURE 6.1 INFRARED SPECTRUM OF $Me_2Ge_2Co_4(CO)_{13}$

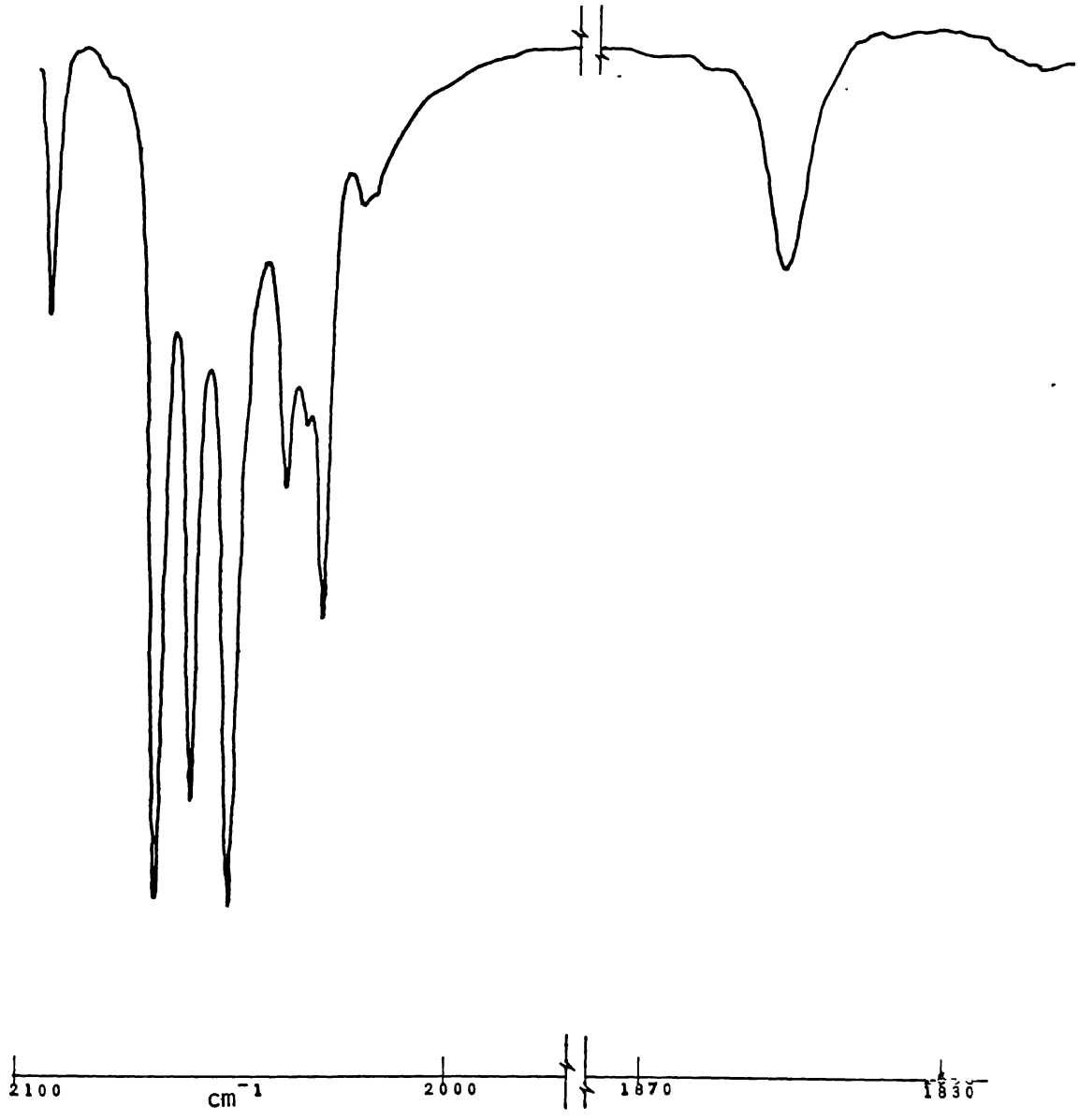

TABLE 6.4 INFRARED SPECTRUM OF $Me_2Ge_2Co_4(CO)_{13}$

2096 m	2016 s
2064 vs	2002 w
2054 vs	1987 w
2043 vs	
2027 m	1843 m
2021 sh w	

C_6H_{14} / CH_2Cl_2 SOLUTION

FIGURE 6.2 PROPOSED STRUCTURE OF $Me(X)Ge_2Co_4(CO)_{13}$.

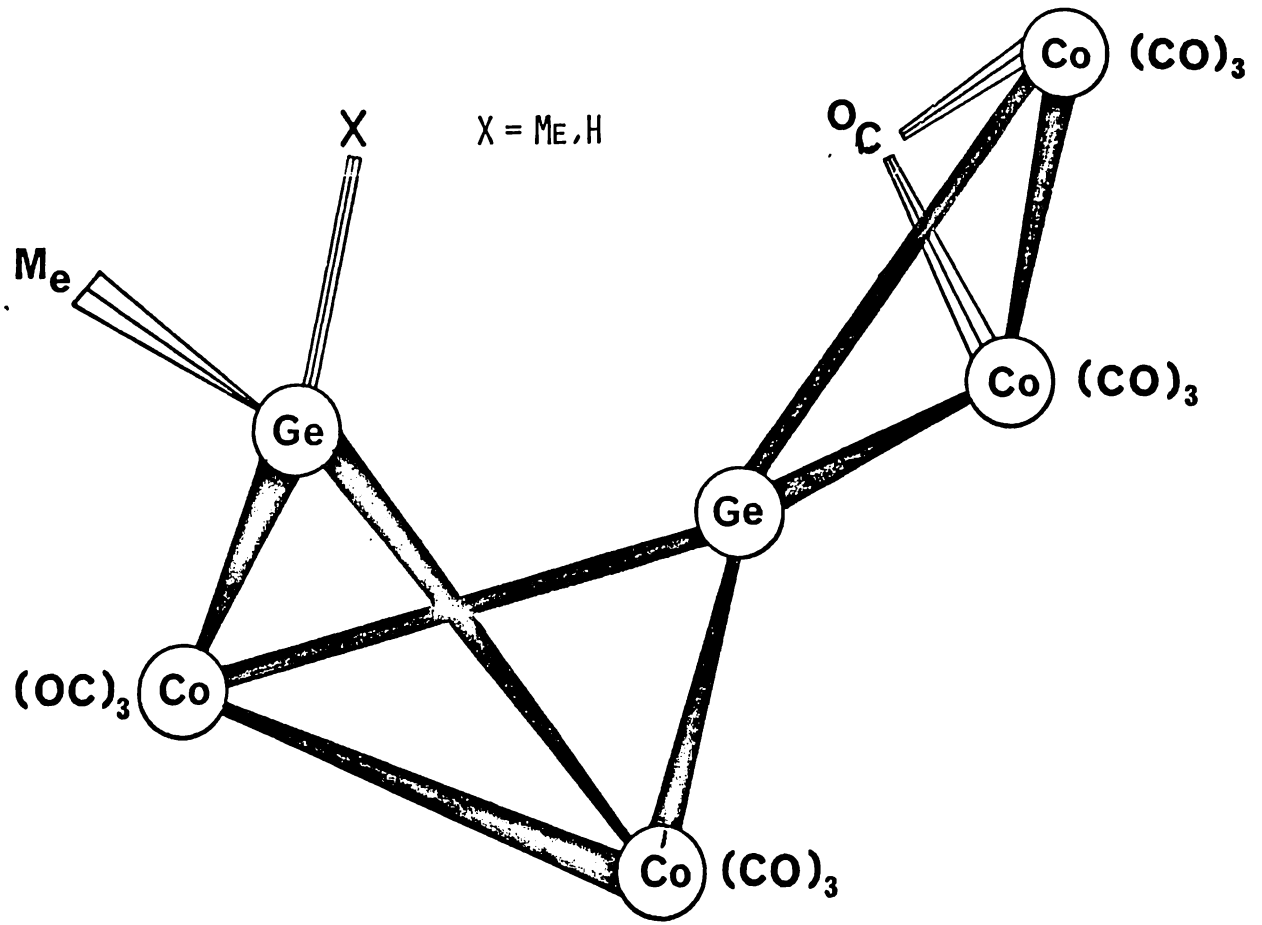

Table 6.5 Preliminary Determination of Crystal Parameters for $Me_2Ge_2Co_4(CO)_{13}$

$C_{15}H_6Co_4Ge_2O_{13}$

M_{calc} = 775.2

Tetragonal, Space Group $P4_12_12$ or $P4_32_12$

a = b = 11.93 $\alpha = \beta = \gamma = 90^0C$

c = 34.01

U = 4840

Assumed $\rho \simeq 2$ Z = 8

Unfortunately instrumental delays meant that the first crystal had decomposed so a second one was rushed to Auckland for the full study. Data and lattice parameters for this crystal were obtained using an Enraf-Nonius CAD 4 diffractometer with graphite-monochromated Mo-Kα radiation. The lattice parameters obtained, closely matched those determined by precession photography (Table 6.5)

The solution of the heavy metal skeleton offered by the program MULTAN for space group $P4_12_12$ was as expected for this structure (see Fig.6.2), with bond lengths and angles consistent with those for related compounds (e.g. $GeCo_4(CO)_{14}$, ref 57). Refinement of this solution by the program SHELX led to location of all but one of the CO groups and both methyl carbon atoms, but only with difficulty. Finally the refinement converged at R = 0.18.

At this stage the data were checked and found to be inconsistent with the determined space group. Attempts to obtain a solution in other space groups more consistent with the data failed. Further precession photographs on a new crystal confirmed the original space group.

It appears that the data were incorrect due most probably to collection from a twinned crystal.

6.3.6 Discussion.

The infrared and mass spectral evidence are consistent with formulation of the compound as $Me_2Ge_2Co_4(CO)_{13}$.

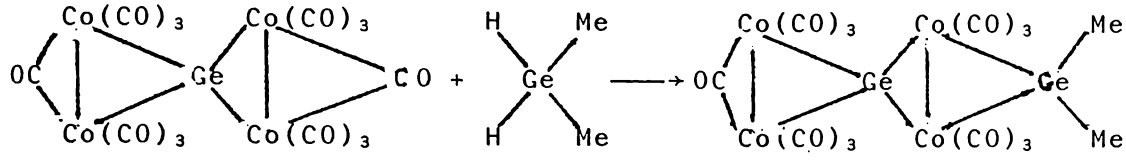

$+ H_2 + CO$

Extrapolation from related reaction systems, in particular the $Me_2GeH_2/Co_2(CO)_8$ system (see section 3.2) strongly suggests that this compound results from the displacement of a bridging CO group in $GeCo_4(CO)_{14}$ by a Me_2Ge group to give a structure as shown in Fig. 6.2.

This is further supported by the crystallographic solution offered by MULTAN which is strongly in favour of the above structure. The lattice parameters obtained by the diffractometer are close to those obtained by precession photography, suggesting the crystal used for collection of data was not grossly twinned. Although the data were good enough to obtain an acceptable solution of the heavy metal atoms, the twinning prevented the correct location of the lighter atoms and refinement of the structure.

6.4. Reaction of $MeGeH_3$ With $GeCo_4(CO)_{14}$

6.4.1 Experimental.

Run 1.

$MeGeH_3$ (96mg, 1.1mmoles) and $GeCo_4(CO)_{14}$ (830mg, 1.18 mmoles) were left to react for 25 weeks and worked up as described in section 2.5. The involatile products were dissolved in CH_2Cl_2 and an infrared spectrum run (see Table 6.6). This shows absorptions due to $GeCo_4(CO)_{14}$, $Ge_2Co_6(CO)_{20}$, $Co_4(CO)_{12}$ and a species with a prominent absorption at $2034cm^{-1}$ and species with weaker absorptions at $2092cm^{-1}$ and $2098cm^{-1}$.

The crystals obtained from a recrystallisation of this solution were found to be enriched in $Ge_2Co_6(CO)_{20}$ and the $2034cm^{-1}$ and $2092cm^{-1}$ species. Further recrystallisations enabled a pure sample (≈20-30mg) of the $2034cm^{-1}$ species to be obtained. This was characterised by X-ray crystallography and found to be the new cluster $(MeGe)_2Co_4(CO)_{11}$ (see chapter 7).

From the volatile fraction were recovered 17mg (0.06mmole) of $MeGeH_2Co(CO)_4$ and 20mg (0.22mmole) of $MeGeH_3$.

Run 2.

$MeGeH_3$ (53mg, 0.58mmoles) and $GeCo_4(CO)_{14}$ (289mg, 0.41 mmoles) were left to react and the reaction mixture sampled, for infrared spectroscopy, after 9 days, 4 weeks and 10 weeks (see Table 6.7). The spectra showed the gradual increase in concentration of a species whose infrared absorptions closely parallel those of $Me_2Ge_2Co_4(CO)_{13}$. A mass spectrum of this species (in a mixture with $GeCo_4(CO)_{14}$), indicated

Table 6.6 Infrared Spectrum* of Products From $MeGeH_3/GeCo_4(CO)_{14}$ Reaction (Run 1).

Peak (cm^{-1})	Rel.Int.	Assignment
2100	vvw	?
2098	vw	$Me(H)Ge_2Co_4(CO)_3$
2092	w	?
2086	w-m	$Ge_2Co_6(CO)_{20}$
2079	w	$GeCo_4(CO)_{14}$
2068	s	$Ge_2Co_6(CO)_{20}$ + $Me(H)Ge_2Co_4(CO)_{13}$
2062	s	$GeCo_4(CO)_{14}$ + $Co_4(CO)_{12}$
2054	s	$Ge_2Co_6(CO)_{20}$ + $Co_4(CO)_{12}$
2040	w	$GeCo_4(CO)_{14}$
2034	m	$(MeGe)_2Co_4(CO)_{11}$
2026	w	$(MeGe)_2Co_4(CO)_{11}$
2020	m	$Ge_2Co_6(CO)_{20}$ + $Me(H)Ge_2Co_4(CO)_{13}$
2011 sh	w	$Me(H)Ge_2Co_4(CO)_{13}$
2005 sh	vw	$Ge_2Co_6(CO)_{20}$ + $GeCo_4(CO)_{14}$
2000 sh	vw	$Me(H)Ge_2Co_4(CO)_{13}$
1865	m	$Co_4(CO)_{12}$
1848 sh	w	$GeCo_4(CO)_{14}$ + $(MeGe)_2Co_4(CO)_{11}$
1842	w-m	$Ge_2Co_6(CO)_{20}$ + $Me(H)Ge_2Co_4(CO)_{13}$

* C_6H_4/CH_2Cl_2 solution.

Table 6.7 Infrared Spectrum* of Products of the $MeGeH_3$/ $GeCo_4(CO)_{14}$ Reaction (Run 2), After 9 Days 4 Weeks and 10 Weeks.

9 days	4 weeks	10 weeks	Assignment
2105 vvw			?
2098 vw	2098 w	2099 w-m	$Me(H)Ge_2Co_4(CO)_{13}$
2079 s	2079 s	2079 s	$GeCo_4(CO)_{14}$
2068 sh w	2068 w-m	2068 vs	$Me(H)Ge_2Co_4(CO)_{13}$
2061 vs	2061 vs	2061 vs	$GeCo_4(CO)_{14}$
2057 sh vw	2057 sh w	2056 sh s	$Me(H)Ge_2Co_4(CO)_{13}$
2047 sh w	2047 m	2047 sh vs	$Me(H)Ge_2Co_4(CO)_{13}$
2040 m	2042 m	2043 vs	$GeCo_4(CO)_{14}$
2031 s	2031 s	2031 m	$GeCo_4(CO)_{14}$
2021 m	2021 m	2021 s	$GeCo_4(CO)_{14} + Me(H)Ge_2Co_4(CO)_{13}$
	2010 sh w	2011 sh m	$Me(H)Ge_2Co_4(CO)_{13}$
2005 sh w	2005 sh w	2004 sh vw	$GeCo_4(CO)_{14}$
	2000 sh vw	2000 sh vw	$Me(H)Ge_2Co_4(CO)_{13}$
1848 m-s	1848 m-s	1848 sh w	$GeCo_4(CO)_{14}$
	1842 sh w	1842 w-m	$Me(H)Ge_2Co_4(CO)_{13}$

* C_6H_{14} /CH_2Cl_2 solution

a parent ion corresponding to $Me(H)Ge_2Co_4(CO)_{13}$ (see following sections). A small quantity of $GeCo_4(CO)_{13}$ is also observed in the spectrum.

Lack of time prevented following this reaction to a further stage.

6.4.2 Mass Spectrum of $Me(H)Ge_2Co_4(CO)_{13}$

This compound was never isolated pure and the mass spectrum thus shows ions due not only to $Me(H)Ge_2Co_4(CO)_{13}$ but also to $GeCo_4(CO)_{14}$ and possibly $Ge_2Co_6(CO)_{20}$. The most significant (and interpretable) ions are listed in Table 6.8.

The feature of the spectrum is the ion corresponding to $Me(H)Ge_2Co_4(CO)_{13}^+$ (assigned as the parent) and ions resulting from the loss of 13 CO groups from this. Ions resulting from methyl loss from the metal skeleton are also observed although these are weak. These parts of the spectrum are similar to those related parts of the $Me_2Ge_2Co_4(CO)_{13}$ spectrum (see section 6.3.3).

6.4.3 Infrared Spectrum of $Me(H)Ge_2Co_4(CO)_{13}$.

The infrared spectrum in the CO stretching region, of a mixture incorporating $Me(H)Ge_2Co_4(CO)_{13}$ is listed in Table 6.7.

The bands in the spectrum attributable to $Me(H)Ge_2Co_4(CO)_{13}$ are very similar in relative intensity (where applicable) and position to those of $Me_2Ge_2Co_4(CO)_{13}$. Eight of the twelve predicted terminal CO stretches ($6a^1 + 6a^{11}$) and the bridging CO stretch are observed.

Table 6.8 Mass Spectrum of

$Me(H)Ge_2Co_4(CO)_{13}/GeCo_4(CO)_{14}$

Mixture above m/e = 380

m/e	rel. int	Assignment	
770-782	W	$Me(H)Ge_2Co_4(CO)_x$,	x = 13
727-740	W		x = 12
699-712	W		x = 11
671-684	M		x = 10
643-656	M		x = 9
615-628	W		x = 8
587-600	S		x = 7
559-572	S		x = 6
531-544	VS		x = 5
503-516	S		x = 4
475-488	S		x = 3
447-460	M		x = 2
419-432	W		x = 1
391-404	S		x = 0
698-704	VW	$GeCo_4(CO)_x$,	x = 14
670-676	W		x = 13
642-646	M		x = 12
614-620	W		x = 11
586-592	M		x = 10
558-564	M		x = 9
530-536	S		x = 8
502-508	S		x = 7
474-480	M		x = 6
446-452	M		x = 5
418-424	M		x = 4
390-396	M		x = 3

6.4.4 Discussion.

It appears that the reaction of $MeGeH_3$ with $GeCo_4(CO)_{14}$, initially follows the $Me_2GeH_2/GeCo_4(CO)_{14}$ reaction, analogously.

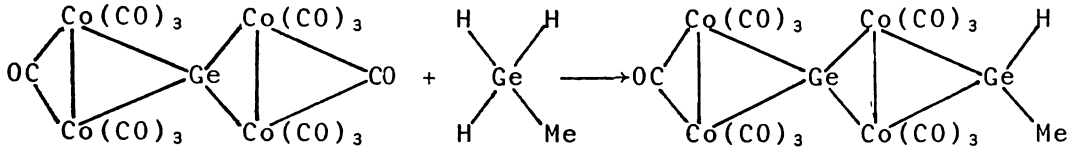

$+ H_2 + CO$

Thus the analogous product $Me(H)Ge_2Co_4(CO)_{13}$ is formed in this reaction. This product has very similar infrared and mass spectral properties to $Me_2Ge_2Co_4(CO)_{13}$, as expected with the replacement of a Me Group for a hydrogen.

The reaction is considerably slower than the $Me_2GeH_2/GeCo_4(CO)_{14}$ reaction however. Thus after $2\frac{1}{2}$ months reaction time, there remained a considerable quantity of unreacted $GeCo_4(CO)_{14}$ (cf. Me_2GeH_2 reaction, quantitative reaction of $GeCo_4(CO)_{14}$ after only 7 weeks). This may be due to the lesser reactivity of $MeGeH_3$ (relative to Me_2GeH_2) due to the decreased methyl substitution (101).

In contrast to the $Me_2GeH_2/GeCo_4(CO)_{14}$ system a further reaction occurs in this system forming the new cluster $(MeGe)_2Co_4(CO)_{11}$. Discussion of this reaction is dealt with in Chapter 8.

6.5 Reaction of Me_3GeH With $GeCo_4(CO)_{14}$.

Me_3GeH (227mg, 1.95mmoles) and $GeCo_4(CO)_{14}$ (670mg, 0.96mmoles) were left to react for 16 weeks and worked up as in 2.5. The infrared spectrum of the relatively involatile products (Table 6.9) shows absorptions due mainly to, unreacted $GeCo_4(CO)_{14}$ and also $Me_3GeCo(CO)_4$. Also present are small quantities of $Co_4(CO)_{12}$, $Me_2Ge_2Co_4(CO)_{13}$, a minor quantity of $GeCo_4(CO)_{13}$ and at least one other species (unidentified) with an infrared absorption at $2008cm^{-1}$. From this were recovered 483mg (0.689mmoles) of $GeCo_4(CO)_{14}$.

Table 6.9 Infrared Spectrum* of the Products From the $Me_3GeH/GeCo_4(CO)_{14}$ Reaction.

Peak (cm^{-1})	Rel.Int	Assignment
2096	w	$Me_2Ge_2Co_4(CO)_{13}$
2093	m	$Me_3GeCo(CO)_4$
2083	w	$GeCo_4(CO)_{13}$
2079	s	$GeCo_4(CO)_{14}$
2063	vs	$GeCo_4(CO)_{14}$, $Me_2Ge_2Co_4(CO)_{13}$
2054	m	$Me_2Ge_2Co_4(CO)_{13}$ + $Co_4(CO)_{12}$
2043	vs	$GeCo_4(CO)_{13}$, $Me_2Ge_2Co_4(CO)_{13}$
2036	s	$Me_3GeCo(CO)_4$
2028	vw	$Me_2Ge_2Co_4(CO)_{13}$ + $GeCo_4(CO)_{14}$
2023	w	$Me_2Ge_2Co_4(CO)_{13}$
2016	m	$Me_2Ge_2Co_4(CO)_{13}$
2006	w	$GeCo_4(CO)_{14}$
2003	vw	$Me_2Ge_2Co_4(CO)_{13}$
1994	vs	$Me_3GeCo(CO)_4$
1866	w-m	$Co_4(CO)_{12}$
1848 sh	w	$GeCo_4(CO)_{14}$
1843	w-m	$Me_2Ge_2Co_4(CO)_{13}$

* C_6H_{14}/CH_2Cl_2 solution.

6.6 The Reactions of Me_2SiH_2 and Me_2SnH_2 With $GeCo_4(CO)_{14}$.

6.6.1 Reaction of Me_2SiH_2.

Me_2SiH_2 (221mg, 3.68mmoles) and $GeCo_4(CO)_{14}$ (485mg, 0.692mmoles) were left to react for 18 weeks and worked up as described in 2.5. The infrared spectrum of the involatile product showed it to consist of virtually pure $GeCo_4(CO)_{14}$ contaminated with a trace of $GeCo_4(CO)_{13}$. Recrystallisation returned 470mg (0.67mmole) of $GeCo_4(CO)_{14}$.

From the volatile fraction, 212mg (3.53mmoles) of unreacted Me_2SiH_2 were recovered.

6.6.2 Reaction of Me_2SnH_2.

$GeCo_4(CO)_{14}$ (480mg, 0.685mmoles) and Me_2SnH_2 (134mg, 0.882mmoles) were left to react for 3 weeks and worked up as in 2.5. The infrared spectrum of the involatile products showed peaks due mainly to $GeCo_4(CO)_{14}$ contaminated with traces of $Me_3SnCo(CO)_4$, $Me_2Sn\{Co(CO)_4\}_2$ and $MeSn\{Co(CO)_4\}_3$. From this, 469mg (0.669mmoles) of unreacted $GeCo_4(CO)_{14}$ were recovered.

No Sn hydrides were observed in the volatile fraction.

6.7 The Reactions of Me_2GeH_2 and Me_2SiH_2 With $MeGeCo_3(CO)_{11}$.

6.7.1 The Reaction of Me_2GeH_2

$MeGeCo_3(CO)_{11}$ (810mg, 1.42mmoles) and Me_2GeH_2 (189mg 1.81mmoles) were left to react for 5 weeks and worked up as described in 2.5. The infrared spectrum of the involatile products (Table 6.10) shows absorptions due mainly to $MeGeCo_3(CO)_{11}$ with some $Me_2GeCo_2(CO)_7$ and $(Me_2Ge)_2Co_2(CO)_6$.

Recrystallisation from this, yielded 642mg (1.12mmoles) of $MeGeCo_3(CO)_{11}$, while vacuum sublimation recovered 35mg (0.12mmoles) of $Me_2GeCo_2(CO)_7$. There remained a small quantity of unseparated $MeGeCo_3(CO)_{11}$, $Me_2GeCo_2(CO)_7$ and $(Me_2Ge)_2Co_2(CO)_6$.

From the volatile fraction, the presence of $Me_2GeHCo(CO)_4$ was identified by infrared and confirmed by nmr spectroscopy (5.20τ (sept), 9.28τ (d), ref.25), (yield; 53mg, 0.19mmoles). Also recovered were 123mg (1.18mmoles) of unreacted Me_2GeH_2. There remained a small quantity of Me_2GeH_2 which was not separated from the hexane.

6.7.2 Reaction of Me_2SiH_2.

Me_2SiH_2 (138mg, 2.30mmoles) and $MeGeCo_3(CO)_{11}$ (730mg, 1.27mmoles) were left to react for 15 weeks and worked up as in 2.5. The infrared spectrum of the involatile product showed it to be pure $MeGeCo_3(CO)_{11}$ (recovered 698mg).

From the volatile fraction, 130mg (2.17mmoles) of unreacted Me_2SiH_2 were recovered. Also observed were traces of $Co_2(CO)_8$ and $HCo(CO)_4$.

Table 6.10 Infrared Spectrum* of the Products from the $Me_2GeH_2/MeGeCo_3(CO)_{11}$ Reaction.

Peak (cm^{-1})	Rel. Int.	Assignment
2093	w-m	$MeGeCo_3(CO)_{11}$
2088	vw	$Me_2GeCo_2(CO)_7$
2080	vs	$MeGeCo_3(CO)_{11}$
2066	m	$(Me_2Ge)_2Co_2(CO)_6$
2054	vs	$MeGeCo_3(CO)_{11}$
2046	w	$MeGeCo_2(CO)_7$
2035 sh	w	$MeGeCo_3(CO)_{11}$
2029	vs	$MeGeCo_3(CO)_{11}$ + $(Me_2Ge)_2Co_2(CO)_6$
2023 sh	vvw	$Me_2GeCo_2(CO)_7$
2017 sh	vvw	$MeGeCo_3(CO)_{11}$
2013	s	$MeGeCo_3(CO)_{11}$
2008 sh	vw	$(Me_2Ge)_2Co_2(CO)_6$
1995 sh	w	$MeGeCo_3(CO)_{11}$
1990 sh	vw	$(Me_2Ge)_2Co_2(CO)_6$
1980 sh	vw	$(Me_2Ge)_2Co_2(CO)_6$
1848	m	$MeGeCo_3(CO)_{11}$
1835	w-m	$MeGeCo_3(CO)_{11}$

* Hexane solution.

6.8 Reaction of Me_2GeH_2 With $Ge_2Co_6(CO)_{20}$.

6.8.1 Experimental

Run 1:

$Ge_2Co_6(CO)_{20}$ (219mg, 0.207mmoles) and Me_2GeH_2 (335mg, 320mmoles) were left to react for 20 weeks and worked up as in 2.5. The infrared spectrum of the involatile products consists of peaks due mainly to the new compound assigned as $(Me_2Ge)_2Ge_2Co_6(CO)_{18}$ (see following sections) and also a small amount of unreacted $Ge_2Co_6(CO)_{20}$.

From the volatile fraction were recovered 24mg (0.09mmoles) of $Me_2GeHCo(CO)_4$ and 235mg of unreacted Me_2GeH_2.

Run 2:

$Ge_2Co_6(CO)_{20}$ (94mg, 0.088mmoles) and Me_2GeH_2 (62mg, 0.59mmoles) were left to react for 5 weeks and worked up as in 2.5. The infrared spectrum of the involatile products was similar to that obtained for Run 1, indicating a near quantitative yield of $(Me_2Ge)_2Ge_2Co_6(CO)_{18}$.

6.8.2 Handling of $(Me_2Ge)_2Ge_2Co_6(CO)_{18}$.

$(Me_2Ge)_2Ge_2Co_6(CO)_{18}$ is an orange solid which is stable at room temperature in the absence of air. Its solubility is similar to $Ge_2Co_6(CO)_{20}$.

Attempts to obtain single crystals for an x-ray study failed, with only twinned needles, similar to those obtained for $Ge_2Co_6(CO)_{20}$, resulting.

6.8.3 Infrared Spectrum of $(Me_2Ge)_2Ge_2Co_6(CO)_{18}$.

The involatility of this compound prevented its characterisation by mass spectrometry, thus the only spectroscopic characterisation was infrared.

The carbonyl stretching region (see Fig.6.3 , Table 6.11) is remarkably similar to that of $Me_2Ge_2Co_4(CO)_{13}$ (see Fig.6.1, Table 6.4). The most notable difference is the absence of a bridging carbonyl mode in this spectrum, suggesting that both bridging CO groups (from $Ge_2Co_6(CO)_{20}$) have been lost (or replaced).

Assuming the most likely structure of this compound as $(Me_2Ge)_2Ge_2Co_6(CO)_{18}$ (see Fig.6.4), then ideally it may have C_{2v} symmetry, from which is predicted 14 infrared active modes for the CO stretches $(5a_1 + 5b_1 + 4b_2)$. Alternatively it may be of C_s (or lower) symmetry, from which are predicted 18 infrared active modes $(9a^1 + 9a^{11})$. A maximum of 9 bands are observed, although the combination of peaks at $\simeq$ 2015cm^{-1} - 1990cm^{-1} suggest there may be unresolved peaks due to accidental overlap. Clearly in molecules of this type, there will be a number of modes of similar energy.

6.8.4 Discussion.

The reactions of Me_2GeH_2 with $GeCo_4(CO)_{14}$ and $Me_2GeCo_2(CO)_7$ clearly show that products arise from the substitution of one bridging CO group by a Me_2Ge group. Thus the reaction of Me_2GeH_2 with the related compound $Ge_2Co_6(CO)_{20}$ may be expected to follow a similar path. Indeed, in this reaction a new product is formed. The

FIGURE 6.3 INFRARED SPECTRUM OF $(Me_2Ge)_2Ge_2Co_6(CO)_{18}$

TABLE 6.11 INFRARED SPECTRUM OF $(Me_2Ge)_2Ge_2Co_6(CO)_{18}$

2087 w	2013 sh m
2065 s-vs	2008 m-s
2053 vs	2002 sh w-m
2041 vs	1985 sh vw
2034 sh w	

C_6H_{14} / CH_2Cl_2 SOLUTION

FIGURE 6.4 PROPOSED STRUCTURE OF $(Me_2Ge)_2Ge_2Co_6(CO)_{18}$.

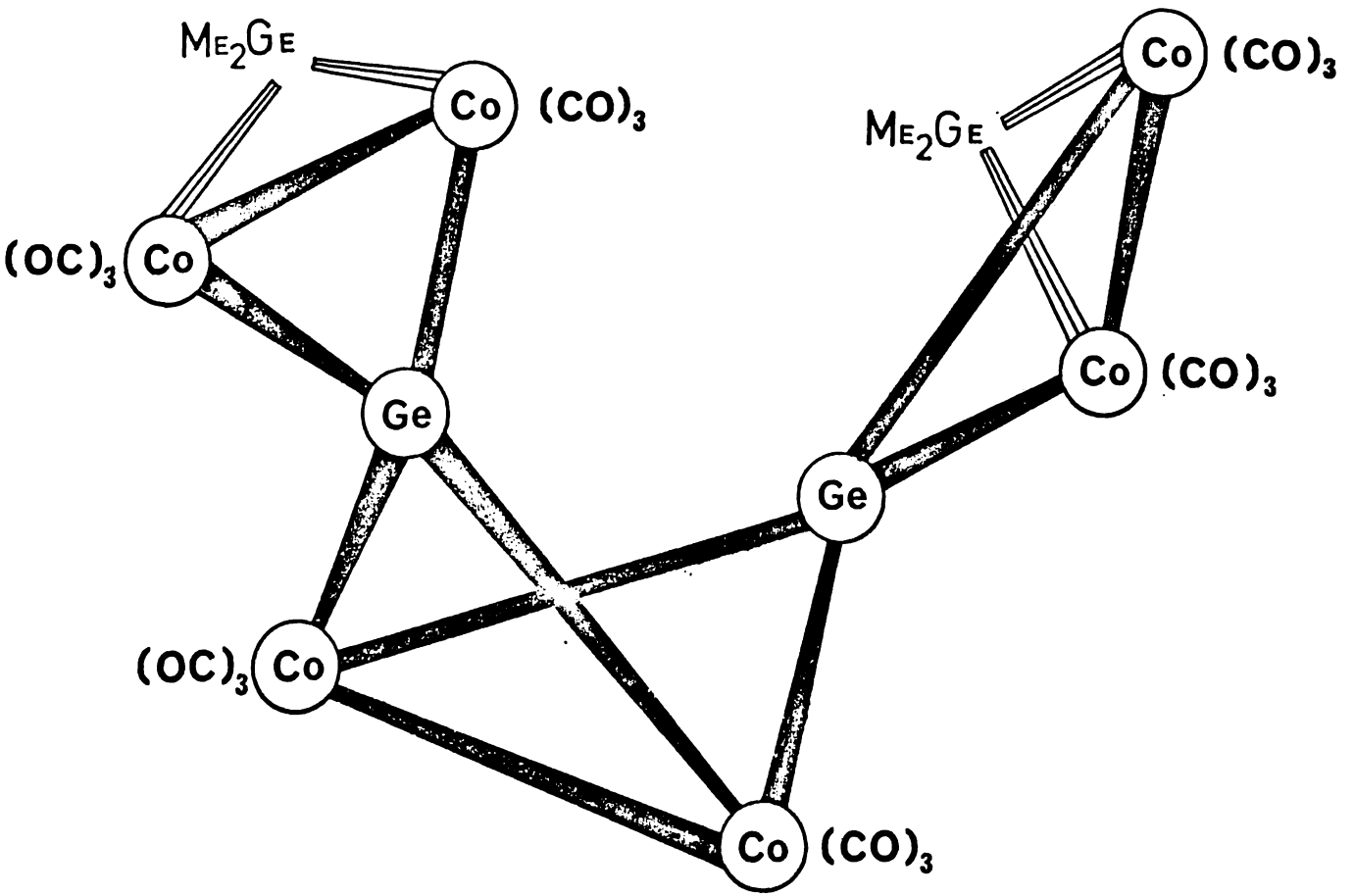

similarity of its infrared spectrum to that of $Me_2Ge_2Co_4(CO)_{13}$ suggests that it has a similar structure and thus also arises from the replacement of bridging CO groups by Me_2Ge groups. The absence of a bridging CO stretching mode suggests that two Me_2Ge groups have been substituted on the molecule.

The low volatility (determined during a mass spectrum attempt) and solubility are also consistent with this type of chain structure. Although a full characterisation cannot be made on the basis of the above evidence, it is strongly suggestive that the formulation as $(Me_2Ge)_2Ge_2Co_6(CO)_{18}$ (see fig.6.4) is correct.

6.9 Reaction of Me_2SiH_2 With $Me_2GeCo_2(CO)_7/Me_2Ge\{Co(CO)_4\}_2$

Me_2SiH_2 (229mg, 3.82mmoles) was added to a hexane solution of mainly $Me_2GeCo_2(CO)_7$ with some $Me_2Ge\{Co(CO)_4\}_2$ and the mixture allowed to react for 16 weeks. The infrared spectrum of the solution after this period showed it to be pure $Me_2GeCo_2(CO)_7$.

From the volatile fraction were recovered 215mg of Me_2SiH_2.

CHAPTER 7. The Crystal and Molecular Structures and Spectroscopic Properties of $(MeGe)_2Co_4(CO)_{11}$ and $\{Co(CO)_4Ge\}_2Co_4(CO)_{11}$.

7.1 The Crystal and Molecular Structure of $(MeGe)_2Co_4(CO)_{11}$.

7.1.1 Experimental

Single crystals of $(MeGe)_2Co_4(CO)_{11}$, suitable for study were grown from a filtered CH_2Cl_2/C_6H_{14} solution as described in Section 2.3. An orange plate-shaped crystal of dimensions 0.375x0.32x0.013mm was mounted with Araldite in a 0.5mm internal diameter glass capillary.

Data and lattice parameters were obtained using an Enraf-Nonius CAD 4 diffractometer at the University of Adelaide. Accurate cell dimensions were obtained using the setting angles of 25 high-angle reflections.

Table 7.1 Crystal Data for $(MeGe)_2Co_4(CO)_{11}$

$C_{13}H_6Co_4Ge_2O_{11}$

M = 719.09

Monoclinic, space group C2/m

a = 13.755(3) Å β = 93.19(5)°

b = 13.94 (2)

c = 10.88 (1)

U = 2082 Å^3

Dcalc = 2.29g cm^{-3}

Z = 4

$F_{(ooo)}$ = 1357.8 $\bar{\mu}$(MoKα) = 58.3 T = 298°K

Niggli-values and cell parameters from the automatic centring routine indicated a C-centred lattice. This was confirmed during data collection, when a check on 28 reflections

with h+k = 2n+1, showed them to be absent.

Intensity data were collected in the range $2.4^0<2\theta<44^0$ using an ω-$\frac{1}{3}\theta$ scan. Horizontal counter apertures and ω scan angles of $(3.00 + 0.5 \tan\theta)$mm and $(1.50 + 0.35 \tan\theta)^0$ respectively were used. The data were corrected for Lorentz and polarisation effects using the SUSCAD program and for linear absorption using ABSORB.

7.1.2 Solution and Refinement

The systematic absences from the intensity data gave three possibilities for the space group; $C2$, Cm or $C2/m$. The initial attempt at solution using the non-centrosymmetric direct method routine of the SHELX program in space group C_2, gave a solution with mirror symmetry. Subsequent solution in $C2/m$ using the centrosymmetric routine of SHELX located the two Ge atoms and the two unique Co atoms. Because of the mirror symmetry, one half of the molecule constituted an unique asymmetric unit and the successful refinement in $C2/m$ confirmed this as the correct choice of space group.

Of the 1214 collected reflections, 954 had $F^2>2.5\sigma(F)^2$ and these were used for refinement. Least squares refinement of the metal atoms with isotropic temperature factors gave R = 0.25 and a subsequent difference map showed both methyl carbons (on the two Ge atoms) and 5 of the 6 unique carbonyl groups. Note that both Ge atoms, the two methyl carbons and the C and O of the bridging carbonyl group, all lay on a mirror plane and were input in the refinement with a site occupancy of 0.5.

Further refinement located the remaining carbonyl group and reduced R to 0.074. At this stage, all atoms were assigned anisotropic temperature factors and the model was refined to R = 0.041. Finally the hydrogen atoms (on the methyl carbons) were included in calculated positions using the AFIX subroutine of SHELX and full matrix least squares refinement to convergence gave R = 0.040 and R_w = 0.042.

The final atomic positional parameters and anisotropic thermal parameters for an asymmetric unit of $(MeGe)_2Co_4(CO)_{11}$ are given in Appendix II.

7.1.3 Discussion of the Structure.

Diagrams of the full molecule are shown in Figs. 7.1 and 7.2 while a stereo unit cell plot looking through the Z orthogonal axis is given in Fig. 7.3. Bonded and selected non-bonded interatomic distances and interatomic angles are given in Tables 7.2 and 7.3 respectively.

The positions of the atoms with respect to the tetracobalt plane are given in Table 7.4.

The molecule lies on a crystallographic mirror plane through Ge_1, Ge_2, C_B, O_B, Cm_1 and Cm_2.

The metallic core of $(MeGe)_2Co_4(CO)_{11}$ consists of 2Ge atoms each quadruply bridging a distorted square planar array of 4 cobalt atoms. Of the 11 carbonyl groups, 8 are completely terminal (2 on each cobalt atom), 1 symmetrically bridges a cobalt-cobalt bond, and the remaining 2 each semi-bridge opposite cobalt-cobalt bonds.

The different cobalt-cobalt bond lengths:

FIGURE 7.1 STRUCTURE OF $(MeGe)_2Co_4(CO)_{11}$.

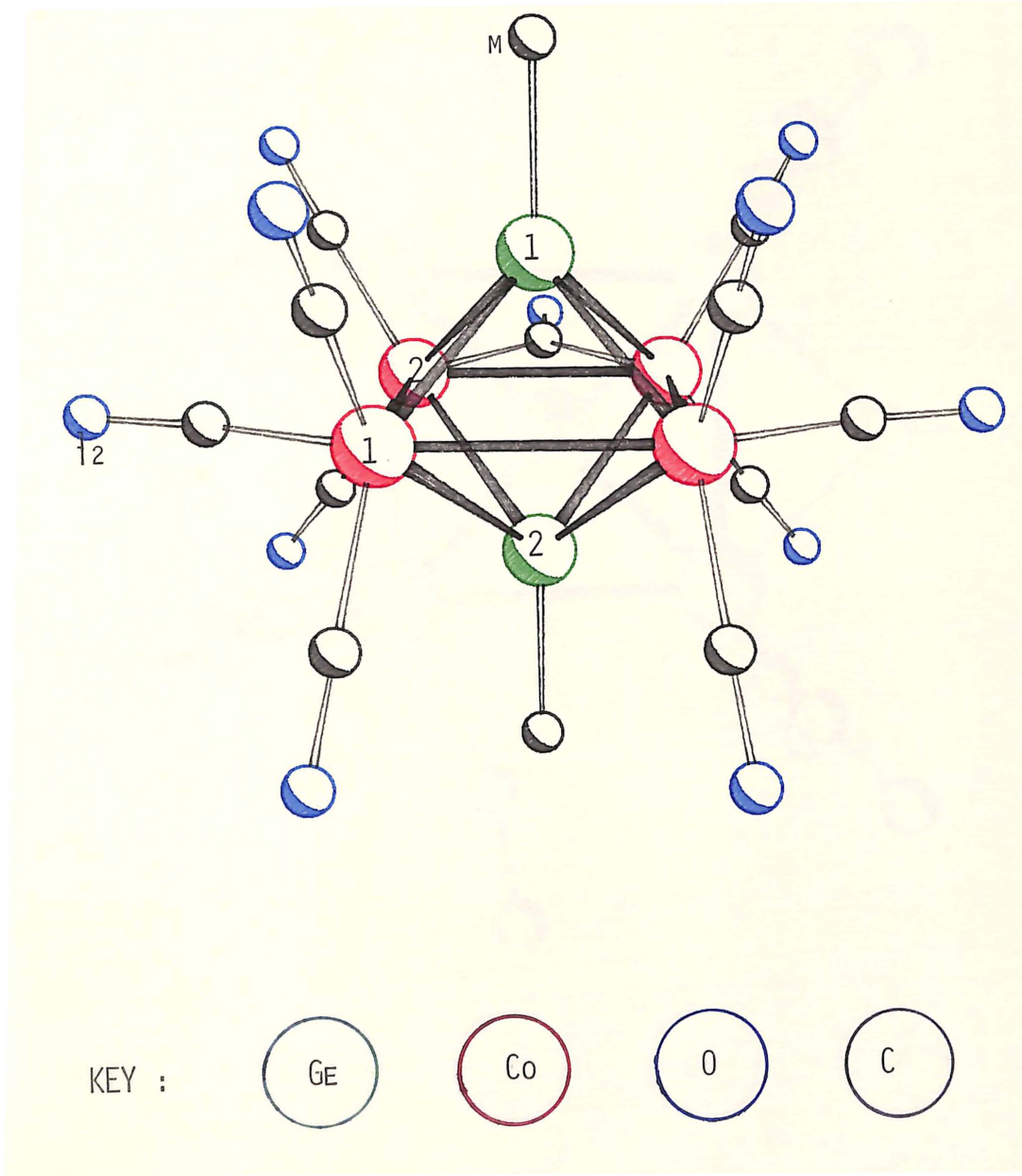

FIGURE 7.2 VIEW OF $(MeGe)_2Co_4(CO)_{11}$ LOOKING THROUGH THE TWO Ge ATOMS.

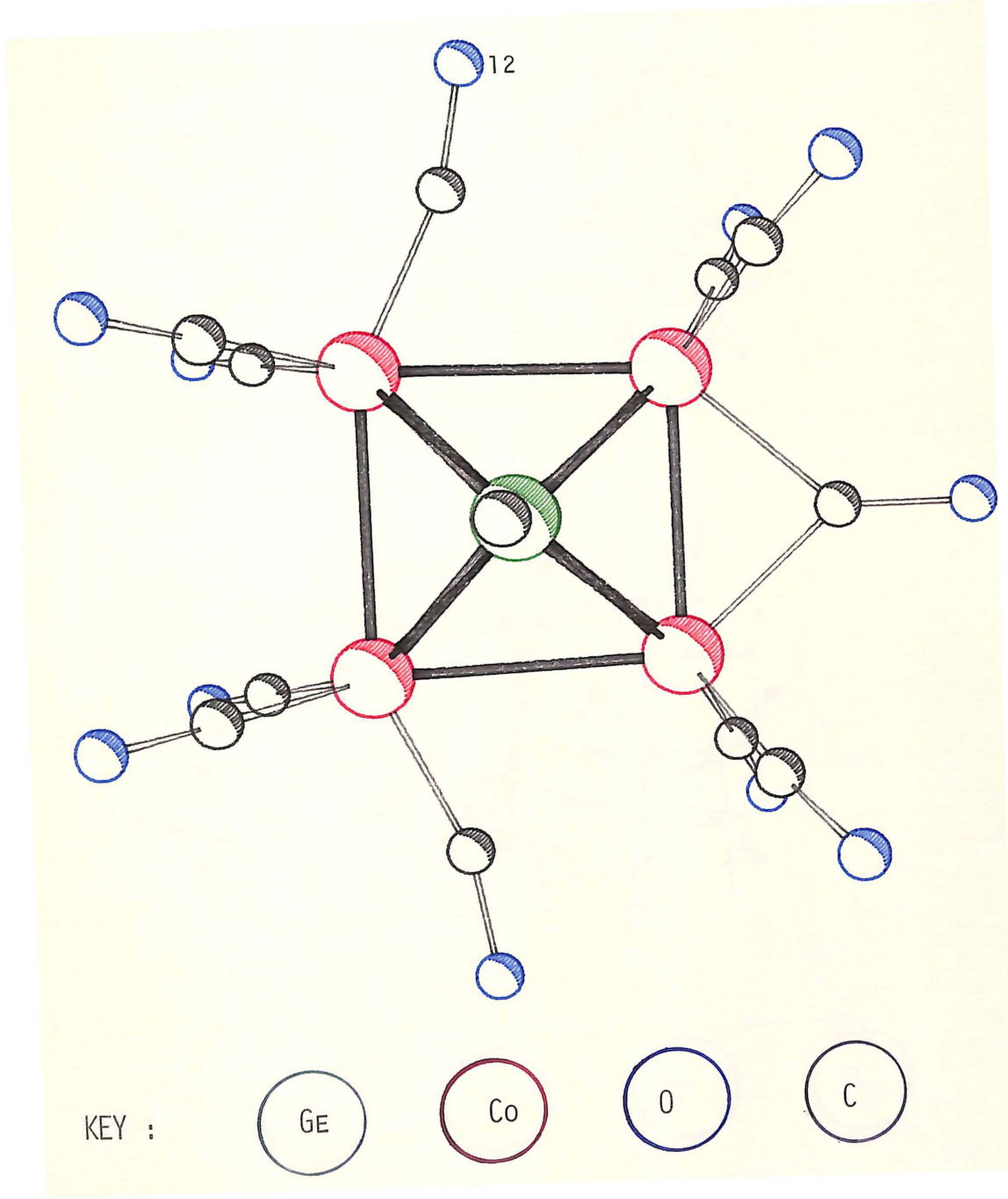

FIGURE 7.3 UNIT CELL PLOT OF $(MeGe)_2Co_4(CO)_{11}$(STEREO) THROUGH THE Z ORTHOGONAL AXIS.

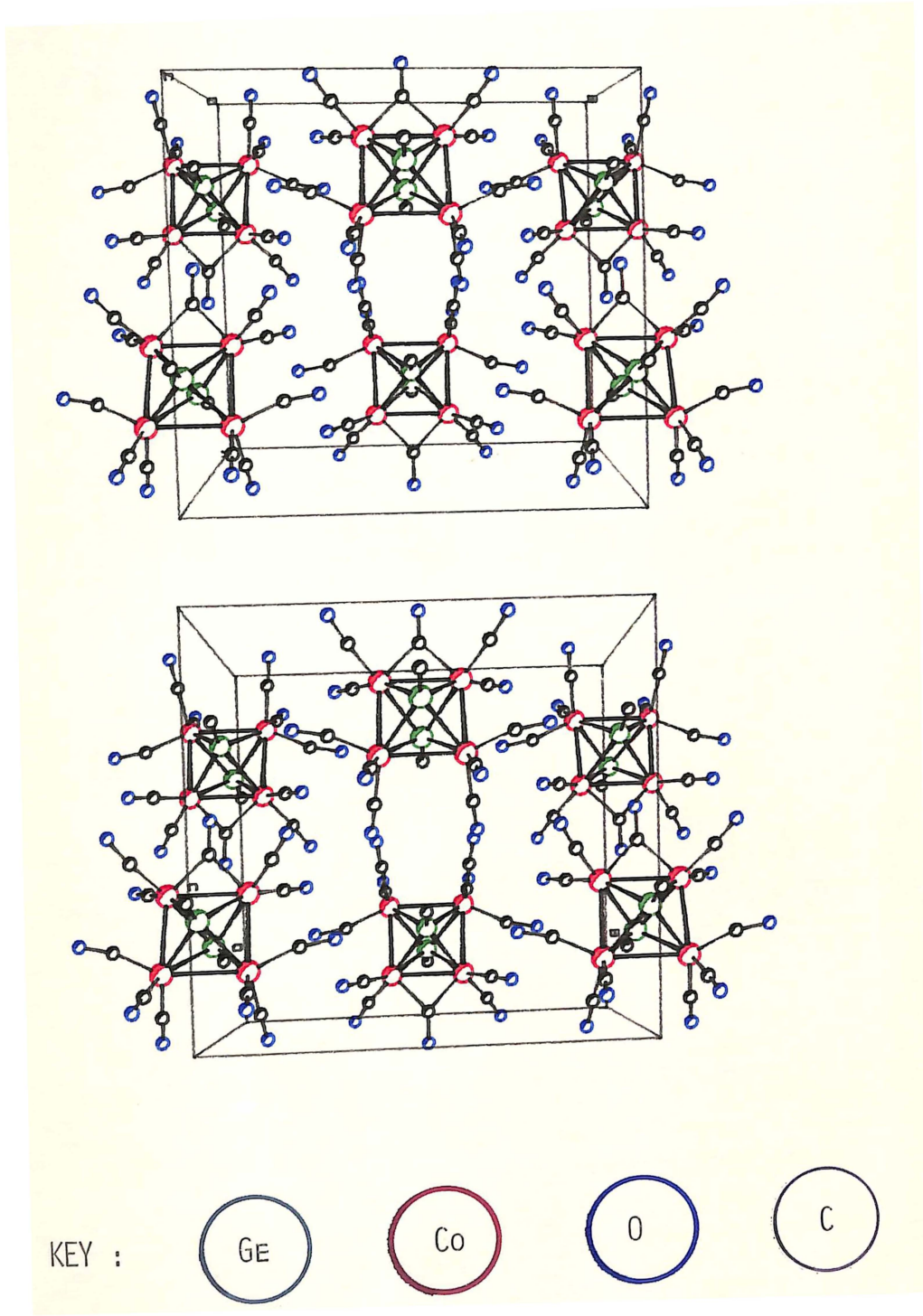

TABLE 7.2 BOND LENGTHS AND SELECTED INTERATOMIC DISTANCES FOR $(MeGe)_2Co_4(CO)_{11}$ (Å).

Ge(1) - Co(1)	2.393(2)	Ge(1)--Ge(2)	2.926(2)
Ge(1) - Co(2)	2.381(2)	Co(2)--C(12)	2.53(1)
Ge(1) - C(M1)	1.94(1)		
Ge(2) - Co(1)	2.399(2)		
Ge(2) - Co(2)	2.385(2)		
Ge(2) - C(M2)	1.96(2)		
Co(1) - Co(2)	2.693(2)		
Co(1) - Co(1')	2.721(2)		
Co(2) - Co(2')	2.580(2)		
Co(1) - C(11)	1.82(1)		
Co(1) - C(12)	1.77(1)		
Co(1) - C(13)	1.80(1)		
Co(2) - C(21)	1.80(1)		
Co(2) - C(B)	1.92(1)		
C(11) - O(11)	1.11(1)		
C(12) - O(12)	1.13(2)		
C(13) - O(13)	1.13(2)		
C(21) - O(21)	1.15(1)		
C(22) - O(22)	1.13(1)		
C(B) - O(B)	1.18(2)		

NOTES: Mirror plane relates Co(1) and Co(1'): Co(2) and Co(2').
All atoms have a mirror image except; Ge(1), Ge(2), C(M1), C(M2), C(B), and O(B).

C(12) and O(12) are the semi-bridging carbonyl.

B = bridging , M= methyl.

TABLE 7.3 SELECTED INTERATOMIC ANGLES FOR $[MeGe]_2Co_4(CO)_{11}$. (°)

Co(1) - Ge(1) - Co(2)	68.7(1)	C(B) - Co(2) - C(21)	93.2(5)
Co(1) - Ge(1) - Co(1)	69.3(1)	C(B) - Co(2) - C(22)	97.6(6)
Co(1) - Ge(2) - Co(2)	68.5(1)	C(21) - Co(2) - C(22)	103.8(5)
Co(1) - Ge(2) - Co(1')	69.1(1)	Co(1) - C(11) - O(11)	179(1)
Co(2) - Ge(1) - Co(2')	65.6(1)	Co(1) - C(12) - O(12)	164(1)
Co(2) - Ge(2) - Co(2')	65.5(1)	Co(2) - C(12) - O(12)	120(1)
Ge(1) - Co(1) - Ge(2)	75.3(1)	Co(1) - C(13) - O(13)	178(2)
Ge(2) - Ge(1) - C(M1)	178.8(2)	Co(2) - C(B) - Co(2)	84.3(3)
Co(1) - Ge(1) - C(M1)	126.7(2)	Co(1) - C(12) - Co(2)	75.2(5)
Co(2) - Ge(1) - C(M1)	128.7(2)	Co(2) - C(B) - O(B)	137.8(3)
Ge(1) - Ge(2) - C(M2)	179.8(2)	Co(2) - C(21) - O(21)	173(1)
Co(1) - Ge(2) - C(M2)	127.9(2)	Co(2) - C(22) - O(22)	176(1)
Co(2) - Ge(2) - C(M2)	127.8(2)		
C(11) - Co(1) - C(12)	99.4(5)		
C(11) - Co(1) - C(13)	102.9(5)		
C(12) - Co(2) - C(21)	87.0(5)		
C(12) - Co(2) - C(22)	83.6(5)	SEE NOTES FOR TABLE 7.2	

TABLE 7.4 DISTANCES OF ATOMS FROM THE TETRACOBALT PLANE IN $(MeGe)_2Co_4(CO)_{11}$ (Å)

Ge(1)	1.458	C(21)	1.396
Ge(2)	-1.466	C(22)	-1.433
C(M1)	3.396	O(11)	-2.267
C(M2)	-3.419	O(12)	0.024
C(11)	-1.414	O(13)	2.270
C(12)	0.002	O(B)	0.108
C(13)	1.411	O(21)	2.247
C(B)	0.025	O(22)	-2.289

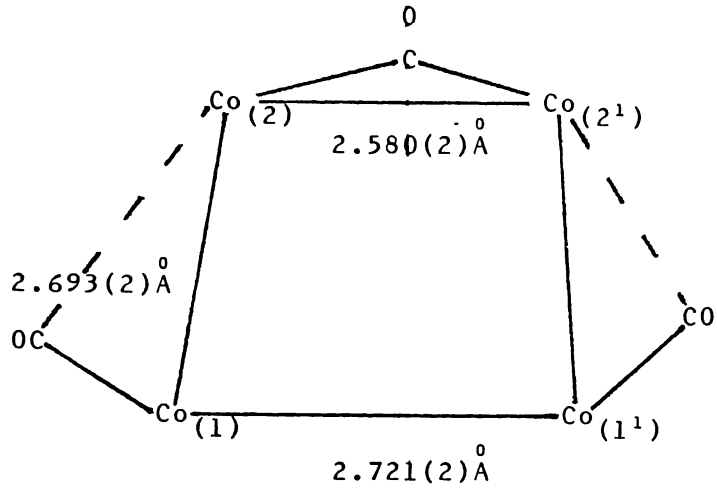

are consistent with previous observations, (91), of the shortening of metal-metal bonds with CO bridging across them. Thus these bond lengths may be explained by the degree of bridging, with the longest bond being the non-CO bridged and the shortest, the symmetrically CO-bridged. The mid Co-Co bond length occurs where there is a weakly semi-bridging CO group. The closeness of this distance (only 0.03Å less) to the non-CO bridged bond is consistent with the very weak bridging nature of this carbonyl.

The Ge-Co distances are all virtually equal. Thus the Ge atoms occupy equivalent positions, symmetrically arranged with respect to the 4 Co atoms. The average of 2.390(9) Å is comparable with the average of 2.36(2) Å in $GeCo_4(CO)_{14}$.

The average Ge-C distance of 1.95(1) Å appears normal for a germanium-aliphatic carbon bond, c.f. Me_3GeCN, average $Ge\text{-}C_{(aliph)}$ = 1.98(4) Å, ref.123. This suggests straightforward σ interaction, despite the 5 coordination of the Ge.

Three different types of carbonyl groups are observed in this cluster. There are eight completely terminal (two

on each Co) with an average Co-C distance of 1.80(1) $\mathring{A}$ and C-O distance of 1.13(2) $\mathring{A}$ (normal for this type of compound , e.g. see ref. 91).

The symmetric bridging carbonyl group lies virtually in the Co_4 plane (see Table 7.4). The Co-C and C-O distances of 1.92(2) $\mathring{A}$ and 1.19(2) $\mathring{A}$ respectively and Co-C-O angle of $137.60(4)^0$ are entirely consistent with those of other such bridging carbonyl groups (see Reference 57 for example).

The two remaining carbonyl groups are semi-bridging, with Co-C distances of 1.79(1) $\mathring{A}$ (to Co(2)) and 2.53(2) $\mathring{A}$ (to Co(1)). The long distance is significantly less than a normal non-bonded distance. In addition these carbonyls lie in the Co_4 plane. These semi-bridging carbonyls are further discussed in Section 7.3.

7.2 The Crystal and Molecular Structure of $\{(CO)_4CoGe\}_2Co_4(CO)_{11}$

7.2.1 Experimental.

Plate-shaped crystals with a longest dimension of approximately 0.3mm, suitable for study were grown from a hot CH_2Cl_2 solution cooled slowly to 4^0C over a period of 4 days.

Initial precession photography showed the crystal to be orthorhombic with space group either Cmca or Aba2 .

Intensity data and refined lattice parameters were obtained at the University of Auckland, using an Enraf-Nonius CAD 4 diffractometer.

Table 7.5 Crystal Data for $\{(CO)_4CoGe\}_2Co_4(CO)_{11}$

$C_{19}Co_6Ge_2O_{19}$

M = 1030.95

Orthorhombic, space group Cmca

a = 17.902

b = 12.783

c = 26.456

U = 6054 $\AA^3$

D_{calc} = 2.26g ml^{-1}

Z = 8

$F_{(ooo)}$ = 3935.4 $\quad \bar{\mu}(MoK\alpha)$ = 50.7 $\quad$ T = 296^0K

Intensity data were collected in the range $1.1^0 \leqslant \theta \leqslant 20.15^0$ using an ω-2θ scan and a horizontal counter aperture and ω scan angle of $(0.80 + 0.35\ Tan\theta)$mm and $(1.7 + 1.2\ Tan\theta)^0$ respectively.

Of the 1227 unique reflections collected, 871 had $F^2>2\sigma(F)^2$ and these were used in the refinement.

7.2.2 Solution and Refinement.

Initial attempts at solution in space group Cmca, using the centrosymmetric EEES and Tang/Phix direct method routines of SHELX, failed. The positions of the heavy metal atoms were obtained by the direct methods program MULTAN (in space group Cmca). The molecule lies on a crystallographic mirror plane.

Least squares refinement of the unique atoms was carried out as for $(MeGe)_2Co_4(CO)_{11}$. Least squares refinement of the metal atoms with isotropic temperature factors gave R = 0.23. Subsequent difference maps allowed the location of the 11 unique carbonyl groups.

Least squares refinement of all the atoms with isotropic temperature factors reduced R to 0.11. The metal atoms were then assigned anisotropic temperature factors and full matrix least squares refinement to convergence gave R = 0.093 and R_w = 0.096.

At this stage the data were corrected for absorption and a subsequent refinement converged at R = 0.0636 and R_w = 0.0700.

7.2.3 Discussion of the Structure.

The structure of $\{(CO)_4CoGe\}_2Co_4(CO)_{11}$ is similar to that of $(MeGe)_2Co_4(CO)_{11}$, with the replacement of the methyl groups

FIGURE 7.4 STRUCTURE OF $[(OC)_4CoGe]_2Co_4(CO)_{11}$.

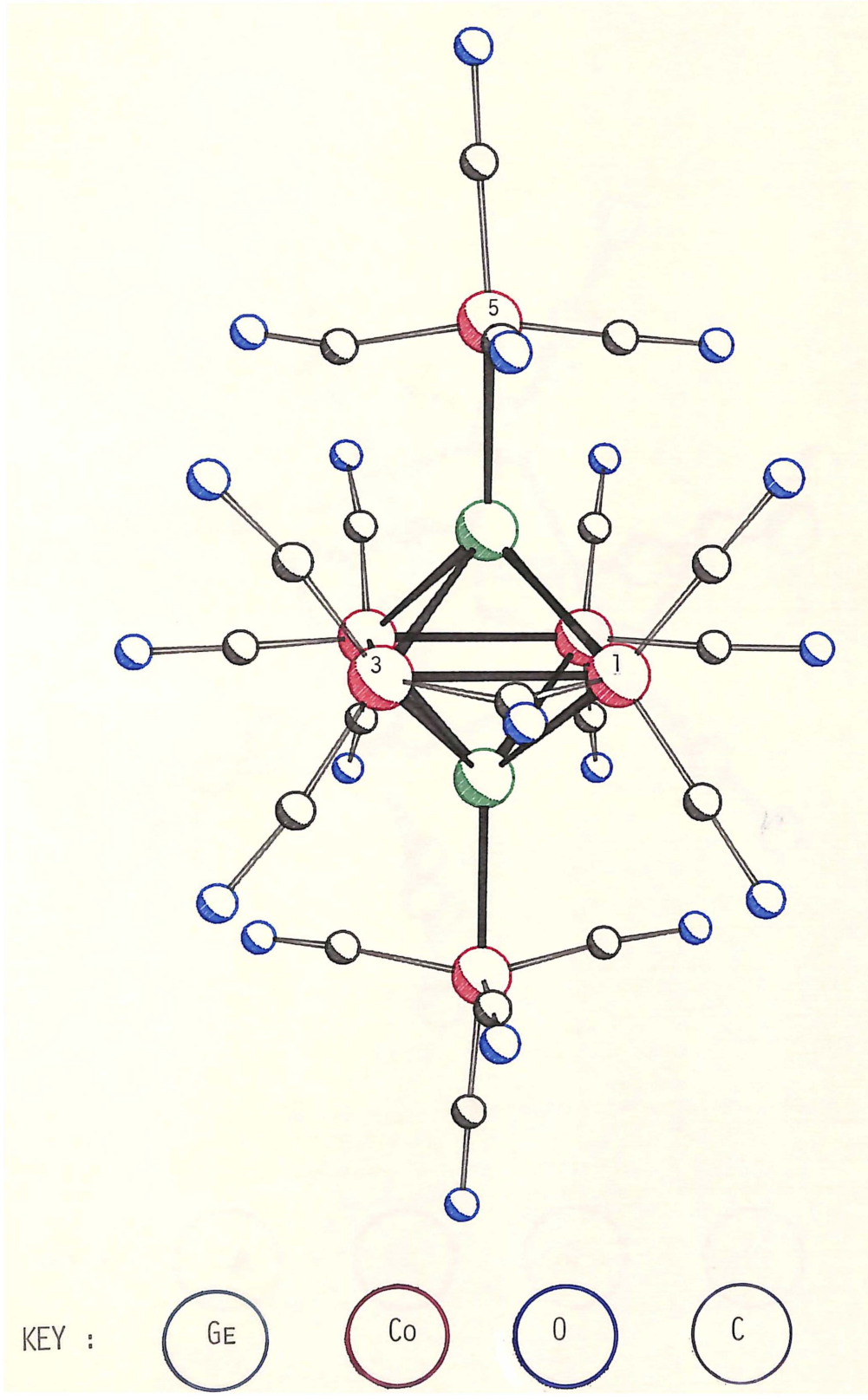

FIGURE 7.5 VIEW OF $[(CO)_4CoGe]_2Co_4(CO)_{11}$ THROUGH THE TWO Ge ATOMS.

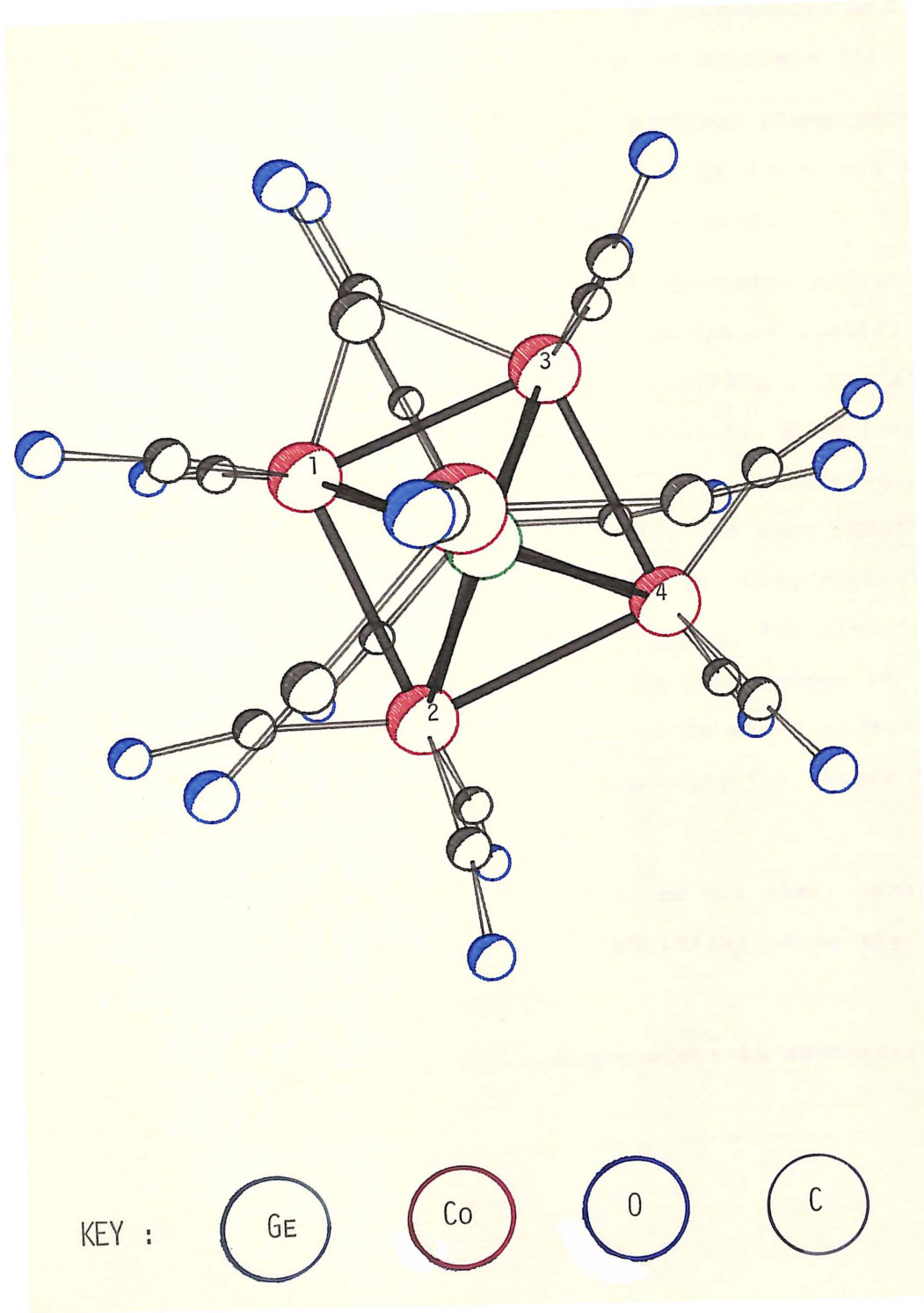

on the two Ge atoms by $-Co(CO)_4$ groups. Diagrams of the molecule are shown in Figs.7.4 and 7.5. Bonded and selected non-bonded interatomic distances, and interatomic angles are given in Tables 7.6 and 7.7 respectively. The final atomic positional parameters and anisotropic thermal parameters are given in Appendix III.

In the molecule, a crystallographic mirror plane passes through the equatorial plane atoms, the two Ge atoms and two apical $-Co(CO)_4$ groups are thus symmetry related.

The Ge-Co bond lengths (to the four clustered cobalt atoms) are again nearly equal, with an average of 2.40(2) $\mathring{A}$, which is very similar to that of $(MeGe)_2Co_4(CO)_{11}$. Of interest is the $Ge\text{-}Co_{(apical)}$ bond length of 2.405(4) $\mathring{A}$. Bond lengths of related compounds are given in Table 7.8. Surprisingly, the $Ge\text{-}Co_{(apical)}$ bond length is virtually the same length as the other Ge-Co bonds in the cluster. In $(CO)_4CoGeCo_3(CO)_9$ (64) and $Co(CO)_4GePh\{Co_2(CO)_7\}$ (44) the $Ge\text{-}Co_{(term)}$ are significantly longer (0.07$\mathring{A}$) than the other Ge-Co. The Ge-Co bonds in $GeCo_5(CO)_{16}^-$, the only other known species in which germanium is bonded to five cobalt atoms, are significantly longer than in $\{(CO)_4CoGe\}_2Co_4(CO)_{11}$.

The reasons for the above effects are not clear however they most likely involve changes in hybridisation on the germanium atoms (see next section).

In this molecule, the tetracobalt plane is asymmetrically distorted.

TABLE 7.6 BOND LENGTHS AND SELECTED INTERATOMIC DISTANCES FOR $[(OC)_4CoGe]_2Co_4(CO)_{11}$ (Å).

Ge(1) - Co(1)	2.406(4)	Ge(1)--Ge(1')	2.995(4)
Ge(1) - Co(2)	2.423(4)	Co(1)--C(22)	2.39(4)
Ge(1) - Co(3)	2.434(5)	Co(4)--C(32)	2.61(4)
Ge(1) - Co(4)	2.390(5)		
Ge(1) - Co(5)	2.405(4)		
Co(1) - Co(2)	2.671(7)		
Co(1) - Co(4)	2.604(7)		
Co(2) - Co(3)	2.693(8)		
Co(3) - Co(4)	2.735(7)		
Co(1) - C(11)	1.71(3)		
Co(1) - C(B)	1.95(4)		
Co(2) - C(21)	1.73(3)		
Co(2) - C(22)	1.70(4)		
Co(3) - C(31)	1.77(3)		
Co(3) - C(32)	1.66(5)		
Co(4) - C(41)	1.72(3)		
Co(4) - C(B)	1.94(4)		
Co(5) - C(51)	1.80(3)		
Co(5) - C(52)	1.77(4)		
Co(5) - C(53)	1.74(3)		
Co(5) - C(54)	1.75(3)		
C(11) - O(11)	1.23(3)		
C(21) - O(21)	1.16(3)		
C(22) - O(22)	1.22(4)		
C(31) - O(31)	1.18(4)		
C(32) - O(32)	1.22(4)		
C(41) - O(41)	1.23(3)		
C(51) - O(51)	1.13(3)		
C(52) - O(52)	1.20(4)		
C(53) - O(53)	1.19(3)		
C(54) - O(54)	1.20(3)		
C(B) - O(B)	1.07(4)		

NOTES: Ge(1) and Ge(1') are related by the mirror plane.

All atoms have a mirror image except; Co(1),Co(2), Co(3),Co(4),C(B),O(B), C(22),O(22),C(32),O(32). (these latter 4 atoms constitute the semi-bridging carbonyls.)

B = bridging.

TABLE 7.7 SELECTED INTERATOMIC ANGLES FOR $[(OC)_4CoGe]_2Co_4(CO)_{11}$

Co(1) - Ge(1) - Co(2)	67.20(2)	C(41) - Co(4) - C(B)	97.3(1)
Co(1) - Ge(1) - Co(3)	103.50(1)	C(41) - Co(4) - C(41')	100.3(2)
Co(1) - Ge(1) - Co(4)	65.80(2)	C(51) - Co(5) - C(52)	91.0(2)
Co(1) - Ge(1) - Co(5)	124.10(1)	C(51) - Co(5) - C(53)	113.2(1)
Co(2) - Ge(1) - Co(3)	67.40(2)	C(51) - Co(5) - C(54)	132.2(1)
Co(2) - Ge(1) - Co(4)	103.00(1)	C(52) - Co(5) - C(53)	97.1(1)
Co(2) - Ge(1) - Co(5)	133.30(2)	C(52) - Co(5) - C(54)	96.7(2)
Co(3) - Ge(1) - Co(4)	69.10(2)	C(53) - Co(5) - C(54)	112.5(1)
Co(3) - Ge(1) - Co(5)	132.00(2)		
Co(4) - Ge(1) - Co(5)	123.30(2)	Ge(1) - Co(5) - C(51)	84.4(1)
		Ge(1) - Co(5) - C(52)	173.0(1)
Ge(1) - Co(1) - Ge(1')	77.00(2)	Ge(1) - Co(5) - C(53)	89.6(1)
Ge(1) - Co(2) - Ge(1')	76.30(2)	Ge(1) - Co(5) - C(54)	82.6(1)
Ge(1) - Co(3) - Ge(1')	75.90(2)		
Ge(1) - Co(4) - Ge(1')	77.60(2)	Co(1) - C(11) - O(11)	174.9(2)
		Co(2) - C(21) - O(21)	176.0(3)
C(11) - Co(1) - C(22)	85.9(1)	Co(2) - C(22) - O(22)	160.8(3)
C(11) - Co(1) - C(B)	95.4(1)	Co(3) - C(31) - O(31)	176.2(3)
C(11) - Co(1) - C(11)	101.6(2)	Co(3) - C(32) - O(32)	168.1(4)
C(22) - Co(1) - C(B)	177.9(1)	Co(4) - C(41) - O(41)	174.5(2)
C(21) - Co(2) - C(22)	100.2(1)	Co(5) - C(51) - O(51)	177.6(3)
C(21) - Co(2) - C(21')	97.3(2)	Co(5) - C(52) - O(52)	177.2(3)
C(31) - Co(3) - C(32)	103.3(2)	Co(5) - C(53) - O(53)	178.2(3)
C(31) - Co(3) - C(31')	94.7(2)	Co(5) - C(54) - O(54)	172.1(3)
		Co(1) - C(B) - Co(4)	83.9(2)
		Co(1) - C(22) - Co(2)	79.4(1)
SEE NOTES FOR TABLE 7.6		Co(1) - C(22) - O(22)	119.7(3)
		Co(1) - C(B) - O(B)	139.7(3)
		Co(4) - C(B) - O(B)	136.4(3)

TABLE 7.8 BOND LENGTHS OF RELATED COMPOUNDS, (Å).

COMPOUND	E - Co	Co - Co	Ref.
$H_3GeCo(CO)_4$	2.416		173
$Cl_3GeCo(CO)_4$	2.310		173
(+)-MePh(nap)$GeCo(CO)_4$	2.458		174
$PhGeCo_3(CO)_{11}$	2.375	2.45	44
	2.392 (a)		
$GeCo_4(CO)_{13}$	2.280	2.61	64
	2.350 (a)		
$GeCo_4(CO)_{14}$	2.339	2.56	57
	2.387		
$HgGeCo_5(CO)_{17}^-$	2.40	2.53	58
	2.32	2.75	
$GeCo_5(CO)_{16}^-$	2.441	2.525	65
	2.335	2.547	
	2.496		
	2.453		
	2.480		
$Ge_2Co_7(CO)_{21}^{2-}$	2.32 (b)	2.60 (d)	66
	2.28 (c)		
$(PhP)_2Co_4(CO)_{10}$	2.24 (d)	2.52 (d)	91
		2.70 (d)	

NOTES : (a) Determined by electron diffraction.

(b) Average for Ge - Co (cluster).

(c) Average for Ge - Co (central).

(d) Average of equivalent bonds.

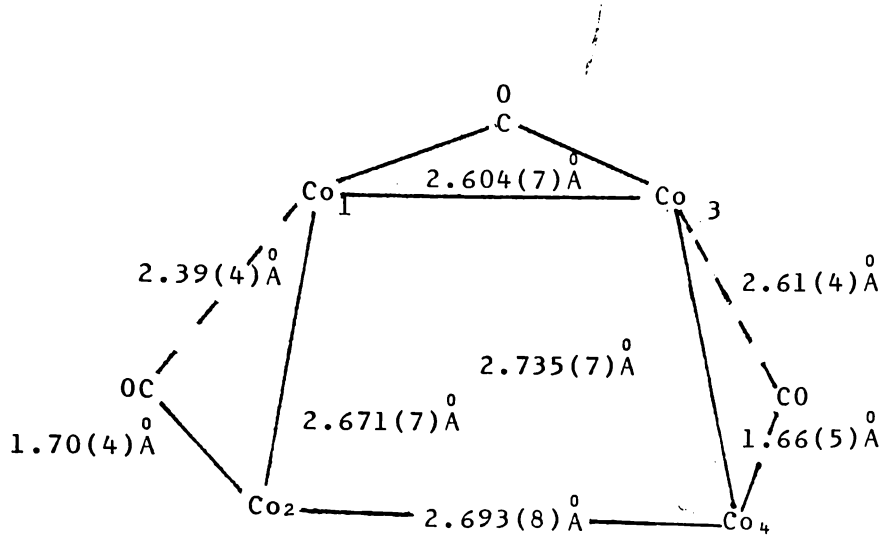

The symmetrically CO-bridged Co-Co bond is again the shortest (as for $(MeGe)_2Co_4(CO)_{11}$), however the longest bond is $Co_{(3)}$-$Co_{(4)}$ which is semi-bridged by an in-plane carbonyl group. This bond is significantly longer than the apparently equivalent $Co_{(1)}$-$Co_{(2)}$. The distortion in these apparently equivalent bonds suggest that this effect is due mainly to crystal packing forces.

This distortion is paralleled by the semi-bridging carbonyls. Thus the longer $Co_{(3)}$-$Co_{(4)}$ bond is semi-bridged by a significantly more asymmetric carbonyl (long Co-Cdistance, 2.61(4) Å, short Co-Cdistance, 1.66(5) Å) than is the shorter $Co_{(1)}$-$Co_{(2)}$ bond (long Co-Cdistance, 2.39(4) Å, short Co-C distance, 1.70(4) Å). These distortions are again most likely due to packing effects.

The remaining 9 cluster carbonyl groups are arranged similarly to those in $(MeGe)_2Co_4(CO)_{11}$, with 8 terminal (2 on each Co atom) and 1 symmetrically bridging carbonyl.

The terminal carbonyls on the apical cobalt atoms are arranged with 3 equatorial and 1 axial, as is normal for a

$-Co(CO)_4$ group (64). The two sets of equatorial carbonyls are perfectly eclipsed as is required by the mirror symmetry. The orientation of these carbonyl groups (i.e. eclipsing the symmetric bridging carbonyl) minimises interaction between these equatorial carbonyls and the upward pointing carbonyls on the cluster cobalt atoms. (See Figs. 7.4 and 7.5).

The equatorial carbonyl groups (on the apical Co atoms) are displaced towards the Ge atoms (see Table 7.7, Ge-Co-C angles of $84.4(1)^0$, $89.6(1)^0$ and $82.6(1)^0$) in the so-called "umbrella" effect. The cause of this effect is not clear, however it has been ascribed to electronic (124), and efficient crystal packing (125), forces.

7.3 Discussion of the Structures of $(MeGe)_2Co_4(CO)_{11}$ and $\{Co(CO)_4Ge\}_2Co_4(CO)_{11}$.

These structures establish an entirely new cluster type for group IVB elements. Analogous clusters with group V and group VI atoms as the hetero atoms (in particular phosphorus and sulphur) have previously been reported by Vahrenkamp (92, 126, 127) and Dahl (91), (See Table 7.9).

Reports of pentacoordinate group IVB atoms,especially with square pyramidal coordination, are extremely rare, and have so far been limited to a few anionic complexes in which Sn or Ge atoms are bonded to four group VI atoms (either O or S) and a halogen (ClorF) (128-131). The only complex previously known where Ge (or any group IVB atom) is bonded to 5 transition metal atoms, is the irregularly coordinated $GeCo_5(CO)_{16}^-$ (See Fig. 1.3(a), ref.65).

The Ge---Ge non-bonded distances in these clusters, of 2.926(2) $\mathring{A}$ and 2.995(4) $\mathring{A}$ are only some 20% longer than the bonded distance in $H_3Ge\text{-}GeH_3$ (132). Although this would appear to imply considerable Ge-Ge interaction, Dahl et al. (91), have suggested that in the analogous phosphorus and sulphur tetracobalt clusters, the close E---E (E = P,S) distance is due mainly to the constraints imposed upon the heteroatoms by the metal-E bond, lengths and angles.

The in-plane semi-bridging carbonyls are observed in both structures. Two distinct types of semi-bridging CO groups have been observed in transition metal complexes. The first type arises in molecules which have an imbalance of charge distribution on two adjacent metal atoms (133). In $C_4(CH_3)_2(OH)_2Fe_2(CO)_6$, (134);

TABLE 7.9 KNOWN $[\mu_4\text{-E}]_2M_4$ CLUSTERS.

COMPOUND	ELECTRON PAIRS AVAILABLE FOR CLUSTER BONDING	REF.
$(PhP)_2Co_4(CO)_8(\mu\text{-}CO)_2$	8	91
$(PhP)_2Co_4(CO)_6(\mu\text{-}CO)_2(PPh_3)_2$	8	91
$S_2Co_4(CO)_8(\mu\text{-}CO)_2$	8	91
$Te_2Co_4(CO)_8(\mu\text{-}CO)_2$	8	91
$(PhP)_2[Fe(CO)_3]_2[Co(CO)_2]_2(\mu\text{-}CO)$	8	92
$S_2[Fe(CO)_3]_2[Co(CO)_2]_2(\mu\text{-}CO)$	8	92
$(PhP)_2Fe_4(CO)_{12}$	8	127
$(PhP)_2Fe_4(CO)_{10}(\mu\text{-}CO)$	7	127
$(MeGe)_2Co_4(CO)_{10}(\mu\text{-}CO)$	8	(a)
$[(OC)_4CoGe]_2Co_4(CO)_{10}(\mu\text{-}CO)$	8	(a)

(a) This Work.

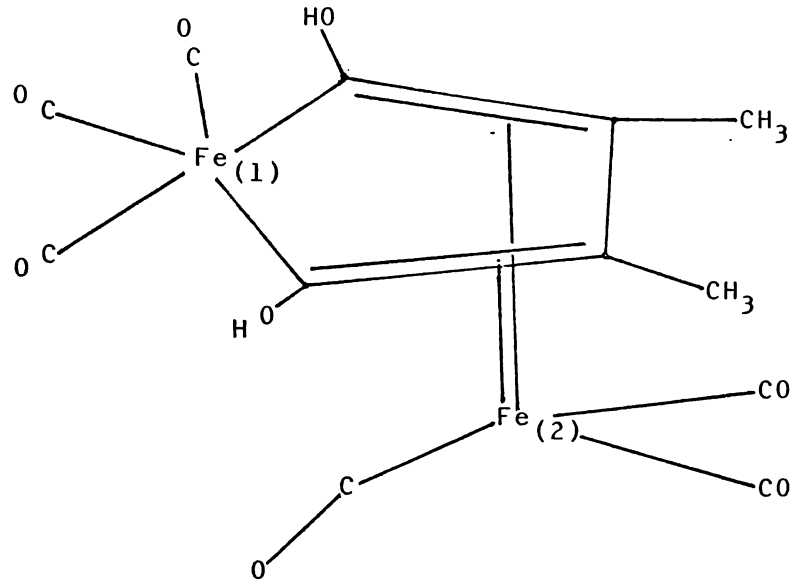

a local electron count gives 16 and 18 electrons on $Fe_{(1)}$ and $Fe_{(2)}$ respectively (not counting the Fe-Fe bond). The Fe-Fe bond is therefore regarded as a donor $Fe_{(2)} \rightarrow Fe_{(1)}$ interaction which leads to a build up of negative charge on $Fe_{(1)}$, which is diminished by donation of electron density from the dπ orbitals on $Fe_{(1)}$ into the pπ* orbital of the semi-bridging carbonyls C atom.

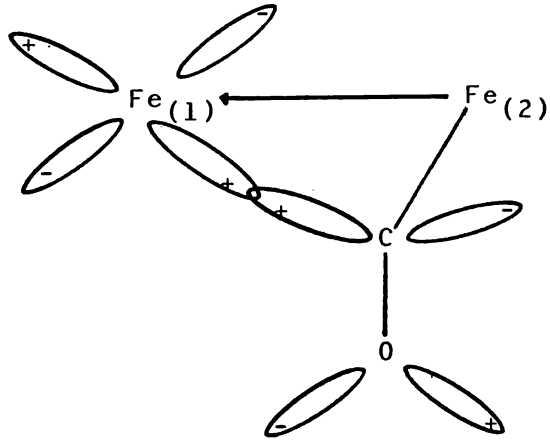

Curtis (135, 136) has discussed another type of semi-bridging carbonyl, which occurs in complexes which are overall formally electron deficient, such as $\{CpMo(CO)_2\}_2$, in which CO acts as a 4 electron donor by donating electron density from the COπ bonds to the adjacent Mo's dπ orbitals.

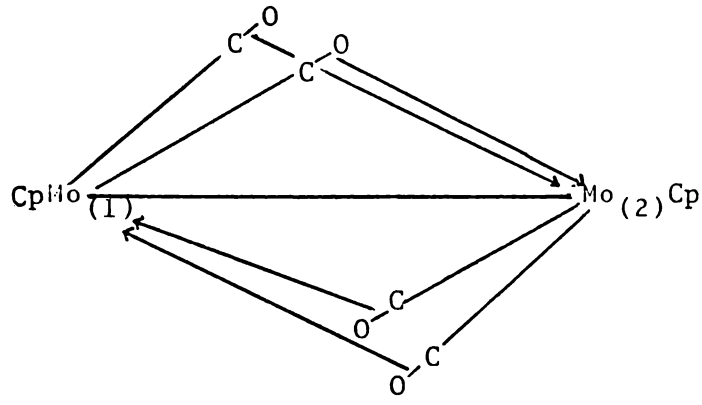

The two types of semi-bridging carbonyls can be distinguished by differences in the bridge asymmetry parameter with respect to the M-C-O angle, θ.

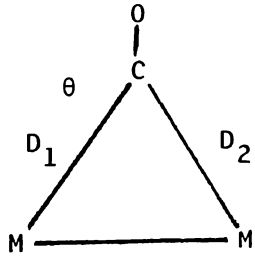

$$\text{Bridge asymmetry parameter} = \frac{(D_2 - D_1)}{D_1}$$

where D_1 = shorter M-C distance

D_2 = longer M-C distance.

Thus for semi-bridging carbonyl groups of the first type, θ varies directly with the degree of bridge asymmetry

and a plot of the two gives essentially a smooth curve. For semi-bridging carbonyls of the second type, the two functions appear independent of each other, as expected, as the interactions between the metal and the C and O of the carbonyl are similar, and the carbonyl remains essentially linear.

The semi-bridging carbonyls in $(MeGe)_2Co_4(CO)_{11}$ and $\{Co(CO)_4Ge\}_2Co_4(CO)_{11}$ are of the first type. Localised electron counting on the two electronically and coordinatively distinct cobalt atoms in the cluster, show the cobalt bonded to the symmetric bridging carbonyl to have 18 electrons and the other cobalt to have 19 electrons. Thus donation of charge from the electron-rich cobalt to the deficient cobalt, leads to a buildup of charge which is diminished by donation of electron density through the semi-bridging carbonyl (as for the Fe complex). The crystallographic evidence supports this assignment with the asymmetry parameters appearing to be related to θ and fitting on the curve of a plot of the two parameters using selected examples (See Fig. 7.6).

Consistent with other reports (137-139), the bonding in these clusters cannot be described in terms of two-centre electron bond pairs. Although by an appropriate electron assignment, the 4 cobalt atoms can formally obtain an 18 electron configuration:

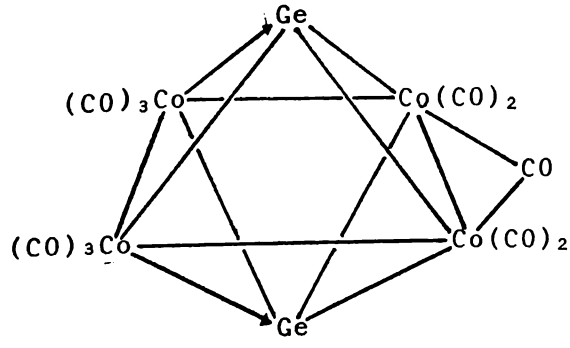

FIGURE 7.6 PLOT OF THE M-C-O ANGLE (Θ) VERSUS THE BRIDGE ASYMMETRY PARAMETER. (Ref. 136).

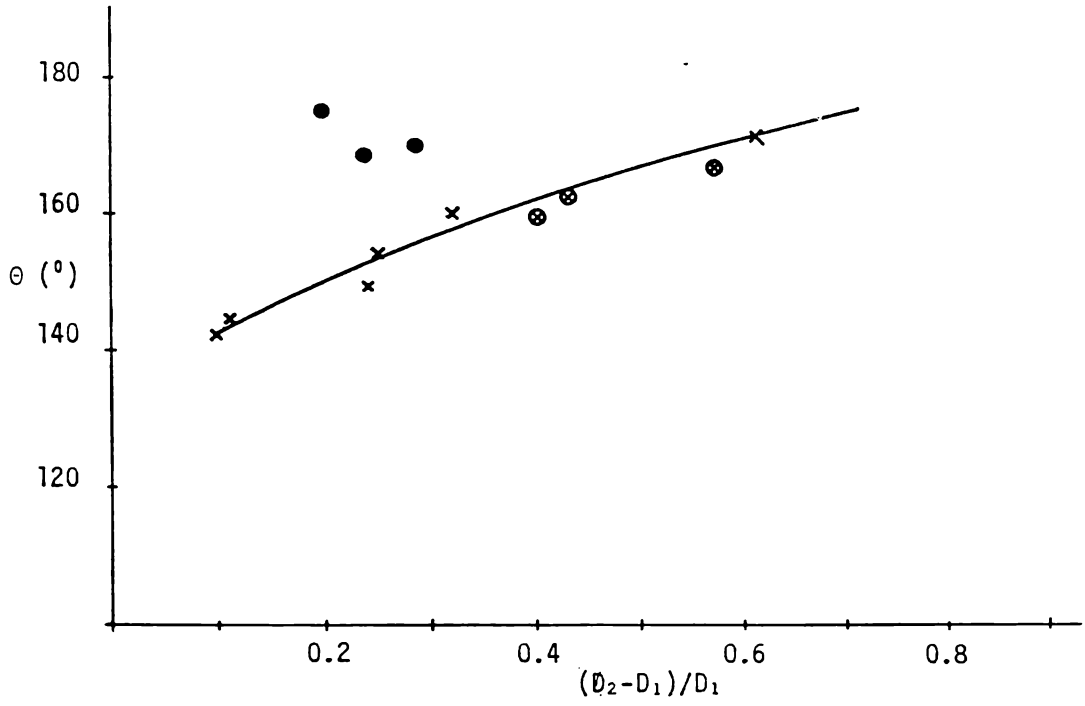

COMPOUND	$(D_2-D_1)/D_1$	Θ	REFERENCE
$Fe_3(CO)_{11}PPh_3$*	0.10	143	164
$Fe_3(CO)_{12}$*	0.11	148	165
$Ru_4(CO)_{13}$	0.24	150	166
$[Fe(py)_6Fe_4(CO)_{13}]$	0.25	155	167
$Fe_2(CO)_7$dipy	0.32	161	168
$Ge_2Co_6(CO)_{19}$	0.40	161	(a)
$(MeGe)_2Co_4(CO)_{11}$	0.43	164	(a)
$Ge_2Co_6(CO)_{19}$	0.57	168	(a)
$Cp_2Mo_2(CO)_6$*	0.61	173	169
$Cp_2Mo_2(CO)_4$	0.20	176	136
$Cp_2V_2(CO)_5$	0.24	169	170
$Cp_2Cr_2(CO)_4$*	0.29	171	171

* Average of all carbonyls , (a) This work.

such exercises serve little purpose in elucidating the bonding in clusters.

Further, the shape of these clusters cannot be predicted by the method of Wade (140, 141):

4 Co atoms (d^9)	:	36 electrons
11 Carbonyl groups	:	22 electrons
2 Ge atoms	:	8 electrons
2 CH_3 groups	:	2 electrons
Total	:	68 electrons.

Subtract:

12 electrons per transition metal	:	48 electrons
and 2 electrons per main group atom	:	4 electrons.
∴ Total electrons available for cluster bonding	:	16 electrons.

Which is 8 skeletal electron pairs (b). The number of skeletal atoms (a) is 6, thus b = a + 2, from which a nido-pentagonal bipyramid is predicted and not the observed pseudo-octahedron.

A survey of structurally related clusters (E_2M_4), (See Table 7.9) shows that this type of cluster appears to favour a, b = a + 2, one electron pair rich configuration. In fact only one example of this type of cluster is known whose structure can be predicted by Wades' rules, $(PhP)_2Fe_4(CO)_{10}(\mu\text{-}C\theta)$, which readily accepts a further molecule of CO to take up the electron-rich configuration, (127).

$$(PhP)_2Fe_4(CO)_{10}(\mu\text{-}CO) + CO \rightleftharpoons (PhP)_2Fe_4(CO)_{10}(\mu\text{-}CO)$$

The relatively easy low energy interconversion of these electronically different clusters, suggests that the extra electron pair in the electron-rich clusters occupies an essentially non-bonding orbital.

Clearly the bonding in these clusters is complex . This is partly shown by the crystallographic evidence. That the Ge atoms in these clusters occupy such a symmetric position, with all Ge-Co bond lengths virtually equal, despite being bonded to two electronically and coordinatively different cobalt atoms, indicates a delocalised type of bonding.

A possible scheme can be developed to represent the overlap of Ge and Co orbitals which would give strong bonding combinations. This scheme (Fig.7.7) is based on analogous schemes for the bonding in $GeFe_2$ triangles (142) and M^1Co_3 tetrahedra (143), and involves the overlap of a Ge Sp_z hybrid orbital and the Ge P_x and P_y orbitals with the appropriate d-orbitals of the 4 cobalt atoms. Although this is not intended as a definitive treatment, it does show that the Ge d-orbitals do not need to be invoked to explain the bonding in these clusters. More detailed molecular orbital treatments would undoubtedly help us to understand the peculiar electron rich configuration of these clusters.

FIGURE 7.7 POSSIBLE OVERLAP OF Ge - Co ORBITALS IN Ge_2Co_4 CLUSTERS

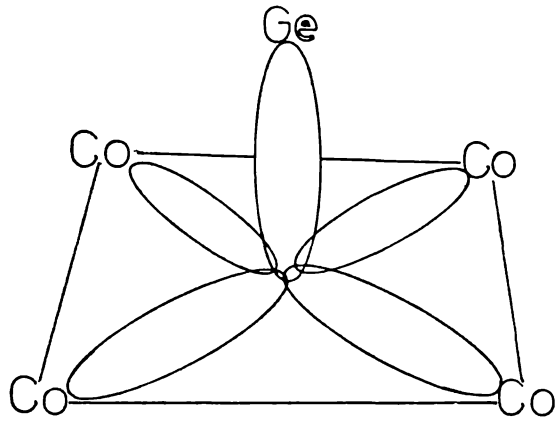

(A) Overlap of a Ge hybrid orbital with inward pointing Co d-orbitals.

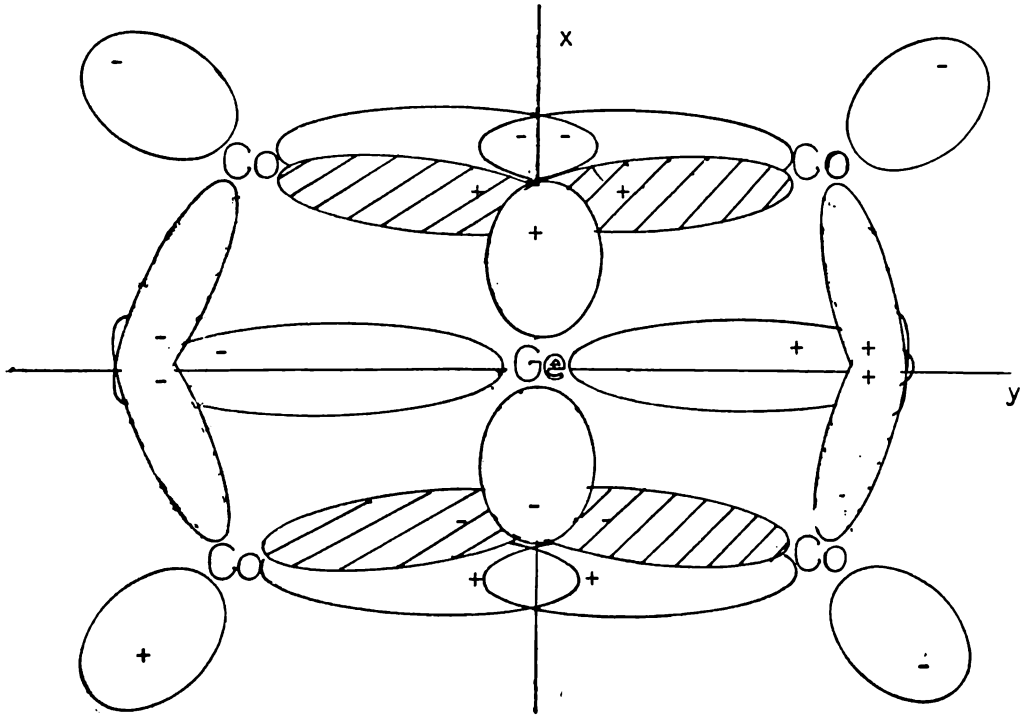

(B) Overlap of Ge p_x and p_y orbitals with Co π-type orbitals.

(note:distortions in orbitals are for the sake of the diagram only)

7.4 The Handling and Spectroscopic Properties of $(MeGe)_2Co_4(CO)_{11}$ and $\{(CO)_4CoGe\}_2Co_4(CO)_{11}$.

7.4.1 Handling.

$(MeGe)_2Co_4(CO)_{11}$ is an orange solid which is stable at room temperature in the absence of air. It decomposes slowly in air, but may be handled for short periods with little decomposition. It is just soluble in hexane and slightly more so in dichloromethane.

$\{(CO)_4CoGe\}_2Co_4(CO)_{11}$ is a black solid, which is extremely stable (relative to the other compounds prepared in this work) to air decomposition. As a solid, it may be handled in air for up to 24 hours with only a small amount of decomposition. It is virtually insoluble in hexane, and only slightly soluble in dichloromethane (at 20^0C).

7.4.2 Mass Spectrum of $(MeGe)_2Co_4(CO)_{11}$

The mass spectrum of $(MeGe)_2Co_4(CO)_{11}$ (See Table 7.10) is remarkably simple, with a very strong series of ions resulting from the successive loss of 11 CO from the parent ion, $Me_2Ge_2Co_4(CO)_{11}^+$, dominating the spectrum (71% of the total ion current is carried by these ions). Ions resulting from methyl loss from the metal skeleton are only of significant intensity when most of the carbonyls have already been lost (although ions resulting from the loss of 2 methyl groups, overlap with ions resulting from CO loss). Of the total ion current, 91% is carried by ions retaining the Ge_2Co_4 skeleton. These figures are unusually high for a group IVB-cobalt cluster (see $Ge_2Co_6(CO)_{20}$ spectrum for example), perhaps suggesting unusual stability.

Table 7.10 Mass Spectrum of $(MeGe)_2Co_4(CO)_{11}$

m/e	rel. int	Assignment	
714-726	10	$(MeGe)_2Co_4(CO)_x^+$,	x = 11
686-698	40		x = 10
658-670	34		x = 9
630-642	22		x = 8
602-614	41		x = 7
574-586	100		x = 6
546-558	44		x = 5
518-530	19		x = 4
490-502	29		x = 3
462-474	37		x = 2
434-446	28		x = 1
400-418	51		x = 0
503-515	5	$MeGe_2Co_4(CO)_x^+$,	x = 4
475-487	10		x = 3
447-459	14		x = 2
419-431	3		x = 1
392-404	49	$(CH)Ge_2Co_4^+$	
376-388	46		x = 0
343-355	3	$(CH)_2Ge_2Co_3^+$	
330-342	13	$(CH)Ge_2Co_3^+$	
317-329	16	$Ge_2Co_3^+$	
284-296	46	$(CH)_2Ge_2Co_2^+$	
271-283	7	$(CH)_2Ge_2Co_2^+$	
258-260	4	$Ge_2Co_2^+$	
144-150	8	$MeGeCo^+$	

Ions resulting from either Co or Ge loss are of relatively weak intensity, except for the envelope at m/e = 284-296, corresponding to $(HC)_2Ge_2Co_2^+$, (loss of 2Co atoms). This fragmentation is interesting in that Vahrenkamp has prepared related clusters by the addition of Co_2 units to E_2M_2 (E = P,S, M = Fe) structures (92).

e.g.

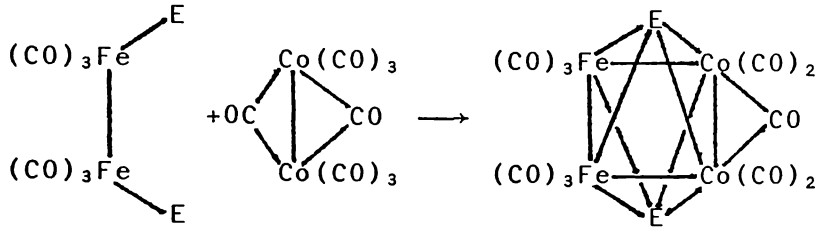

7.4.3 Mass Spectrum of $\{(CO)_4CoGe\}_2Co_4(CO)_{11}$.

A good mass spectrum of $\{(CO)_4CoGe\}_2Co_4(CO)_{11}$ could not be obtained due to its involatility. One spectrum however produced as an identifiable ion pattern $Ge_2Co_6^+$ (m/e = 494-506), which dominated (in intensity) all ions above m/e = 400. Patterns above this representing carbonylation of the skeleton, were too weak to attribute above the noise level.

7.4.4 Infrared Spectrum of $(MeGe)_2Co_4(CO)_{11}$

The infrared spectrum of the carbonyl stretching region of $(MeGe)_2Co_4(CO)_{11}$ is shown in Fig. 7.8 and listed in Table 7.11. In solution, the molecule is probably of C_{2v} symmetry (See Figs. 7.1 and 7.2) from which we predict 8 infrared active modes for the terminal (and semi-bridging) carbonyls. The spectrum is however simpler than this with only 5 bands observed (one of which may be a $\nu^{13}CO$) for the terminal carbonyls.

FIGURE 7.8 INFRARED SPECTRUM OF $(MeGe)_2Co_4(CO)_{11}$

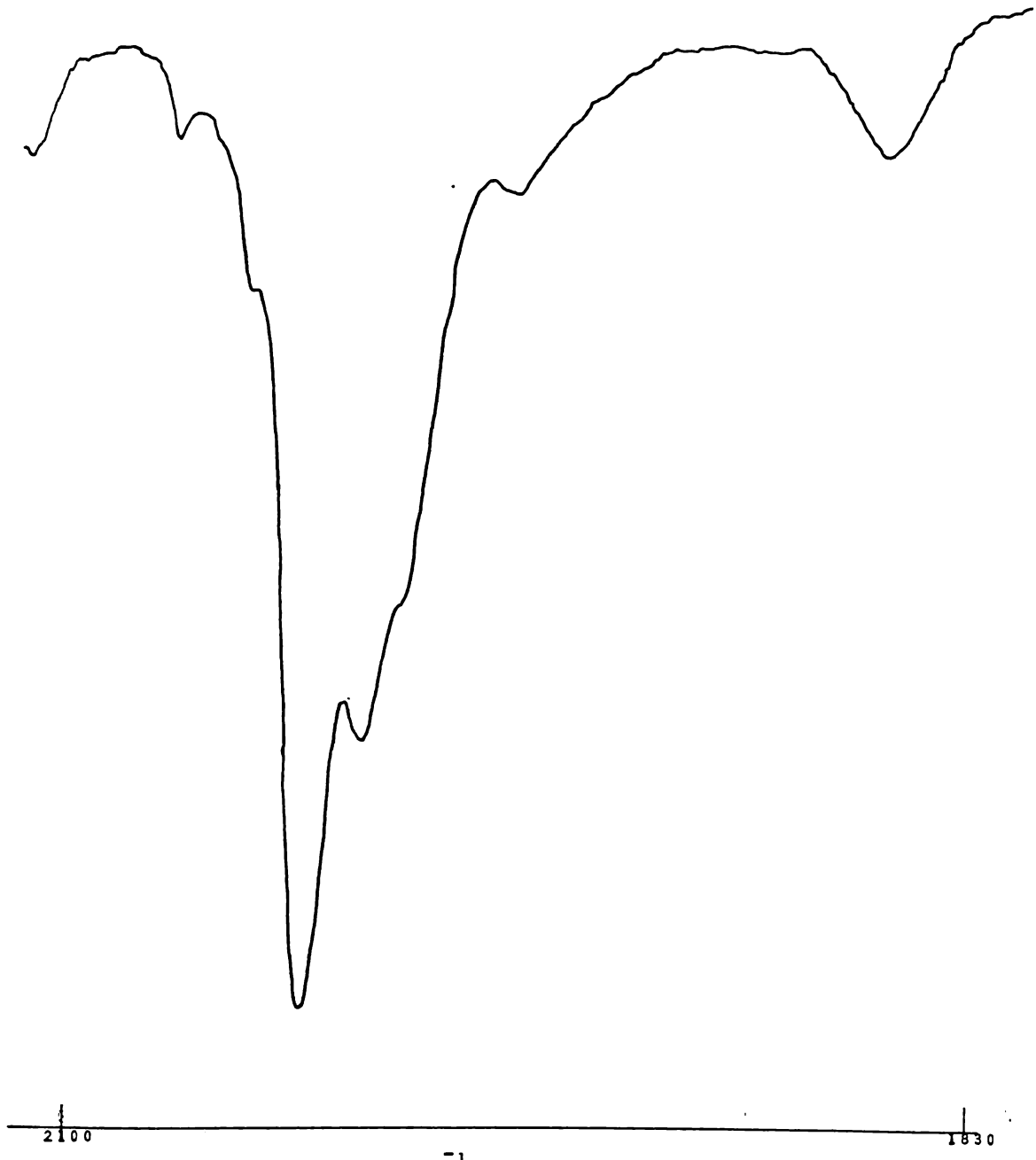

TABLE 7.11 INFRARED SPECTRA OF $(MeGe)_2Co_4(CO)_{11}$ and $(MeP)_2Co_4(CO)_{11}$

$(MeGe)_2Co_4(CO)_{11}$: 2034 vs, 2015 s, 2004 sh m, 1990 w, 1985 vw, 1850 br w.

$(MeP)_2Co_4(CO)_{11}$: 2030 vs, 2025 s, 2006 m, 1983 m, 1832 s. Ref. 126.

DICHLOROMETHANE SOLUTION

The band at ca. 1850cm^{-1} is in the expected region for a normal bridging carbonyl stretch. Note that the 8 axial carbonyl groups lie in approximate D4h symmetry (for a $Co_4(CO)_8$ group of D4h symmetry we predict 3 infrared active bands, $A_{2u}+E_g+E_u$), thus also taking into account the 2 equatorial (semi-bridging) carbonyls, we may expect a 5 band spectrum, as is observed.

The spectrum is similar to that of the iso-structural cluster $(MeP)_2Fe_4(CO)_{11}$ (See Table 7.11) and also the iso-electronic clusters $(PhP)_2Co_4(CO)_{12}$ (91), and $\{PhP\}_2Fe_4(CO)_{12}$. It therefore appears likely that this type of cluster may have a characteristic spectrum (as do the $OCCo_3(CO)_9$ clusters, see Section 3.3.3.3).

7.4.5 Infrared Spectrum of $\{(CO)_4CoGe\}_2Co_4(CO)_{11}$.

The infrared spectrum of $\{(CO)_4CoGe\}_2Co_4(CO)_{11}$ in the carbonyl stretching region is similar to that of $(MeGe)_2Co_4(CO)_{11}$. The spectrum can be resolved as due to vibrations of two groups with little vibrational coupling between them. The vibrations of the $-Co_4(CO)_{11}$ group may be assigned as for $(MeGe)_2Co_4(CO)_{11}$ and subtraction of these leave two bands (at 2100cm^{-1} and 2050cm^{-1}) and possibly a third (at 2065cm^{-1}), although this may be due to a trace of $Co_4(CO)_{12}$, which may be ascribed to vibrations of the $-Co(CO)_4$ groups. With local symmetry of C_{3v} for the $-Co(CO)_4$ group, we expect 3 infrared active modes ($2a_1+e$) for the carbonyl stretches. If the assignment of the above bands is accepted, then this puts these bands at considerably higher frequency than for, say $Me_3GeCo(CO)_4$ (20). This may be explained by the electron

FIGURE 7.9 INFRARED SPECTRUM OF $[(OC)_4CoGe]_2Co_4(CO)_{11}$

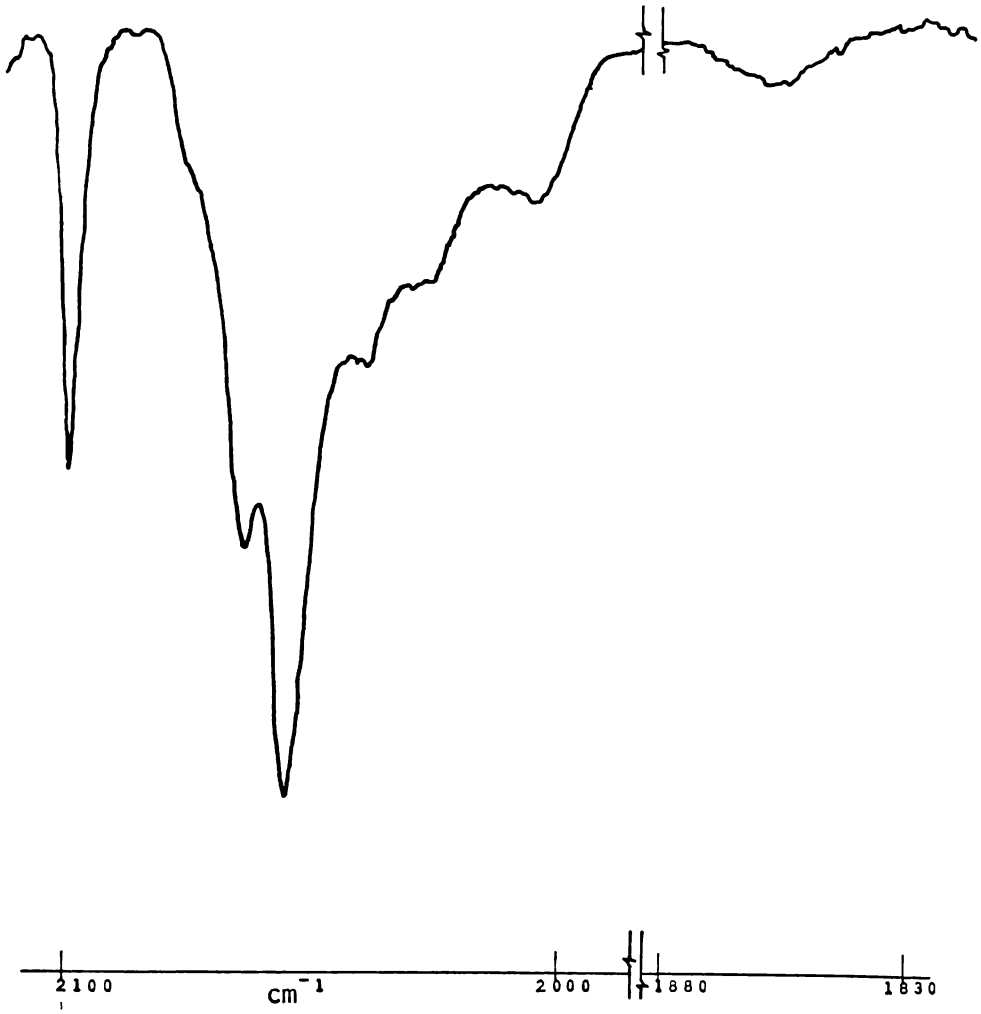

TABLE 7.12 INFRARED SPECTRUM OF $[(OC)_4CoGe]_2Co_4(CO)_{11}$

2100 s	2003 sh w
2065 sh w	1990 sh w
2050 s	
2037 vs	1844 br w
2014 m	

DICHLOROMETHANE SOLUTION

withdrawing effect of the $-Co_4(CO)_{11}$ group on the Ge atoms which results in a strengthening of the C-O bonds and raises the energy of νCO (see for example, the spectra of $X_3GeCo(CO)_4$ species, X = Cl, Br, I, ref.23).

This effect is not reflected in the spectrum of $(CO)_4CoGeCo_3(CO)_9$ (64) where the $-Co(CO)_4$ group carbonyl stretches are at lower frequency. This may well be due to the lesser electronic demands of the $Co_3(CO)_9$ (relative to the tetracoordinate $-Co_4(CO)_{11}$ group) on the Ge atom.

CHAPTER 8. Discussion.

8.1 On the Mechanism of the Group IVB Hydride/$Co_2(CO)_8$ Reaction.

8.1.1 Reaction of Me_3GeH With $Co_2(CO)_8$.

Before discussing the reactions of various germanes with $Co_2(CO)_8$, reported in Chapters 3, 4 and 5, it is worth considering the reaction of Me_3GeH. This was studied briefly because:

(i) the products arising from the reaction:

$$2Me_3GeH + Co_2(CO)_8 \longrightarrow 2Me_3GeCo(CO)_4 + H_2$$

are well established (20) and thus this aspect was not pursued. and (ii) it is a simple hydride, having only one position for substitution, and it therefore offers a simple system from which to obtain general mechanistic information.

Experimental:

The reaction of Me_3GeH with $Co_2(CO)_8$ was monitored by measurement of the evolved H_2.

Table 8.1 H_2 Production From the Reaction of $Me_3GeH/Co_2(CO)_8$.

Me_3GeH (249mg, 2.10mmoles), $Co_2(CO)_8$ (360mg, 1.05mmoles)

2:1 Ratio.

Time.	mmoles H_2	% of Total.
15 min.	0.92	88
75 min.	1.04	99
7 days	1.06	101

Me_3GeH (267mg, 2.25mmoles), $Co_2(CO)_8$ (770mg 2.25mmoles)

1:1 Ratio.

15 min.	1.07	95
20 hours.	1.14	102

The molecular weight was checked and confirmed as H_2 (experimentally Determined 2.8, Calc. 2.00).

8.1.2 The Reactions of the Monogermanes.

The mechanism for the reaction of a group IVB hydride with $Co_2(CO)_8$, proposed by Chalk and Harrod (See Section 1.4) is under question (13).

(1) $Me_3SiH + Co_2(CO)_8 \rightarrow Me_3SiCo(CO)_4 + HCo(CO)_4$

(2) $Me_3SiH + HCo(CO)_4 \longrightarrow Me_3SiCo(CO)_4 + H_2$

(3) $2HCo(CO)_4 \longrightarrow Co_2(CO)_8 + H_2$

This reaction system is complicated by the instability of $HCo(CO)_4$ which readily decomposes at room temperature (according to equation 3) regenerating $Co_2(CO)_8$. Thus equation 2 may not take place. Further, $HCo(CO)_4$ has never been observed in significant quantities to quantify equation 1.

Although it has not been the intention of this work to elaborate the mechanism of the reaction, some interesting points have emerged.

The measurement of the incondensable gases produced during the reactions at room temperature of Me_2GeH_2, GeH_4, Me_2SiH_2 and Ge_2H_6 with $Co_2(CO)_8$ (See Chapters 3, 4 and 5) all show initially a greater evolution of CO than H_2(relative to the expected reaction stoichiometric ratios). As the reaction proceeds the ratio of $CO:H_2$ approximates more closely to the expected stoichiometric ratio. An explanation for this may be formulated using the $Me_2GeH_2/Co_2(CO)_8$ reaction as an example.

As (in this case) CO is evolved (neglecting $Co_4(CO)_{12}$ production) from the production of $Me_2GeCo_2(CO)_7$:

(4) $Me_2GeH_2 + Co_2(CO)_8 \longrightarrow Me_2GeCo_2(CO)_7 + H_2 + CO$

the retardation of H_2 evolution suggests production via an intermediate species, most probably with a Co-H bond. Thus some intermediate such as $Me_2(H)Ge - Co(CO)_x - Co(H)(CO)_x$ seems reasonable. A model compound is $HCo(CO)_4$ (which could actually form by further reaction of the postulated intermediate).

Sternberg et al. (108) have measured the decomposition of $HCo(CO)_4$ (equation 3) and found it to be a second order process with a rate constant, k_2, of approximately 3×10^{-3} $(mole/litre)^{-1}$ sec^{-1}. The half life of a solution of $HCo(CO)_4$ can thus be calculated using equation 5.

(5) $$t_{0.5} = \frac{1}{k_2 a}$$

where a = initial concentration (mol l^{-1})
Assuming (in run 4, section 3.1.2) that the reaction is extremely rapid (using the figure for CO production as representing the degree of reaction), then after 1 hour a maximum of 5.6mmoles of $HCo(CO)_4$ is produced. In the 10ml of hexane, the solution is 0.56mol l^{-1} in $HCo(CO)_4$. Using equation 5, after 70 minutes (3 half lives) we expect 2.45mmoles of H_2 which agrees closely with the observed value after 60 minutes, of 2.4mmoles.

Despite the major assumptions in the above argument, the agreement is striking and supports the proposal that $HCo(CO)_4$ or a more complex related Co-H species is produced in major quantities as an intermediate.

From the low temperature ($\simeq 4^0C$) reaction of GeH_4 with $Co_2(CO)_8$ (See Section 5.2.1) a considerable quantity (43mg,

0.25mmoles) of $HCo(CO)_4$ was isolated. This is as expected, as it has previously been observed (50) that $HCo(CO)_4$ decomposes slowly at or below 0^0C. Consistent with this result was the measurement of the incondensable gases evolved during this experiment which indicated after 74 days, that while 96% of the total possible CO had been evolved, only 63% of the total possible H_2 had been evolved.

The reaction of Me_3GeH with $Co_2(CO)_8$ (Section 8.1), evolved H_2 considerably quicker than the reactions previously mentioned, and is virtually complete within an hour. This result may be explained by two different arguments:

(i) If we assume Me_3GeH reacts only with $Co_2(CO)_8$ (and not $HCo(CO)_4$):

$$Me_3GeH + Co_2(CO)_8 \longrightarrow Me_3GeCo(CO)_4 + HCo(CO)_4$$

then H_2 evolution is hastened only by faster $HCo(CO)_4$ decomposition. This may be explained by the report of Chalk and Harrod (13) who have shown that certain trisubstituted silanes accelerate the decomposition of $HCo(CO)_4$.

It is therefore likely that Me_3GeH also increases the decomposition of $HCo(CO)_4$. This implies a difference in behaviour towards $HCo(CO)_4$ decomposition between Me_3GeH and the other hydrides used for these measurements. Note that in Chalk and Harrod's report only the effect of trisubstituted silanes were measured.

(ii) The second argument assumes that Me_3GeH reacts rapidly not only with $Co_2(CO)_8$ but also with $HCo(CO)_4$.

$$Me_3GeH + HCo(CO)_4 \longrightarrow Me_3GeCo(CO)_4 + H_2$$

Thus H_2 evolution would be rapid. Note that this also implies differences in behaviour between Me_3GeH and the other hydrides

used. The reaction of Me_2GeH_2 with $HCo(CO)_4$ would need to be slow to explain the observed retarded H_2 evolution.

Finally comment should be made on the measurement of the incondensable gases produced during the reaction of excess GeH_4 with $Co_2(CO)_8$ ($1GeH_4:1Co_2(CO)_8$ See Section 5.2.1 run 9). The equal quantities of CO and H_2 observed after $1\frac{1}{2}$ hours of reaction are consistent with the formation of species that will not readily condense and evolve CO, most likely partially substituted germanes, rather than H_2 evolution not being retarded. The formation of quantities of these partially substituted products in the reactions of excess hydride with $Co_2(CO)_8$ is confirmed by the isolation of quantities of $GeH_3Co(CO)_4$ and $HGe\{Co(CO)_4\}_3$ from the reaction of GeH_4 with $Co_2(CO)_8$ (1:1 ratio, run 8, Section 5.1.2).

8.2 On the Reaction of Ge_2H_6 with $Co_2(CO)_8$.

Although quantitative cleavage of the Ge-Ge bond in Ge_2H_6 was effected in this reaction, the high yield of $Ge_2Co_6(CO)_{20}$ obtained (relative to the GeH_4 and $Me_3M^1GeH_3$ reactions) suggests that a different mechanism of formation holds for this reaction (the mechanism of formation of $Ge_2Co_6(CO)_{20}$ in the other reactions is discussed in the following section).

It seems most likely that during the initial reaction, an intermediate is formed in which the Ge-Ge bond is weakened or even cleaved but in which the two Ge atoms are held in a favourable position for further reaction. A possible scheme is given in Fig. 8.1. This scheme gives two possible routes

FIGURE 8.1 POSSIBLE MECHANISM FOR THE $Ge_2H_6/Co_2(CO)_8$ REACTION

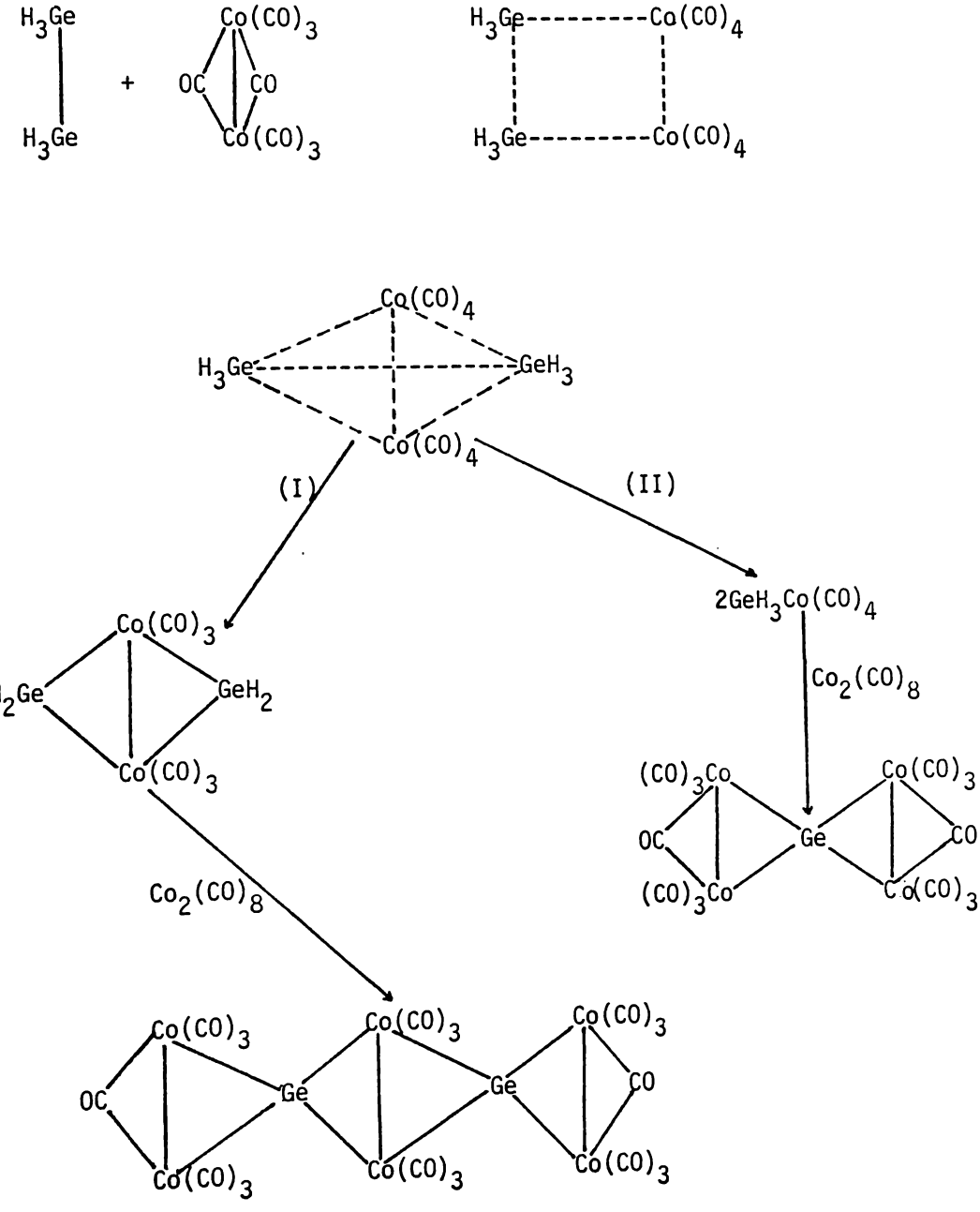

for reaction of the intermediate (A); (I) to ultimately form $Ge_2Co_6(CO)_{20}$ and (II) to ultimately form $GeCo_4(CO)_{14}$. If this scheme is correct, the moderately high yield of $GeCo_4(CO)_{14}$ in the Ge_2H_6 reaction, suggests there is only a small difference (whether thermodynamic or kinetic) between the two paths. Further, changing the relative ratios of Ge_2H_6:$Co_2(CO)_8$ also affected the relative yields of $Ge_2Co_6(CO)_{20}$ and $GeCo_4(CO)_{14}$ obtained (See Section 5.3) which suggests the concentration of $Co_2(CO)_8$ may influence which path is taken for reaction.

8.3 On the Building of $GeCo_2$ Linked Clusters.

It has been shown in this work that GeH_2 groups may replace a bridging carbonyl group in compounds of type $GeCo_2(CO)_7$, to form an extended $GeCo_2$ linked cluster.

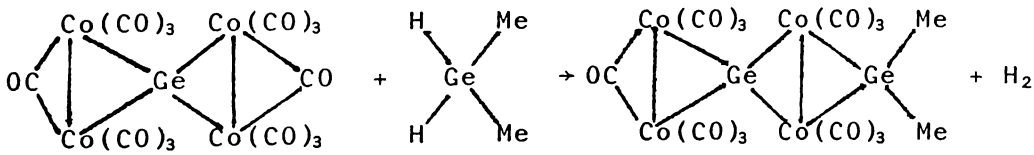

This occurs in the following reactions:

(i) $Me_2GeH_2 + Me_2GeCo_2(CO)_7 \rightarrow (Me_2Ge)_2Co_2(CO)_6 + CO + H_2$

(ii) $Me_2GeH_2 + \{Co_2(CO)_7\}Ge\{Co_2(CO)_7\} \rightarrow \{Co_2(CO)_7\}Ge\{Co_2(CO)_6\}(\mu\text{-}GeMe$
$+ H_2 + CO$

(iii) $MeGeH_3 + \{Co_2(CO)_7\}Ge\{Co_2(CO)_7\} \rightarrow \{Co_2(CO)_7Ge\{Co_2(CO)_6\}(\mu\text{-}Ge(H)M$
$+ H_2 + CO$

(iv) $Me_2GeH_2 + Ge_2Co_6(CO)_{20} \rightarrow (\mu Me_2Ge)Ge_2Co_6(CO)_{18}(\mu\text{-}GeMe_2)$
$+ H_2 + CO$

An interesting feature of reactions (ii), (iii) and (iv)

is the difference in behaviour between $GeCo_4(CO)_{14}$ and $Ge_2Co_6(CO)_{20}$. Despite use of an excess of Me_2GeH_2 in all these reactions, the Me_2Ge group substituted only for one bridging carbonyl in $GeCo_4(CO)_{14}$, whereas it substituted for both bridging carbonyls in $Ge_2Co_6(CO)_{20}$.

A reason may be indicated by the changes in Co-Co bond lengths in $GeCo_4(CO)_{14}$ (57) and $(CO)_4CoHgGeCo_4(CO)_{13}$ (58). In $GeCo_4(CO)_{14}$, both Co-Co bonds are essentially equal with an average of 2.56 $\mathring{A}$. However in $(CO)_4CoHgGeCo_4(CO)_{13}$ (which has a bridging carbonyl replaced by a bridging Hg atom), the Hg bridged Co-Co bond has shortened slightly (relative to $GeCo_4(CO)_{14}$) to 2.54 $\mathring{A}$, but the unbridged Co-Co bond has significantly increased to 2.75 $\mathring{A}$. Thus if substitution of a Me_2Ge group on one end of $GeCo_4(CO)_{14}$ also significantly increases the other Co-Co bond, then this may make substitution at the lengthened bond, less favoured. Obviously the crystal structure of $Me_2Ge_2Co_4(CO)_{13}$ would clarify this, and it is unfortunate it could not be refined.

$Ge_2Co_6(CO)_{20}$ on the other hand is sufficiently extended so that the effect of substitution at one end will be diminished through the chain such that the effect on the other (CO-bridged) Co-Co bond will be small. Thus substitution may occur at both ends.

These reactions may also explain other products observed. Thus the appearance of small quantities of $Ge_2Co_6(CO)_{20}$ in the reactions of GeH_4 (and $Me_3M^1GeH_3$) with $Co_2(CO)_8$ may occur by the side reaction of GeH_4 with $GeCo_4(CO)_{14}$ (the major product of reaction.

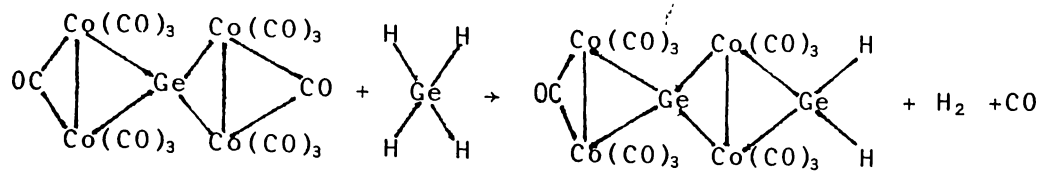

The functional hydrogens may react further to ultimately form $Ge_2Co_6(CO)_{20}$. Likewise the appearance of the $2094cm^{-1}$ species in these (and the Ge_2H_6) reactions, if it is assumed that it is the homologous $Ge_3Co_8(CO)_{26}$, may be explained by a similar reaction.

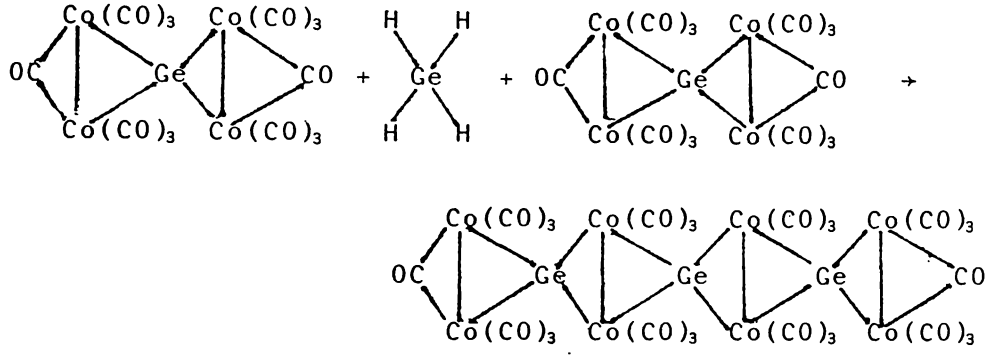

In the reaction of GeH_4 with $GeCo_4(CO)_{14}$ (Section 6.2), small quantities of $Ge_2Co_6(CO)_{20}$ and the $2094cm^{-1}$ species were observed. That the $GeCo_4(CO)_{14}$ remained largely unreacted is probably consistent with the low reactivity of GeH_4 (relative to methyl substituted germanes) (101). Note also that the reaction of $MeGeH_3$ with $GeCo_4(CO)_{14}$ was significantly slower than the corresponding Me_2GeH_2 reaction.

The reaction of Me_3GeH with $GeCo_4(CO)_{14}$ yielded as a product, in low yield, $Me_2Ge_2Co_4(CO)_{13}$. As the sample of Me_3GeH used was very pure and free of $MeGeH_3$ or Me_2GeH_2, this implies a cleavage of a Ge-C bond.

$$GeCo_4(CO)_{14} + Me_3GeH \rightarrow Me_2Ge_2Co_4(CO)_{13} + ?$$

Although $Me_2Ge_2Co_4(CO)_{13}$ was formed in low yield this result is surprising considering the mild reaction conditions used

(room temperature, absence of light) and indicates a peculiar reactivity of $GeCo_4(CO)_{14}$. The fate of the cleaved methyl group was not determined, although a likely fate is as CH_4.

In a number of these systems, no reaction occurred or only a minor side reaction was observed. In the reaction of Me_2GeH_2 with $MeGeCo_3(CO)_{11}$, the only products observed were; $Me_2GeCo_2(CO)_7$, $(Me_2Ge)_2Co_2(CO)_6$ and $Me_2GeHCo(CO)_4$. No substitution product (expected, $MeCo(CO)_4Ge\{Co_2(CO)_6\}\{\mu\text{-}GeMe_2\}$) was observed. Graham has determined the crystal structure of the phenyl analogue, $PhGeCo_3(CO)_{11}$ and found that the bridging carbonyl lies on the same side of the Ge atom as the $-Co(CO)_4$ group (44).

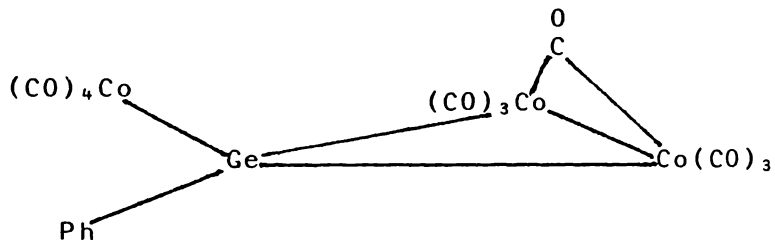

The two bridging carbonyl stretching modes in the infrared spectrum have been attributed to the existence of a second isomer in solution, in which the bridging carbonyl group lies on the same side of the CoGeCo triangle as the phenyl ring. An identical infrared spectrum is observed for $MeGeCo_3(CO)_{11}$ (24).

It is therefore possible that $MeGeCo_3(CO)_{11}$ is less able to accept a bridging Me_2Ge group than the more tightly constrained $GeCo_4(CO)_{14}$, because of the "free" $-Co(CO)_4$ group. Thus the minor pathway may involve formation of an intermediate such as:

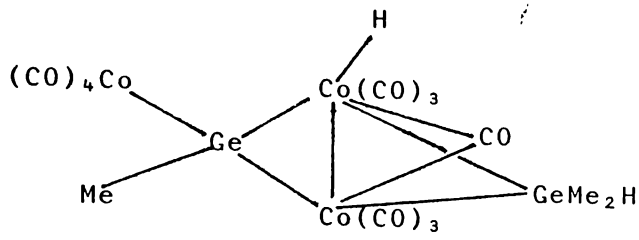

which extrudes $Me_2GeCo_2(CO)_7$. The fate of the MeGe unit is not clear, but the formation of $(MeGe)_2Co_4$ clusters in other reactions may be significant.

Me_2SiH_2 failed to react with $GeCo_4(CO)_{14}$, $Me_2GeCo_2(CO)_7$/ $Me_2Ge\{Co(CO)_4\}_2$ and $MeGeCo_3(CO)_{11}$. Although failure to react with $MeGeCo_3(CO)_{11}$ is not surprising in light of the previous result, the other two species do react with Me_2GeH_2. As noted previously, the reactions of silanes with $Co_2(CO)_8$, tend to form more partially-substituted products than do the analogous germanes (Section 1.4). Thus it appears there may be a lower reactivity of silanes towards such species, although the reason for this is not clear. Perhaps an approach to extended silicon clusters may be through reaction of $SiCo_4(CO)_{14}$ (56).

Finally Me_2SnH_2 appears to have reacted with $GeCo_4(CO)_{14}$, but no Me_2Sn substituted $GeCo_4$ product was identified. The isolation of quantities of $Me_{4-x}Sn\{Co(CO)_4\}_x$, (x = 1,2,3), suggest that, as in the $MeGeCo_3(CO)_{11}$ /Me_2GeH_2 reaction, an initial product may have formed, however structural stresses may have caused it to disproportionate. The structural effect in this case is the reluctance of Sn to bridge a Co-Co bond due to its large covalent radius, (68).

8.4 On the Mechanisms of Formation of $\{Co(CO)_4Ge\}_2Co_4(CO)_{11}$ and $(MeGe)_2Co_4(CO)_{11}$.

Both the compounds characterised by X-ray crystallography in this work, arise from major rearrangements. Perhaps the more clearly envisaged of these is that forming $\{Co(CO)_4Ge\}_2Co_4(CO)_{11}$.

This compound is formed by the gentle heating of $Ge_2Co_6(CO)_{20}$. A possible mechanism for formation is shown in Fig. 8.2. This mechanism is of course a simplification, showing only the rearrangement of the metal atoms and not the carbonyl groups, which are undoubtedly intimately involved. Note also that the arrows are not intended to represent the transfer of electron pairs, only the breaking and forming of bonds.

From the diagrams it is obvious that the labelled cobalt atoms ($Co_{(1)}$ and $Co_{(2)}$) are close together in $Ge_2Co_6(CO)_{20}$ (this structure is an extrapolation based on the related structure of $GeCo_4(CO)_{14}$, ref (57)), such that as the outer Co-Co bonds break they may form a bond and thus initiate the "clusterification". Note that the decarbonylation of $Ge_2Co_6(CO)_{20}$ to the digermanium-tetra cobalt cluster $\{Co(CO)_4Ge\}_2Co_4(CO)_{11}$ is a direct parallel of the decarbonylation of the lower homologue $GeCo_4(CO)_{14}$ to the monogermanium-tricobalt cluster $(CO)_4CoGeCo_3(CO)_9$ (57).

While a similar mechanism can be envisaged for $(MeGe)_2Co_4(CO)_{11}$ using $\{\mu\text{-}Me(H)Ge\}\{Co_2(CO)_6\}Ge\{Co_2(CO)_7\}$ as a precursor, the addition of an extra methyl group to the molecule complicates matters. Thus it is not known whether this additional methyl group arises from the incorporation of 2 molecules of $MeGeH_3$ into the cluster with extrusion of the

FIGURE 8.2 POSSIBLE REARRANGEMENT DURING DECARBONYLATION OF $Ge_2Co_6(CO)_{20}$

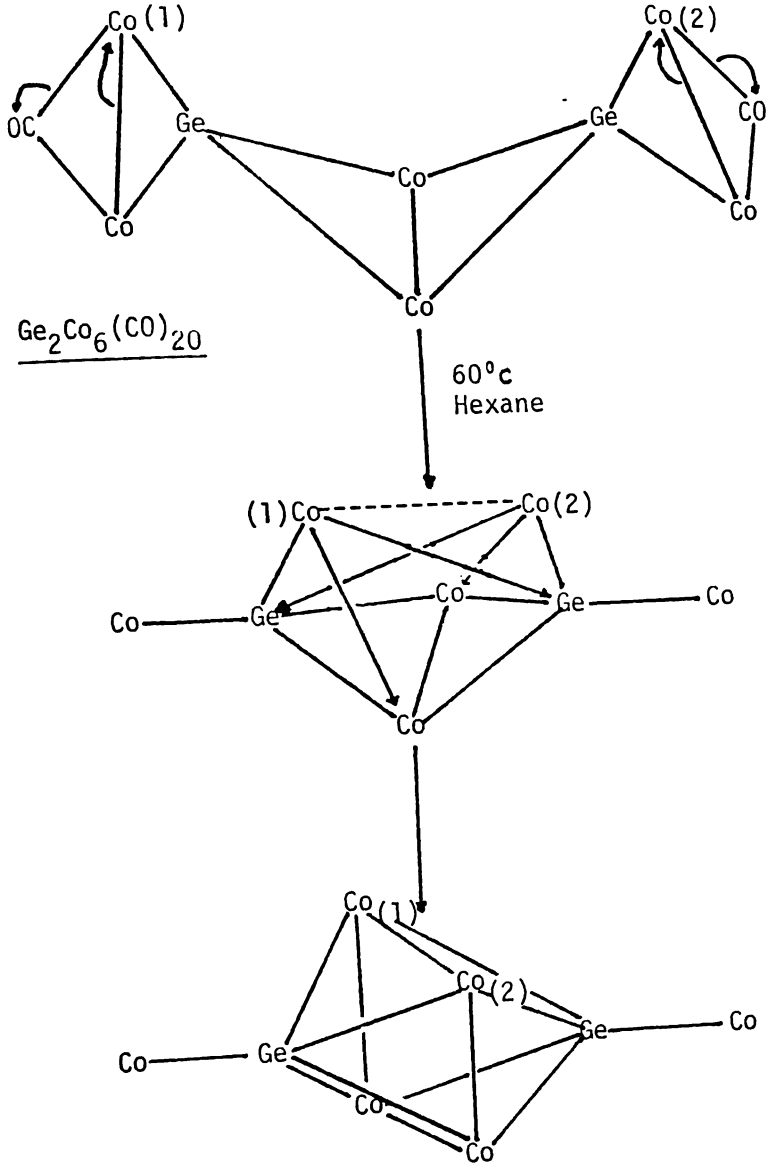

central Ge atom or if it arises from Ge-C cleavage and bond formation (on the central Ge atom). Further the identification of quantities of $Ge_2Co_6(CO)_{20}$ suggest this may result from an intermolecular (rather than intra molecular) reaction, although the possibility of this being an initial impurity in the $GeCo_4(CO)_{14}$ cannot be excluded.

This rearrangement proceeds under very mild conditions (room temperature, absence of light), thus if $Me(H)Ge_2Co_4(CO)_{13}$ is accepted as a precursor to the formation of $(MeGe)_2Co_4(CO)_{11}$, it appears that the functional hydrogen (on the Ge atom) initiates the rearrangement. Note that $Me_2Ge_2Co_4(CO)_{13}$ has shown no tendency to rearrange under similar conditions.

8.5 Overview and Suggestions for Further Work.

This work has confirmed and extended the usefulness of group IVB hydrides as reagents for the synthesis of group IVB-cobalt carbonyl compounds.

Previously, only the reactions of simple mononuclear substituted group IVB hydrides with $Co_2(CO)_8$ have been investigated (See Section 1.4). This work has re-investigated some of these reactions and found some new products can be obtained by varying the reactant ratios and the amount of CO present during and after reaction.

The reactions of some polynuclear group IVB hydrides with $Co_2(CO)_8$ have been investigated and it has been found that $Co_2(CO)_8$ quantitatively cleaves an M^1-M^1 bond. However

in the cases of the Ge_2H_6, Ge_3H_8 and $(GeH_3)_2SiMe_2$ reactions an extended homologue of $GeCo_4(CO)_{14}$, $Ge_2Co_6(CO)_{20}$ has been isolated in good yield. There are indications that higher homologues are produced in these reactions (the $2094cm^{-1}$ species), however reaction of Ge_3H_8 with $Co_2(CO)_8$ yielded only a very small quantity of a species which may be the trigermanium homologue of $GeCo_4(CO)_{14}$ and $Ge_2Co_6(CO)_{20}$.

This work has established that germanium hydrides react with some species related to $Co_2(CO)_8$, in a similar manner. Thus the reaction of Me_2GeH_2 with $Co_2(CO)_8$ and $GeCo_4(CO)_{14}$ leads to the replacement of a bridging carbonyl group by a Me_2Ge group in both species.

e.g. $Co_2(CO)_8 + Me_2GeH_2 \rightarrow Me_2GeCo_2(CO)_7 + H_2 + CO$

and $GeCo_4(CO)_{14} + Me_2GeH_2 \rightarrow Me_2Ge_2Co_4(CO)_{13} + H_2 + CO.$

This is thus a method for extending the chain length of existing clusters.

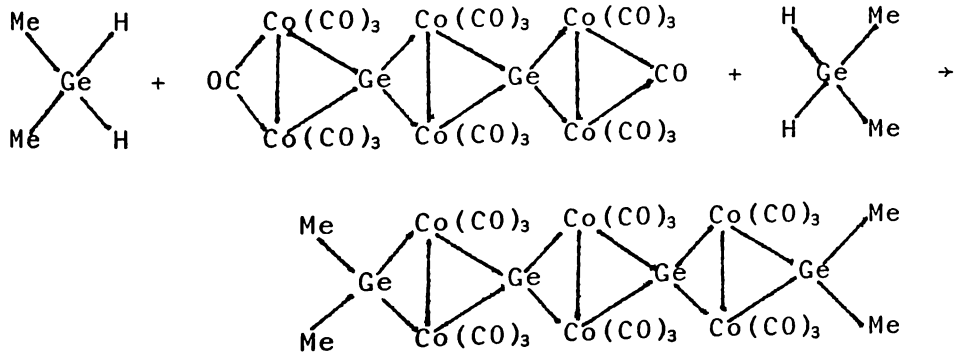

An unfortunate property of these extended chain compounds, particularly the symmetrically substituted species (i.e. $Ge_2Co_6(CO)_{20}$, $(Me_2Ge)_2Ge_2Co_6(CO)_{18}$ and the $2094cm^{-1}$ species) is their failure to form crystals suitable for an X-ray crystallography study, despite prolonged attempts. It is felt that the shape of these compounds and the number of

possible isomeric forms (with the combinations of $GeCo_2$ triangles facing the same or opposite ways), contributes to this.

Thus further compounds may be built up by a series of steps:

(i) $Me_2GeCo_2(CO)_7 + MeGeH_3 \rightarrow (Me_2Ge)Co_2(CO)_6(\mu\text{-}GeMeH) + H_2 + CO$

$(Me_2Ge)Co_2(CO)_6(\mu\text{-}GeMeH) + \frac{1}{2}Co_2(CO)_8 \rightarrow$

$Me_2GeCo_2(CO)_6(\mu\text{-}GeMeCo(CO)_4) + \frac{1}{2}H_2$

or

(ii) $GeCo_4(CO)_{14} + MeGeH_3 \rightarrow Me(H)Ge_2Co_4(CO)_{13} + H_2 + CO$

$Me(H)Ge_2Co_4(CO)_{13} + \frac{1}{2}Co_2(CO)_8 \rightarrow MeCo(CO)_4Ge_2Co_4(CO)_{13} + \frac{1}{2}H_2$

etc.

This work has been largely exploratory and the aim has been to specifically build group IVB cobalt carbonyls. Thus reaction conditions used have been mild in order to keep the reactions simple, so that generally it is only the reactants used that are involved in reaction and not decomposition products. e.g. If $GeCo_4(CO)_{14}$ was reacted with Me_2GeH_2 at 40°C, $GeCo_4(CO)_{13}$ would form from the decomposition of $GeCo_4(CO)_{14}$ (57) and may thus complicate the reaction.

These reactions however are slow (reaction times of a minimum of 2 months are generally needed), thus it is felt that a study of these reactions (and others) using more forcing conditions (temperature, photolysis, catalysis etc.) would be useful.

These reactions have also been limited to group IVB hydrides and cobalt carbonyls, thus an extension to other main group hydrides and transition metal carbonyls seems logical. In particular, of the 1st row elements, an extension

to iron carbonyls would seem to be the most promising, as much of their chemistry parallels that of the cobalt carbonyls used in this work, (6).

The decarbonylations of these compounds has been shown by the $GeCo_4(CO)_{14}$ (57) and $Ge_2Co_6(CO)_{20}$ (this work) reactions to be a good method for forming closed clusters. Thus the application to some of the more extended structures such as $(Me_2Ge)_2Ge_2Co_6(CO)_{18}$ may yield unusual clusters of high nuclearity.

This work has also established the new group IVB - transition metal cluster type $\{RGe\}_2Co_4(CO)_{11}$, (R = Me,$Co(CO)_4$). There exists considerable scope for studying the chemistry of these clusters. Synthetically, the most accessible is $\{(CO)_4CoGe\}_2Co_4(CO)_{11}$. Thus the reactions of this cluster with hydrides (e.g. replacement of the bridging carbonyl) and with nucleophiles such as $Co(CO)_4^-$, $Mn(CO)_5^-$ may be explored. Vahrenkamp (127) has found that the analogous iron cluster $(RFe)_2Co_4(CO)_{12}$ can readily lose CO and add bases such as phosphines. Perhaps of interest also will be the electrochemistry of these electron rich clusters.

Thus this work has shown that main group-transition metal carbonyls can be specifically built by the reactions of main group hydrides
with selected transition metal carbonyls. Thus with suitable strategy (144) and a fair degree of rationale, the techniques used in this work have great potential for building further main group transition-metal clusters.

CHAPTER 9. The Preparation and Properties of $MeSnH_2Mn(CO)_5$ and $Me_2SnHMn(CO)_5$.

9.1. Introduction.

The thermal stability of the hydrides of the group IVB metals decreases with the increase in atomic size, for example $SiH_4>GeH_4>SnH_4>>PbH_4$ (101). This decrease in thermal stability parallels the decreasing strength of the M^1-H bond. (table 9.1).

Table 9.1. Bond Energy of M^1-H.

Bond.	Energy $kJMol^{-1}$	Ref.
Si-H	321.3	145
Ge-H	298.8	145
Sn-H	253.7	145
Pb-H	205.8	145

The quantity of work on group IVB hydrides appears to be directly related to their thermal stability, thus while the hydrides of Si and Ge are relatively stable and well studied, the hydrides of Sn and Pb are comparatively unstable and many fewer derivatives are known.

SnH_4 and Sn_2H_6 are the only known binary hydrides of Sn (IV) (c f. binary hydrides of Ge containing up to 9 Ge atoms are known (101)). SnH_4 decomposes readily to its (119) elements at room temperature, but can be stored for months in the presence of traces of oxygen with little decomposition. It is thought that the SnH_4 decomposes upon the fresh tin surface, and the O_2 inhibits this process by forming an oxide film on the tin surface. The other known binary hydride of tin is Sn_2H_6 which decomposes above -112^0C. (147).

The thermal stability of tin hydrides increases with

alkyl or aryl substitution (148), and decreases with substitution with electronegative groups (148). Thus while $MeSnH_3$ can be stored at room temperature(103), SnH_3Cl decomposes even at -70°C. (149)

Transition metal carbonyl derivatives of tin have been studied extensively (6), however there have been few reports of these compounds containing Sn-H bonds (see table 9.2) The most widely used method of preparation is the reduction of the halogen compounds:

$$\{(CO)_5Mn\}_2\ SnCl_2 \xrightarrow[(iso\text{-}Bu)_2AlH]{hexane} H_2Sn\{Mn(CO)_5\}_2 \qquad (150)$$

One of the more interesting derivatives is the novel di-tin species $\{\{(CO)_5Mn\}_2\ SnH\}_2$, prepared by the reaction of $HMn(CO)_5$ with $SnCp_2$(151). This has been characterized by

$$4HMn(CO)_5+2SnCp_2 \xrightarrow{benzene} \{\{Mn(CO)_5\}_2\ SnH\}$$

crystallographic methods. The compound is remarkably stable to thermal decomposition (decomposes at 150°C) and also has a very low Sn-H stretching frequency in the infrared at $1725cm^{-1}$. These features have been explained by substantial p character of the Sn-H bonds.

Finally, mention should be made of the unstable $SnH_3Mn(CO)_5$(113), prepared by the alkali-halide coupling reaction of unstable SnH_3Cl with $NaMn(CO)_5$.

$$SnH_3Cl+NaMn(CO)_5 \longrightarrow NaCl+SnH_3Mn(CO)_5$$

This compound has been characterised by infrared, nmr and mass spectroscopic evidence, however it appears to be unstable at room temperature, readily decomposing to give $HMn(CO)_5$ and other unidentified products.

Table 9.2 Transition Metal Carbonyl Derivatives of Tin Hydrides.

Compound	M.P. (°C)	Ref.
$(OC)_5MnSnPh_2H$	Oil	150
$(OC)_5ReSnPh_2H$	Oil	150
$\{(OC)_5Mn\}_2SnH_2$	89-92	150
$\{(OC)_5Re\}_2SnH_2$	94-97	150
$\{(OC)_5Mn\}_3SnH$	127-130	150
$\{n\text{-}Bu_3PCo(CO)_3\}_3SnH$	160-162	152
$\{Mn(CO)_5\}_4Sn_2H_2$	150 (dec.)	151
$(CO)_5MnSnH_3$	-	113

9.2. Preparation and Characterisation of $MeSnH_2Mn(CO)_5$.

9.2.1 Experimental.

Run 1.

The preparation of $MeSnH_2Cl$ was based on the method of Amberger (149) for the preparation of SnH_3Cl. Excess $MeSnH_3$ (931mg, 6.76mmoles) was allowed to react with anhydrous HCl (220mg, 6.03mmoles) at -70°C for 1½ hours until H_2 evolution

$$Me_2SnH_2 + HCl \longrightarrow Me_2SnHCl + H_2$$

appeared complete, as described in section 2.4.7. The green solution of $Mn(CO)_5^-$ was decanted away from the excess amalgam and the product from the $MeSnH_3$/HCl reaction was condensed on top of it. The mixture was then allowed to warm and react for 10 minutes at room temperature, while the solution changed to a pale orange colour and small crystals of sodium chloride were deposited.

The volatile products from the reaction were removed and fractionated to yield a pale yellow liquid at -45°C. This was identified as $MeSnH_2Mn(CO)_5$ (121mg, 0.37mmoles) by infrared, nmr, and mass spectroscopy, and by its reactions, (yield 6% based on consumed $MeSnH_3$).

Further separation of the fraction volatile at -45°C yielded 11mg (0.08mmoles) of $MeSnH_3$.

Run 2.

$MeSnH_2Cl$ was prepared from $MeSnH_3$ (163mg, 1.19mmoles) and dry HCl (35mg, 0.96mmoles) and reacted with $Mn(CO)_5^-Na^+$ (prepared from 388mg, 0.995mmoles of $Mn_2(CO)_{10}$) as in Run 1. Work up yielded 17mg(0.05mmoles) of $MeSnH_2Mn(CO)_5$ (5.3%, yield based on HCl).

9.2.2. Handling and Reaction of $MeSnH_2Mn(CO)_5$

9.2.2.1 Handling

$MeSnH_2Mn(CO)_5$ is a clear volatile liquid with a vapour pressure of ca. 2-3mm at room temperature. Its thermal stability appears to be considerably greater than the related $SnH_3Mn(CO)_5$(113) since a sample left at room temperature in vacuo for 1 hour showed no sign of decomposition.

9.2.2.2 Reaction with CCl_4

40mg (0.12mmoles) of $MeSnH_2Mn(CO)_5$ was condensed onto excess CCl_4 (ca. 200mg, ca. 1mmole) and the mixture allowed to warm slowly to room temperature. Upon warming the clear solution quickly turned pale yellow. Removal of the volatile compounds from the reaction vessel left 51mg (0.13mmoles) of a pale yellow solid identified as $MeSnCl_2Mn(CO)_5$ from its infrared spectrum (153).

9.2.3. Spectroscopic Characterisation of $MeSnH_2Mn(CO)_5$

9.2.3.1 Mass Spectrum

Mass spectra of species containing tin are easily recognisable by the relative abundances of the ten naturally occuring isotopes of tin (six having an abundance greater than 5%).

Table 9.3. The Naturally Occurring Isotopes of Tin.

Mass	Abundance %	Spin.
112	0.96	
114	0.66	
115	0.35	½

Table 9.3 Continued.

Mass	Abundance %	Spin
116	14.30	0
117	7.61	$\frac{1}{2}$
118	24.03	0
119	8.58	$\frac{1}{2}$
120	32.85	0
122	4.72	
124	5.94	

The mass spectrum of $MeSnH_2Mn(CO)_5$ is shown in table 9.4. A tin envelope between 326-336 mass units corresponds to $MeSnH_2Mn(CO)_5^+$ and confirms the formulation of the compound. Of the tin containing fragments, the most intense series of ions corresponds to the loss of CO from the parent, as has been observed with the analogous $MeGeH_2Mn(CO)_5$(155) and other related species (22, 155). The series of ions resulting from M^1-C cleavage are however much more intense for $MeSnH_2Mn(CO)_2$ than for $MeGeH_2Mn(CO)_5$ (154) reflecting the weaker Sn-C bond strength.(Ge-C 255, Sn-C 193 $kJmol^{-1}$, ref 143)

Rearrangement ions involving formation of new Sn-C bonds are also observed in the spectrum ($Me_3SnH_X^+$ and $Me_2SnH_X^+$). This relative ease of cleavage and formation of Sn-C bonds has also been observed in reaction systems (see Chapter 3). where conditions that do not affect Ge-C bonds readily cleave Sn-C bonds.

In the spectrum, the ions $Mn(CO)_X^+$ and $HMn(CO)_X^+$ are unusually intense. Although $HMn(CO)_5$ is a product of the decomposition of $SnH_3Mn(CO)_5$(113) and would be expected to form from the decomposition of $MeSnH_2Mn(CO)_5$, the most likely

Table 9.4 Mass Spectrum of $MeSnH_2Mn(CO)_5$

m/e	rel. int	Assignment
326-336	9	$MeSnHxMn(CO)y$, y = 5
298-308	12	y = 4
270-280	46	y = 3
242-252	25	y = 2
214-224	10	y = 1
186-196	24	y = 0
311-321	21	$SnHxMn(CO)y$, y = 5
283-293	23	y = 4
255-265	20	y = 3
227-237	15	y = 2
199-209	15	y = 1
171-181	18	y = 0
168	33	$HMn(CO)_4^+$
167	12	$Mn(CO)_4^+$
161-171	46	Me_3SnHx
146-156	70	Me_2SnHx
131-140	65	$MeSnHx$
116-125	58	$SnHx$
140	11	$HMn(CO)_3^+$
139	7	$Mn(CO)_3^+$
112	28	$HMn(CO)_2^+$
111	31	$Mn(CO)_2^+$
84	15	$HMn(CO)^+$
83	40	$Mn(CO)^+$
56	30	HMn^+
55	33	Mn^+

explanation for these unusually high intensities (see $Me_2SnHMn(CO)_5$ spectrum for comparison) is that the sample used for the mass spectrum was contaminated with $HMn(CO)_5$. Because of these high intensities, the percentage of the ion current carried by ions containing both metal atoms is low (36% of the total ion current) compared to the germanium analogue (ca. 75% of the total ion current). Even allowing for the contamination with $HMn(CO)_5$ the percentage ion current carried by Sn-Mn species appears to be relatively low.

9.2.3.2 NMR Spectrum

The ^1H nmr spectrum of neat $MeSnH_2Mn(CO)_5$ (with ca.10% added TMS) showed a quartet at 5.75±0.03τ and a triplet at 9.36±0.03τ in the relative intensity of 2:3 with J=3.8±0.2 H_Z The chemical shifts of related species are shown in Table 9.5.

The observed spectrum is consistent with that expected for a $MeSnH_2X$ species. Further, the chemical shift of the $Sn-H_2$ signal is consistent with the noted trend, (25) that the addition of a methyl group has the effect of deshielding the group IVB protons and thus moving the signal to lower field. Thus the replacement of one of the protons in $SnH_3Mn(CO)_5$ by a methyl group has significantly shifted the Sn-H signal to lower field, even allowing for the $SnH_3Mn(CO)_5$ spectrum being recorded in benzene (which shifts signals to higher field).

9.2.3.3. Infrared Spectrum

The vibrational spectra of molecules of the type $R_3M^1Mn(CO)_5$ have been found to be generally best discussed

Table 9.5 NMR Chemical Shifts of $R_3M^1Mn(CO)_5$

Compound	Chemical Shift (τ)		JHH(Hz)	Solvent	Ref.
	M^1H	CH_3			
$SiH_3Mn(CO)_5$	6.41			Neat	160
$Me_3SiMn(CO)_5$		9.51		C_6H_{12}	161
$GeH_3Mn(CO)_5$	6.72			C_6H_6	155
	6.36			$SiCl_4$	25
$MeGeH_2Mn(CO)_5$	6.30	9.33	4.0	$SiCl_4$	154
$Me_2GeHMn(CO)_5$	5.8	9.3	3.6	$SiCl_4$	25
	5.6	8.94	3.6	Neat	25
$Me_3GeMn(CO)_5$		9.38		$CDCl_3$	162
$SnH_3Mn(CO)_5$	6.53			C_6H_6	113
$MeSnH_2Mn(CO)_5$	5.75	9.36	3.8	Neat	(a)
$Me_2SnHMn(CO)_5$	5.40	9.07	3.2	Neat	(a)
$Me_3SnMn(CO)_5$		9.53		Neat	158

in terms of local symmetry around the two metal atoms (155). While $MeSnH_2Mn(CO)_5$ is of overall C_s symmetry, it will be discussed here in terms of C_s symmetry for $MeSnH_2X$ (X=-$Mn(CO)_5$) and C_{4v} symmetry for $YMn(CO)_5$ (Y=$MeSnH_2$).

The infrared spectrum of $MeSnH_2Mn(CO)_5$ is given in Table 9.6 along with the spectra of the related $MeGeH_2Mn(CO)_5$, (154), and $SnH_3Mn(CO)_5$. (113). The most imposing part of the spectrum is the carbonyl stretching region (ca. 2100-1950cm^{-1}). Local C_{4v} symmetry predicts $2a_1+b_1+e$ vibrational modes with the b_1 mode infrared inactive. The frequencies, intensities and contours of the carbonyl stretches of the -$Mn(CO)_5$ group vary little upon changing the group IVB species and so these modes can be assigned according to previous spectra, (113,154,155). Thus the band centred at 2101cm^{-1} is of type -A contour with a strong Q branch and weak P branch and is assigned as the a_1 axial carbonyl stretch. The band centred at 2026cm^{-1} also shows type -A contour, and is thus assigned as the a_1 symmetric equatorial carbonyl stretch. The very strong band at 2012cm^{-1} must therefore be the e asymmetric mode. As expected for complexes of this type, the e mode is considerably the most intense of the spectrum (153). The final band in this region (at 1976cm^{-1}) is in the correct position for a ν^{13} CO band.

Of the remaining $5a_1+8e$ infrared active modes of the -$Mn(CO)_5$ group, only 3 are observed. The 2 very strong bands at ca.660cm^{-1} can be assigned as a_1 and e Mn-C-O deformations on the basis of the $HMn(CO)_5$ spectrum, (156), although exact assignment cannot be made without Raman evidence. The final observed $Mn(CO)_5$ mode is the band at 476cm^{-1}, which can be confidently assigned as the a_1 axial Mn-C stretch from comparisons with related species, (154, 156). The a_1 and e

Table 9.6 Infrared Spectrum* of

$MeSnH_2Mn(CO)_5$

Peak (cm^{-1})	rel. int	Assignment	$SnH_3Mn(CO)_5$	$MeGeH_2Mn(CO)_5$
2994	VW	νCH_3 asym		2963
2920	VW	νCH_3 sym		2926
				2877
2104 R			2109	
2101 Q	VS	νCO axial a^1	2106	2107
2098 P			2103	
2029 R			2021	
2026 Q	S	νCOeq a^1	2018	2029
2023 P			2015	
2012	VVS	νCOeq e		2018
1976	W-M	ν^{13}CO	1983	1985
1828 R			1846	
1825 Q	S	νSnH_2 sym	1843	
1822 P			1840	
1346	VW	δCH_3		1460
				1080
				1030
768	M	ρCH_3		877
766				838
718 R			696	
715 Q	M	δSnH_2 sym	694	695
712 P			692	
666	VS	δMn-CO	667	670
658			657	660
575	M-S	ρSnH		583
517	M	νSn-C		
514				
476	M	νMn-C	474	482

* Gas phase.

a) ref. 113 b) ref. 154

equatorial Mn-C stretches are expected to occur in the region, 430-300cm^{-1}, (154), but were not observed in this spectrum.

Sn-H stretches unlike Ge-H stretches occur in a region of the infrared removed from terminal carbonyl absorptions, (1900-1800cm^{-1}) and so are more easily observed in compounds of this type. The contour of the medium intensity band centred at 1825cm^{-1} suggests that it is the symmetric Sn-H_2 stretch. This leaves the weak band at higher frequency (1845cm^{-1}) as the asymmetric Sn-H_2stretch. The remainder of the Sn-H_2 modes can be assigned by comparison with the spectrum of Me_2SnH_2, (157). Thus the band at 575cm^{-1} may be ascribed to the rocking of the -SnH_2 group (at 574cm^{-1} for Me_2SnH_2). The assignment of the band centred at 715cm^{-1} is however uncertain, as for Me_2SnH_2 both the H-Sn-H deformation (at 726cm^{-1}) and the SnH_2 wag (at 712cm^{-1}) lie close to each other. The contour of the band is similar to that of the Sn-H_2 symmetric stretch which suggests that we are observing the a^1 symmetric deformation. If this is so, then it appears that the SnH_2 wag is accidentally degenerate in energy with this mode and that it lies beneath it.

This leaves only the CH_3 related modes which may be assigned as for $MeSnH_3$, (157). The peaks at 2994cm^{-1} and 2930cm^{-1} may be ascribed to the asymmetric and symmetric CH_3 stretches respectively. Likewise the very weak band at 1346cm^{-1} can be assigned to a CH_3 deformation. The remaining CH_3 deformation must be too weak in intensity to observe. The assignment is complete with the identification of the CH_3 rock (767cm^{-1}) and the Sn-C stretch (515cm^{-1}), both at almost identical energies as the corresponding modes for

$MeSnH_3$, (157). The small splitting of these bands may indicate a distorted A or B contour.

9.3. Synthesis of $Me_2SnHMn(CO)_5$

9.3.1. Experimental

Run 1.

The reaction techniques and conditions used in this preparation were similar to those used in 9.2.1. Me_2SnH_2 (451mg, 2.99mmoles) was reacted with anhydrous HCl (119mg, 3.26mmoles) for ca. 60 minutes at -70°C after which H_2 evolution appeared complete. Gases volatile at this temperature were removed and the remaining volatile gases were condensed onto, and allowed to react with a diethyl ether solution of $NaMn(CO)_5$, prepared from the reduction of 1178mg (3.02mmoles) of $Mn_2(CO)_{10}$. After 15 minutes at room temperature, the initially green solution had turned pale orange and crystals of NaCl had precipitated out. Fractionation of the volatile components from the reaction through -45°C, gave an infrared spectrum consisting of peaks due mainly to $HMn(CO)_5$, (156), plus a further weak peak at 2006cm^{-1}. Attempts to free the 2006cm^{-1} species from $HMn(CO)_5$ failed.

Run 2:

401mg (2.64mmoles) of Me_2SnH_2 was allowed to react with 103mg (2.82mmoles) of anhydrous HCl at -70°C and the volatile products of the reaction were condensed onto and allowed to react with a diethyl solution of $NaMn(CO)_5$ (prepared from 1350mg, 3.46mmoles of $Mn_2(CO)_{10}$) as in run 1. The volatile components produced from the reaction were

fractionated through -63.5°C to leave a small quantity of a white solid. This solid was freed from traces of $HMn(CO)_5$ by further fractionation.

9.3.2. Spectroscopic Characterisation.

9.3.2.1 NMR Spectrum

An nmr spectrum of the white solid dissolved in a small quantity of T.M.S. (ca.30% T.M.S. by volume) was recorded (Table 9.7).

Table 9.7 NMR Spectrum of White Solid

Chemical Shift (τ)	Rel.Int.	Assignment
9.53 singlet	100*	$Me_3SnMn(CO)_5$
5.40 septet	1	$Me_2SnHMn(CO)_5$
9.07 doublet	6	$Me_2SnHMn(CO)_5$

J_{H-H} = 3.2Hz

* Approximate.

The strong singlet can be assigned as due to $Me_3SnMn(CO)_5$ (reported τ = 9.54, ref. 158). The weaker septet and doublet are the expected spectrum of a Me_2SnHX species. The chemical shift of the septet is in the correct position for a Sn-H resonance and further shows the expected trend to lower field with increased Me substitution on the tin atom (see Table 9.5). The coupling constant, J_{H-H} is also smaller than the one for $MeSnH_2Mn(CO)_5$ as expected (see section 9.2). Thus the nmr spectrum supports the synthesis of $Me_2SnHMn(CO)_5$, (and $Me_3SnMn(CO)_5$) from the reaction.

9.3.2.2 Mass Spectrum.

The mass spectrum of the most volatile fraction of the

white solid is shown in Table 9.8. Although the $Me_2SnHMn(CO)_5$ obtained from the reaction is contaminated with a considerable amount of $Me_3SnMn(CO)_5$, the weakness of the $Me_3SnMn(CO)_5^+$ ion in the mass spectrum suggests that there is little (if any) $Me_3SnMn(CO)_5$ in the sample used.

The observed spectrum is complicated by overlap of ions, in particular those arising from the loss of two methyl groups being roughly equivalent to the loss of one CO group. Therefore $Me_2SnH_xMn(CO)y^+$ ions overlap with $SnH_xMn(CO)y^+$ ions, and $Me_3SnMn(CO)y^+$ ions overlap with $MeSnH_xMn(CO)y^+$ ions. Again, the dominant feature of the spectrum is CO loss with the higher mass ions of the series $Me_2SnH_xMn(CO)y^+$ being particularly intense. Methyl loss from the 2 metal fragment is only significant when most CO groups have been lost. 56% of the total ion current is carried by fragments containing both metal atoms, compared with the 52% reported for the $Me_2GeHMn(CO)_5$ spectrum (25). Although these two spectra may have been run under different conditions, this result agrees remarkably well with the spectra obtained for the $Me_3M^1Mn(CO)_5$ species (M^1=Sn,Ge) where the proportion of the total ion current carried by fragments containing both metal atoms is greater for the Sn compound (59%) than for the Ge compound (52%), (159).

The very high intensity of $Me_3SnH_x^+$ is consistent with that observed in other systems, (159), and probably reflects the very high stability of this ion.

9.3.2.3. Infrared Spectrum

The gas phase infrared spectrum of the most volatile

Table 9.8 Mass Spectrum of $Me_2SnHMn(CO)_5$

m/e	rel. int	Assignment	
356-364	7	$Me_3SnMn(CO)_5^+$	
341-350	50	$Me_2SnHxMn(CO)y^+$,	y = 5
313-322	42		y = 4
285-294	34		y = 3
257-266	32		y = 2
229-238	12		y = 1
201-210	24		y = 0
326-335	1	MeSnHxMn(CO)y,	y = 5
298-307	1		y = 4
270-279	2		y = 3
242-251	5		y = 2
214-223	36		y = 1
186-195	36		y = 0
171-180	30	$SnHxMn^+$	
161-170	100	Me_3SnHx^+	
146-155	15	Me_2SnHx^+	
131-140	70	$MeSnHx^+$	
116-125	14	$SnHx^+$	
168	30	$HMn(CO)_4^+$	
167	10	$Mn(CO)_4^+$	
139	5	$Mn(CO)_3^+$	
111	4	$Mn(CO)_2^+$	
83	5	$Mn(CO)^+$	

Table 9.9 Infrared Spectrum* of

$Me_2SnHMn(CO)_5$

Peak (cm^{-1})	rel. int	Assignment
2977	VW	νCH_3 asym
2916	VW	νCH_3 sym
2094	VS	νCO axial a_1
2024	VS	νCO eq. a_1
2006	VVS	νCO eq. e
1970	M	ν^{13}CO
1810 R 1808 Q 1805 P	M-S	νSn-H
867	W	ρCH_3
766	M-S	
728	W	δSn-H
669 657	VS	δMn-Co
555	M	νSn-C asym
507	M-S	νSn-C sym
477	M	νMn-C

* Gas Phase.

fraction of the white solid was run (Table 9.9). The spectrum appeared to consist of only one carbonyl containing species and the identification of Sn-H vibrational modes suggests that the sample is pure $Me_2SnHMn(CO)_5$.

The assignment of the carbonyl modes follows that for $MeSnH_2Mn(CO)_5$ (see 9.2.3.3). The CH_3 stretches are assigned as for Me_2SnH_2(157) however no δCH_3 are observed. The involatility of $Me_2SnHMn(CO)_5$ and fear of contamination with $Me_3SnMn(CO)_5$ precluded the obtaining of a stronger spectrum to observe these modes. The band at $766cm^{-1}$ is assigned as a CH_3 rock from comparison with Me_2SnH_2 ($774cm^{-1}$). The band at $867cm^{-1}$ may also be a CH_3 rock although it is at a particularly high frequency. Alternatively, the weakness of the band suggests it may be a combination band.

The Sn-C stretches can be assigned to the bands at $555cm^{-1}$ and $507cm^{-1}$ by comparison with Me_2SnH_2, (157). The band at higher energy is the asymmetric stretch in both cases. The average values of the Sn-C stretch, $528cm^{-1}$ (for Me_2SnH_2) and $531cm^{-1}$ (for $Me_2SnHMn(CO)_5$) are in good agreement with each other. The increased separation of these two bands in the $Me_2SnHMn(CO)_5$ spectrum suggests increased coupling with a $Mn(CO)_5$ mode, possibly νMn-C.

Finally the Sn-H modes can be assigned with reference to the spectrum of Me_3SnH (157).

9.4. Discussion.

The new compounds $MeSnH_2Mn(CO)_5$ and $Me_2SnHMn(CO)_5$ have been synthesized by the established alkali-halide salt

elimination method (6).

$Me_{3-x}SnH_xCl + Na^+Mn(CO)_5^- \longrightarrow Me_{3-x}SnH_xMn(CO)_5 + NaCl$

(x = 1,2)

Both compounds have been characterised by infrared, mass spectral and nmr evidence which are all fully consistent with the assigned structures. In addition $MeSnH_2Mn(CO)_5$ has been further characterised by reaction with CCl_4 to give quantitatively, the known compound $MeSnCl_2Mn(CO)_5$ (153).

$MeSnH_2Mn(CO)_5 \xrightarrow{CCl_4} MeSnCl_2Mn(CO)_5$

The substitution of M^1-H bonds for M^1-Cl bonds by CCl_4 has been observed previously in reaction with $MeGeH_2Mn(CO)_5$ (154). Identified as products from that reaction were $CHCl_3$ and CH_2Cl_2. Although the fate of the CCl_4 was not determined in the $MeSnH_2Mn(CO)_5$ reaction, it is likely that $CHCl_3$ and/or CH_2Cl_2 are the end products.

The series of compounds has now been completed and characterised $Me_{3-x}SnH_xMn(CO)_5$ (x=0,1,2,3 Refs.113, 159) spectroscopically. Although the instability of $SnH_3Mn(CO)_5$ prevents a full comparison of the spectroscopic properties of all these compounds, a few interesting trends have emerged.

The carbonyl stretching frequencies for this series and the analogous germanium series are given in Table 9.10. It can be seen that with increasing methyl substitution on the group IVB atom the frequencies of the carbonyl stretches decrease. This can be explained by the greater electron-donating ability of Me (relative to H) having a significant effect on increasing σ electron density between manganese and carbon which in turn increases the π - back donation between the two and consequently weakens the CO bond. This relationship between methyl substitution and a lowering of

Table 9.10 νCO of $XMn(CO)_5$ Species.

Mode	X: H_3Ge[a]	$MeGeH_2$[b]	Me_2GeH[c]	Me_3Ge[d]
νCOaxial a_1	2117R, 2114Q, 2111P > m	2107m	2106R, 2102Q, 2098P > m-s	2101 m
νCOeq. a_1	2022R, 2019Q, 2016P > vvs	2029vs	2032	
νCOeq. e	2019* vvs	2018vs	2011 vs	2009 vs
	H_3Sn[e]	$MeSnH_2$[f]	Me_2SnH[f]	Me_3Sn[d]
νCOaxial a_1	2109R, 2106Q, 2103P > ms	2104R, 2101Q, 2098P > vs	2094 vs	2093 m
νCOeq. a_1	2021R, 2018Q, 2015P > vvs	2029R, 2026Q, 2023P > s	2024 vs	
νCOeq. e	2018* vvs	2012 vvs	2006 vvs	2002 vs

* e modes and a modes overlap

a = ref. 155

b = ref. 154

c = ref. 25

d = ref. 159

e = ref. 113

f = this work.

νCO frequencies is most striking with a plot of the number of substituted methyl groups on the Sn atom versus the frequency of the e mode of the νCO vibrations (see Fig. 9.1) which shows a virtual linear relationship between the two. A similar plot for the germanium analogues does not give such a good linear relationship, however it should be noted that the spectra of the four compounds were run on four different infrared spectrometers.

A further point to note from the vibrational spectra of the tin compounds is the decrease in the observed Sn-H stretching frequency with increasing methyl substitution. This trend has been noted previously for the methylstannanes. (157).

FIGURE 9.1 PLOT OF NUMBER OF METHYL SUBSTITUENTS ON $Me_{3-x}SnH_xMn(CO)_5$ VERSUS E MODE OF νCO FREQUENCY.

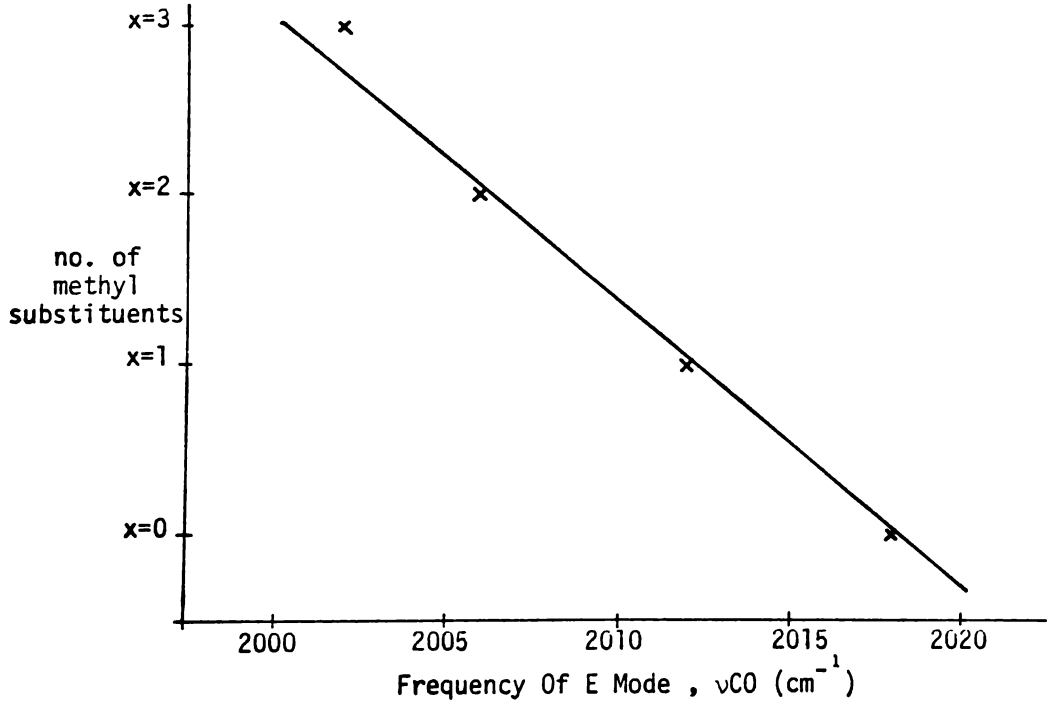

APPENDIX I COMPUTING FACILITIES AND PROGRAMS USED IN THIS WORK.

All the following programs were used on a Vax 11/780 computer at the University of Waikato. Diagrams were plotted on a Hewlett Packard 7221B plotter.

MOLASZ: This was used for processing of crystal data obtained from Precession Photography, to calculate setting angles and density.

SHELX : The direct methods program SHELX has two subroutines available for structure solution; the centrosymmetric automatic origin defining EEES routine and the origin defining TANG/PHIX routine. Both were used in this work. SHELX was also used for ; the production of Difference Maps, interatomic distances and angles, and least squares refinement of models.

MULTAN : The direct methods stucture solving program MULTAN, was used for solution of non-centrosymmetric structures, and when SHELX failed to give an acceptable solution.

PLUTO : This was used for the plotting of structures and unit cell packing.

MEANPLANE : This calculated planes of best fit and distances of atoms from these planes.

GRAPHPAR : This converts a SHELX output into a suitable format for MEANPLANE.

NOTES: (A) SHELX , Ref.175

(B) MULTAN, Ref. 176

(C) PLUTO, Ref. 177

APPENDIX II FURTHER CRYSTALLOGRAPHIC INFORMATION FOR $(MeGe)_2Co_4(CO)_{11}$.

FINAL ATOMIC POSITIONAL COORDINATES OF.

$(MeGe)_2Co_4(CO)_{11}$

GE1	0.30500	0.00000	0.12227
GE2	0.23922	0.00000	0.37346
CO1	0.18063	0.09761	0.20347
CO2	0.36704	0.09252	0.29312
CM1	0.34576	0.00000	-0.04568
H1	0.41046	-0.04400	-0.03874
H2	0.35884	0.06227	-0.10147
H3	0.28610	-0.04094	-0.08769
CM2	0.19574	0.00000	0.54149
H4	0.13871	-0.05335	0.53657
H5	0.16860	0.06523	0.58075
H6	0.25674	-0.02633	0.59857
C11	0.07098	0.11352	0.28751
C12	0.23450	0.21149	0.22921
C13	0.13695	0.11177	0.04599
CB	0.46617	0.00000	0.33836
C21	0.44455	0.15765	0.19530
C22	0.37305	0.16067	0.43462
O11	0.00403	0.12382	0.33790
O12	0.24937	0.29143	0.23419
O13	0.10642	0.12004	-0.05181
OB	0.54949	0.00000	0.37040
O21	0.50133	0.19682	0.14029
O22	0.37848	0.20728	0.52003

ANISOTROPIC TEMPERATURE PARAMETERS FOR $(MeGe)_2Co_4(CO)_{11}$

GE1	0.03407	0.03442	0.02799	0.00000	0.00002	0.00000
GE2	0.03674	0.03309	0.02929	0.00000	0.00295	0.00000
CO1	0.03692	0.04131	0.04216	0.00798	0.00325	0.00904
CO2	0.03877	0.03331	0.03460	-0.00559	0.00249	-0.00686
CM1	0.05823	0.07585	0.03033	0.00000	0.00533	0.00000
CM2	0.05360	0.05583	0.04095	0.00000	0.00445	0.00000
C11	0.04213	0.05342	0.04481	0.00170	0.00911	0.01605
C12	0.05512	0.04579	0.11965	0.02661	0.01950	-0.00324
C13	0.07096	0.13219	0.04599	0.02736	0.00965	0.05606
CB	0.03849	0.05759	0.02718	0.00000	0.00746	0.00000
C21	0.05700	0.03576	0.06280	-0.01104	0.00426	-0.01133
C22	0.05437	0.06063	0.06120	-0.02502	0.00981	-0.00080
O11	0.07517	0.06100	0.08347	0.00074	0.02932	0.01736
O12	0.06928	0.04474	0.21660	0.02575	0.02336	-0.00340
O13	0.14768	0.25023	0.04816	0.03903	-0.01415	0.08927
OB	0.03593	0.09141	0.06114	0.00000	-0.00356	0.00000
O21	0.07983	0.05795	0.08886	-0.00575	0.03948	-0.02607
O22	0.10050	0.09352	0.08482	-0.05467	0.02069	-0.02107

OBSERVED AND CALCULATED STRUCTURE FACTORS FOR $(MeGe)_2Co_4(CO)_{11}$

H	K	L	FO	FC	H	K	L	FO	FC	H	K	L	FO	FC	H	K	L	FO	FC	H	K	L	FO	FC
2	0	0	284	-271	5	5	0	203	-206	1	11	0	58	-59	-1	1	1	492	487	-2	4	1	33	32
4	0	0	48	-49	7	5	0	66	76	3	11	0	21	18	1	1	1	392	-386	0	4	1	49	-52
6	0	0	105	113	9	5	0	102	104	5	11	0	39	40	5	1	1	44	-39	2	4	1	55	53
8	0	0	65	66	11	5	0	200	-178	7	11	0	53	-53	7	1	1	37	32	4	4	1	150	-147
10	0	0	15	-17	13	5	0	69	74	9	11	0	32	-33	9	1	1	38	-43	6	4	1	236	231
14	0	0	33	-32	0	6	0	6	-5	0	12	0	151	150	11	1	1	21	-24	8	4	1	35	-31
1	1	0	78	-78	2	6	0	33	-32	2	12	0	87	-89	13	1	1	22	-12	10	4	1	88	-78
3	1	0	20	24	4	6	0	242	237	4	12	0	32	-34	-14	2	1	48	47	12	4	1	77	78
5	1	0	125	109	6	6	0	119	-123	6	12	0	20	22	-12	2	1	50	-52	-13	5	1	30	28
7	1	0	83	-92	8	6	0	17	-17	8	12	0	19	-7	-10	2	1	45	40	-9	5	1	22	-41
9	1	0	13	-27	10	6	0	21	12	1	13	0	42	-42	-8	2	1	84	-83	-7	5	1	33	-36
11	1	0	77	78	12	6	0	17	10	3	13	0	34	37	-6	2	1	105	120	-5	5	1	99	93
13	1	0	61	56	1	7	0	28	28	5	13	0	12	-9	-4	2	1	107	-107	-1	5	1	227	-216
0	2	0	307	301	3	7	0	48	45	0	14	0	41	41	-2	2	1	76	-75	1	5	1	77	75
2	2	0	203	-203	5	7	0	101	-99	2	14	0	44	-46	2	2	1	22	24	3	5	1	296	293
4	2	0	16	-9	7	7	0	86	88	4	14	0	62	60	4	2	1	184	-173	5	5	1	301	-296
6	2	0	50	47	9	7	0	86	93	-14	0	1	68	67	6	2	1	46	45	7	5	1	92	86
8	2	0	67	-71	11	7	0	73	-75	-12	0	1	30	31	8	2	1	102	-90	9	5	1	19	10
10	2	0	10	3	0	8	0	183	183	-10	0	1	30	-31	10	2	1	95	102	13	5	1	19	-7
12	2	0	15	-18	2	8	0	111	-112	-8	0	1	170	-168	12	2	1	13	-5	-12	6	1	119	-126
14	2	0	25	-28	4	8	0	75	74	-6	0	1	328	300	14	2	1	40	-38	-10	6	1	147	180
1	3	0	34	-33	6	8	0	4	5	-4	0	1	86	-104	-13	3	1	38	38	-8	6	1	36	-37
3	3	0	74	71	8	8	0	43	-46	-2	0	1	97	-100	-11	3	1	25	17	-6	6	1	99	-98
5	3	0	112	-114	10	8	0	19	11	2	0	1	54	51	-9	3	1	24	-28	-4	6	1	53	54
7	3	0	51	54	12	8	0	13	3	4	0	1	65	61	-5	3	1	49	48	-2	6	1	28	25
9	3	0	65	64	1	9	0	8	7	6	0	1	91	-74	-3	3	1	84	85	0	6	1	24	-26
11	3	0	79	-85	3	9	0	18	18	8	0	1	104	-118	1	3	1	112	-110	2	6	1	40	39
13	3	0	61	63	5	9	0	30	32	10	0	1	173	195	3	3	1	418	409	4	6	1	155	-154
0	4	0	77	-78	7	9	0	46	-47	12	0	1	29	-26	5	3	1	101	-102	6	6	1	229	223
2	4	0	184	-177	9	9	0	13	0	14	0	1	73	-77	7	3	1	94	89	8	6	1	31	-30
4	4	0	278	275	11	9	0	23	15	-13	1	1	8	-12	9	3	1	41	-41	10	6	1	101	-97
6	4	0	147	-154	0	10	0	338	340	-11	1	1	12	-8	-12	4	1	158	-144	12	6	1	67	55
8	4	0	7	0	2	10	0	166	-166	-9	1	1	22	-22	-10	4	1	173	192	-11	7	1	3	-7
10	4	0	18	-3	4	10	0	14	4	-7	1	1	147	145	-8	4	1	31	-37	-9	7	1	36	-39
1	5	0	186	-178	6	10	0	55	54	-5	1	1	217	-258	-6	4	1	69	-75	-7	7	1	17	20
3	5	0	35	35	8	10	0	18	8	-3	1	1	45	-46	-4	4	1	103	100	-5	7	1	72	76

OBSERVED AND CALCULATED STRUCTURE FACTORS

H	K	L	FO	FC	H	K	L	FO	FC	H	K	L	FO	FC	H	K	L	FO	FC	H	K	L	FO	FC
-3	7	1	15	-2	6	10	1	11	-18	10	0	2	34	38	-1	3	2	14	12	-6	6	2	31	31
-1	7	1	21	-16	8	10	1	50	-48	12	0	2	13	-14	1	3	2	16	19	-4	6	2	22	20
1	7	1	73	-73	10	10	1	112	103	14	0	2	21	22	3	3	2	94	-91	-2	6	2	271	-268
3	7	1	212	212	-7	11	1	53	53	-11	1	2	52	-46	5	3	2	129	127	0	6	2	219	217
5	7	1	198	-194	-5	11	1	110	-107	-9	1	2	121	-118	7	3	2	121	-117	2	6	2	77	78
7	7	1	57	54	-1	11	1	188	187	-7	1	2	247	295	9	3	2	98	92	4	6	2	274	-270
9	7	1	14	2	1	11	1	165	-166	-5	1	2	203	-216	11	3	2	54	-45	6	6	2	163	160
11	7	1	18	4	3	11	1	35	37	-3	1	2	30	-30	13	3	2	22	26	8	6	2	17	-7
-12	8	1	47	-57	5	11	1	27	24	-1	1	2	47	44	-12	4	2	26	-18	10	6	2	18	2
-10	8	1	54	56	7	11	1	31	27	1	1	2	37	36	-10	4	2	8	-6	-11	7	2	69	86
-8	8	1	71	-69	9	11	1	21	-30	3	1	2	41	41	-8	4	2	21	-22	-9	7	2	95	-100
-6	8	1	36	36	-8	12	1	50	-51	5	1	2	73	-71	-6	4	2	49	46	-7	7	2	18	16
-4	8	1	57	-56	-6	12	1	68	67	7	1	2	145	-131	-4	4	2	92	93	-5	7	2	19	-21
-2	8	1	16	-17	-4	12	1	14	-19	9	1	2	279	243	-2	4	2	194	-187	-3	7	2	55	52
0	8	1	4	-7	-2	12	1	48	-48	11	1	2	145	-154	0	4	2	217	208	-1	7	2	17	-19
2	8	1	25	-28	2	12	1	59	60	13	1	2	9	1	2	4	2	135	135	1	7	2	14	-7
4	8	1	112	-110	4	12	1	10	-12	-14	2	2	12	4	4	4	2	277	-279	3	7	2	56	-61
6	8	1	56	58	8	12	1	59	-56	-12	2	2	15	25	6	4	2	179	177	5	7	2	113	116
8	8	1	42	-42	-5	13	1	20	-20	-10	2	2	16	-18	8	4	2	62	-62	7	7	2	105	-106
10	8	1	12	30	-1	13	1	61	61	-8	2	2	64	76	12	4	2	14	4	9	7	2	26	26
-9	9	1	33	-38	1	13	1	56	-60	-6	2	2	183	-191	-13	5	2	97	-89	11	7	2	22	-26
-7	9	1	77	74	3	13	1	54	55	-4	2	2	214	210	-11	5	2	147	185	-10	8	2	30	-32
-5	9	1	93	-91	5	13	1	46	-46	-2	2	2	46	-48	-9	5	2	117	-126	-8	8	2	65	66
-3	9	1	33	-36	0	14	1	4	-8	0	2	2	50	-46	-7	5	2	72	-72	-6	8	2	77	-78
-1	9	1	177	180	2	14	1	34	29	2	2	2	35	-34	-5	5	2	95	93	-4	8	2	59	54
1	9	1	176	-179	4	14	1	45	-43	4	2	2	67	68	-3	5	2	186	178	-2	8	2	78	-76
3	9	1	75	75	-10	0	2	9	27	6	2	2	57	57	-1	5	2	57	-51	0	8	2	5	-7
5	9	1	12	-19	-8	0	2	138	124	8	2	2	95	-85	1	5	2	28	-27	2	8	2	36	35
7	9	1	19	4	-6	0	2	198	-243	10	2	2	4	12	3	5	2	71	-74	4	8	2	57	-58
-10	10	1	20	-3	-4	0	2	115	-115	12	2	2	20	15	5	5	2	236	240	6	8	2	53	55
-8	10	1	73	-74	-2	0	2	180	181	-13	3	2	50	-52	7	5	2	132	-130	8	8	2	19	-20
-6	10	1	149	145	0	0	2	334	-328	-11	3	2	108	101	9	5	2	43	-43	-11	9	2	14	11
-4	10	1	31	-31	2	0	2	18	17	-9	3	2	63	-80	11	5	2	42	43	-9	9	2	61	-67
-2	10	1	27	-25	4	0	2	25	21	-7	3	2	68	71	13	5	2	67	54	-7	9	2	153	156
0	10	1	18	4	6	0	2	77	77	-5	3	2	56	-57	-10	6	2	19	-12	-5	9	2	130	-128
4	10	1	6	7	8	0	2	104	-91	-3	3	2	51	51	-8	6	2	25	28	-1	9	2	10	-2

OBSERVED AND CALCULATED STRUCTURE FACTORS

H	K	L	FO	FC	H	K	L	FO	FC	H	K	L	FO	FC	H	K	L	FO	FC	H	K	L	FO	FC
1	9	2	26	-25	5	13	2	16	20	0	2	3	154	148	-1	5	3	375	376	8	8	3	57	57
5	9	2	18	8	-2	14	2	49	-50	2	2	3	64	65	1	5	3	155	-155	10	8	3	82	-82
7	9	2	55	-54	0	14	2	36	34	4	2	3	39	-38	3	5	3	181	-178	-9	9	3	43	44
9	9	2	123	120	2	14	2	22	27	6	2	3	25	-23	5	5	3	140	136	-7	9	3	61	-61
11	9	2	102	-98	-14	0	3	75	65	8	2	3	146	142	7	5	3	19	5	-5	9	3	99	98
-10	10	2	21	3	-12	0	3	129	-123	10	2	3	168	-160	9	5	3	20	12	-3	9	3	49	-47
-8	10	2	47	48	-10	0	3	7	9	12	2	3	88	72	11	5	3	22	2	1	9	3	25	-24
-6	10	2	110	-108	-8	0	3	205	246	-13	3	3	7	1	-12	6	3	57	68	3	9	3	99	101
-4	10	2	60	58	-6	0	3	258	-284	-11	3	3	14	8	-10	6	3	74	-80	5	9	3	56	-55
-2	10	2	87	90	-4	0	3	84	88	-9	3	3	21	-20	-8	6	3	39	-39	9	9	3	43	42
0	10	2	145	-144	-2	0	3	82	78	-7	3	3	71	-67	-6	6	3	61	63	-8	10	3	103	106
2	10	2	37	36	2	0	3	144	134	-5	3	3	101	105	-4	6	3	124	124	-6	10	3	169	-169
4	10	2	33	31	4	0	3	162	-164	-3	3	3	219	-217	-2	6	3	128	-127	-4	10	3	37	36
6	10	2	18	9	6	0	3	22	24	-1	3	3	34	35	0	6	3	21	-22	-2	10	3	17	31
8	10	2	68	-66	8	0	3	182	173	1	3	3	262	-256	2	6	3	17	-15	0	10	3	19	0
10	10	2	20	23	10	0	3	284	-233	3	3	3	67	-67	4	6	3	82	84	2	10	3	33	31
-9	11	2	50	-52	12	0	3	69	81	5	3	3	45	48	6	6	3	97	-98	4	10	3	70	-72
-7	11	2	136	138	-13	1	3	48	49	7	3	3	75	-71	8	6	3	27	-29	6	10	3	14	20
-5	11	2	94	-94	-11	1	3	13	9	9	3	3	41	41	10	6	3	23	22	8	10	3	96	91
-1	11	2	12	31	-9	1	3	56	63	13	3	3	25	-18	12	6	3	84	75	-9	11	3	20	7
1	11	2	27	25	-7	1	3	127	-139	-12	4	3	42	48	-9	7	3	19	23	-7	11	3	84	-84
3	11	2	19	9	-5	1	3	169	170	-10	4	3	78	-86	-7	7	3	21	-22	-5	11	3	104	103
5	11	2	17	-26	-3	1	3	45	-47	-8	4	3	70	-67	-5	7	3	16	19	-3	11	3	8	-19
7	11	2	53	-51	-1	1	3	81	-76	-6	4	3	14	-8	-3	7	3	169	-167	-1	11	3	63	-61
9	11	2	140	137	1	1	3	29	27	-4	4	3	121	116	-1	7	3	212	212	1	11	3	47	-47
-8	12	2	32	36	3	1	3	307	295	-2	4	3	91	-90	1	7	3	90	-88	3	11	3	123	120
-6	12	2	99	-96	5	1	3	94	-91	0	4	3	52	-51	3	7	3	70	-68	5	11	3	54	-53
-4	12	2	90	91	7	1	3	50	-49	2	4	3	52	-53	5	7	3	84	83	7	11	3	45	-44
0	12	2	46	-46	9	1	3	84	76	4	4	3	74	75	7	7	3	13	-6	-6	12	3	79	-78
4	12	2	33	33	13	1	3	20	8	6	4	3	83	-81	9	7	3	8	3	-4	12	3	31	31
6	12	2	32	36	-14	2	3	46	41	8	4	3	4	-29	-8	8	3	87	88	0	12	3	23	18
-5	13	2	28	-26	-12	2	3	73	-63	10	4	3	17	-7	-6	8	3	71	-68	4	12	3	40	-40
-3	13	2	12	12	-8	2	3	150	159	12	4	3	61	54	-4	8	3	102	100	6	12	3	17	-12
-1	13	2	18	6	-6	2	3	167	-170	-7	5	3	38	40	0	8	3	52	53	-5	13	3	47	49
1	13	2	32	34	-4	2	3	101	100	-5	5	3	41	39	2	8	3	81	81	-3	13	3	66	-65
3	13	2	18	-20	-2	2	3	54	51	-3	5	3	291	-290	4	8	3	19	19	-1	13	3	33	36

OBSERVED AND CALCULATED STRUCTURE FACTORS

H	K	L	FO	FC	H	K	L	FO	FC	H	K	L	FO	FC	H	K	L	FO	FC	H	K	L	FO	FC
1	13	3	61	-60	0	2	4	195	-195	9	5	4	116	113	1	9	4	9	13	2	0	5	105	-106
3	13	3	12	16	2	2	4	248	247	-10	6	4	12	2	3	9	4	78	-78	4	0	5	197	199
5	13	3	18	14	4	2	4	147	-148	-8	6	4	39	39	5	9	4	58	59	6	0	5	66	-65
0	14	3	11	5	6	2	4	71	67	-6	6	4	56	-51	7	9	4	15	-4	8	0	5	92	-94
-12	0	4	65	-52	8	2	4	34	33	-4	6	4	128	-132	9	9	4	88	-82	10	0	5	18	26
-10	0	4	33	-38	-13	3	4	49	-57	-2	6	4	312	314	-8	10	4	23	-27	12	0	5	51	46
-8	0	4	29	-32	-11	3	4	38	45	0	6	4	260	-261	-6	10	4	46	44	-13	1	5	73	-60
-6	0	4	69	69	-9	3	4	60	-61	2	6	4	45	-47	-4	10	4	33	-33	-9	1	5	14	24
-4	0	4	94	-89	-7	3	4	22	19	4	6	4	53	57	-2	10	4	82	-81	-7	1	5	34	36
-2	0	4	193	-189	-5	3	4	43	41	6	6	4	27	30	0	10	4	31	-32	-5	1	5	37	39
0	0	4	18	-18	-3	3	4	63	-67	8	6	4	50	-49	2	10	4	153	154	-3	1	5	168	-169
2	0	4	225	222	-1	3	4	79	78	10	6	4	21	6	4	10	4	154	-152	1	1	5	227	222
4	0	4	382	-371	3	3	4	32	-32	-9	7	4	69	-74	8	10	4	42	41	3	1	5	353	-350
6	0	4	18	-16	5	3	4	13	13	-7	7	4	55	59	-7	11	4	77	-74	5	1	5	164	160
8	0	4	65	63	7	3	4	39	-36	-5	7	4	26	21	-5	11	4	43	41	-12	2	5	88	99
10	0	4	27	-25	11	3	4	14	18	-3	7	4	140	-135	-3	11	4	32	34	-10	2	5	67	-68
12	0	4	26	21	-12	4	4	14	29	-1	7	4	20	21	1	11	4	15	12	-8	2	5	42	44
-13	1	4	153	-130	-10	4	4	3	-9	1	7	4	45	46	3	11	4	53	-59	-6	2	5	18	-19
-11	1	4	98	115	-8	4	4	58	60	5	7	4	16	-28	5	11	4	60	68	-4	2	5	28	26
-9	1	4	29	31	-6	4	4	33	-33	7	7	4	65	-62	7	11	4	18	30	-2	2	5	12	2
-7	1	4	166	-173	-4	4	4	158	-154	9	7	4	38	34	-6	12	4	65	63	0	2	5	12	-18
-5	1	4	98	96	-2	4	4	273	273	11	7	4	41	36	-4	12	4	37	-34	2	2	5	28	-26
-1	1	4	29	28	0	4	4	259	-259	-10	8	4	14	14	-2	12	4	28	24	4	2	5	96	93
1	1	4	57	54	2	4	4	13	11	-6	8	4	25	24	0	12	4	66	-64	6	2	5	52	-46
3	1	4	118	-117	4	4	4	84	85	-4	8	4	65	-63	2	12	4	121	125	10	2	5	12	-7
5	1	4	125	121	6	4	4	35	32	-2	8	4	120	115	4	12	4	84	-82	12	2	5	21	13
7	1	4	19	24	12	4	4	19	-10	0	8	4	118	-113	6	12	4	18	11	-13	3	5	21	-5
9	1	4	159	-156	-11	5	4	9	8	2	8	4	87	87	-3	13	4	13	-26	-11	3	5	13	-6
11	1	4	73	67	-9	5	4	97	-93	4	8	4	82	-87	-1	13	4	16	12	-9	3	5	21	17
13	1	4	14	-6	-7	5	4	148	151	6	8	4	59	54	1	13	4	15	-11	-7	3	5	73	-71
-12	2	4	3	-13	-5	5	4	71	72	10	8	4	21	-9	-12	0	5	136	128	-5	3	5	30	32
-10	2	4	21	15	-3	5	4	101	-99	-9	9	4	15	11	-10	0	5	68	-74	-3	3	5	90	85
-8	2	4	26	-27	-1	5	4	95	94	-7	9	4	90	-90	-8	0	5	81	-82	-1	3	5	125	-123
-6	2	4	108	110	1	5	4	37	38	-5	9	4	67	67	-4	0	5	100	102	1	3	5	143	143
-4	2	4	101	-101	3	5	4	95	92	-3	9	4	18	12	-2	0	5	99	-102	3	3	5	87	-90
-2	2	4	113	112	7	5	4	79	-74	-1	9	4	14	19	0	0	5	16	-22	5	3	5	61	61

OBSERVED AND CALCULATED STRUCTURE FACTORS

H	K	L	FO	FC	H	K	L	FO	FC	H	K	L	FO	FC	H	K	L	FO	FC	H	K	L	FO	FC
7	3	5	57	-55	8	6	5	149	145	-5	11	5	5	16	-4	2	6	110	-111	1	5	6	26	-29
9	3	5	21	21	10	6	5	68	-67	-3	11	5	64	-64	-2	2	6	136	142	3	5	6	70	-72
11	3	5	15	-3	-11	7	5	17	7	-1	11	5	19	21	0	2	6	4	8	5	5	6	62	-66
-12	4	5	32	32	-9	7	5	25	16	1	11	5	120	124	2	2	6	173	-172	7	5	6	171	168
-10	4	5	98	-93	-7	7	5	77	-76	3	11	5	162	-165	4	2	6	138	132	9	5	6	133	-136
-8	4	5	188	183	-5	7	5	25	29	5	11	5	73	73	6	2	6	54	-57	-8	6	6	82	-76
-6	4	5	128	-125	-3	7	5	97	98	-4	12	5	27	32	8	2	6	13	21	-6	6	6	90	87
-4	4	5	24	-23	-1	7	5	156	-157	2	12	5	20	4	10	2	6	20	-24	-4	6	6	32	33
-2	4	5	95	94	3	7	5	33	-32	4	12	5	45	46	-11	3	6	50	-48	-2	6	6	64	-64
0	4	5	11	-11	5	7	5	86	85	-1	13	5	29	-30	-9	3	6	99	93	0	6	6	13	-19
4	4	5	12	10	7	7	5	80	-78	1	13	5	64	64	-7	3	6	143	-139	2	6	6	113	114
6	4	5	87	-88	9	7	5	22	20	-12	0	6	22	23	-5	3	6	61	59	4	6	6	21	21
8	4	5	151	148	-10	8	5	62	-56	-10	0	6	37	38	-3	3	6	40	-40	6	6	6	122	-127
10	4	5	91	-86	-8	8	5	64	61	-8	0	6	26	29	-1	3	6	10	-15	8	6	6	79	75
12	4	5	38	-32	-6	8	5	8	-17	-6	0	6	80	79	1	3	6	15	8	-9	7	6	134	125
-11	5	5	16	3	-4	8	5	3	-10	-4	0	6	236	-233	3	3	6	19	6	-7	7	6	94	-88
-9	5	5	42	40	2	8	5	30	-28	-2	0	6	311	309	5	3	6	52	-52	-5	7	6	47	47
-7	5	5	103	-98	4	8	5	51	51	0	0	6	42	42	7	3	6	109	108	-1	7	6	21	18
-5	5	5	29	31	6	8	5	55	-54	2	0	6	203	-205	9	3	6	93	-89	1	7	6	8	10
-3	5	5	199	198	8	8	5	30	30	4	0	6	260	259	11	3	6	52	45	3	7	6	7	-1
-1	5	5	227	-226	-9	9	5	17	-1	6	0	6	9	-5	-12	4	6	26	-23	5	7	6	47	-49
1	5	5	81	78	-5	9	5	30	29	8	0	6	29	-27	-10	4	6	10	-8	7	7	6	99	100
3	5	5	61	69	-3	9	5	63	-67	10	0	6	21	-20	-8	4	6	79	-76	9	7	6	71	-73
5	5	5	29	30	1	9	5	121	121	-11	1	6	40	-42	-6	4	6	101	99	-8	8	6	14	-11
7	5	5	106	-105	3	9	5	168	-175	-9	1	6	11	-3	-2	4	6	43	-45	-6	8	6	61	60
9	5	5	63	59	5	9	5	100	97	-7	1	6	13	12	0	4	6	6	-10	-4	8	6	66	-66
11	5	5	11	5	7	9	5	19	-16	-5	1	6	124	123	2	4	6	59	58	-2	8	6	65	64
-10	6	5	119	-115	-8	10	5	22	-25	-3	1	6	162	-159	4	4	6	53	-50	0	8	6	9	-2
-8	6	5	186	177	-4	10	5	51	51	1	1	6	15	-10	6	4	6	127	-125	2	8	6	46	-46
-6	6	5	111	-107	-2	10	5	34	-33	3	1	6	117	116	8	4	6	92	91	4	8	6	101	100
-4	6	5	75	-74	0	10	5	16	-17	5	1	6	53	-56	10	4	6	18	-14	6	8	6	68	-70
-2	6	5	83	81	2	10	5	72	-70	9	1	6	10	3	-11	5	6	53	-47	8	8	6	24	26
0	6	5	33	33	4	10	5	88	89	11	1	6	80	72	-9	5	6	162	154	-7	9	6	32	-26
2	6	5	28	29	6	10	5	15	-24	-10	2	6	11	-2	-7	5	6	210	-202	-5	9	6	48	52
4	6	5	24	-26	8	10	5	37	-34	-8	2	6	20	-13	-3	5	6	38	40	-3	9	6	62	-63
6	6	5	97	-97	-7	11	5	29	21	-6	2	6	42	43	-1	5	6	26	-26	-1	9	6	20	17

OBSERVED AND CALCULATED STRUCTURE FACTORS

H	K	L	FO	FC	H	K	L	FO	FC	H	K	L	FO	FC	H	K	L	FO	FC	H	K	L	FO	FC
1	9	6	22	-18	7	1	7	49	-47	-3	5	7	51	-50	5	9	7	24	-25	8	2	8	19	-3
3	9	6	66	67	9	1	7	43	-43	-1	5	7	75	-75	-6	10	7	37	39	-9	3	8	9	3
5	9	6	17	-19	-10	2	7	8	-16	1	5	7	215	224	-4	10	7	87	-88	-7	3	8	33	34
7	9	6	9	17	-8	2	7	19	-16	3	5	7	140	-145	-2	10	7	68	71	-5	3	8	19	-7
-6	10	6	51	48	-6	2	7	57	57	5	5	7	66	-66	2	10	7	9	12	-3	3	8	17	15
-4	10	6	119	-117	-4	2	7	134	-130	7	5	7	96	96	4	10	7	18	-15	-1	3	8	19	-22
-2	10	6	133	132	-2	2	7	22	23	9	5	7	36	-37	-3	11	7	131	128	3	3	8	40	38
0	10	6	17	13	0	2	7	17	-9	-10	6	7	90	83	-1	11	7	70	-74	5	3	8	19	-26
2	10	6	115	-122	2	2	7	11	-15	-8	6	7	121	-112	1	11	7	32	-35	7	3	8	11	3
4	10	6	101	106	8	2	7	17	-18	-6	6	7	55	51	3	11	7	50	50	9	3	8	34	36
6	10	6	21	-22	10	2	7	70	68	0	6	7	21	-22	-8	0	8	18	-17	-8	4	8	30	28
-5	11	6	64	60	-11	3	7	14	8	2	6	7	38	-36	-6	0	8	24	-24	-6	4	8	12	-3
-3	11	6	83	-84	-9	3	7	12	5	4	6	7	26	26	-4	0	8	220	212	-4	4	8	43	-45
1	11	6	8	-5	-7	3	7	59	58	6	6	7	82	84	-2	0	8	175	-167	-2	4	8	30	-28
3	11	6	32	35	-5	3	7	36	-35	8	6	7	99	-99	0	0	8	15	-18	0	4	8	207	208
5	11	6	40	-43	-3	3	7	90	89	-9	7	7	10	-9	2	0	8	35	37	2	4	8	179	-181
-2	12	6	70	72	-1	3	7	68	-70	-7	7	7	45	42	4	0	8	75	76	4	4	8	75	71
0	12	6	21	11	1	3	7	128	133	-5	7	7	26	-23	6	0	8	110	-108	6	4	8	19	17
2	12	6	91	-93	3	3	7	65	-64	-3	7	7	52	54	8	0	8	9	18	8	4	8	25	-26
-10	0	7	46	-44	5	3	7	18	-8	-1	7	7	69	-67	-9	1	8	97	96	-9	5	8	79	-74
-8	0	7	68	65	7	3	7	69	74	1	7	7	125	130	-7	1	8	17	-21	-7	5	8	32	24
-6	0	7	67	64	9	3	7	23	-31	3	7	7	52	-54	-5	1	8	116	-115	-5	5	8	24	23
-4	0	7	195	-197	-10	4	7	84	79	5	7	7	46	-47	-3	1	8	102	101	-3	5	8	30	-34
-2	0	7	92	94	-8	4	7	129	-122	7	7	7	44	46	-1	1	8	27	-26	-1	5	8	31	-29
0	0	7	27	-28	-6	4	7	80	77	-8	8	7	47	-42	1	1	8	11	-17	1	5	8	11	-3
2	0	7	36	36	-4	4	7	11	15	-6	8	7	20	24	3	1	8	15	-6	3	5	8	51	53
4	0	7	15	-19	-2	4	7	15	15	-4	8	7	60	-61	5	1	8	51	-52	5	5	8	16	-4
6	0	7	19	-22	0	4	7	14	-19	-2	8	7	22	22	7	1	8	86	94	7	5	8	60	-63
8	0	7	37	37	2	4	7	39	-40	0	8	7	39	-39	-8	2	8	27	-23	-8	6	8	25	24
10	0	7	69	69	4	4	7	26	24	2	8	7	18	-9	-6	2	8	31	-30	-4	6	8	35	-32
-5	1	7	124	-124	6	4	7	97	94	4	8	7	11	3	-4	2	8	91	92	-2	6	8	10	-25
-3	1	7	258	257	8	4	7	102	-107	-7	9	7	14	16	-2	2	8	91	-96	0	6	8	160	161
-1	1	7	147	-146	10	4	7	73	76	-5	9	7	99	-90	0	2	8	58	61	2	6	8	176	-182
1	1	7	51	-51	-9	5	7	33	-30	-3	9	7	123	122	2	2	8	62	-63	4	6	8	57	64
3	1	7	97	96	-7	5	7	73	75	-1	9	7	88	-86	4	2	8	64	70	6	6	8	28	28
5	1	7	7	-9	-5	5	7	19	3	3	9	7	34	38	6	2	8	51	-55	-7	7	8	19	17

OBSERVED AND CALCULATED STRUCTURE FACTORS

H	K	L	FO	FC	H	K	L	FO	FC	H	K	L	FO	FC	H	K	L	FO	FC	H	K	L	FO	FC
-5	7	8	17	10	-7	1	9	26	27	-4	4	9	59	-58	-4	0	10	36	-35	-2	4	10	33	-30
-1	7	8	36	-35	-5	1	9	60	56	0	4	9	19	23	-2	0	10	47	-52	0	4	10	64	-65
1	7	8	14	13	-3	1	9	86	-86	4	4	9	39	-40	0	0	10	81	83	2	4	10	74	75
3	7	8	51	53	-1	1	9	16	-9	6	4	9	13	-10	2	0	10	17	-31	4	4	10	11	-33
5	7	8	20	-17	1	1	9	32	29	-7	5	9	21	11	4	0	10	71	-72	-5	5	10	97	-98
7	7	8	23	-23	3	1	9	63	63	-5	5	9	82	-78	6	0	10	95	99	-3	5	10	52	54
-6	8	8	27	-29	5	1	9	100	-102	-3	5	9	42	39	-7	1	10	41	40	-1	5	10	34	33
-4	8	8	44	42	7	1	9	77	83	-1	5	9	80	81	-5	1	10	12	13	3	5	10	20	-23
-2	8	8	60	-59	-8	2	9	71	-69	1	5	9	162	-163	-3	1	10	12	16	-4	6	10	103	93
0	8	8	71	75	-6	2	9	13	15	3	5	9	107	111	-1	1	10	23	-21	-2	6	10	8	-29
2	8	8	79	-77	-4	2	9	28	28	5	5	9	22	-25	1	1	10	10	-14	0	6	10	83	-86
4	8	8	23	27	0	2	9	11	-2	-6	6	9	70	69	5	1	10	65	69	2	6	10	81	79
-5	9	8	40	-39	2	2	9	6	9	-4	6	9	60	-57	-6	2	10	42	-40	-4	0	11	14	18
-3	9	8	68	65	4	2	9	32	-36	0	6	9	32	36	-4	2	10	21	19	-2	0	11	32	-33
-1	9	8	38	-38	6	2	9	79	77	2	6	9	29	30	-2	2	10	26	-30	0	0	11	13	8
1	9	8	15	-18	8	2	9	56	-56	4	6	9	40	-43	0	2	10	28	32	-3	1	11	43	-41
-2	10	8	86	-87	-9	3	9	14	-13	-5	7	9	34	-35	2	2	10	14	2	-1	1	11	107	114
0	10	8	28	25	-7	3	9	14	18	-3	7	9	22	24	4	2	10	58	-58	1	1	11	101	-108
2	10	8	25	22	-5	3	9	44	-44	-1	7	9	50	50	6	2	10	71	77	-4	2	11	42	44
-8	0	9	94	-90	-3	3	9	8	-1	1	7	9	111	-114	-7	3	10	75	73	-2	2	11	39	-37
-6	0	9	18	-20	-1	3	9	68	68	3	7	9	78	81	-5	3	10	55	-53	0	2	11	10	16
-4	0	9	112	109	1	3	9	104	-102	5	7	9	4	-7	-3	3	10	36	38	-3	3	11	82	-76
2	0	9	30	-29	3	3	9	71	70	-4	8	9	15	12	-1	3	10	13	3	-1	3	11	49	51
4	0	9	25	-22	5	3	9	70	-73	-2	8	9	27	-24	1	3	10	22	11	1	3	11	10	-16
6	0	9	130	131	7	3	9	32	31	0	8	9	17	9	5	3	10	16	7	-2	4	11	19	-21
8	0	9	89	-89	-8	4	9	31	-28	2	8	9	20	24	-6	4	10	59	-60	0	4	11	21	2
-9	1	9	4	-16	-6	4	9	48	50	-1	9	9	16	21	-4	4	10	77	78					

APPENDIX III FURTHER CRYSTALLOGRAPHIC DETAILS OF $[(OC)_4CoGe]_2Co_4(CO)_{11}$, FINAL ATOMIC POSITIONAL COORDINATES OF $[(OC)_4Co]_2Co_4(CO)_{11}$.

GE1	0.41635	0.24528	0.12448
C01	0.50000	0.29690	0.05780
C02	0.50000	0.38513	0.14934
C03	0.50000	0.19454	0.19273
C04	0.50000	0.11060	0.09762
C05	0.28292	0.23399	0.11534
C11	0.42584	0.34260	0.02331
C21	0.42746	0.43982	0.18351
C22	0.50000	0.46489	0.09773
C31	0.42713	0.22788	0.23517
C32	0.50000	0.06468	0.19366
C41	0.42642	0.02512	0.09283
C51	0.28907	0.14280	0.16695
C52	0.18424	0.22803	0.11667
C53	0.29496	0.17545	0.05641
C54	0.29004	0.37019	0.11268
C8	0.50000	0.15764	0.02772
O11	0.37332	0.36836	-0.00378
O21	0.37886	0.48168	0.20465
O22	0.50000	0.54405	0.07185
O31	0.37973	0.24540	0.26516
O32	0.50000	-0.02829	0.20381
O41	0.37718	-0.04158	0.09209
O51	0.29088	0.08371	0.19871
O52	0.11743	0.22114	0.11932
O53	0.30167	0.13337	0.01636
O54	0.29465	0.46250	0.10463
O8	0.50000	0.12156	-0.00863

ANISOTROPIC TEMPERATURE PARAMETERS FOR THE Ge AND Co ATOMS OF $[(OC)_4CoGe]_2Co_4(CO)_{11}$.

GE1	0.01583	0.02723	0.03070	-0.00073	-0.00105	0.00339
CO1	0.01673	0.02907	0.02942	0.00330	0.00000	0.00000
CO2	0.02623	0.02605	0.03618	-0.00918	0.00000	0.00000
CO3	0.03212	0.04005	0.02492	0.00287	0.00000	0.00000
CO4	0.01568	0.02236	0.04333	-0.00059	0.00000	0.00000
CO5	0.01635	0.03379	0.04238	-0.00065	-0.00042	-0.00026

ISOTROPIC TEMPERATURE PARAMETERS FOR THE O AND C ATOMS OF $[(OC)_4CoGe]_2Co_4(CO)_{11}$.

C11	0.03776	O11	0.06085
C21	0.04438	O21	0.07355
C22	0.02626	O22	0.07050
C31	0.06026	O31	0.09824
C32	0.05167	O32	0.07266
C41	0.03720	O41	0.06689
C51	0.04747	O51	0.07352
C52	0.07049	O52	0.07873
C53	0.04244	O53	0.05066
C54	0.05728	O54	0.07003
CB	0.02938	OB	0.04417

OBSERVED AND CALCULATED STRUCTURE FACTORS FOR $[(OC)_4CoGe]_2Co_4(CO)_{11}$

H	K	L	FO	FC	H	K	L	FO	FC	H	K	L	FO	FC	H	K	L	FO	FC	H	K	L	FO	FC
2	0	0	712	644	6	10	0	461	470	6	0	2	137	130	13	7	2	260	-291	5	7	3	287	-293
4	0	0	723	698	8	10	0	310	328	10	0	2	101	95	0	8	2	87	74	9	7	3	221	-221
6	0	0	186	189	2	12	0	115	-127	1	1	2	1079	949	1	9	2	147	151	13	7	3	114	-122
8	0	0	530	484	4	12	0	202	-212	3	1	2	310	282	3	9	2	180	-178	0	8	3	133	133
10	0	0	1286	1175	5	1	1	81	-78	5	1	2	654	569	5	9	2	173	-177	2	8	3	186	-172
12	0	0	369	418	0	2	1	197	-208	7	1	2	512	-460	7	9	2	448	-418	6	8	3	97	-88
14	0	0	859	866	2	2	1	116	112	9	1	2	669	627	3	11	2	252	249	7	9	3	160	-154
16	0	0	159	148	4	2	1	149	-135	11	1	2	382	369	5	11	2	310	308	0	10	3	174	-189
0	2	0	941	-934	1	3	1	71	-73	13	1	2	666	615	7	11	2	376	389	7	11	3	104	113
4	2	0	94	-86	3	3	1	63	-58	15	1	2	248	233	1	3	3	189	-185	0	12	3	108	109
6	2	0	367	356	5	3	1	310	352	17	1	2	128	-104	5	3	3	99	91	0	0	4	875	-1006
8	2	0	90	95	7	3	1	189	-170	0	2	2	80	-84	9	3	3	123	-104	2	0	4	73	82
10	2	0	406	-394	9	3	1	77	86	4	2	2	123	-121	13	3	3	103	-93	4	0	4	386	-325
12	2	0	230	-225	0	4	1	438	441	1	3	2	146	-114	2	4	3	548	-529	6	0	4	302	288
14	2	0	352	-351	8	4	1	84	72	3	3	2	150	154	4	4	3	213	-187	8	0	4	79	80
16	2	0	176	201	10	4	1	146	125	5	3	2	299	328	6	4	3	207	-205	10	0	4	501	-467
0	4	0	592	568	14	4	1	99	89	7	3	2	604	559	8	4	3	196	-187	12	0	4	226	-227
2	4	0	109	-114	1	5	1	106	111	9	3	2	88	-80	12	4	3	284	-268	14	0	4	416	-398
4	4	0	486	-456	3	5	1	200	187	13	3	2	239	-229	14	4	3	82	-77	16	0	4	212	205
6	4	0	745	-704	5	5	1	154	147	15	3	2	118	121	1	5	3	325	308	5	1	4	118	103
8	4	0	273	-259	7	5	1	280	251	17	3	2	277	274	3	5	3	386	372	7	1	4	80	-74
14	4	0	90	102	11	5	1	167	160	0	4	2	325	-321	5	5	3	361	328	9	1	4	85	74
16	4	0	277	-309	0	6	1	191	-204	2	4	2	120	-107	7	5	3	113	120	0	2	4	503	527
0	6	0	534	-572	4	6	1	125	-123	4	4	2	181	176	9	5	3	196	216	2	2	4	297	-279
6	6	0	354	346	3	7	1	139	-147	8	4	2	82	-76	11	5	3	221	207	4	2	4	62	-58
8	6	0	120	116	5	7	1	107	-101	16	4	2	78	-63	13	5	3	261	232	6	2	4	480	-465
10	6	0	162	-213	7	7	1	184	-177	1	5	2	188	204	15	5	3	102	118	8	2	4	238	-223
12	6	0	149	-146	11	7	1	116	-128	3	5	2	181	-167	0	6	3	62	56	10	2	4	205	209
14	6	0	190	-210	0	8	1	282	304	5	5	2	235	-227	2	6	3	299	304	14	2	4	165	187
0	8	0	495	535	1	9	1	65	-48	7	5	2	707	-645	4	6	3	166	169	16	2	4	277	-310
6	8	0	282	-268	7	9	1	183	169	13	5	2	277	247	6	6	3	308	304	1	3	4	150	-158
8	8	0	95	-87	6	10	1	153	158	0	6	2	130	143	8	6	3	246	232	3	3	4	90	91
10	8	0	192	193	8	10	1	102	102	1	7	2	396	-388	10	6	3	109	112	9	3	4	140	-143
0	10	0	152	-157	0	0	2	108	166	7	7	2	215	213	12	6	3	167	172	0	4	4	680	-670
2	10	0	234	231	2	0	2	68	-68	9	7	2	276	-255	1	7	3	175	-185	2	4	4	339	324
4	10	0	296	307	4	0	2	156	139	11	7	2	146	-166	3	7	3	124	-119	4	4	4	292	259

OBSERVED AND CALCULATED STRUCTURE FACTORS

H	K	L	FO	FC	H	K	L	FO	FC	H	K	L	FO	FC	H	K	L	FO	FC	H	K	L	FO	FC
6	4	4	546	570	7	3	5	114	106	0	12	5	104	-111	11	7	6	232	238	13	5	7	138	-136
8	4	4	376	371	11	3	5	67	67	0	0	6	211	-221	13	7	6	289	340	0	6	7	102	131
10	4	4	130	-135	0	4	5	318	-329	2	0	6	62	66	8	8	6	67	42	2	6	7	266	-273
14	4	4	125	-142	2	4	5	233	-226	6	0	6	83	75	1	9	6	387	-382	4	6	7	111	-118
16	4	4	272	292	4	4	5	257	-213	1	1	6	122	-110	3	9	6	88	-87	6	6	7	267	-255
1	5	4	62	-66	6	4	5	101	-121	3	1	6	215	223	5	9	6	88	-82	8	6	7	206	-200
3	5	4	59	45	8	4	5	129	-150	5	1	6	278	249	7	9	6	172	161	12	6	7	141	-139
5	5	4	112	108	10	4	5	177	-175	7	1	6	673	611	9	9	6	234	-218	1	7	7	111	103
0	6	4	671	673	12	4	5	151	-150	9	1	6	131	-126	1	11	6	151	140	13	7	7	90	105
4	6	4	83	67	14	4	5	155	-148	13	1	6	264	-238	5	11	6	130	-128	0	8	7	369	-362
6	6	4	250	-234	1	5	5	222	-228	15	1	6	111	112	7	11	6	151	-149	2	8	7	58	58
10	6	4	264	287	3	5	5	417	-415	17	1	6	291	276	1	1	7	190	204	4	8	7	145	-154
12	6	4	193	192	5	5	5	200	-166	0	2	6	113	95	3	1	7	115	107	8	8	7	99	-80
14	6	4	247	259	7	5	5	452	-452	2	2	6	122	-119	5	1	7	83	88	10	8	7	185	-192
7	7	4	85	-67	11	5	5	256	-243	6	2	6	85	-86	7	1	7	109	107	3	9	7	126	127
0	8	4	478	-472	13	5	5	110	-121	12	2	6	63	-52	9	1	7	113	103	5	9	7	95	73
2	8	4	147	-136	15	5	5	118	-135	1	3	6	68	62	13	1	7	107	83	7	9	7	169	152
4	8	4	142	-169	0	6	5	377	381	3	3	6	528	-489	15	1	7	69	81	0	10	7	272	274
6	8	4	150	158	2	6	5	179	192	5	3	6	416	-414	2	2	7	374	381	4	10	7	121	132
10	8	4	282	-257	4	6	5	246	246	7	3	6	840	-805	8	2	7	138	122	2	12	7	104	97
12	8	4	213	-230	6	6	5	246	228	13	3	6	122	111	12	2	7	209	191	0	0	8	626	642
0	10	4	217	204	8	6	5	240	243	15	3	6	136	-153	14	2	7	82	94	2	0	8	357	-370
6	10	4	288	-275	10	6	5	226	251	0	4	6	570	-593	1	3	7	129	-126	4	0	8	473	-434
8	10	4	158	-160	12	6	5	115	141	4	4	6	61	-12	7	3	7	143	-134	6	0	8	715	-650
0	12	4	85	-110	14	6	5	165	160	10	4	6	132	-131	0	4	7	166	-161	8	0	8	342	-340
4	12	4	94	98	1	7	5	118	117	14	4	6	102	-116	2	4	7	219	222	10	0	8	96	102
1	1	5	116	115	3	7	5	149	144	1	5	6	286	-296	4	4	7	76	81	16	0	8	297	-303
3	1	5	63	-62	7	7	5	289	272	3	5	6	129	116	6	4	7	114	119	5	1	8	116	-114
5	1	5	629	-557	11	7	5	82	99	7	5	6	505	512	12	4	7	120	111	7	1	8	136	138
7	1	5	106	84	0	8	5	145	-152	9	5	6	140	-135	16	4	7	74	85	9	1	8	67	-76
11	1	5	74	-63	10	8	5	95	-92	13	5	6	253	-240	1	5	7	221	-221	11	1	8	81	80
17	1	5	81	46	1	9	5	115	116	0	6	6	178	183	3	5	7	148	-131	13	1	8	82	-73
0	2	5	93	-93	5	9	5	166	169	1	7	6	533	539	5	5	7	187	-164	0	2	8	801	-766
4	2	5	111	-105	9	9	5	189	191	3	7	6	132	127	7	5	7	142	-154	2	2	8	192	198
6	2	5	123	-119	2	10	5	114	-111	7	7	6	146	-130	9	5	7	225	-226	4	2	8	413	401
1	3	5	149	153	6	10	5	80	-96	9	7	6	321	321	11	5	7	96	-103	6	2	8	687	672

OBSERVED AND CALCULATED STRUCTURE FACTORS

H	K	L	FO	FC	H	K	L	FO	FC	H	K	L	FO	FC	H	K	L	FO	FC	H	K	L	FO	FC
8	2	8	316	301	6	2	9	282	270	14	0	10	129	148	3	11	10	68	-56	0	8	11	392	408
10	2	8	125	-101	8	2	9	262	225	1	1	10	194	198	1	1	11	231	-252	4	8	11	199	177
14	2	8	126	-128	10	2	9	204	192	3	1	10	157	-182	3	1	11	208	-216	10	8	11	188	198
16	2	8	270	294	12	2	9	236	214	5	1	10	208	-194	5	1	11	189	-201	3	9	11	178	-164
5	3	8	56	45	14	2	9	183	167	7	1	10	724	-671	7	1	11	218	-209	5	9	11	187	-193
7	3	8	115	-133	16	2	9	117	123	13	1	10	257	227	9	1	11	201	-185	7	9	11	162	-153
0	4	8	378	399	1	3	9	142	154	0	2	10	183	215	11	1	11	150	-149	9	9	11	107	-108
2	4	8	263	-258	3	3	9	209	237	2	2	10	168	190	15	1	11	115	-110	0	10	11	190	-187
4	4	8	216	-197	5	3	9	274	266	4	2	10	100	-106	0	2	11	323	-317	1	11	11	77	-83
6	4	8	566	-571	7	3	9	107	115	8	2	10	75	73	2	2	11	202	-214	0	0	12	530	-530
8	4	8	323	-343	9	3	9	182	184	12	2	10	69	64	4	2	11	261	-269	2	0	12	82	89
10	4	8	100	98	11	3	9	147	141	1	3	10	235	-235	6	2	11	246	-271	6	0	12	334	335
5	5	8	195	-187	13	3	9	168	156	3	3	10	57	48	8	2	11	252	-235	8	0	12	169	165
7	5	8	201	241	2	4	9	86	-90	5	3	10	199	187	10	2	11	255	-226	10	0	12	250	-233
0	6	8	629	-624	3	5	9	71	51	7	3	10	516	541	12	2	11	163	-149	12	0	12	124	-117
2	6	8	105	-98	7	5	9	152	151	11	3	10	85	-71	14	2	11	148	-143	14	0	12	173	-175
6	6	8	224	215	0	6	9	220	-232	13	3	10	298	-277	1	3	11	189	201	3	1	12	112	-128
10	6	8	260	-268	2	6	9	101	-98	0	4	10	132	139	3	3	11	273	302	5	1	12	142	158
12	6	8	133	-166	1	7	9	139	137	2	4	10	104	-112	5	3	11	359	357	7	1	12	230	-215
14	6	8	230	-224	5	7	9	107	99	1	5	10	273	248	7	3	11	229	224	9	1	12	154	140
0	8	8	677	714	7	7	9	146	-128	3	5	10	73	-55	9	3	11	178	189	11	1	12	105	-89
2	8	8	210	208	9	7	9	160	162	5	5	10	76	-74	11	3	11	197	190	0	2	12	631	661
4	8	8	151	148	13	7	9	109	102	7	5	10	312	-322	13	3	11	142	141	2	2	12	96	101
10	8	8	321	326	2	8	9	101	-87	9	5	10	179	165	15	3	11	118	120	6	2	12	261	-280
12	8	8	210	225	4	8	9	135	-139	13	5	10	215	218	0	4	11	305	311	10	2	12	316	267
0	10	8	350	-380	6	8	9	206	-210	2	6	10	168	167	2	4	11	104	112	12	2	12	228	205
6	10	8	126	109	8	8	9	165	-163	4	6	10	136	-126	4	4	11	135	159	14	2	12	251	248
1	1	9	218	-224	1	9	9	208	-200	1	7	10	262	-253	6	4	11	142	136	9	3	12	119	-98
3	1	9	328	-356	3	9	9	99	-103	7	7	10	328	320	8	4	11	169	170	11	3	12	126	134
5	1	9	165	-155	5	9	9	237	-250	9	7	10	83	-99	10	4	11	140	165	0	4	12	657	-670
7	1	9	176	-170	9	9	9	232	-219	11	7	10	132	-131	14	4	11	121	106	2	4	12	112	-98
11	1	9	184	-171	6	10	9	79	88	0	8	10	91	87	11	5	11	78	44	6	4	12	182	171
13	1	9	187	-168	0	0	10	687	717	1	9	10	265	274	0	6	11	151	-128	10	4	12	261	-284
0	2	9	235	239	2	0	10	130	-152	7	9	10	200	-192	2	6	11	94	80	12	4	12	156	-165
2	2	9	333	349	10	0	10	188	174	0	10	10	90	-66	5	7	11	88	77	14	4	12	231	-224
4	2	9	369	383	12	0	10	134	-122	1	11	10	206	-214	7	7	11	163	169	5	5	12	109	105

OBSERVED AND CALCULATED STRUCTURE FACTORS .

H	K	L	FO	FC	H	K	L	FO	FC	H	K	L	FO	FC	H	K	L	FO	FC	H	K	L	FO	FC
7	5	12	99	-110	7	3	13	119	-105	11	5	14	133	-129	0	2	16	603	-665	6	6	17	106	-112
9	5	12	126	117	9	3	13	181	-186	13	5	14	204	-195	2	2	16	191	-188	8	6	17	127	-127
0	6	12	352	348	6	4	13	115	100	0	6	14	145	132	6	2	16	124	127	10	6	17	107	-110
2	6	12	62	-78	5	5	13	116	104	2	6	14	97	-103	10	2	16	297	-300	7	7	17	152	-163
4	6	12	97	-82	0	6	13	114	138	3	7	14	202	-189	12	2	16	237	-219	0	0	18	163	165
6	6	12	309	-320	5	7	13	139	-150	5	7	14	325	-293	5	3	16	137	134	2	0	18	256	-278
8	6	12	198	-186	9	7	13	139	-131	7	7	14	388	-407	7	3	16	173	-168	12	0	18	161	-154
12	6	12	87	77	0	8	13	79	90	2	8	14	99	111	9	3	16	110	99	1	1	18	141	143
3	7	12	125	144	2	8	13	134	119	3	9	14	163	163	0	4	16	527	501	5	1	18	198	-198
0	8	12	181	-160	4	8	13	130	140	5	9	14	308	292	2	4	16	202	233	7	1	18	364	-388
2	8	12	65	61	6	8	13	167	146	7	9	14	254	238	4	4	16	140	146	11	1	18	77	74
4	8	12	163	163	0	10	13	97	-80	1	1	15	70	112	10	4	16	302	279	0	2	18	257	-268
6	8	12	343	323	0	0	14	257	-260	7	1	15	102	122	12	4	16	243	273	2	2	18	117	122
8	8	12	169	183	2	0	14	232	242	0	2	15	128	128	7	5	16	137	123	1	3	18	374	-379
3	9	12	75	-69	6	0	14	136	154	2	2	15	101	110	9	5	16	92	-75	3	3	18	162	-166
7	9	12	106	-102	8	0	14	141	152	4	2	15	101	88	0	6	16	255	-250	9	3	18	197	-191
0	10	12	161	161	14	0	14	143	-125	8	2	15	93	103	4	6	16	159	162	11	3	18	231	-237
6	10	12	207	-180	1	1	14	398	-394	5	3	15	118	-125	6	6	16	337	337	4	4	18	128	130
1	1	13	112	138	7	1	14	198	203	2	4	15	76	84	8	6	16	208	198	10	4	18	109	81
3	1	13	182	200	9	1	14	282	-257	6	4	15	138	112	7	7	16	85	-86	1	5	18	219	230
5	1	13	187	195	11	1	14	147	-163	1	5	15	89	-90	2	8	16	163	-155	7	5	18	178	-147
7	1	13	188	183	13	1	14	275	-269	7	5	15	104	-92	4	8	16	303	-271	9	5	18	71	71
9	1	13	162	149	0	2	14	212	214	2	6	15	226	-219	6	8	16	364	-348	0	6	18	94	-114
11	1	13	110	93	2	2	14	119	-120	6	6	15	93	-103	8	8	16	214	-215	3	7	18	165	161
13	1	13	91	99	14	2	14	93	77	2	8	15	73	85	5	9	16	90	-81	5	7	18	220	233
0	2	13	160	-183	1	3	14	460	473	0	10	15	120	124	7	3	17	204	-188	7	7	18	327	327
2	2	13	195	-191	3	3	14	177	191	0	0	16	493	467	0	4	17	71	75	0	8	18	111	116
4	2	13	217	-229	7	3	14	124	-137	6	0	16	220	-242	2	4	17	162	171	2	2	19	125	130
6	2	13	234	-249	9	3	14	274	279	8	0	16	87	-92	6	4	17	73	72	1	3	19	115	-113
8	2	13	193	-195	11	3	14	290	288	10	0	16	171	182	12	4	17	111	114	3	3	19	131	-135
10	2	13	166	-163	13	3	14	355	350	12	0	16	133	121	3	5	17	202	213	7	3	19	125	-125
12	2	13	134	-126	0	4	14	236	-227	5	1	16	105	-133	5	5	17	75	83	2	4	19	191	-196
14	2	13	123	-111	1	5	14	322	-326	7	1	16	184	196	7	5	17	252	231	4	4	19	104	-77
1	3	13	178	-209	5	5	14	80	90	9	1	16	91	-116	11	5	17	138	137	6	4	19	157	-150
3	3	13	90	-95	7	5	14	280	259	11	1	16	104	106	0	6	17	152	-138	8	4	19	138	-145
5	3	13	130	-130	9	5	14	150	-154	13	1	16	101	-74	2	6	17	177	-168	1	5	19	140	137

OBSERVED AND CALCULATED STRUCTURE FACTORS

H	K	L	FO	FC	H	K	L	FO	FC	H	K	L	FO	FC	H	K	L	FO	FC	H	K	L	FO	FC
3	5	19	145	138	0	2	20	290	319	8	4	20	75	-18	3	1	22	238	215	5	5	22	74	97
7	5	19	128	108	6	2	20	284	-268	5	5	20	76	52	5	1	22	380	365	2	6	22	117	-105
2	6	19	121	128	8	2	20	138	-124	0	6	20	166	185	7	1	22	327	332	2	0	24	125	-116
6	6	19	82	111	10	2	20	106	93	4	6	20	117	-120	9	1	22	126	145	4	0	24	295	-282
2	0	20	183	177	1	3	20	114	-86	6	6	20	216	-203	0	2	22	163	176	6	0	24	310	-316
4	0	20	322	326	5	3	20	124	-113	0	8	20	135	-142	2	2	22	83	-78	4	2	24	125	120
6	0	20	427	480	9	3	20	149	-128	2	4	21	101	-91	1	3	22	189	178	6	2	24	208	207
8	0	20	306	352	0	4	20	311	-325	0	0	22	168	-164	7	3	22	156	-163	0	4	24	232	217
7	1	20	170	-184	2	4	20	137	-152	2	0	22	166	174	0	4	22	117	-109	2	4	24	128	118
9	1	20	113	119	6	4	20	109	97	4	0	22	100	-110	1	5	22	163	-152	0	0	26	92	84
11	1	20	100	-98																				

REFERENCES

1) E.W. Abel and F.G.A. Stone; Quart. Rev., 23, (1969), 325; 24, (1970), 498

2) M. Orchin; Accts Chem. Res., 14, 9, (1981), 259.

3) H.M. Feder and J. Halpern; J. Am. Chem. Soc., 97 (1975), 7186.

4) M.A. Bennet and P.B. Donaldson; Inorg. Chem. 17, (1978), 1995.

5) K.M. Mackay and R. Watt; Organometal. Chem. Revs. (A), 4, (1969), 137.

6) K.M. Mackay and B.K. Nicholson; Comprehensive Organometallic Chemistry, Pergammon Press, (1982), ch 43.

7) N.S. Vyazankin, G.A.Razuvaev and O.A. Kruglaya; Organometal. Chem. Rev, 3A, (1968), 323.

8) E.H. Brooks and R.J. Cross; Organomet. Chem. Rev. 6A, (1970), 227.

9) H.G. Ang and P.T. Lau; Organomet. Chem. Rev. 8A, (1972), 235.

10) B.J. Aylett and J.M. Campbell; J. Chem. Soc. (A), (1969), 1910.

11) A.P. Hagen and A.G. MacDiarmid; Inorg. Chem., 6, (1967), 686.

12) A.J. Chalk and J.F. Harrod; J. Am. Chem. Soc., 87, (1965), 1133.

13) A.J. Chalk and J.F. Harrod; J. Am. Chem. Soc., 89, (1967), 1640.

14) R.R. Schrieke and B.O. West; Aust. J. Chem., 22, (1969), 49.

15) Y.L Baay and A.G. MacDiarmid; Inorg. Nucl. Chem. Lett., 3, (1967), 159.

16) S.K. Gondal and A.G. MacDiarmid; Inorg. Nucl Chem. Lett., 5, (1969), 413.

17) L.H. Sommer and J.E. Lyons; J. Am. Chem. Soc., 90, (1968), 4197.

18) R.C. Kerber and T. Pakkanen; Inorg. Chim. Acta, 37, (1979), 61.

19) R.D. George, K.M. Mackay and S.R. Stobart; J. Chem. Soc., (Dalton), (1972), 974.

20) G.F. Bradley and S.R. Stobart; J. Chem. Soc. (Dalton), (1974), 264.

21) W. Heiber and R. Breu; Chem. Ber., 90, (1957), 1270.

22) D.J. Patmore and W.A.G. Graham; Inorg. Chem., 6, (1967), 981.

23) D.J. Patmore and W.A.G. Graham; Inorg. Chem., 7, (1968), 771.

24) R.F. Gerlach, B.W.L. Graham and K.M. Mackay; J. Organometal. Chem., 182, (1979), 285.

25) R.F. Gerlach; M.Sc. Thesis, University of Waikato, (1976).

26) J.P. Collman, J.K. Hoyano and D.W. Murphy; J. Am. Chem. Soc., 95, (1973), 3424.

27) R.F. Gerlach; D.Phil. Thesis; University of Waikato, (1978).

28) F.S. Wong; D.Phil. Thesis; University of Waikato, (1978).

29) O. Kahn and M. Bigorgne; J. Organomet. Chem., 10, (1967), 137.

30) F. Hein and W. Jehn; Justus Liebig Annalen der Chemie, 684, (1965), 4.

31) L.F. Wuyts and G.P. Van der Kelen; Spect. Acta, 32A, (1976), 689.

32) L.F. Wuyts and G.P. Van der Kelen; Spect. Acta, 32A, (1976), 1705.

33) B.P. Bir'yukov, Y.T. Struchkov, K.N. Ansimov, N.E. Kolobova, O.P. Osipova and M.Y. Zhakarova; Chem. Comm., (1967), 749.

34) A.N. Nesmayanov, K.N. Anisimov, N.E. Koldsova and M.Y. Zakharova; Izv. Akdd. Nauk. SSSR, Ser. Khim., (1965), 1127.

35) D.J. Patmore and W.A.G. Graham; Inorg. Chem., 6, (1967), 1879.

36) B.J. Aylett and J.M. Campbell; Chem. Comm., (1967), 159.

37) D.J. Patmore and W.A.G. Graham; Inorg. Chem., 5, (1966), 1586.

38) R.C. Job and M.D. Curtis; Inorg. Chem., 12 (1973), 2514.

39) A.J. Cleland, S.A. Fieldhouse, B.H. Freeland, and R.J. O'Brien; Chem. Comm., (1971), 155.

40) F. Bonati, S. Cenini, D. Marelli and R. Ugo; J. Chem. Soc. (A), (1966), 1052.

41) D.J. Patmore and W.A.G. Graham; Inorg. Nucl. Chem. Lett., 2, (1966), 179.

42) K. Triplett and M.D. Curtis; Inorg. Chem., 15, (1976), 431.

43) D.J. Patmore and W.A.G. Graham; Inorg., Chem., 5, (1966), 2222.

44) R. Ball, M.J. Bennet, E.H. Brookes, W.A.G. Graham, J. Hoyano and S.M. Illingworth; Chem. Comm., (1970), 592.

45) G. Schmid and G. Etzrodt; J. Organometal. Chem., 131, (1977), 477.

46) R. Thomson; M.Sc. Thesis, University of Waikato (1981).

47) P. W. Sutton and L.F. Dahl; J.Am.Chem. Soc., 89, (1967), 261.

48) S.A. Fieldhouse, B.H. Freeland and R.J. O'Brien; Chem. Comm., (1969), 1297.

49) A.J. Cleland, S.A. Fieldhouse, B.H. Freeland and R.J. O'Brien; J. Organometal. Chem., 32, (1971), C15.

50) B.W. Graham; D. Phil. Thesis, University of Waikato (1973)

51) J.A. Christie, D.N. Duffy, K.M. Mackay and B.K. Nicholson; J. Organometal. Chem, 226, (1982), 165.

52) G. Etzrodt and G. Schmid; J. Organomet. Chem., 169, (1979), 259.

53) R.D. Adams and F.A. Cotton; J. Am. Chem. Soc., 92, (1970), 5003.

54) M.D. Curtis and R.C. Job; J. Am. Chem. Soc., 94, (1972), 2153.

55) R.D. Adams, F.A. Cotton, W.R. Cullen, D.L. Hunter and L. Mihichuk; Inorg. Chem., 14, (1975), 1395.

56) K.M. Mackay and Tan Cham Chee; J. Chem. Res. (S), (1982), 229.

57) R.F. Gerlach, K.M. Mackay, B.K. Nicholson and W.T. Robinson; J. Chem. Soc. (Dalton), (1981), 80.

58) D.N. Duffy, K.M. Mackay, B.K. Nicholson, and W.T. Robinson; J. Chem. Soc. (Dalton), (1981), 381.

59) P.F. Lindley and P. Woodward; J. Chem. Soc. (A), (1967), 382.

60) B.K. Nicholson, K.M. Mackay and R.F. Gerlach; Rev. Silicon, Germanium and Tin Compounds, 5, (1981), 67.

61) B.R. Penfold and B.H. Robinson; Accts. Chem. Res. 6, (1973), 73.

62) G. Schmid, V. Bätzel and G. Etzrodt; J. Organometal. Chem. 112, (1976), 345.

63) G. Schmid and G. Etzrodt; J. Organometal. Chem., 137, (1977), 367.

64) R. Boese and G. Schmid; Chem. Comm., (1969), 349.

65) R.A. Croft, D.N. Duffy and B.K. Nicholson; J. Chem. Soc. (Dalton), (1982), 1023.

66) D.N. Duffy, K.M. Mackay, B.K. Nicholson, and R.A. Thomson; J. Chem. Soc. (Dalton), (1982), 1029.

67) K.E. Schwarzans; Z. Naturforsch., 34b, (1979), 1456.

68) G. Schmid; Angew. Chem. Int. Ed., 17, (1978), 392.

69) V.G. Albano, P. Chini, G. Ciani, M. Sansoni, D. Strumab, B.T. Heaton and S. Martinengo; J. Am. Chem. Soc., 98 (1976), 5027.

70) V.G. Albano, P. Chini, S. Martinengo, M. Sansoni and D. Strumolo; Chem. Comm., (1974), 299.

71) G. Bör, G. Cervasio, R. Rosetti and P.L. Stranghellini; Chem. Comm., (1978), 841.

72) V. G. Albano, P. Chini, G. Ciani, S. Martinengo and M. Sansoni; J. Chem. Soc. (Dalton), (1978), 463.

73) S. Martinengo, G. Ciani, A. Sironi, B.T. Heaton and J. Mason; J. Am. Chem. Soc., 101, (1979), 7095.

74) P. Chini, G. Ciani, S. Martinengo, A. Sironi, L. Longhetti and B.T. Heaton; Chem. Comm., (1979), 188.

75) G. Schmid, V. Bätzel, G. Etzrodt and R. Pfeil; J. Organometal. Chem., 86, (1975), 257.

76) K.E. Schwarzans and H. Steiger; Angew Chemie Int. Ed. 11, (1972), 535.

77) G. Schmid and V. Bätzel; J. Organometal. Chem., 81, (1974), 321.

78) W.P. Griffith; Adv. Organometallic Chem., 7, (1968), 211.

79) F. Calderazzo, R. Ercoli and G. Natta, in I. Wender and P. Pino (Eds), Organic Synthesis via Metal Carbonyls, Wiley Interscience, New York, (1968).

80) A. Visi-Orosz, V. Galamb, G. Pályi, L. Marko, G. Bör and G. Natile; J. Organometal. Chem., 107, (1976), 235.

81) A.S. Foust, M.S. Foster and L.F. Dahl; J. Am. Chem. Soc., 91, (1969), 5633.

82) A.S. Foust, M.S. Foster and L.F. Dahl; J. Am. Chem. Soc., 91, (1969), 5631.

83) F.A. Cotton and G. Wilkinson; Advanced Inorganic Chemistry, Wiley, 3rd Edition, 1972, p370-372.

84) A. Vizi-Orosz; J. Organometal. Chem., 111, (1976), 61.

85) A. Vizi-Orosz, G. Palyi and L. Marko; J. Organometal. Chem., 60, (1973), C25.

86) D. Seyferth and R.S. Henderson; J. Organometal. Chem., 162, (1978), C35.

87) D. Seyferth and J.S. Merola; J. Am Chem. Soc., 100, (1978), 6783.

88) F. Richter, H. Beurich and H. Vahrenkamp; J. Organometal. Chem., 166, (1979), C5.

89) H. Beurich, T. Madoch, F. Richter and H. Vahrenkamp; Angew Chem. Int. Ed. 18, (1979), 690.

90) E. Keller and H. Vahrenkamp; Angew. Chem. Int. Ed., 16, (1977), 731.

91) R.C. Ryan and L.F. Dahl; 97, (1975), 6904. and R.C. Ryan, C.U. Pittman Jr., J.P. O'Connor and L.F. Dahl; J. Organometal. Chem., 193, (1980), 247.

92) H. Vahrenkamp and E.J. Wucherer; Angew.Chem.Int.Ed., 20, (1981), 680.

93) A.S. Foust and L.F. Dahl; J. Am. Chem Soc., 92, (1970), 7337.

94) C.H. Wei and L.F. Dahl; Inorg. Chem., 6, (1967), 1229.

95) C.E. Strouse and L.F. Dahl; J. Am. Chem. Soc., 93, (1971), 6032.

96) F. Richter and H. Vahrenkamp; Angew. Chem. Int. Ed., 17, (1978), 864.

97) F. Richter and H. Vahrenkamp; Angew. Chem. Int. Ed., 18, (1979), 531.

98) F. Richter and H. Vahrenkamp; Angew. Chem. Int. Ed., 19, (1980), 65.

99) C.H. Wei and L.F. Dahl; J. Am Chem. Soc., 90, (1968), 3960.

100) D. Seyferth, C.N. Rudie and J.S. Merola; J. Organometal. Chem., 144, (1978), C26.

101) E. Wiberg and E. Amberger; Hydrides of the Elements of Main Groups I-IV ,Elsevier Publishing Co., (1971).

102) F. Glockling; The Chemistry of Germanium, Academic Press, (1969).

103) H.G. Kuivila; The Organometallic and Coord. Chem. of Germanium, Tin and Lead, (1978), 31.

104) Y.L. Baay and A.G. MacDiarmid; Inorg. Chem., 8, (1969), 986.

105) E.H. Brooks and W.A.G. Graham; Abstracts 4th International Conference on Organometallic Chemistry, Bristol, (1969).

106) E.J. Bulten and H.A. Budding; J. Organometal. Chem., 82, (1974), 121.

107) S.A. Fieldhouse, A.J. Cleland, B.H. Freeland, C.D.M. Mann and R.J. O'Brien; J. Chem. Soc (A), (1971), 2536.

108) H.W. Sternberg, I. Wender, R.A. Friedel and M. Orchin; J. Am. Chem. Soc., 75, (1953), 2717.

109) R.D. Ball and D. Hall; J. Organometal. Chem. 56, (1973), 209.

110) D. Grant and J.R. Van Wazer; J. Organometal. Chem., 4, (1965), 229.

111) Chemical Rubber Company, Handbook of Chemistry and Physics, CRC Press, 58th Edition, (1977-1978), C713-C720.

112) J.E. Drake and W.L. Jolly; Inorg. Synth. 7, (1963), 36.

113) S.P. Foster; M.Sc. Thesis, University of Waikato, (1979).

114) A. Gilliland and D. Blanchard; Inorg. Synth., 2 (1946), 81.

115) F.A. Cotton and J.M. Troup; J. Am. Chem. Soc., 96, (1974), 3438.

116) C.D.M. Mann, A.J. Cleland, S.A. Fieldhouse, B.H. Freeland and R.J. O'Brien; J. Organometal. Chem., 24, (1970) C61.

117) F. Klanberg, W.B. Askew and L.J. Guggenberger; Inorg. Chem., 7, (1968), 2265.

118) K.M. Mackay and R.A. Mackay; Introduction to Modern Inorganic Chemistry, 2nd Ed., Intertext Books (1973).

119) H.J. Emeléus and S.F.A. Kettle; J. Chem. Soc., (1958), 244.

120) G. Bör; J. Organometal. Chem., 94, (1975), 181.

121) B.J. Aylett and H.M. Colquhoun; J. Chem. Soc. (Dalton) (1977), 2058.

122) G. Bör and L. Markó; Spectochim. Acta., 16, (1960), 1105.

123) E.O. Schlemper and D. Britton; Inorg. Chem., 5, (1966), 511.

124) J.K. Burdett; J. Chem. Soc., Faraday Trans., II, (1974), 1599.

125) J.A. Zubieta and J.J. Zuckerman; Prog. Inorg. Chem., 24, (1978), 336.

126) H. Vahrenkamp and D. Wolters; J. Organometal. Chem., 224, (1982), C17.

127) H. Vahrenkamp and D. Wolters; Organometallics, 1, (1982), 874.

128) A.C. Sau, R.O. Day, R.R. Holmes; J. Am. Chem. Soc., 103, (1981), 1264.

129) A.C. Sau, R.O.Day, R.R.Holmes; J. Am. Chem. Soc., 102, (1980), 7972.

130) A.C. Sau, R.R. Holmes; Inorg. Chem., 20, (1981), 4129.

131) R.O. Day, T.M. Holmes, A.C. Sau and R.R. Holmes; Inorg. Chem., 21, (1982), 281.

132) L. Pauling, A.W. Laubengayer and J.L. Hoard; J. Am Chem. Soc., 60, (1938), 1605.

133) F.A. Cotton; Prog. Inorg. Chem., 21, (1976), 1.

134) A.A. Hock and O.S. Mills; Acta Crystallogr., 14, (1961), 139.

135) M.D. Curtis, K.R. Han and W.M. Butler; Inorg. Chem., 19, (1980), 2096.

136) R.J. Klingler, W.M. Butler and M.D. Curtis, J. Am. Chem. Soc., 100, (1978), 5034.

137) M.R. Churchill, J. Wormald, J. Knight and M.J. Mays; Chem. Comm., (1970), 458.

138) E.R. Corey, L.F. Dahl and W. Beck; J. Am. Chem. Soc., 85, (1963), 1202.

139) A. Sirigu, M. Bianchi and E. Benedetti; Chem. Comm., (1969), 596.

140) K. Wade; Chem. in Britain, 11, (1975), 177.

141) K. Wade; Adv. Inorg. Chem. Radiochem., 18, (1976), 1.

142) R.H. Summerville and R. Hoffman; J. Am. Chem. Soc., 101, (1979), 3821.

143) C.F. Shaw and A.L. Allred; Organometal. Chem. Rev., A, 5, (1970), 96.

144) H. Vahrenkamp; Transition Metal Chemistry (Eds. A. Müller and E. Diemann), Verlag Chemie, (1981), 35.

145) S.R. Gunn; J. Phys. Chem., 68, (1964), 949.

146) F.E. Saalfield and H.J. Suec; Inorg. Chem., 2, (1963), 46

147) W.L. Jolly: Angew. Chemie, 72, (1960), 268.

148) A.K. Sawyer and H.G. Kaivila; J. Org. Chem. 27, (1962), 8

149) E. Amberger; Angew. Chemie, 72, (1960), 78.

150) J.P. Collman, J.K. Hoyano and D.W. Murphy; J. Am. Chem. Soc., 95, (1973), 3424.

151) K.D. Bos, E.J. Bulten, J.G. Noltes and A.L. Spek; J. Organometal. Chem., 92, (1975), 33.

152) P. Hackett and A.R. Manning; J. Organometal. Chem. 66, (1974), C17.

153) N.A.D. Carey and H.C. Clark: Inorg. Chem., 7, (1968), 94.

154) B.W.L. Graham, K.M. Mackay and S.R. Stobart; J. Chem. Soc. (Dalton), (1975), 475.

155) R.D. George, K.M. Mackay and S.R. Stobart; J. Chem. Soc. (Dalton), (1972), 1505.

156) W.F. Edgell, J.W. Fisher, G. Asato and W.M. Risen; Inorg. Chem., 8, (1969), 1103.

157) C.R. Dillard and L. May; J. Mol. Spec., 14, (1964), 250.

158) R.E.J. Bichler, M.R. Booth, H.C. Clark and B.K. Hunter; Inorg. Synth., 12, (1970), 61.

159) R.A. Burnham and S.R. Stobart; J. Chem. Soc. (Dalton), (1973), 1269.

160) B.J. Aylett and J.M. Campbell; J. Chem. Soc. (A), (1969), 1910.

161) E.A.V. Ebsworth, S.G. Frankiss and A.G. Robiette; J. Mol. Spec., 12, (1964), 299.

162) H.C. Clark, J.D. Cotton and J.H. Tsai; Inorg. Chem. 5, (1966), 1582.

163) V.G. Albano, M. Sansoni, P. Chini and S. Martinengo; J. Chem. Soc. (Dalton), (1973), 651.